

JAG/NN 8201
no. 1361

**Proton NMR studies on *Megasphaera elsdenii* flavodoxin:
structure elucidation by 2D-NMR and implications**



CENTRALE LANDBOUWCATALOGUS

0000 0394 7203

LSN 522123

BIBLIOTHEEK
LANDBOUWUNIVERSITEIT
WAGENINGEN

Promotoren:	dr. F. Müller	oud-hoogleraar in de Biochemie
	dr. H.J.C. Berendsen	hoogleraar in de Fysische Chemie aan de Rijksuniversiteit Groningen
Co-promotor:	dr.ir. J. Vervoort	universitair docent in de Biochemie

Carlo van Mierlo

**Proton NMR studies on *Megasphaera elsdenii* flavodoxin:
structure elucidation by 2D-NMR and implications**

Proefschrift

ter verkrijging van de graad van
doctor in de landbouw- en milieuwetenschappen,
op gezag van de rector magnificus,
dr. H. C. van der Plas,
in het openbaar te verdedigen
op vrijdag 15 juni 1990
des namiddags te vier uur in de aula
van de Landbouwuniversiteit te Wageningen

aan pa en ma en
iedereen die ik
liefheb

1. De experimenteel aangetoonde watertoegankelijkheid van het fosfaat bindingsgebied en een gedeelte van het isoalloxazine-bindingsgebied van *Megasphaera elsdenii* flavodoxine impliceert dat watermoleculen betrokken zullen moeten worden in beschouwingen (en berekeningen) betreffende de verklaring van de redox-eigenschappen (structuur in relatie tot functie) van dit eiwit.

Dit proefschrift.

2. Bij verwijdering van het flavine uit *Megasphaera elsdenii* flavodoxine blijft de secundaire en tertiäre structuur van het apo-eiwit grotendeels behouden; dit is in tegenspraak met vroegere observaties.

Studies of Flavin-Protein interaction in Flavoproteins Using Protein Fluorescence and Circular Dichroism, D'Anna, J.A. & Tollin, G. (1972) *Biochemistry* 11, 1073-1080.

Dit proefschrift.

3. Het vermelden van het percentage toegekende NOE-kruispijken bij publicatie van een eiwitstructuur die bepaald is met behulp van NMR-gegevens is nuttig.
4. Bij reductie van *Megasphaera elsdenii* flavodoxine naar de semiquinon toestand treden subtiele, functioneel belangrijke, conformatieveranderingen op in het flavine bindingsgebied. De tertiäre structuur buiten het isoalloxazine-bindingsgebied van het eiwit blijft ongewijzigd.

Dit proefschrift.

5. De te betreuren algemene opvatting dat men bij het verwisselen van een academische research positie voor een baan in de industrie eindelijk een 'echte baan' gevonden heeft beperkt zich niet tot uitsluitend het Nederlandse publiek.

Who cares about science, Blakemore, C. (1990) *Sci. publ. Affairs* 4, 97-119.

6. Gedurende de eerste maanden na de monetaire unie van Oost- met West-Duitsland mag verwacht worden dat menig Oost-Duitsler over deze unie zwaar gedesillusioneerd zal raken. Een explosieve toename van de werkloosheid in Oost-Duitsland, waarvan de gevolgen amper te overzien zijn, zal daar debet aan zijn.
7. De slot-opmerking van Powell en Rogers dat de per toeval door hun gecreëerde transgene haarloze muis-variant een mogelijk waardevol systeem zal blijken te zijn voor dermatologische studies die een naakt diersmodel vereisen valt buiten het kader van hun publicatie; het verlegt de grens van wat toelaatbaar is.

Cyclic hair-loss and regrowth in transgenic mice overexpressing an intermediate filament gene. B.C. Powell and G.E. Rogers, (1990) *The EMBO Journal*, vol. 9, no. 5, 1485-1493.

8. Een kristalstructuur die zich zonder temperatuurs- en verfijningsfactoren in de Protein Data Bank bevindt dient in de nieuw te creëren categorie 'tentative structures' geplaatst te worden.
9. De financiële ondersteuning door het Department of Energy Funding aan J. Hanssen (NASA Goddard Institute for space studies) werd na zijn openbare bekendmaking van het vermoeden van een broeikast-effect (1988) stopgezet. De gebruikte motivatie dat het onderzoek economische en industriële vooruitgang belemmert, illustreert het enorme belang van onafhankelijke financiële subsidiebronnen voor het ondersteunen van wetenschappelijk onderzoek.

Science (1990), 248, 672-673.

10. Het is niet verassend (gezien de voorzorgsmaatregelen) dat er onder honderden wetenschappers die met het HIV virus gewerkt hebben (met concentraties van het virus ver boven het niveau in AIDS patienten) de laatste 5 jaar geen AIDS-gevallen gerapporteerd zijn, dit in tegenstelling tot Duesberg's opvatting.

Human immunodeficiency virus and acquired immunodeficiency syndrome: correlation but not causation, Duesberg, P.H. (1989), *Proc. Nat. Acad. Sci. USA* 86, 755-764.

11. Eiwitvouwingsmodellen verkregen via resultaten uit in vitro experimenten kunnen slechts met grote voorzichtigheid doorgetrokken worden naar de in vivo situatie.
12. Demokratische instellingen binnen de universiteit kunnen gekwalificeerd worden als lachspierversterkende middelen.

Stellingen behorende bij het proefschrift 'Proton NMR studies on *Megasphaera elsdenii* flavodoxin: structure elucidation by 2D-NMR and implications'.

Carlo van Mierlo

Wageningen, 15 juni 1990.

Voorwoord

Ik wil op deze plaats graag een aantal mensen bedanken die belangrijk zijn geweest voor de totstandkoming van dit proefschrift.

Franz Müller voor het nauwgezet bestuderen en becommentarieren van de manuscripten; Herman Berendsen voor de genereus ter beschikking gestelde computertijd in Groningen.

Chrit Moonen en Rolf Boelens, die me in de beginfase op weg hebben geholpen.

Willem van Berkel, Willy van de Berg, Anita van Berkel en vooral niet te vergeten Marja Snoek, die onmisbaar waren met betrekking tot het flavodoxine zolang het nog niet in de NMR-buis zat.

Paul Folkers, Frank Vergeldt, Tinka Spronk, Peter van Woensel, Boudewijn van der Sanden, Philip Lijnzaad, Annette van der Toorn en Arnoud Kalverda die in het kader van een doctoraalproject een belangrijke bijdrage aan het onderzoek hebben geleverd. Jullie zijn voor mij een van de factoren geweest die de lol in het werk bepaald hebben!

Jacob de Vlieg, die samen met Philip Lijnzaad, een groot aandeel in het uitvoeren van de moleculaire dynamica berekeningen zowel in Groningen als op het EMBL in Heidelberg heeft gehad. Het is een prachtige en interessante samenwerking geweest! Gert Vriend was een vaardige steun in het gebruik van de WHATIF programmatuur.

Sybrein Wijmenga die het voortouw in de 3D-NMR experimenten heeft gehad, zonder hem zou hoofdstuk 6 niet bestaan hebben. Sybrein, ik heb het fantastisch gevonden!

Jos Joordens: zoals je ziet kunnen ook varkensmesters en koeiemelkers een proefschrift schrijven. Bedankt voor het tip-top in orde houden van de 500 en 600 MHz'en en de gezelligheid. Ook de andere mensen in de groep van Hilbers hebben er voor gezorgd dat het naar Nijmegen gaan zeker geen straf was.

Cees Veeger die met grote inzet ervoor gezorgd heeft dat ik een tijdelijke aanstelling op de vakgroep Biochemie heb gekregen. De leden van de vakgroep Biochemie wil ik bedanken voor de gezelligheid, ik heb me echt thuis gevoeld.

Robert Hall, voor het corrigeren van gedeeltes van dit proefschrift.

Ruud Scheek en Klaas Dijkstra die zo vriendelijk waren meettijd ter beschikking te stellen toen dat elders niet mogelijk was.

I would like to thank David Neuhaus for giving me the possibility to finish part of this thesis during the first months of my stay in Cambridge.

Mijn familie, mijn vrienden en mijn huisgenoten wil ik bedanken voor de aandacht en steun die ik de afgelopen jaren heb gehad. Dat was erg belangrijk.

Als laatste wil ik eindigen met de belangrijkste persoon betreffende het proefschrift: Jacques Vervoort. Jacques, je enthousiasme, je onvoorwaardelijke steun en absolute vertrouwen in mij is geweldig geweest. In tijden van depressies wist je me snel uit de put (en op de kast?) te krijgen. Ondanks menige gezonde botsing (eigen aan onze karakters) zal ik aan de vruchtbare samenwerking met de grootst mogelijke vreugde terug denken. Een betere collega had ik me niet kunnen wensen!

Chapter 2 has been published and chapters 3, 4, 5, 6 and 7 will be published seperately.

- Chapter 2: van Mierlo, C.P.M., Vervoort, J., Müller, F. & Bacher, A. (1990) *Eur. J. Biochem.* 187, 521-541.
- Chapter 3: van Mierlo, C.P.M., Müller, F. & Vervoort, J. (1990) *Eur. J. Biochem.*, (in press).
- Chapter 4: van Mierlo, C.P.M., Lijnzaad, P., Vervoort, J., Müller, F., Berendsen, H.J.C. & de Vlieg, J. (1990) *Eur. J. Biochem.*, (submitted).
- Chapter 5: van Mierlo, C.P.M., van der Sanden, B.P.J., van Woensel, P., Müller, F. & Vervoort, J. (1990) *Eur. J. Biochem.*, (submitted).
- Chapter 6: Wijmenga, S.S. & van Mierlo, C.P.M. (1990) *Eur. J. Biochem.*, (submitted).
- Chapter 7: van Mierlo, C.P.M., van der Toorn, A. & Vervoort, J. (1990) *FEBS Lett.*, (submitted).

The work described in this thesis was carried out under the auspices of the Netherlands Foundation for Chemical Research (SON) with financial aid from the Netherlands Organization for the Advancement of Pure Research (NWO).

List of Abbreviations

1D, 2D, 3D	one-, two-, three-dimensional
BT	back transfer
Cosy	2D scalar correlated spectroscopy
DQF	double quantum filter
EM	energy minimization
FMN	riboflavin 5'-phosphate
HMQ	heteronuclear multiple quantum coherence
HoHaHa	Homonuclear Hartmann Hahn transfer experiment
MD	molecular dynamics
NMR	nuclear magnetic resonance
NOE	nuclear Overhauser enhancement
NOESY	nuclear Overhauser enhancement spectroscopy
RMD	restrained molecular dynamics
RMS	root mean square
RMSD	root mean square difference
ROE	<i>rotating frame nuclear Overhauser enhancement</i>
TOCSY	total correlation spectroscopy
TSP	trimethylsilylpropionate
Ala	A alanine
Arg	R arginine
Asn	N asparagine
Asp	D aspartic acid
Cys	C cysteine
Gln	Q glutamine
Glu	E glutamic acid
Gly	G glycine
Ile	I isoleucine
Leu	L leucine
Lys	K lysine
Met	M methionine
Phe	F phenylalanine
Pro	P proline
Ser	S serine
Thr	T threonine
Trp	W tryptophane
Tyr	Y tyrosine
Val	V valine

Contents

	Page
Chapter 1	1
Introduction (outline of this thesis).	
Chapter 2	11
A two-dimensional ^1H NMR study on <i>Megasphaera elsdenii</i> flavodoxin in the reduced state: sequential assignments.	
Chapter 3	55
Secondary and tertiary structure characteristics of <i>Megasphaera elsdenii</i> flavodoxin in the reduced state as determined by two-dimensional ^1H NMR.	
Chapter 4	83
Tertiary structure characteristics of two-electron reduced <i>Megasphaera elsdenii</i> flavodoxin and some implications, as determined by two-dimensional ^1H NMR and restrained molecular dynamics.	
Chapter 5	127
A two-dimensional ^1H NMR study on <i>Megasphaera elsdenii</i> flavodoxin in the oxidized state and some comparisons with the two-electron reduced state.	
Chapter 6	163
Three-dimensional Clean TOCSY-NOESY NMR study of <i>Megasphaera elsdenii</i> flavodoxin in the oxidized state.	
Chapter 7	193
A two-dimensional ^1H NMR study on the apoflavodoxin of <i>Megasphaera elsdenii</i> .	
Summary	213
Samenvatting	216
Curriculum Vitae	220

Chapter 1

Introduction (outline of this thesis)

Megasphaera elsdenii flavodoxin, the flavoprotein studied in this thesis, contains a tightly but non-covalently bound prosthetic group called FMN (riboflavin-5'-phosphate). FMN is one of the yellow chromophores called "flavin". The first flavin has been discovered more than 100 years ago in milk [1]. Many proteins (more than 100) have until now be found to contain a flavin as functional part of the molecule. In the thirties the structures of several flavins were elucidated [2-5]. Figure 1 depicts the structures of the most common flavin coenzymes including the internationally accepted numbering system.

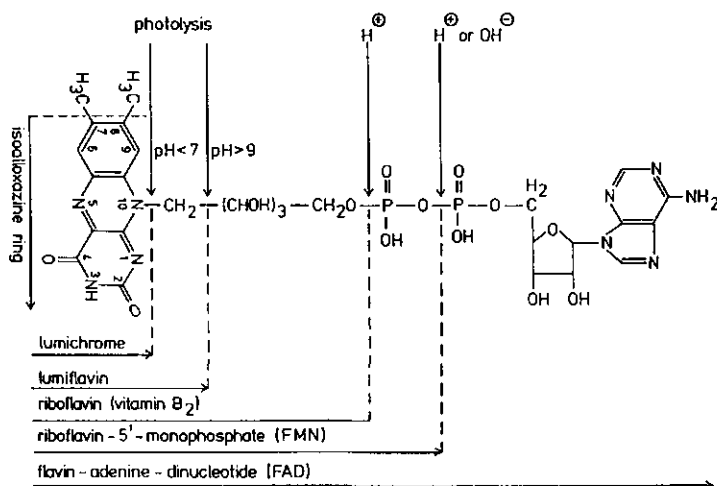


Fig. 1

The chemical entity responsible for the diverse biological activity of flavoproteins is the isoalloxazine moiety of the flavocoenzyme (Fig. 1). The most prominent features of this group, in regard to the protein studied in this thesis, are the redox properties. Flavins can exist in three redox states: the oxidized or quinone state, the one-electron reduced or semiquinone (radical) state and the two-electron reduced or hydroquinone state. The flavoquinone and flavohydroquinone state are diamagnetic, whereas the flavosemiquinone state is paramagnetic.

Free flavin is an amphoteric molecule existing as neutral, anionic and cationic species in all three redox states (see Fig. 2). Only the neutral flavoquinone, the neutral and anionic flavosemiquinone, and the neutral and anionic hydroquinone are of biological relevance in flavoproteins, because the proteins are not stable at

pH<2 or pH>9. Free flavins are unique among all known redox coenzymes as they can undergo both one and two-electron redox transitions.

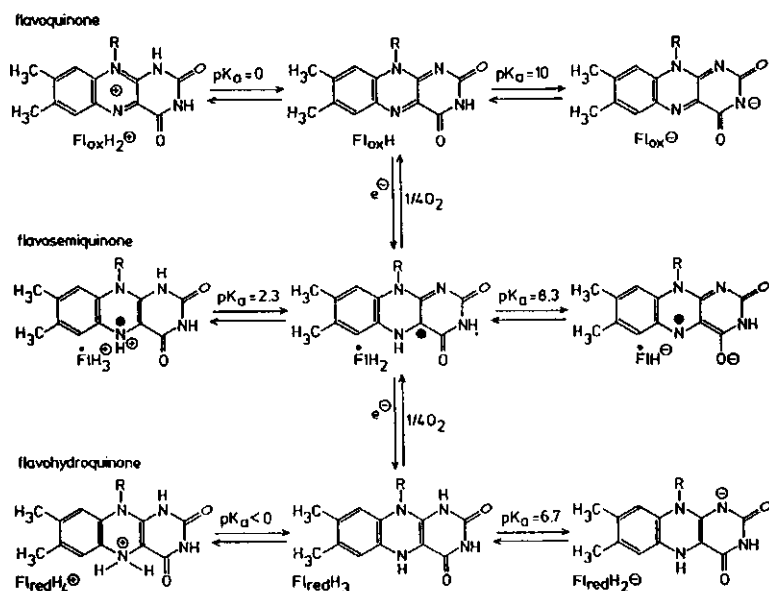


Fig. 2

Flavodoxins are small molecular weight flavoproteins, which contain one molecule of FMN per polypeptide chain [6]. The reaction partners of flavodoxins are other redox proteins. It has been demonstrated that flavodoxins can replace ferredoxins, which are one-electron transfer proteins, in some biological reactions [6]. The amount of ferredoxin or flavodoxin synthesized in the cell depends on the iron content of the medium, i.e. at low iron concentration flavodoxin is preferentially synthesized at the expense of ferredoxin and vice versa [6].

On binding to apoflavodoxins the redox potentials of FMN are strongly altered as compared to those of free flavin. This is the most prominent feature of these proteins. The specific interaction between the flavin coenzyme and the apoprotein is expected to be responsible for the modified chemical and physical properties of the flavin. In case of *Megasphaera elsdenii* flavodoxin the redox potential for the transition from the oxidized to the semiquinone state (E2) is -115 mV, whereas the transition from the semiquinone to the hydroquinone state (E1) has a much lower redox potential of -375 mV [6]. The corresponding values for free FMN are E2=-314 mV and E1=-124 mV [7]. In flavodoxins E2 is always much more positive than E1.

Another feature of flavodoxins is that they act (as ferredoxin) as one-electron transferring proteins, the two-electron transition of the flavin is not of biological relevance. This feature of an one-electron transferring system requires stabilization of the radical state. In flavodoxins the neutral flavosemiquinone is quantitatively formed. The transition between the semiquinone and hydroquinone state is the biologically relevant one, as has been demonstrated for *Megasphaera elsdenii* flavodoxin [8,9]. An high activation barrier occurring between the oxidized and the semiquinone state predestinates the protein for one-electron transitions between the semiquinone and hydroquinone state.

Questions arising are: how does a specific flavodoxin regulate the redox potential of FMN, and what is the cause for the activation barrier occurring in the transition between the oxidized and the semiquinone states of flavodoxins?

In order to gain answers to the forementioned questions, several flavodoxins have been crystallized and their corresponding three-dimensional structures have been determined to high resolution, including *Clostridium MP* flavodoxin in the oxidized and one-electron reduced state [10-12], *Desulfovibrio vulgaris* flavodoxin in the oxidized state [13] and *Anacystis nidulans* flavodoxin in the oxidized state [14-16]. Some results have been published concerning the shape of the dihydro-isoalloxazine ring in two-electron reduced *Clostridium MP* flavodoxin (in addition the positions of Ser7 OH, Ser87 OH, the carbonyl group of Gly57, and the sidechain positions of Glu59, Met56 and Trp90 were published) [12]. A conformational change between the oxidized and one-electron reduced *Clostridium MP* flavodoxin structure has been observed and believed to explain the activation barrier existing between these redox states. Conformational effects exerted by the apoflavodoxin on the flavin ring were argued to be the main factors governing the redox potential modulation [17]. ¹³C and ¹⁵N nuclear magnetic resonance (NMR) results showed this hypothesis to be too simple [18]. Charge-charge interactions were proposed to be probably the main factor in determining the redox properties of flavodoxins [19].

In the past, NMR spectroscopy has proven to be a valuable tool for studying flavoproteins in detail. By using ¹³C and ¹⁵N enriched flavins it was possible to study the electronic and conformational structure of the protein-bound flavin [20,21]. The reconstituted flavoproteins did not differ in any chemical property from the original flavoproteins. ¹³C and ¹⁵N chemical shifts did reveal the π electron density and the presence of hydrogen bonds to the isoalloxazine moiety in the different redox states. ³¹P NMR showed that the phosphate group of FMN is bound in the dianionic form in case of *Megasphaera elsdenii* flavodoxin [8]. In addition dynamical information concerning the proteins could be extracted from the NMR

results. Only a few results however, were gathered concerning the apoflavodoxins [22,23].

The aim of this research project was to obtain answers to the forementioned questions regarding the redox potential regulation, and the activation barrier occurring between the oxidized and one-electron reduced redox states of *Megasphaera elsdenii* flavodoxin. Therefore the interaction between the flavin coenzyme and the apoprotein has to be determined, a solution structure of the protein is necessary. *Megasphaera elsdenii* flavodoxin is an uncrystallizable protein consisting of 137 amino acid residues (molecular mass 15 kDa).

^1H NMR is an excellent technique to get detailed information on the protein structure and its dynamics. However, the enormous amount of resonances present when acquiring ^1H NMR spectra of a protein the size of *Megasphaera elsdenii* flavodoxin, make interpretation of this information difficult. The recent development of the two-dimensional NMR techniques (2D-NMR) [24], and the great advances in NMR instrumentation make it possible to attempt solving the solution structure of flavodoxin by NMR. Of great importance is the progress made in the main bottleneck: the assignment of the ^1H resonances of a specific protein. Development of the sequential resonance assignment procedure by the group of Wüthrich [25-28] make it possible to assign in principle every proton of a (relatively small) protein in solution. Assignment of virtually all protons of two-electron reduced *Megasphaera elsdenii* flavodoxin using this procedure is described in chapter 2 of this thesis. Use has been made of the special properties of flavodoxin regarding its three redox states.

The dipole-dipole interaction between the protons of a protein is the basis for structure determination by NMR. This interaction can result in magnetisation transfer, the nuclear Overhauser enhancement (NOE) [29], which can be measured in solution. The size of the NOE effect is dependent on the distance (r^{-6} distance dependence), NOE's can only be measured between protons having relatively short internuclear distances ($<5\text{\AA}$). Using 2D-NOE spectra (NOESY spectra) it is possible to determine the size of the NOE effect between two protons, as this is reflected in the size of the off-diagonal cross peak connecting these proton resonances, and hence obtain structural information.

The NOE between NH , C_αH and C_βH protons of *Megasphaera elsdenii* flavodoxin is extensively exploited for assigning amino acid residues (chapter 2). The same effect is also used for secondary structure determination. The secondary structure of a protein is characterized by several characteristic NOE connectivities. Helices show strong connectivities between neighbouring amide protons: NH_i and NH_{i+1} , corresponding to short distances. The regions of helicity are further confirmed by the observation of medium-range connectivities between $\text{C}_\alpha\text{H}_i$ and

NH_{i+3} , and between $\text{C}_\alpha\text{H}_i$ and $\text{C}_\beta\text{H}_{i+3}$. In contrast to helices, strong NOE connectivities between $\text{C}_\alpha\text{H}_i$ and NH_{i+1} are characteristic for extended backbone conformations. In chapter 3 the determination of the secondary structure elements of two-electron reduced *Megasphaera elsdenii* flavodoxin is described.

The tertiary structure of a protein is determined by long-range NOE's. These NOE's connect resonances of protons from amino acid residues which are far apart in the primary sequence (at least four positions apart) but in close spatial proximity of each other as a result of tertiary folding of the protein. The global fold of *Megasphaera elsdenii* flavodoxin is described in chapter 3 of this thesis, using these long-range NOE's.

Subsequently, a detailed structure of *Megasphaera elsdenii* flavodoxin can be generated by employing all interresidual NOE connectivities observed. Based mainly on information obtained in chapter 3 a starting structure of flavodoxin is generated. Restrained molecular dynamics calculations [30-32], solving the classical Newtonian equations of motions, are applied to this structure. Beside terms describing the potential energy of the molecular system, NOE's were used as 'non-physical' distance restraints. The calculations performed in vacuo resulted in a structure satisfying the experimental restraints very well. The first structure of a two-electron reduced flavodoxin is obtained hereby. Generating the detailed structure of two-electron reduced *Megasphaera elsdenii* flavodoxin is described in chapter 4 of this thesis. The structure is discussed considering NMR parameters (lineshapes, exchange characteristics and chemical shifts) and some implications with respect to redox potential regulation are drawn (chapter 4).

In chapter 5, using information gathered in the previous chapters of this thesis, the ^1H NMR assignment of all amino acid residues of the oxidized state of *Megasphaera elsdenii* flavodoxin is described. Special attention is given to conformational differences observed between oxidized and two-electron reduced flavodoxin, by using NOESY spectra, in order to explain the previously mentioned activation barrier. Attention is also given to proton chemical shift differences observed between both reduction states of the protein.

In chapter 6 the interpretation of a three-dimensional ^1H NMR experiment ('Clean TOCSY-NOESY' 3D-NMR) is theoretically described. The interpretation and assignment method is applied to the 'Clean TOCSY-NOESY' spectrum of oxidized *Megasphaera elsdenii* flavodoxin with the aim of demonstrating the use of such an experiment in assigning a complex protein. Furthermore the experiment provides a check on the assignments found by 2D-NMR methods.

Finally, in chapter 7 the apo flavodoxin of *M. elsdenii* is studied using 2D-NMR techniques. Information about the tertiary structure of this protein in solution is obtained and the structures of the apo- and holoproteins are compared.

This thesis is a reflection of the enormous progress made in NMR-spectroscopy on proteins, NMR has become an invaluable tool in studying several specific biochemical problems, as shown. Many important studies however, can still be performed on the interesting flavoprotein studied in this thesis. The structure of this flavodoxin can still be refined by taking into account for example intraresidual NOE contacts. Calculating the structure with water molecules is expected to emerge in a better biologically defined tertiary structure of this protein, which might have implications on the local structure in the immediate neighbourhood of the flavin. Amino acid residue replacement in the flavin binding region by genetic manipulation of the gene encoding for *Megasphaera elsdenii* flavodoxin is expected to emerge in information concerning the specific roles these residues play on redox potential regulation. ^1H 2D- and 3D-NMR methods will than reveal easily the accompanied structural changes involved. NMR will continue to play a dominant role in explaining the relation between structure and function of this biomolecule.

References

1. Blyth, A.W. (1879) *J. Chem. Soc.* 35, 530-539.
2. Kuhn, R., Reinemund, K. & Weygand, F. (1934) *Ber. Dtsch. Chem. Ges.* 67, 1460-1462.
3. Karrer, P., Schöpp, K. & Benz, F. (1935) *Helv. Chim. Acta* 18, 426-429.
4. Theorell, H. (1935) *Biochem. Z.* 278, 263-290.
5. Warburg, O. & Christian, W. (1938) *Biochem. Z.* 254, 294.
6. Mayhew, S.G. & Ludwig, M.L. (1975) *The enzymes* 3rd Ed., 57-118.
7. Anderson, R.F. (1983) *Biochem. Biophys. Acta* 723, 78-82.
8. Moonen, C.T.W. & Müller, F. (1982) *Biochemistry* 21, 408-414.
9. Moonen, C.T.W. & Müller, F. (1984) *Eur. J. Biochem.* 140, 303-309.
10. Burnett, R.M., Darling, G.D., Kendall, D.S., Lequesne, M.E., Mayhew, S.G., Smith, W.W. & Ludwig, M.L. (1974) *J. Biol. Chem.* 249, 4383-4392.
11. Smith, W.W., Burnett, R.M., Darling, G.D. & Ludwig, M.L. (1977) *J. Mol. Biol.* 117, 195-225.
12. Ludwig, M.L., Burnett, R.M., Darling, G.D., Jordan, S.R., Kendall, D.S. & Smith, W.W. (1976) in *Flavins and Flavoproteins* (Singer, T.P., ed.) pp. 393-404, Elsevier, Amsterdam.
13. Watenpaugh, K.D., Sieker, L.C. & Jensen, L.H. (1973) *Proc. Nat. Acad. Sci. Us* 70, 3857-3860.
14. Smith, W.W., Patridge, K.A., Ludwig, M.L., Petschko, G.A., Tsernoglou, D., Tanakar, M. & Yasunobu, K.T. (1983) *J. Mol. Biol.* 165, 737-755.

15. Ludwig, M.L., Pattridge, K.A. & Tarr, G. (1984) in *Flavins and Flavoproteins* (Bray, R.C., Engel, P.C. & Mayhew, S.G. eds.) pp. 253-259, Walter de Gruyter & Co., Berlin-New York.
16. Laudenbach, D.E., Straus, N.A., Pattridge, K.A. & Ludwig, M.L. (1987) in *Flavins and Flavoproteins* (Edmondson, D.E. & McCormick, D.B. eds.) pp. 249-260, Walter de Gruyter & Co., Berlin-New York.
17. Simondson, R.P. & Tollin, G. (1980) *Mol. Cell. Biochem.* 33, 13-24.
18. Moonen, C.T.W., Vervoort, J. & Müller, F. (1984) *Biochemistry* 23, 4868-4872.
19. Moonen, C.T.W., Vervoort, J. & Müller, F. (1984) in *Flavins and Flavoproteins* (Bray, R.C., Engel, P.C. & Mayhew, S.G., eds.) pp. 493-496, Walter de Gruyter & Co., Berlin-New-York.
20. Moonen, C.T.W. (1983) *Thesis*, Agricultural University Wageningen.
21. Vervoort, J (1986) *Thesis*, Agricultural University Wageningen.
22. Moonen, C.T.W. & Müller, F. (1984), *Eur. J. Biochem.* 140, 311-318.
23. Moonen, C.T.W., Scheek, R.M., Boelens, R. & Müller, F. (1984) *Eur. J. Biochem.* 141, 323-330.
24. Ernst, R.R., Bodenhausen, G. & Wokaun, A. (1987) *Principles of Nuclear Magnetic Resonance in One and Two dimensions*, Clarendon Press, Oxford.
25. Wüthrich, K., Wider, G., Wagner, G. & Braun, W. (1982) *J. Mol. Biol.* 155, 311-319.
26. Wagner, G. & Wüthrich, K. (1982) *J. Mol. Biol.* 155, 321-346.
27. Billeter, M., Braun, W. & Wüthrich, K. (1982) *J. Mol. Biol.* 155, 321-346.
28. Wüthrich, K. (1986) *NMR of Proteins and Nucleic Acids*, Wiley, New York.
29. Noggle, J.H. & Schirmer, R.E. (1977) *The Nuclear Overhauser Effect-Chemical Applications*, Academic, New York.
30. van Gunsteren, W.F., Kaptein, R. & Zuiderweg, E.R.P. (1983) in *Nucleic Acid Conformation and Dynamics* (Olson, W.K. ed.) Report of NATO/CECAM Workshop, pp. 79-92, Orsay, France.
31. Kaptein, R., Zuiderweg, E.R.P., Scheek, R.M., Boelens, R. & van Gunsteren, W.F. (1985) *J. Mol. Biol.* 182, 179-182.
32. Clore, G.M., Brünger, A.T., Karplus, M. & Gronenborn, A.M. (1986) *J. Mol. Biol.* 191, 523-551.

Chapter 2

A two-dimensional ^1H NMR study on *Megasphaera elsdenii* flavodoxin in the reduced state: sequential assignments

Carlo P.M. van Mierlo¹, Jacques Vervoort¹, Franz Müller^{1*} and Adelbert Bacher²

1. Department of Biochemistry, Agricultural University, Wageningen, The Netherlands.

1*. Present address: Sandoz, Agro Ltd., Department of Toxicology, Basle, Switzerland.

2. Department of Organic Chemistry and Biochemistry, Technical University of Munich, Garching, Federal Republic Germany.

Summary

Assignments for the 137 amino acid residues of *Megasphaera elsdenii* flavodoxin in the reduced state have been made using the sequential resonance assignment procedure. Several hydroxyl and sulfhydryl protons were observed at 41 °C at pH 8.3. Spin systems were sequentially assigned using phase-sensitive 2D-correlated spectroscopy (DQF-Cosy, HoHaHa-spectroscopy, DQ-spectroscopy) and phase-sensitive nuclear Overhauser enhancement spectroscopy (NOESY). Spectra of the protein in H₂O and of protein preparations either completely or partly exchanged against ²H₂O were obtained.

Use of the fast electron shuttle between the paramagnetic semiquinone and the diamagnetic hydroquinone state greatly simplified the NMR spectra, making it possible to assign easily the ¹H resonances of amino acid residues located in the immediate neighbourhood of the isoalloxazine ring.

The majority of the nuclear Overhauser effect contacts between the flavin and the apoprotein correspond to the crystal structure of the flavin domain of *Clostridium MP* flavodoxin, but differences are also observed. The assignments provide the basis for the structure determination of *M. elsdenii* flavodoxin in the reduced state as well as for assigning the resonances of the oxidized flavodoxin.

Introduction

Megasphaera elsdenii flavodoxin is a non-crystallizable protein which contains riboflavin-5'-monophosphate (FMN) as a prosthetic group and functions as an electron carrier in biological reactions. The FMN molecule is noncovalently but very tightly bound to the apoprotein [1]. Under iron-deficient conditions the protein is produced in large quantities by *M. elsdenii* as a substitute for ferredoxin [1]. The protein-bound flavin can occur in the oxidized, the one-electron reduced (semiquinone) and the two-electron reduced (hydroquinone) state. *In vivo* the flavodoxin shuttles between the semiquinone and hydroquinone states owing to a high activation barrier occurring between the oxidized and the semiquinone state. This activation barrier predestinates the protein for one-electron transfer reactions [2,3].

The flavodoxins form a class of relatively small proteins (15-23 kDa); the flavodoxin from *M. elsdenii* has a molecular weight of 15 kDa and consists of 137 amino acid residues. The sequence of the protein is known [4,5]. Upon binding to the apoprotein the chemical and physical properties of the flavin are modified. The most striking property of the flavodoxins is the strongly altered redox potential of the

semiquinone/hydroquinone transition (from -400 mV to -500 mV) as compared to free FMN (-124 mV) [1,6].

With regard to NMR spectroscopy several studies were done to probe the electronic and conformational structure of the protein-bound flavin using ^1H , ^{13}C , ^{15}N and ^{31}P NMR techniques [2,3,7-10]. The present 2D-NMR study is a continuation of previous 1D- and preliminary 2D- ^1H NMR studies [7,10,11]. These studies showed that *M. elsdenii* flavodoxin is very suitable for 2D-NMR experiments, because it is easily available in large quantities and is highly soluble. The protein is also remarkably stable in the three redox states over a long period of time at different temperatures and pH values. Furthermore the 1D-NMR spectrum is well resolved. The aim of this paper is to assign the resonances in the ^1H NMR spectrum of *M. elsdenii* flavodoxin by 2D-NMR techniques. These data will then form the basis for the elucidation of the three-dimensional structure and dynamical properties of the protein. It is assumed that these studies will lead to a better insight into the structural requirements which determine the biological functions of this flavoprotein.

In the past few years two-dimensional NMR has been applied successfully for sequential resonance assignments in spectra of several relatively small-sized proteins. The technique was first successfully applied for the elucidation of the structure of the 58 amino acid residue-containing BPTI by the group of Wüthrich [12,13]. Till 1987 sequential resonance assignments were made only on proteins not exceeding 90 amino acid residues [13-29]. The sequential resonance assignments for larger proteins is hampered by the larger intrinsic linewidths and the substantial increase in numbers of cross peaks, both resulting in a considerable overlap of resonances in the $\text{NH-C}_\alpha\text{H}$ region of 2D-NMR spectra.

Assignments of proteins of larger sizes (more than 90 residues) have only recently been made, including those for spinach plastocyanin (99 residues [30]), hen egg white lysozyme (129 residues [31]), horse ferricytochrome c (104 residues [32,33]), *Escherichia Coli* thioredoxin (108 residues [34]) and plastocyanine (97 residues [35]). The assignment of the 137 amino acid residues in *M. elsdenii* flavodoxin represented a considerable challenge. The fact that it was possible to achieve an almost complete assignment is in fact due to the "right" physical properties of the protein which have been already mentioned above. The full assignment in the spectrum of *M.elsdenii* flavodoxin demonstrates that modern NMR techniques are capable of tackling relatively large, biologically interesting macromolecules. In the final stage of this two-dimensional NMR study it became evident that the three-dimensional structure of *M. elsdenii* flavodoxin closely resembles that of the known crystal structure of *Clostridium MP* flavodoxin.

Materials and Methods

Flavodoxin from *M. elsdenii* was isolated and purified as previously described [36]. For the removal of all exchangeable protons of the flavodoxin, the apoflavodoxin was prepared according to the method of Wassink & Mayhew [37]. The apoflavodoxin was then dissolved in $^2\text{H}_2\text{O}$ and freeze dried, this procedure was repeated at least two times. The reconstitution with FMN was done in $^2\text{H}_2\text{O}$ at pH 8.3. Reconstitution using isotopically enriched FMN molecules were done in an analogous way. FMN molecules selectively enriched with ^{13}C in the ribityl side chain were prepared according to Le Van et al. [38]. Excess FMN was removed from reconstituted flavodoxin by molecular sieve chromatography (Biogel P-6Dg).

Reduction and reoxidation experiments were conducted by the addition of the desired amount of a dithionite solution to the anaerobic solution of flavodoxin in the oxidized state. Anaerobic solutions were achieved by carefully flushing the flavodoxin solution in the NMR tube with argon for about 20 min. The desired degree of reoxidation was obtained by injecting small volumes of air into the NMR tube containing the anaerobic flavohydroquinone solution, followed by gentle mixing.

All samples contained 6 to 10 mM flavodoxin in solutions consisting of potassium phosphate or potassium pyrophosphate or a mixture of both phosphates in total concentrations ranging from 75 mM to 200 mM, pH 8.3.

All measurements were done using a mixture of 10% $^2\text{H}_2\text{O}$ /90% H_2O , except in cases where a specific deuterium content was desired.

^{13}C and ^{31}P NMR spectra were acquired on a Bruker CXP-300 NMR spectrometer. The conditions to acquire these spectra have been described previously [2,8].

2D-NMR spectra were acquired on a Bruker WM500 and a Bruker AM500 spectrometer operating at 500 MHz and more recently on a Bruker AM600 operating at 600 MHz. The spectra on the WM500 spectrometer, were collected with the carrier frequency at the extreme left of the spectrum [11] whereas the other spectra were acquired with the carrier frequency in the middle of the spectrum coinciding with the water resonance.

Double quantum filtered Cosy spectra were acquired according to Marion & Wüthrich [39] and Rance et al. [40]. Phase sensitive NOESY spectra were obtained using Time Proportional Phase Increments (TPPI) [39,41]. Mixing times of 25, 50, 100, 150 and 200 ms were used. No zero quantum filter was applied. The NOESY spectrum corresponding to a mixing time of 150 ms was used as the basic NOESY spectrum for making sequential assignments. Double quantum spectra were acquired using delay times τ of 16 ms and 32 ms [42,43].

2D Homonuclear Hartmann Hahn transfer experiments using MLEV17 composite pulse cycling [44] were acquired using mixing times varying between 10 and 160 ms. The MLEV17 part was sandwiched between two 2.5 ms trimpulses. TPPI was used in the DQ and HoHaHa experiments for frequency discrimination in the ω_1 direction. In the DQF Cosy and NOESY experiments specific irradiation of the water resonance took place at all times, except during the data acquisition period. In the DQ and HoHaHa experiments irradiation took place during the relaxation delay period.

Irradiation of the water protons for 2.5 s with 13-40 dB attenuation from 0.2 Watt power was sufficient to saturate the protons, the power of irradiation depended on the solvent used (H_2O or $^2\text{H}_2\text{O}$). Experiments were done at 30, 33, 37 and 41 °C.

The number of increments varied between 355 and 729 whereas the number of scans varied between 32 and 144. Four dummy scans were performed during each 2D-NMR experiment. The total acquisition time varied between 14 h and 50 h (the latter for the spectra acquired using the WM500 instrument, where a relatively low signal-to-noise ratio was obtained).

After data acquisition all further data handling was performed on a Microvax II computer using software obtained from Dr. R. Boelens, modified to our specific requirements. The data were digitally filtered by using sine bell or squared sine bell window functions shifted by various amounts as described in the Figure legends. After zero filling, spectra with a digital resolution varying between 2.9 and 11.8 Hz per point were obtained. After the double Fourier transformation of the data of the 2D-NMR experiment baseline corrections with a fourth order polynomial were performed according to Pearson [45] in both frequency directions. The 2D-NMR spectra are presented as contour plots with levels increasing by a factor 1.3.

Results and Discussion

General Remarks

The assignments in the NMR spectra of flavodoxin in the reduced state were done by applying the sequential resonance assignment procedure for proteins as developed by the group of Wüthrich [12-14,46,47]. In the first step of the two-stage procedure as many individual spin systems as possible were searched for using experiments like Double quantum filtered Cosy and HoHaHa which give information about scalar coupled protons within a particular spin system. At this stage it was possible to assign some amino acid residues possessing unique spin patterns which could be detected completely in the 2D-NMR spectra. Other spin systems were collected as groups of spin systems showing the same spin pattern

characteristics in the 2D-NMR spectra. In the second stage, assignments of spin systems to specific amino acid residues in the flavodoxin were made using sequential NOE effects involving neighbouring NH, C α H and C β H protons. In this way several sequential fragments were collected. Comparing these sequential fragments with the known primary structure of flavodoxin [4,5] resulted in sequence-specific assignments.

During the assignment procedure in spectra of reduced flavodoxin use of the special property of flavodoxin was made, i.e. the fast electron shuttle between the hydroquinone and the semiquinone state [3]. Moonen and Müller [3] showed that this electron-exchange reaction is diffusion-controlled and consequently no conformational change occurs in the transition from the semiquinone to the hydroquinone state.

Due to the paramagnetic properties of the isoalloxazine ring in the semiquinone state [48] resonances of protons located in the immediate neighbourhood of the isoalloxazine ring become broadened or disappear completely from the spectrum. Since the electron exchange between the one-electron reduced semiquinone state and the two-electron reduced diamagnetic hydroquinone state is diffusion-limited it is possible to create a varying proton sphere around the flavin. Protons in this sphere are characterized in the 2D-NMR spectra by either complete disappearance or broadening of the corresponding cross peaks, depending on the distance from the flavin. The proton sphere can be created as desired by varying the concentration of the semiquinone in the sample. This property of flavodoxin has two advantages; firstly, as already mentioned, protons of amino acid residues in the immediate neighbourhood of the isoalloxazine moiety are easily recognized facilitating the assignment procedure; secondly, the complex 2D-NMR spectra of *M. elsdenii* flavodoxin are simplified. Some areas in the 2D-NMR spectrum are no longer overcrowded, an advantage which should not be underestimated in 2D-NMR spectroscopy applied to a protein of this size.

Another property of flavodoxin concerning the differences between the oxidized and the two-electron reduced state was also exploited. In the case of the diamagnetic two-electron reduced state the flavin contains two additional electrons as compared to the diamagnetic oxidized state. Protons of amino acids in the immediate neighbourhood of the flavin moiety experience thereby different local magnetic fields caused by the different ring current effects of the flavin moiety. These protons are characterized in the 2D-NMR spectra by altered resonance positions on going from the oxidized to the reduced state of the flavodoxin and are thereby easily recognized. This property did not generate simpler 2D-NMR spectra, in terms of containing fewer cross peaks, but it solved overlap problems in several spectral regions.

During the two-stage procedure of the sequential assignments, also information was gathered about secondary structure elements, i.e. α -helices and β -sheets, and the tertiary structure. α -Helices are characterized by strong NOE intensities between neighbouring amide protons ($\text{NH}_i\text{-NH}_{i+1}$), additionally also medium range NOE's between $\text{C}_\alpha\text{H}_i\text{-NH}_{i+3}$ and $\text{C}_\alpha\text{H}_i\text{-C}_\beta\text{H}_{i+3}$ protons [46,47,49] are observed. β -Sheets are characterized by strong $\text{C}_\alpha\text{H}_i\text{-NH}_{i+1}$ NOE contacts. After determining the helicity and β -sheet characteristics of the protein this information was exploited to confirm assignments and to search for missing spin systems. Similarly information about the tertiary structure, gathered by non-sequential interresidual NOE contacts, was collected during the assignment procedure. As a result of the above procedure there was a continuous feedback between the different stages of this process.

Moreover, spectra were recorded at different temperatures and of protein preparations in which the amide protons were partly exchanged against deuterons to solve ambiguities in different spectral regions.

The investigation of reduced flavodoxin in dependence on the pH of the solution was limited by the fact that full reduction of flavodoxin requires a high pH value, i.e. approximately pH 8.3 [50].

For convenience the one letter code for amino acid residues is used in the text.

Analysis of spin systems

M. elsdenii flavodoxin is composed of 137 amino acid residues including 5 proline residues. The fingerprint region of the DQF Cosy spectrum should therefore contain 132 cross peaks (or pairs of cross peaks in the case of glycine residues) for the $\text{NH-C}_\alpha\text{H}$ contacts.

In the DQF Cosy spectrum 118 cross peaks can be observed at 33 °C (Fig. 1), implicating that 14 cross peaks could not be detected. This suggests three things. Firstly, the $\text{NH-C}_\alpha\text{H}$ coupling constant may be too small or the linewidth too large, resulting in cancellation of the cross peak intensity by overlap of the anti-phase components of the cross peak [15]. Secondly, a $\text{NH-C}_\alpha\text{H}$ cross peak can vanish because the α -proton resonates at the same position as the water signal, which results in a concomitant loss of intensity during the saturation of the water resonance. This problem can be overcome by varying the temperature and thereby shifting the water resonance position. Thirdly, an amide proton can exchange very rapidly and thereby saturation of the solvent can be transferred to these protons. In addition the chemical shift difference between the NH- and the solvent resonance might be too small with respect to the exchange rate [47]. In the case of reduced flavodoxin the measurements were done at pH 8.3. Under this condition the minimum hydrogen exchange rate as determined for model peptides is far

exceeded and thereby this condition is far above the normally chosen experimental conditions for acquiring two-dimensional NMR spectra [51]. One would therefore expect that several exchangeable protons of flavodoxin will be effected by the basic environment.

Fig. 1 500 MHz NH-C α H-connectivity region of a double-quantum filtered C α Sy spectrum of *M. elsdenii* flavodoxin in the reduced state in 90% H $_2$ O/10% 2 H $_2$ O, pH 8.3, 33 $^{\circ}$ C. The spectra were collected with the carrier positioned in the centre of the spectrum and processed with a sine-bell shifted by 15 $^{\circ}$ in t_2 and a squared sine-bell shifted by 22.5 $^{\circ}$ in t_1 dimension. The digital resolution is 3.4 Hz/point in ω_2 and 6.8 Hz/point in ω_1 dimension. Positive cross peaks are represented as filled circles, negative cross peaks as open circles. NH-C α H-cross peaks are identified by labels. Underlined labels indicate cross peaks which were not visible in the 500 MHz spectrum, mainly due to a slight oxidation of the sample during the experiment, these cross peaks were obtained and added using a 600 MHz DQF-C α Sy spectrum which contained however a lot of t_1 noise above the aromatic C α Sy connectivities and is therefore not presented here.

corresponding spin systems (including A29, D30, one NH-C α H cross peak of G53 and M120). In the case of A29, D30 and M120, we detected at 41 °C HoHaHa cross peaks very close to the waterline revealing the corresponding C α H resonance positions.

Six amide proton resonances (V41, D48, G80, N118, D122 and E126) appeared to be influenced by the high pH of the solution, resulting in a high exchange rate of these protons with the solvent. These amide resonances are characterized by their low NMR intensities in the NOESY spectra. Three of them (V41, D48 and G80) could not be detected in the DQF-Cosy and in the HoHaHa spectra of the reduced state of the protein. Recording 2D-NMR spectra of the protein in the oxidized state or in the partly reduced state, where a lower pH of the solution could be used, resulted in a clear observation of these amide resonances at the same resonance positions as in the reduced state (the amide resonance position of D48 could not be detected in the fully reduced state because of loss of NMR intensity). The amide proton of the N terminus of flavodoxin could not be assigned in the three redox states, because it is expected to exchange too rapidly with the solvent molecules to be detected.

The remaining 7 missing DQF-Cosy cross peaks are assumed to result from spin systems with a small NH-C α H coupling constant (G11, F36, G53 (one C α H-NH Cosy cross peak at ω_1 is 1.80 ppm), A75, G90, G92 and W96). Their NH's were assigned during the second stage of the sequential resonance assignment procedure.

The remarkable feature that almost all NH resonances could be observed in the NOESY spectra in the range 30 °C-41 °C at pH 8.3 indicates that the structure of flavodoxin is stable and compact in the reduced state. The protein environment must therefore considerably decrease the amide exchange rate as compared to the amide protons freely accessible by solvent [51].

Almost all NH resonances could also be observed in samples containing varying ratios of semiquinone/hydroquinone (with the exception of amide resonances influenced by the paramagnetism of the flavin moiety) and in samples containing the oxidized state of the protein. This indicates that in all three redox states the protein is very stable.

The majority of the double quantum filtered Cosy cross peaks in the fingerprint region of the spectrum have the same antiphase fine structure, when using a resolution as described in the legend of Fig. 1. Therefore no specific amino acid residue can be assigned to such cross peak, solely on the basis of only the fine structure, with the exception of glycines which can give rise to two cross peaks resulting from the coupling of one NH proton with two α protons. The latter was observed for 4 glycines. The other glycine residues gave rise to only one Cosy

the C β H-position are usually difficult to identify because the C β H and C γ H resonance positions are very similar and therefore give rise to cross peaks very close to the diagonal. In addition, the coupling patterns in which overlap of antiphase components leads to cancellation of cross peak intensity are very complex to analyze.

In the following the strategy and the results for the analysis of spin systems of flavodoxin in the reduced state is given, thus comprising thereby the first stage of the sequential resonance assignment procedure.

Glycines

Flavodoxin contains 14 glycine residues (see Table 1). Glycine spin systems give rise to a single Cosy connectivity of the two α protons in the region around 4 ppm in $^2\text{H}_2\text{O}$, characterized by a large coupling constant. Gly can give rise to two fingerprint region Cosy cross peaks, as discussed above, as well as two HoHaHa cross peaks in the same spectral region. Gly can also give rise to a unique remote connectivity at the amide resonance position in the ω_2 direction and the $\omega_{\alpha 1} + \omega_{\alpha 2}$ position in ω_1 direction in a double-quantum spectrum [43]. Using the double-quantum spectrum six Gly were completely assigned (G11, G28, G58, G80, G94 and G108).

G58, G94, G113 and G131 gave rise to two Cosy cross peaks in the fingerprint region and G84, G87 and G90 were found via their two HoHaHa cross peaks in the fingerprint region of the spectrum. Three glycines could not be identified at this stage (G9, G53 and G92).

Threonines

Flavodoxin contains 8 Thr residues (see Table 1). Threonine spin systems have a unique spin pattern and give rise to a strong C β H-C γ H₃ Cosy cross peak in addition to a Cosy peak between C α H-C β H, which sometimes is not detected because of degeneration of the C α H and C β H resonances. In the HoHaHa spectrum relay connectivities from the amide proton to the C α H, C β H and C γ H protons can be found thus distinguishing Thr from Ala. In this way T39, T72, T104, T110 and T114 were completely assigned whereas for T10 only the C β H-C γ H connectivity was found but it was not known at this stage whether this connectivity belonged to an alanine or threonine residue.

Alanines

Flavodoxin contains 18 Ala residues (see Table 1). Alanine is one of the most easily detectable spin systems giving unique spin patterns characterized by a strong C α H-C β H Cosy connectivity and strong NH-C β H relay connectivities in HoHaHa spectra recorded in H_2O . A56 had already been assigned [7,11]. 17 Ala spin systems could be assigned completely at this stage. For A75 only the C α H-C β H connectivity was found. In a later stage of the assignment procedure we could

assign the NH proton of A75 via strong NOE connectivities between the amide proton and the C α H and the C β H protons. No Cosy or relay connectivities could be found for the amide proton of A75 suggesting a small NH-C α H coupling.

Valines

Flavodoxin contains 13 Val spin systems (see Table 1). Valine residues are rather easily assigned, characterized by pairs of methyl cross peaks with their C α H and C β H spin system protons in HoHaHa spectra in $^2\text{H}_2\text{O}$. In HoHaHa spectra obtained in H_2O one can observe relay connectivities between the amide and methyl protons.

All valine spin systems, except those of V83 and V111, appeared to have inequivalent methyl groups and could be assigned at this stage along with their amide protons, except for the amide resonance of V41 which appeared to be influenced by the high pH of the flavodoxin solution. In the case of degeneracy of the methyl groups (V83, V111) the generally different resonance positions of the C β H protons of valine spin systems and threonine spin systems in proteins can easily be distinguished [54]. 16 Valine spin systems were assigned, thus 3 spin systems (I4, I50 and L52) were first wrongly assigned as valines. In the case of I4 and I50 only parts of the spin systems resembling a valine spin system with equivalent methyl groups were detected, causing the false assignments at this stage. In the case of L52 the absence of relay connectivities from the amide and α proton to the methyl groups in combination with the crowded high field part of the spectra led to the assignment of L52 to a valine spin system.

Leucines

Flavodoxin contains 7 leucine residues (see Table 1). Leucine spin systems, as well as valine spin systems, are characterized by pairs of methyl resonances connected via pairs of cross peaks to one or several protons of the spin system, depending on the type of techniques used. L51 and L85 were completely assigned using the HoHaHa spectra in H_2O . For L62 the C δ H and the C γ H protons were already assigned [7,11]. Using the HoHaHa spectra also the C β H and C α H protons could be assigned. At this stage of the spin system analysis it appeared not possible, using correlated spectroscopy, to connect the aliphatic resonances of L62 to their amide resonance due to serious overlap problems. In NOESY spectra the many interresidual NOE contacts of the methyl groups of L62 also made it impossible to assign the amide resonance unambiguously.

K101 was wrongly assigned at this stage as a leucine spin system due to overlap problems.

Isoleucines

Flavodoxin contains 5 isoleucine residues (see Table 1). Identification of two C γ H Cosy cross peaks with a single δ methyl resonance clearly separates this spin

system from valine and leucine spin systems which have pairwise cross peaks in the same spectral region. Starting with the methyl resonance, I20 and I112 could be completely assigned using the HoHaHa spectra recorded in H₂O.

M97 has been wrongly assigned as an Ile residue at this stage, caused by the high upfield shift of one C β H proton of this particular spin system (due to the ring current of a nearby aromatic residue) thereby resembling a methyl proton. One C γ H proton resonance and two δ -methyl proton resonances of this "Ile" were missing however in the scalar correlated spectra.

AMX side chain spin systems

Flavodoxin contains 34 AMX side chain spin systems including Asn, Asp, Cys, Phe, Ser, Trp and Tyr (see Table 1). These spin systems can be recognized on the basis of their specific C α H-C β H Cosy coupling patterns or by the observation of relay connectivities between the amide resonance and the C β H resonances (with chemical shifts in the region 2.5-3.9 ppm) in HoHaHa spectra. No attempt was made at this time to connect AMX side chains with C δ H ring resonances of aromatic residues via strong intraresidual NOESY cross peaks. However this was done at later stages of the assignment procedure. The side chains of the aromatic residues Y89 and W91 had already been completely assigned [10,11] and we could, using HoHaHa spectra, also assign the corresponding amide resonance positions. (The C(2,6)H protons of Y89 appeared not to be inequivalent as interpreted by Moonen et al. [11]).

The amide and side chain resonance positions of Y6, N18, D30, D38, N40, D42, D43, C54, F70, F71, D73, F86, D106, D122 and N123 were assigned. Spin systems having AMX spin system characteristics are classified as type J [30,31].

The C β H side chain protons of serines are expected to resonate at lower field than the other AMX side chain spin systems, namely in the region 3.5-5 ppm. All serine spin systems (S8, S33, S46, S59, S65, S88 and S93) including the corresponding amide resonance could be determined at this stage.

AMPTX side chain and other long side chain amino acid residues

Flavodoxin contains 38 amino acid residues with long aliphatic side chains (2 Arg, 1 Gln, 16 Glu, 9 Lys, 5 Met and 5 Pro, see Table 1). The assignment of these amino acid residues occurred mainly on the basis of their C β H resonance positions (1.6-2.5 ppm). Spin systems belonging to this group are classified as type U.

Each assigned side chain in this group of spin systems could be connected to its corresponding amide proton. No proline residues were detected. The (partly) assigned spin systems at this stage included E3, E32, E61, E95, Q102, E105, E119, E126, E129 and E132.

K128 could be completely assigned with the help of a HoHaHa spectrum obtained with 100 ms MLEV17 composite pulse cycling, the amide resonance being connected to all side chain protons by relay connectivities.

In summary, the analysis of spin systems using correlated spectroscopy has led to the correct identification of 88 of the 137 spin systems. These included 54 unique spin systems (for which 51 through-bond connectivities with the amide protons were obtained), 24 AMX spin systems and 10 'long side chain' spin systems, both types including their amide resonances. In addition 5 spin systems including their amide resonances were assigned to wrong amino acid residues.

The 44 spin systems, not assigned at this stage of the analysis, are classified as type X.

Sequential assignments of backbone protons

Before starting the search for sequential connectivities in a NOESY spectrum, the already assigned spin systems using correlated spectroscopy, have to be transferred to the corresponding NOESY spectrum. A 500 MHz NOESY spectrum of flavodoxin acquired in 90% H_2O /10% $^2\text{H}_2\text{O}$, pH 8.3, at 33 $^\circ\text{C}$ using a mixing time of 0.2 s, was used in the beginning of our study. Later on, when we had access to a 600 MHz spectrometer, a superior NOESY spectrum acquired at 41 $^\circ\text{C}$ with a mixing time of 0.15 s was used as the main NOESY spectrum. The higher temperature had the advantage to increase T_2 resulting in a sharpening of lines in the NMR spectrum. Increasing the temperature from 33 $^\circ\text{C}$ to 41 $^\circ\text{C}$ influenced several resonance positions which had the beneficial effect of solving some ambiguities in spectral overlap regions. The chemical shift changes were relatively small, there was no problem to transfer the assigned cross peaks from the 33 $^\circ\text{C}$ to the 41 $^\circ\text{C}$ NOESY spectrum.

Fig. 5 shows the amide region of the NOESY spectrum recorded at 41 $^\circ\text{C}$. The water resonance position (in the center of the spectrum) is positioned at the right side. Fig. 5 illustrates the quality of the 2D-NMR spectra and demonstrates the overwhelming number of NOE contacts. Some selected parts of Fig. 5 will be discussed during the second stage of the sequential resonance assignment procedure.

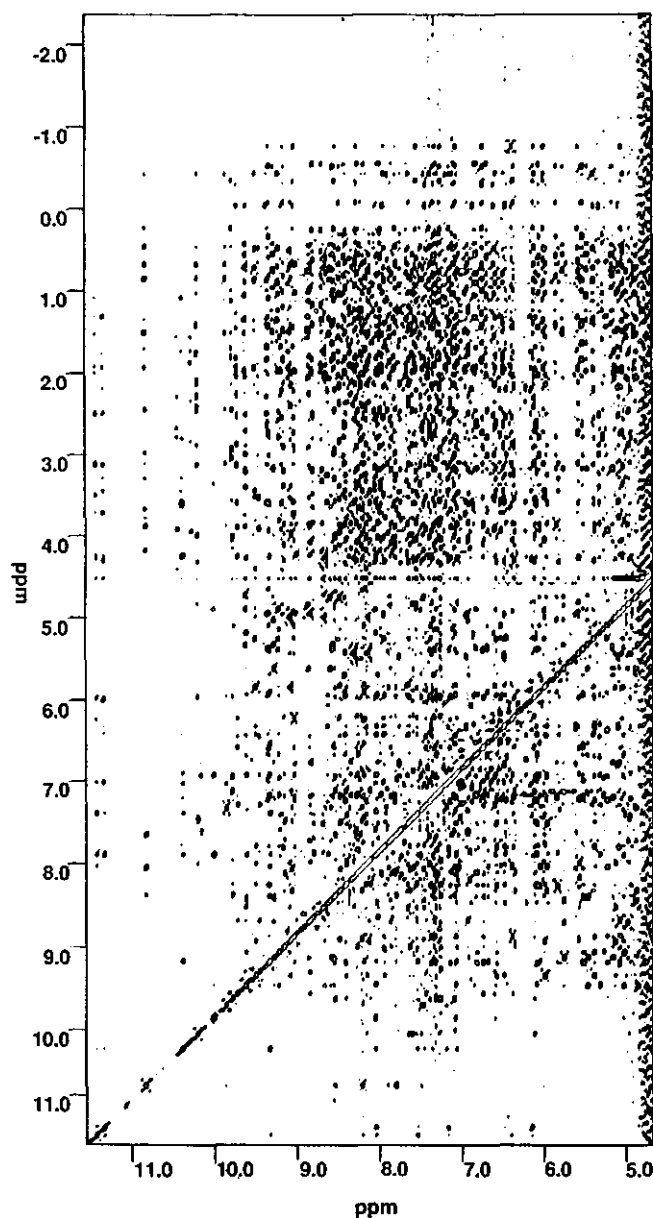


Fig. 5 Part of a 600 MHz NOESY spectrum of reduced *M. elsdenii* flavodoxin in 90% H_2O /10% D_2O , pH 8.3, 41 $^\circ\text{C}$, showing the wealth of NOE contacts observed in the complete left (amide region) part of the spectrum. The carrier coincides with the water resonance position in the centre of the spectrum, which corresponds with the extreme right of the Figure shown. The mixing time was 150 ms, the spectral resolution is 4.1 Hz/point in ω_2 direction and 8.1 Hz/point in ω_1 direction.

The NOESY spectrum shows a superior resolution in the NH-C α H region as compared to, for example, the Cosy spectrum where the multiplet structure is exaggerated by antiphase patterns [16]. In crowded regions it became possible therefore, using the NOESY spectrum, to assign the exact NH-C α H resonance positions of spin systems during the sequential assignment procedure. In other, more empty, spectral regions there is a clear coincidence of connectivities observed in 2D-NMR spectra obtained via correlated spectroscopy and the cross peaks in the NOESY spectrum.

The second stage of the assignment procedure [12-14,46,47] involved the assignment of a NH-C α H cross peak to a specific amino acid residue in the protein sequence. Therefore the NOESY spectrum of flavodoxin was searched for sequential d_{NN}, d α N and d β N connectivities which are summarized in Fig. 6.

The length of a sequentially assigned peptide fragment was determined by several factors. Overlapping amide or C α H resonances of neighbouring amino acid residues made it impossible to find the d_{NN} or d α N connectivities, almost the same effect is exerted by an amide proton which has a low NMR intensity because of rapid exchange with the saturated solvent molecules. For reduced flavodoxin the latter is the case for the amide protons of V41, D48, G80, N118, D122 and E126. In addition, C α H resonances coinciding with the water resonance give rise to a break in the detection of d α N connectivities.

In practice proline residues can also give rise to breaks because one has to search for d $\alpha\delta$, d $N\delta$ and d $\beta\delta$ connectivities which are more difficult to assign unambiguously in combination with the difficulty in obtaining a continuous assignment pathway across a Pro spin system [47]. In the case of flavodoxin no proline residue could be assigned during the spin system analysis.

Another problem is the overlap of amide or C α H resonances of non neighbouring residues. These can also give rise to ambiguities in the sequential assignment procedure [31].

Some of the problems mentioned can however be overcome by standard methods such as varying the temperature or making use of differences in hydrogen exchange rate. In our case we also had the unique opportunity of using the already mentioned special properties of flavodoxin in its three redox states.

Using the sequential NOE contacts we tried to find sequential fragments which could be placed in a unique way in the known protein sequence. The longer the sequential fragments are the greater the chance of having a unique fragment.

We started, while searching for these fragments, with amino acid residues that had been uniquely identified in the fingerprint region, including glycines, valines, threonines, leucines and isoleucines (and A56, L62, Y89 and W91). Starting with the latter residues increased the chance of finding a unique protein fragment.

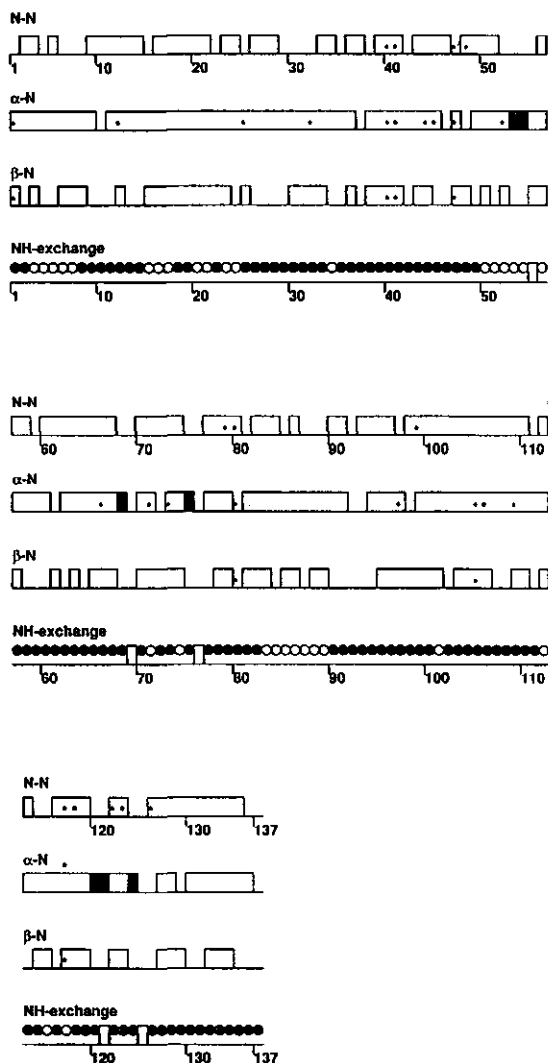


Fig. 6 Sequential NOE contacts observed in a NOESY spectrum with a mixing time of 150 ms of *M. elsdenii* flavodoxin in the reduced state, pH 8.3, 41 °C. Contacts labeled with asterisks indicate that the NOESY spectrum of the oxidized state has been used either to solve ambiguities or to find NOE contacts which were missing in the NOESY spectrum of the reduced state (caused by the high pH of the reduced solution, see text). No differences in NOE contact intensities have been made. The grey boxes represent respectively $d_{N\delta}$, $d_{\alpha N}$, $d_{N\delta}$, $d_{N\delta}$, $d_{\alpha\delta}$, $d_{\alpha N}$ and $d_{\alpha\delta}$ connectivities involving proline residues. Black-filled, grey-filled and open circles indicate amides with fast, intermediate and slow exchange rates, respectively. Amide resonances with slow exchange rates were present during the 19.4 h taking $^2\text{H}_2\text{O}$ exchange NOESY experiment (pH 8.3, 41 °C). Amide resonances corresponding to the black-filled circles had no detectable intensity in the $^2\text{H}_2\text{O}$ exchange NOESY experiment.

resolved $C_{\alpha}H$ proton resonances of a tyrosine ring system thereby specifying this J type spin system as a tyrosine residue (not shown). This tyrosine residue can be connected via a single prominent $d_{\alpha N}$ connectivity to the intraresidual $NH-C_{\alpha}H$ Cosy cross peak of a valine spin system. The $C_{\alpha}H$ resonance of this valine spin system can be connected via a NOE connectivity to the amide resonance of another valine spin system, whereas the amide resonance shows a strong $d_{\alpha N}$ connectivity to another valine spin system whose intraresidual $NH-C_{\alpha}H$ connectivity is very weak in the NOESY spectra (see Fig. 7) but prominently present in the Cosy and HoHaHa spectra.

Thus, an ambiguity in making the sequential resonance assignments arose which had to be solved. In this special case both connectivity trajectories lead to the same spin system sequence V-V-Y-X-S so we cannot exclude a connectivity trajectory by searching for its occurrence in the primary sequence of the protein [16]. The connectivity trajectory V-Y-X-S corresponds to the specific sequence V5-S8 in the protein sequence; the sequence V-V5-S8 does not exist, it should be I-V5-S8. Reinvestigation of both possible sequential neighbours showed that one valine spin system was wrongly assigned and was in fact an isoleucine spin system excluding thereby the other spin system as sequential neighbour. No obvious additional d_{NN} or $d_{\beta N}$ connectivities from both possible neighbours to V5 could be found that could also have helped in excluding one of the two possibilities. The remaining NOE connectivity between the $C_{\alpha}H$ proton of V5 and the other valine residue was found to occur from a nonsequential neighbour of V5, namely V34, which is in agreement with the β -sheet character of this region of the protein.

The amide resonance of I4 has a strong $d_{\alpha N}$ connectivity (see Fig. 7) in addition to a d_{NN} and $d_{\beta N}$ connectivity (not shown) with an J type amino acid residue which was identified as E3. The amide resonance of I4 also exhibits a NOE connectivity with the $C_{\alpha}H$ resonance of S33 in accordance with the secondary structure in this region of the protein.

In Fig. 7 the sequential connectivity trajectory of V49 to G53 is also indicated and shows the same secondary structure characteristics as the region E3-W7.

The same well-resolved spectral region as shown in Fig. 7 is chosen to demonstrate the special properties of flavodoxin. By varying the percentage semiquinone in the sample, a varying proton sphere around the flavin group is affected by the paramagnetism of this moiety. This results, as already mentioned, in a gradually simplified 2D-NMR spectrum as illustrated in Figs. 8 and 9. The number of cross peaks was substantially decreased on going from the fully reduced to the semiquinone state. It appeared possible to influence maximally 35 amino acid residues. This fact yields an extra check whether or not a connectivity trajectory is correctly determined, i.e. the decrease of intensity of a proton resonance of

neighbouring amino acid residues should not show abrupt discontinuities upon reoxidation of reduced flavodoxin.

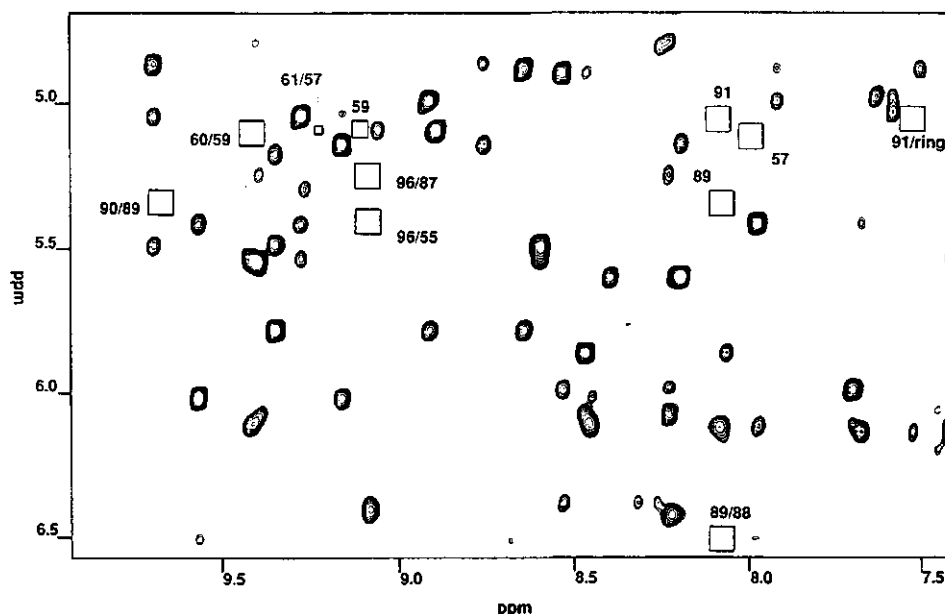


Fig. 8 600 MHz NOESY spectrum of *M. elsdenii* flavodoxin as presented in Fig. 7. In this case the sample contained approximately 80% hydroquinone and 20% semiquinone ($T = 41^\circ\text{C}$). The positions of cross peaks missing due to the paramagnetism of the flavin moiety in the semiquinone state, as compared to the fully reduced state of the protein, are labeled (mixing time 150 ms).

The discussed sequential fragments in Fig. 7 (E3-W7; V49-G53) were only partly affected by the reduction state of the flavin: the W7 and G53 resonances, respectively, broaden or disappear on going from the hydroquinone to the semiquinone state. The proton resonances of the other amino acid residues in these fragments were, as judged by eye, not influenced by the paramagnetism of the flavin, so W7 and G53 must be in the vicinity of the flavin ring. Amino acid residues that were being influenced by the paramagnetism of the flavin as detected by NMR include: W7, S8, G9, T10, N12, T13, G53, C54, P55, A56, M57, G58, S59, E60, E61, L62, E63, G87, S88, Y89, G90, W91, G92, S93, G94, E95, W96, M97, D98, A99, I116, V117, N118 and E119. This yields information about the tertiary structure of flavodoxin.

Proton resonances of the amino acid residues A56, M57, G58, S59, E60, E61, Y89, G90, W91 and G92 disappeared almost immediately in the 2D-NMR spectra upon slight oxidation of a reduced flavodoxin solution (90%

hydroquinone/10%semiquinone). These amino acid residues must therefore be in the immediate neighbourhood of the isoalloxazine ring.

It could be argued that NOESY difference spectra, obtained by subtracting NOESY spectra of flavodoxin in the reduced and in the partly reduced state, as performed by Moonen et al. [11], can be used to acquire a 2D-NMR spectrum of solely those amino acid residues which are located close to the isoalloxazine ring. However, this turned out to be incorrect, as will be discussed in the following.

Moonen et al. [11] presented a NOESY difference spectrum by displaying only the positive contour levels. Such a presentation is wrong because it assumes that the chemical shift differences of all protons in flavodoxin remain unaffected on going from the fully reduced to the partly reduced state. However, if a chemical shift difference occurs between the two spectra and the corresponding proton is not localized in the immediate vicinity of the protein-bound prosthetic group, then this proton resonance will appear in the difference spectra suggesting that it is in the vicinity of the flavin.

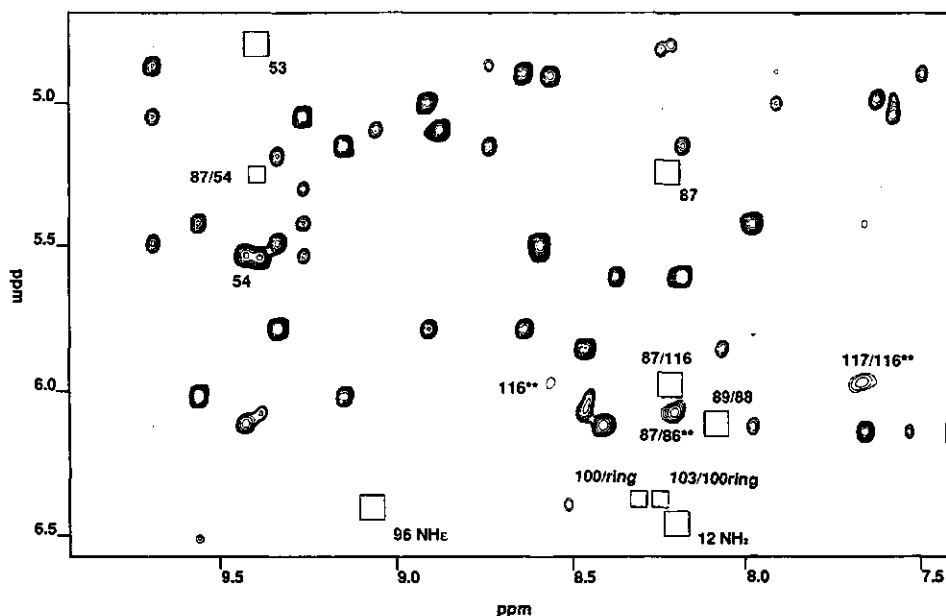


Fig. 9 NOESY spectrum of *M. elsdenii* flavodoxin as presented in Figs. 7 and 8. In this case the NOESY spectrum of *M. elsdenii* flavodoxin was acquired using approximately 100% semiquinone ($T = 41^\circ\text{C}$). Positions of cross peaks which completely disappeared on going from the partly reduced state (as presented in Fig. 8) to the 100% semiquinone state are labeled by boxes; broadened cross peaks are labeled by asterisks (mixing time 150 ms).

It is expected that on reoxidation the pH of a reduced flavodoxin solution will decrease depending on the amount of excess dithionite used for reduction, because oxidation of one mole of dithionite generates four protons [50]. We therefore checked the pH of the NMR sample whenever partially oxidized flavodoxin solutions were prepared from solutions reduced by excess dithionite. ^{31}P NMR was used to determine the pH of solutions of flavodoxin in 0.2 M potassium pyrophosphate, pH 8.3, at 33 °C. On comparison of the ^{31}P resonance position of the buffer containing flavodoxin with a calibration curve, we found a pH decrease of 0.5 unit on going from the fully reduced state to a mixture of approximately 90% hydroquinone and 10% semiquinone state. Further reoxidation did no longer affect the pH, as expected. If a flavodoxin solution is buffered by potassium phosphate, which has a low buffering capacity at pH 8.3, (the buffer used in reference [11]), an even larger pH decrease can be expected. Recalculation of the difference NOESY spectrum presented by Moonen et al. [11] clearly demonstrates that many cross peaks appeared as pairs consisting of one cross peak with a positive intensity and another with a negative intensity, owing to the varying peak shifts of several proton resonances. Proton resonances of amino acid residues in the immediate vicinity of the flavin appeared, as expected, exclusively as positive cross peaks (not shown).

On adjustment of the pH to 8.3 (accuracy is ± 0.1 pH unit using ^{31}P NMR) of a partially reduced sample (80% hydroquinone/20% semiquinone) we obtained the NOESY difference spectrum shown in Fig. 10. Fig. 10 clearly demonstrates small peak shifts for several proton resonances very likely to be caused by a small pH difference between the samples. The two separate NOESY spectra of the two samples are similar concerning the NOE connectivities and cross peak intensities as judged by eye (clearly proton resonances which are not present anymore due to the paramagnetism of the flavin cannot be compared). Consequently conformation differences between the flavodoxin molecules in the two samples cannot explain the peak shifts. Although the difference spectra have proven to be less valuable than previously believed, they still contain a large number of cross peaks, they were useful in showing that several cross peaks belong together as they exhibited the same peak shifts. The side chain resonances of M1 were detected using a HoHaHa difference spectrum of a reduced and partly reduced flavodoxin solution without pH adjustments, showing a considerable downfield shift of the C_αH resonance position in going to the partly reduced flavodoxin. In addition a strong $d_{\alpha\text{N}}$ connectivity to V2 was observed.

Four amino acid residues influenced by the paramagnetism of the flavin moiety were already (partly) assigned, including A56, L62, Y89 and W91 [7,10,11]. The search for sequential connectivities in the region around the flavin therefore started

with the resonance positions of these amino acid residues. The sequential assignments of these amino acid residues will be discussed now in detail.

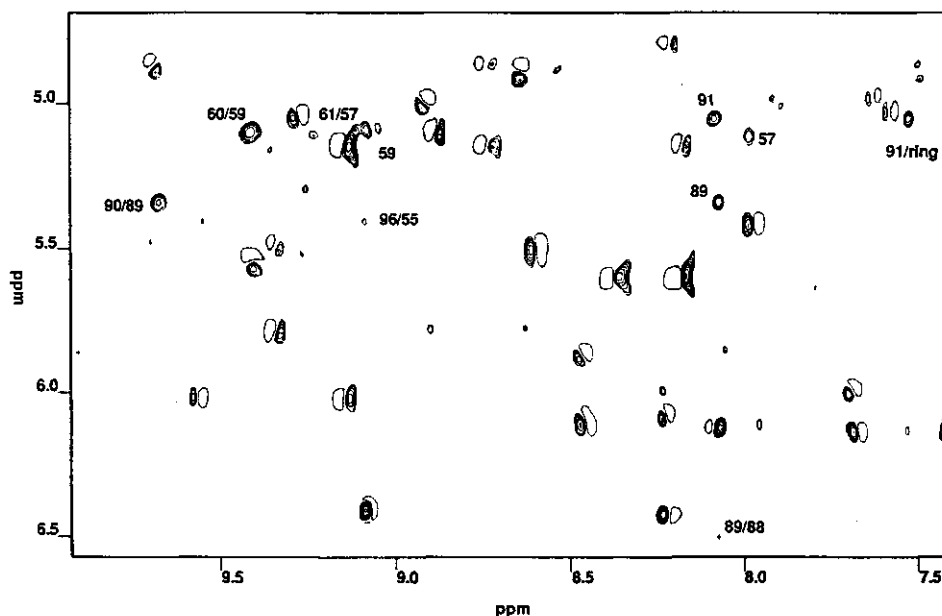


Fig. 10 Difference NOESY spectrum ($T = 41^\circ\text{C}$) obtained by subtracting the NOESY spectrum of the fully reduced (Figs. 5 and 7) from the NOESY spectrum of the partly reduced flavodoxin (as in Fig. 8). Care was taken to equal the pH of both samples (see text). Positive cross peaks are presented as filled areas, whereas negative cross peaks are presented as open areas. Cross peaks which disappeared on going from the fully reduced to the partly reduced (80% hydroquinone/20% semiquinone) state are labeled in this 2D difference NOESY spectrum. Note the varying shifts several NOE connectivities underwent on switching from the fully to the partly reduced state of flavodoxin.

The following connectivity trajectory could be established: G-S-Y89-G-W91 representing the protein sequence from residue number 87 to 91. The resonances of G87 were only slightly influenced by the paramagnetism of the flavin. A $d_{\alpha\text{N}}$ connectivity could be established from the $\text{C}_{\alpha}\text{H}$ resonance position of W91 to a $^2\text{H}_2\text{O}$ exchangeable proton resonance which showed no detectable intraresidual $\text{C}\alpha\text{H}$ or $\text{H}\alpha\text{H}\alpha$ cross peaks in the corresponding spectra. Starting with this proton resonance no further sequential connectivities could be established. The resonance immediately disappears in the presence of a very small amount of semiquinone in the hydroquinone samples. This resonance was therefore assigned to the amide resonance of G92.

The starting point for the assignment of the fragment S93-A99 was the unique S-G pair (the other two possibilities: S8-G9 and G87-S88 had already been assigned at that time), by using sequential connectivities resulting in the sequence S-G-U- X_a -I- X_b -A. The NH- C_α H intraresidual cross peak of S93 and the corresponding interresidual $d_{\alpha N}$ connectivity to G94 were observed in the NOESY spectrum at 33 °C and were not visible in the NOESY spectrum acquired at 41 °C, because of bleaching through water irradiation. X_a showed no NH- C_α H Cosy or HoHaHa cross peak. Its position was detected purely on the basis of d_{NN} , $d_{\alpha N}$ and $d_{\beta N}$ NOE connectivities. The corresponding C_β H proton resonances showed clear NOE connectivities to an aromatic resonance as would be expected for X_a representing W96 in the primary sequence of the protein. M97 had been wrongly assigned to an Ile residue as already mentioned, as became apparent when almost all spin systems were sequentially assigned. X_b could be assigned to an AMX side chain spin system representing D98. The A99 proton resonances were only slightly affected on going from the fully reduced to the semiquinone state of the flavodoxin. Therefore, the protein chain points away from the flavin on going from amino acid residue 93 to 99.

Starting with A56 the sequence P-A56-X-G-S was established, determining firstly the proline spin system via a strong $d_{\alpha N}$ connectivity (and weaker $d_{\beta N}$ connectivities) to the amide resonance of A56 and then using Cosy and HoHaHa spectra to complete the assignments of this spin system. The C_β H resonance positions of S59 almost coincided with the C_α H resonances of G58 causing difficulties in its assignment. X represents M57.

The methyl resonance of A56 was used as an indicator of the reduction state of the protein during the experiments [3]. Its resonance position is clearly resolved in the high field part of the 1D proton NMR spectrum and the resonance is very sensitive to the reduction state. A trace amount of semiquinone is enough to decrease the resonance intensity [3].

During the assignment procedure of the reduced state of flavodoxin it was difficult to use the spectra of the oxidized state for solving ambiguities in assigning amino acid residues in the neighbourhood of the flavin. Proton resonances of these amino acid residues manifested considerable chemical shift differences between the two reduction states, so it was often impossible to find and assign these resonances without knowing all the proton resonances in the reduced state.

The C_β H resonances of P55 have strong NOE connectivities with the C_α H resonance of a spin system classified J and assigned to C54. The amide resonance of C54 almost coincides with the amide resonance of the already assigned G53 in the NOESY spectra at 33 °C and 41 °C accounting for undetectable d_{NN} , $d_{\alpha N}$ and $d_{\beta N}$ connectivities between these spin systems. Starting at the C_α H resonance

position of S59 a strong $d_{\alpha N}$ connectivity leads to the amide resonance of a spin system of type X, being E60, again connected via a $d_{\alpha N}$ connectivity to an U type spin system, being E61. The amide resonance position of L62 was found via a weak d_{NN} connectivity to the amide resonance of E63, E63 being assigned via its NOE connectivities to D64 which was completely assigned at this stage of the assignment procedure. An extra $d_{\beta N}$ connectivity from E61 to the amide resonance of L62 further confirmed the correct assignment of this resonance.

Two sequential fragments influenced by the paramagnetism of the flavin moiety, G53-E63 and G87-A99, have now been discussed. Two fragments remain: W7-T13 and I116-E119. The amide resonance of G9 could be detected via strong d_{NN} and $d_{\beta N}$ connectivities from the already assigned S8 spin system to G9. The $C_{\alpha}H$ resonances of G9 appeared to be degenerated. The connectivity trajectory G9-X-X-G-X-X-X-A could be established using strong d_{NN} connectivities between the individual components of this sequence confirmed by additional $d_{\alpha N}$ and $d_{\beta N}$ connectivities. The proton resonances of the sequence W7-T13 only disappeared completely in the presence of a high amount of semiquinone in the reduced flavodoxin sample. In the presence of approximately 20% semiquinone the resonances are still present in the spectra as a consequence of the relatively large distance between these amino acid residues and the flavin ring.

Starting at the $C_{\alpha}H$ resonance position of A115 a strong $d_{\alpha N}$ connectivity led to the amide resonance of a spin system type X, its corresponding $C_{\alpha}H$ resonance could be connected to the amide resonance of a valine spin system via a strong $d_{\alpha N}$ connectivity. So the sequence A115-I116-V117 was established, from there on a problem existed: no consistent sequential connectivities could be made.

Comparing the spectra of the reduced state with those of the oxidized state (pH 7.0 in the oxidized state compared to pH 8.3 in the reduced state) it was easy to detect A115-V117 as almost no shifts in this region had occurred. The same connectivity trajectory could be established, including a strong $d_{\alpha N}$ connectivity from the $C_{\alpha}H$ resonance position of V117 to an amide resonance belonging to a J type spin system representing N118. Starting with the $C_{\alpha}H$ resonance of N118 the amide resonance of a U type spin system representing E119 was detected via a strong $d_{\alpha N}$ connectivity in the NOESY spectra of the oxidized state. Comparing the spectra of the oxidized state with the spectra of the reduced state the spin system representing E119 was also detected in the spectra of the reduced state. Almost no chemical shift differences between the two spectra concerning these residues were observed. Again comparing both spectra the amide resonance of N118 was detected for the reduced state of flavodoxin. It showed weak relay connectivities to the $C_{\alpha}H$ and one $C_{\beta}H$ proton in a HoHaHa spectrum and even weaker connectivities in the NOESY spectrum where in addition the intraresidual NH- $C_{\alpha}H$

connectivity was absent. In the reduced state of flavodoxin the weak intensity of the amide resonance of N118 was very probably caused by the high pH of the solution in combination with the accessibility of this proton for solvent molecules, resulting in a high exchange rate of this proton with the saturated solvent. The $^2\text{H}_2\text{O}$ exchange characteristics are in agreement with the latter: the amide proton of N118 is accessible to water molecules and cannot be detected in a NOESY spectrum of flavodoxin acquired immediately after dissolving flavodoxin in $^2\text{H}_2\text{O}$ (Fig. 6).

In the case of a high percentage semiquinone in the sample the amide resonance of N118 completely disappeared due to its proximity to the flavin, despite the lower pH in the solution as compared to the reduced solution.

The sequential fragments influenced by the paramagnetism of the flavin moiety have now been discussed. The sequence specific assignments for the rest of the protein were (already) obtained following the same principles as already described.

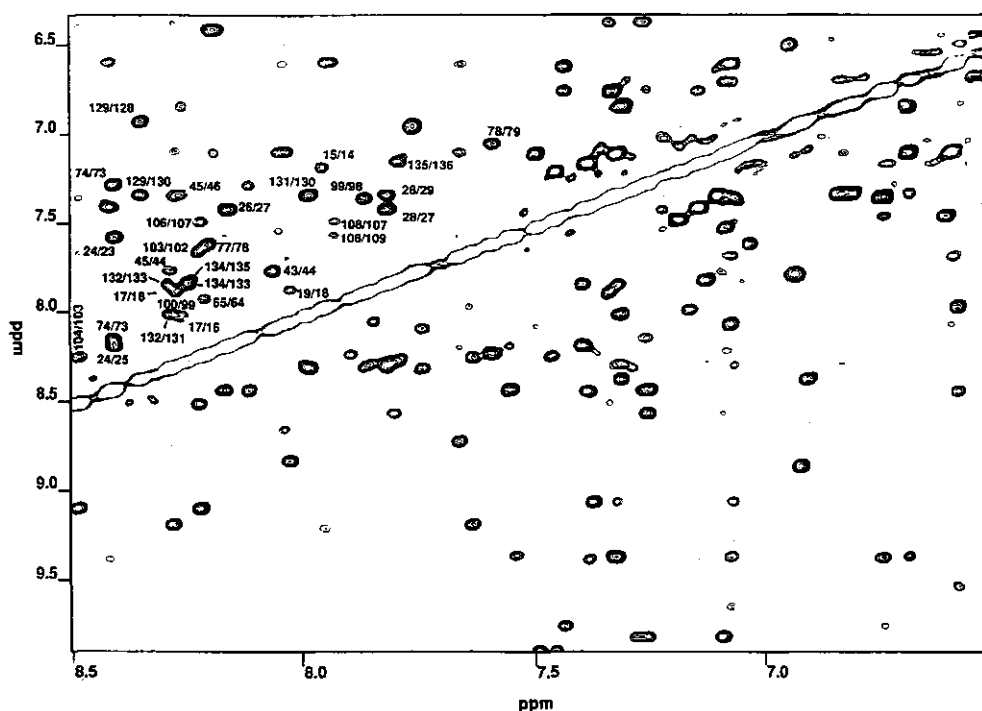


Fig. 11 A Detail of the NOESY spectrum of Fig. 5 showing part of the d_{NN} region of reduced *M. elsdenii* flavodoxin. The lowest contour level in this Figure is higher than in Fig. 5 for reasons of clarity. The cross peaks are labeled $\text{NH}(\omega_2)/\text{NH}(\omega_1)$.

Figs. 11 and 12 show several of the d_{NN} and $d_{\alpha N}$ connectivities used and Fig. 6 summarizes all d_{NN} , $d_{\alpha N}$ and $d_{\beta N}$ connectivities. No overlapping sequential connectivities could be made for K25-A26 and G53-C54 due to their coinciding amide resonances. In oxidized flavodoxin these amide resonances could be separated and thereby sequential connectivities became apparent consisting of $d_{\alpha N}$ and $d_{\beta N}$ connectivities thus confirming the assignments. The connectivities to the amide proton of G92 have been tackled before; starting at the proton resonances of P69 and P76 no sequential connectivities could be made to their sequential neighbours which had already been uniquely determined by their subsequent neighbours.

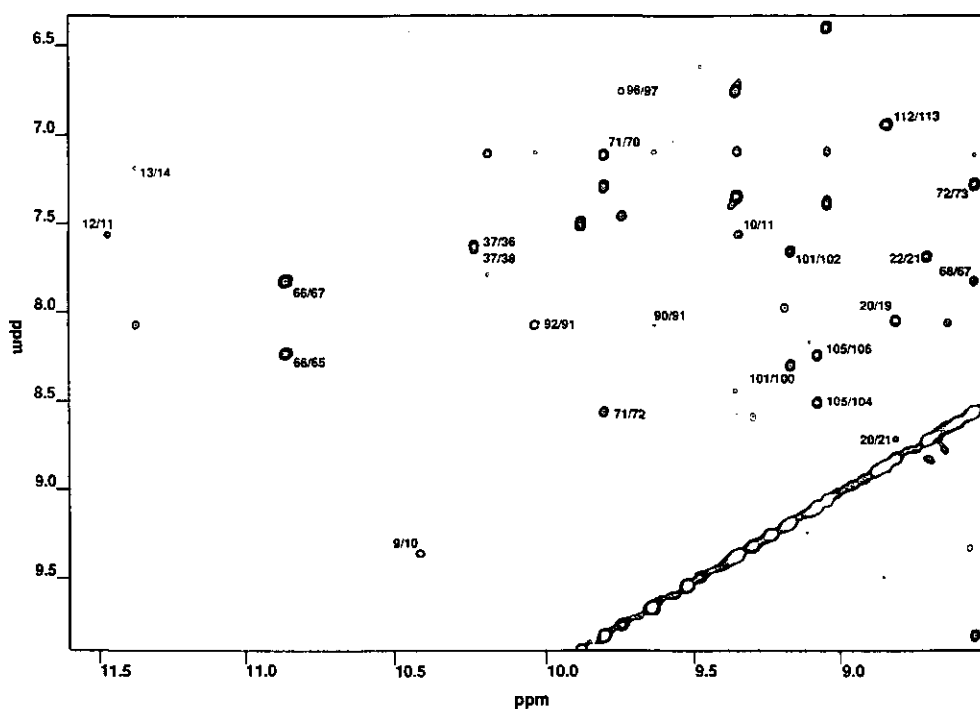


Fig. 11 B Another part of the d_{NN} region of *M. elsdenii* flavodoxin, the lowest contourlevel is identical to the one used in Fig. 11a.

Only sequential NOE contacts are presented in Fig. 11a and 11b, the contacts shown represent the strongest d_{NN} connectivities observed for this protein.

The assignment of P121, P125, E126 and C127 was established after the three-dimensional structure of *M. elsdenii* flavodoxin had been generated.

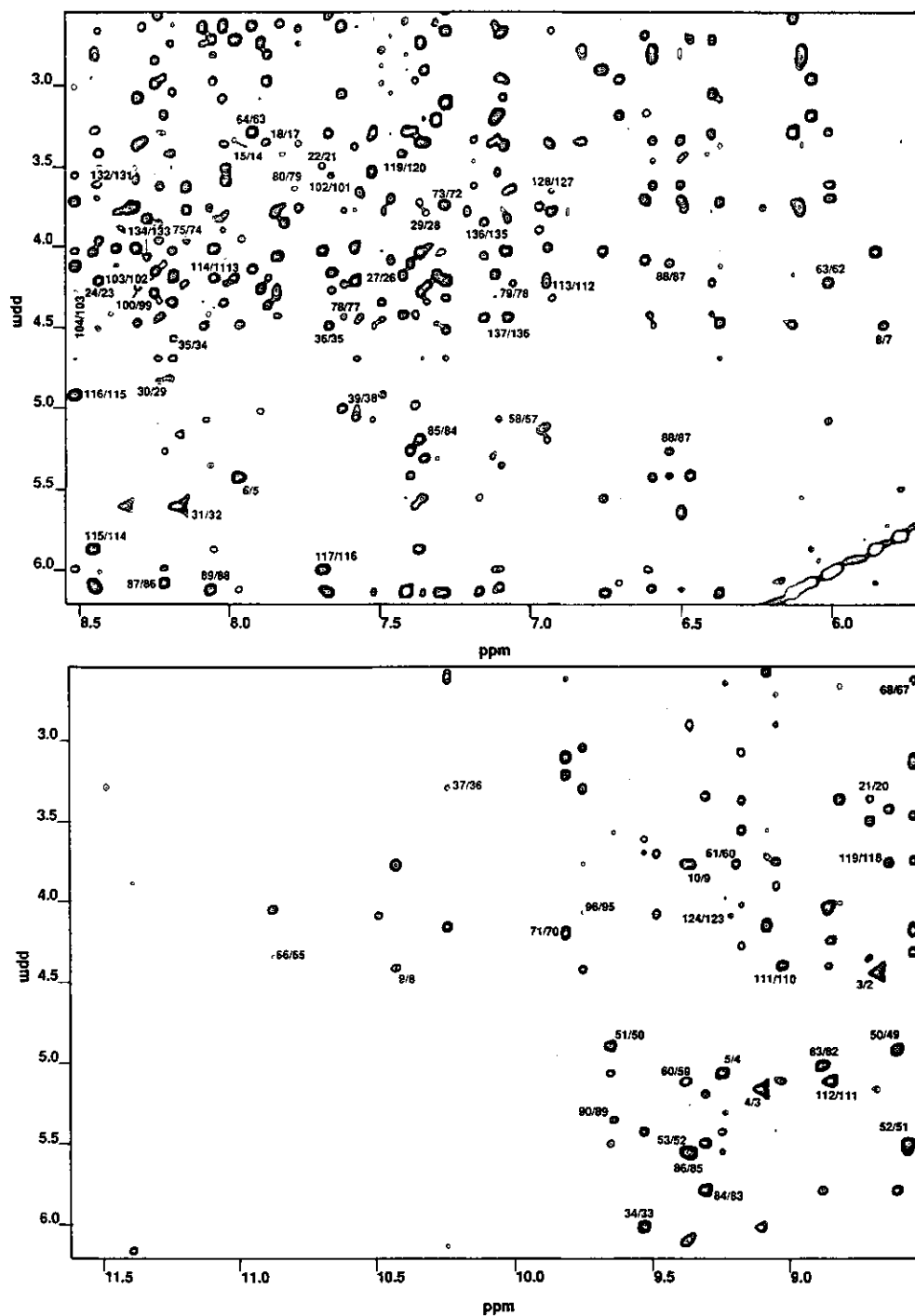


Fig. 12 The fingerprint region of the phase sensitive NOESY spectrum of Fig. 5. The lowest contour level in these Figures is higher than the one used in Fig. 5. In this Figure the major $d_{\alpha N}$ connectivities are labeled $NH(\omega_2)/C_{\alpha}H(\omega_1)$.

Additional assignments

Once the sequence specific assignment had been unambiguously made for a backbone proton which had not yet been (completely) assigned to its side chain protons during the previous spin system analysis, we started searching for additional assignments for protons in that side chain. Consequently, these additional assignments were largely made during the sequential assignment procedure and not at the end of this procedure.

In the case of a J-type residue representing an amino acid residue with an aromatic side chain, we searched in the $^2\text{H}_2\text{O}$ spectra for NOE connectivities between the C_βH protons and aromatic resonances representing the C_δH protons. All C_δH resonances for the ten aromatic residues could be detected in that way. Using a combination of Cosy, HoHaHa and NOESY spectra the remaining aromatic resonances including the four indole amide protons could be assigned (see Table 1). In case of ambiguities, resulting from overlapping resonances starting at the aromatic resonances, we made use of the structural information we had gathered at that time about the protein: i.e. the strong structural homology between *Clostridium MP* flavodoxin and *M. elsdenii* flavodoxin.

For *Clostridium MP* flavodoxin the three dimensional structure is known in the oxidized and semiquinone state [55-57]. Some NOE connectivities starting at the amide resonance could be ascribed to a specific proton using the three dimensional structure of *Clostridium MP* flavodoxin.

In the majority of X-type residues, assignments for the C_βH protons could be made using intra- and interresidual $\text{NH-C}_\beta\text{H}$ NOE connectivities which could be connected to their corresponding C_αH resonance via Cosy or HoHaHa connectivities. Sometimes the connectivity trajectory could then be completed using correlated spectroscopy starting at the assigned C_αH resonance position, as in the case of T13.

In addition, the hydroxyl proton of T13 could be detected as also of S8, S88, T104 and T107. The presence of these solvent-exchangeable resonances, including the SH resonance of C54 and NH_2 resonances of N12 and N118, complicated the analysis of the NOESY spectra. For example, the $\text{OH-C}_\alpha\text{H}$ connectivity of T13 in the HoHaHa spectrum was, for a long time thought to originate from a backbone $\text{NH-C}_\alpha\text{H}$ connectivity.

The observation of several hydroxyl resonances of flavodoxin at pH 8.3 (41 $^\circ\text{C}$) is remarkable. The exchange rate of these protons is too high to be observed by NMR [47,51] if they are solvent accessible. In the proteins studied so far by NMR such exchangeable hydroxyl resonances have not been observed [54]. This implies that these exchangeable protons in flavodoxin are shielded from water and/or are

tightly bounded by hydrogen bonds. These results provide interesting structural information. Amide exchange experiments against $^2\text{H}_2\text{O}$ (Fig. 6) showed that 32 amide protons exchanged very slowly with the solvent during one 2D-NMR experiment. Even after several weeks at room temperature the majority of these 32 exchangeable protons were still present (unpublished results). These 32 amide protons must also be tightly bonded or shielded from the solvent molecules. These exchange characteristics must be related to the spatial protein structure as will be discussed in a forthcoming paper.

Table 1: ^1H chemical shifts (ppm) of *M. elsdenii* flavodoxin in the reduced state, pH 8.3, 41 $^\circ\text{C}$.

Residue	NH	C $^\alpha$ H	C $^\beta$ H	Others
Met1		3.74	2.21,2.04	C γ H 2.51
Val2	8.33	4.40	2.03	C γ H 0.81, 0.71
Glu3	8.69	5.15	2.17,1.85	
Ile4	9.11	5.05	2.08	C γ H3 1.02, C γ H2 1.61, C $^\delta$ H 0.64
Val5	9.25	5.42	1.48	C γ H 0.60, -0.31
Tyr6	7.95	6.11	2.73,2.78	C $^\delta$ H 6.60, C $^\epsilon$ H 6.49
Trp7	8.43	4.46	3.24	NH 9.89, C $^\delta$ 1H 7.50, C $^\zeta$ 2H 7.47, C η 2H 7.19, C $^\zeta$ 3H 7.06, C $^\epsilon$ 3H 7.38
Ser8	5.82	4.36	3.58,3.43	OH 8.06
Gly9	10.43	3.79,3.79		
Thr10	9.35	4.66	4.59	C γ H 1.21
Gly11	7.55	3.64,4.43		
Asn12	11.49	4.63	2.64,3.25	NH $_1$ 6.42, NH $_2$ 8.21
Thr13	11.40	3.86	4.43	C γ H 1.49, OH 6.17
Glu14	7.17	3.30		
Ala15	7.97	4.16	1.65	
Met16	8.01	3.79	2.58	C γ H 3.03*, CH3 2.15**
Ala17	8.27	3.30	0.91	
Asn18	7.86	4.32	2.93,2.76	
Glu19	8.04	3.97	2.13,2.09	
Ile20	8.81	3.33	1.29	C γ H3 0.38, C γ H2 1.53, 0.74 C $^\delta$ H -0.43
Glu21	8.71	3.47	2.09,2.02	
Ala22	7.67	3.98	1.46	
Ala23	7.57	4.18	1.61	
Val24	8.42	3.38	2.12	C γ H 1.08, 0.77

Lys25	8.17	4.31	1.83	C ^δ H 1.73*, 1.65* C ^ε H 2.96*
Ala26	8.17	4.14	1.50	
Ala27	7.40	4.39	1.47	
Gly28	7.83	3.75,4.25		
Ala29	7.33	4.81	1.36	
Asp30	8.22	4.75	2.69,2.53	
Val31	8.17	5.60	2.06	C ^γ H 0.95, 0.88
Glu32	8.15	4.66	1.99,2.10	C ^γ H 2.25
Ser33	8.43	6.01	3.66,3.58	
Val34	9.53	4.53	2.06	C ^γ H 0.97, 0.84
Arg35	8.17	4.45		
Phe36	7.65	3.25	2.52,2.43	C ^δ H 6.12, C ^ε H 7.40, C ^ζ H 7.15
Glu 37	10.24	4.13	2.20,2.27	C ^γ H 2.40
Asp38	7.62	4.98	3.00,2.59	
Thr39	7.56	5.03	3.97	C ^γ H 1.15
Asn40	9.24	5.29	2.91,2.91	
Val41	8.49	3.31	1.62	C ^γ H 0.55, 0.44
Asp42	7.98	4.31	2.57,2.60	
Asp43	8.07	4.45	2.70,2.59	
Val44	7.75	3.72	2.25	C ^γ H 1.35, 1.05
Ala45	8.30	3.98	1.48	
Ser46	7.28	4.45	4.12,4.03	
Lys47	7.59	4.54	1.98**,1.90**	
Asp48	7.85+	4.55	2.74,2.83	
Val49	7.48	4.89	2.06	C ^γ H 0.98, 0.85
Ile50	8.61	4.87	1.64	C ^γ H3 0.85, C ^γ H2 1.45
Leu51	9.65	5.49	2.10,1.18	C ^γ H 1.47, C ^δ H 0.68, 0.56
Leu52	8.57	5.54	1.95,1.52	C ^γ H 1.75, C ^δ H 1.11, 0.99
Gly53	9.37	4.79,1.80		
Cys54	9.36	5.60	2.86,2.86	SH 5.05
Pro55	---	5.40	2.32,2.07*	C ^γ H 1.85, C ^δ H 4.39, 4.95
Ala56	6.46	2.67	0.09	
Met57	7.96	5.11	1.15,1.60**	C ^γ H 2.29*
Gly58	6.95	3.72,3.86		
Ser59	9.05	5.10	3.71,3.90	
Glu60	9.39	3.73	2.41*,2.10*	C ^γ H 2.62*
Glu61	9.19	4.54	2.07,1.79	C ^γ H 2.34, 2.34
Leu62	7.56	4.19	1.39,0.73	C ^γ H 1.06, C ^δ H -0.22, -0.64
Glu63	6.00	3.24	1.47,0.74*	C ^γ H -0.30, 1.22*

Asp64	7.91	4.10	2.58,2.68	
Ser65	8.22	4.31	3.93,3.82	
Val66	10.88	4.02	1.65	C γ H 0.97, 0.80
Val67	7.82	2.57	2.05	C γ H 0.59, 0.37
Glu68	8.55	4.15		
Pro69	---	4.27	2.25*	C γ H 1.82, C δ H 3.43, 3.11
Phe70	7.10	4.13	3.15,3.15	C δ H 7.30, C ϵ H 7.34, C ζ H 7.11
Phe71	9.81	4.19	3.06,3.06	C δ H 7.27
Thr72	8.55	3.71	4.28	C γ H 1.23
Asp73	7.26	4.48	2.62,2.46	
Leu74	8.42	3.93	1.92	C γ H 1.66, C δ H 1.28, 1.05
Ala75	8.13	3.73	1.13	
Pro76	---	4.46	2.41,1.80	C γ H 1.98, C δ H 3.59
Lys77	8.21	4.39	1.89	
Leu78	7.60	4.19	2.10	C δ H 0.89**, 0.68**
Lys79	7.05	3.60	1.99,1.82*	C δ H 1.59, C ϵ H 3.07
Gly80	7.77	4.21,3.89		
Lys81	8.15	4.68	1.97,1.85*	C γ H 1.43*, C δ H 1.66*
Lys82	7.88	5.00	2.18,2.18	C γ H 1.57*, 1.42*, C δ H 1.67*, C ϵ H 3.03
Val83	8.88	5.79	1.59	C γ H 0.88, 0.88
Gly84	9.31	5.18,3.32		
Leu85	7.35	5.54	1.52,0.46	C γ H 0.94, C δ H 0.05, -0.39
Phe86	9.29	6.08	3.14,2.91	C δ 1H 6.69, C ϵ 1H 6.84, C ζ H 6.82, C ϵ 2H 7.32, C δ 2H 7.09
Gly87	8.20	5.25,4.06		
Ser88	6.53	6.11	3.72,3.72	OH 6.49
Tyr89	8.05	5.34	3.13,2.64	C δ H 7.08, C ϵ H 6.60
Gly90	9.64	4.41,3.54		
Trp91	8.06	5.05	3.49,3.27	NH 10.20, C δ 1H 7.11, C ζ 2H 7.78, C η 2H 6.95, C ζ 3H 7.10, C ϵ 3H 7.52
Gly92	10.05	---		
Ser93	9.65	4.63	4.01,3.88	
Gly94	9.48	4.04,3.67		
Glu95	8.86	4.03	2.17,2.03	C γ H 2.70*, 2.38
Trp96	9.75	4.39	3.26,3.00	NH 9.05, C δ 1H 6.40, C ζ 2H 7.38 C ϵ 3H 7.45, C ζ 3H 6.61, C η 2H 7.10
Met97	6.74	3.99	1.39,-0.17	C γ H 2.10**, 2.01, CH3 1.56**
Asp98	7.35	4.24	2.71,2.68	

Ala99	7.88	4.22	1.57	
Trp100	8.29	4.44	3.33,3.03	NH 6.12, C ^δ 1H 6.36, C ^ε 2H 6.73 C ^η 2H 7.33 ^{**} , C ^ε 3H 7.08 ^{**}
Lys101	9.18	3.52	1.96,1.59	C ^γ H 1.31, 1.13, C ^δ H 1.59 C ^ε H 2.85
Gln102	7.65	4.12	2.25	
Arg103	8.23	4.25		
Thr104	8.50	3.99	4.08	OH 3.68, CH 0.96
Glu105	9.09	4.12	2.27,2.12 ^{**}	C ^γ H 2.53
Asp106	8.23	4.56	2.95,2.80	
Thr107	7.48	4.31	4.42	OH 5.39, C ^γ H 1.52
Gly108	7.94	4.44,3.91		
Ala109	7.55	4.65	1.30	
Thr110	8.86	4.37	3.99	C ^γ H 1.13
Val111	9.03	5.09	2.09	C ^γ H 0.79, 0.79
Ile112	8.85	4.21	1.91	C ^γ H3 0.68 ^{**} , C ^γ H2 0.87, 1.09 C ^δ H 0.57
Gly113	6.93	4.15,3.97		
Thr114	8.03	5.86	3.99	C ^γ H 0.95
Ala115	8.44	4.90	1.14	
Ile116	8.50	5.99	2.26	C ^γ H3 0.79, C ^γ H2 1.15, 1.67 C ^δ H 0.61
Val117	7.67	4.38	2.16	C ^γ H 0.89, 0.72
Asn118	8.33	3.70	2.47,2.30	NH1 6.91, NH2 6.23
Glu119	8.65	3.39	2.34,2.15	C ^γ H 2.02 [*]
Met120	7.41	4.44	2.06	C ^γ H 2.71 [*] , 2.57 [*]
Pro121		4.46		C ^δ H 3.48, 4.36 [*]
Asp122	8.05	4.55	2.68,2.41	
Asn123	10.49	4.06	2.91,2.81	
Ala124	9.22	4.55	1.68	
Pro125		4.29	2.42,2.01	C ^γ H 2.18, C ^δ H 4.19 ^{**} ,4.14 ^{**}
Glu126	10.32	4.08	1.85,1.99	C ^γ H 2.96, 2.47
Cys127	7.07	3.62	3.33,2.61	SH 1.90
Lys128	6.92	3.74	1.89,1.79	C ^γ H 1.38, 1.30, C ^δ H 1.61 C ^ε H 2.92
Glu129	8.36	3.98	2.02,2.02	C ^γ H 2.38, 2.24
Leu130	7.32	4.20		C ^γ H 1.34, C ^δ H 0.71, 0.67
Gly131	7.99	3.55,3.47		
Glu132	8.30	3.70	2.07,1.93	C ^γ H 2.43

Ala133	7.83	4.02	1.45	
Ala134	8.26	3.79	1.35	
Ala135	7.80	3.81	1.49	
Lys136	7.14	4.41	1.74, 1.66	C γ H 1.50, C δ H 1.97, C ϵ H 2.97
Ala137	7.06	3.99	1.43	

- One asterisk indicates resonances belonging to a specific amino acid residue (manifested via Cosy or HoHaHa cross peaks) with a tentatively determined position in the amino acid residue side chain.
- Two asterisks indicate resonance positions of the amino acid residue side chain determined exclusively via NOESY spectra.
- + The amide resonance position of D48 has been determined using the 2D-NMR spectra of the partially-reduced state and of the fully oxidized state of the protein.

NMR studies have shown that the flavin binding region of *M. elsdenii* flavodoxin and *Clostridium MP* flavodoxin are identical [8,52]. Therefore we could make use of the three dimensional structure of *Clostridium MP* flavodoxin to check, using the 2D-NMR results, if the assignments of the flavin in *M. elsdenii* flavodoxin were in accordance with the three-dimensional structure of *Clostridium MP* flavodoxin [55-57].

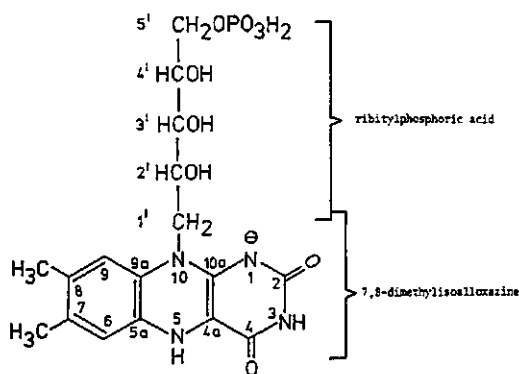


Fig. 13 Structure of two-electron reduced riboflavin 5'-phosphate (FMNH⁻).

The resonances of C(6)H, C(9)H, CH₃(7 α) and CH₃(8 α) were tentatively assigned by Moonen and Müller [10] and these resonance positions were confirmed by this 2D-NMR study (Table 2). Resonances due to the isoalloxazine

moiety are clearly very sensitive to traces of semiquinone in the sample, so care had to be taken to get a perfectly reduced sample. The C(6)H resonance gave rise to a strong NOE connectivity to the unambiguously determined N(5)H resonance [10] as would be expected regarding the isoalloxazine structure (Fig. 13). The C(6)H resonance showed low intensity NOE connectivities to the CH₃(7 α) and CH₃(8 α) protons and a strong NOE connectivity to the amide resonance of G58. The latter connectivity is in accordance with the three-dimensional structure of the flavin domain of *Clostridium MP* flavodoxin in the semiquinone state (the structure of this state will be very similar to the structure of the reduced state taking into account the fast electron exchange between the one- and two-electron reduced flavodoxin; the structure of the reduced state of *Clostridium MP* flavodoxin has never been published). A clear NOE connectivity between C(6)H and the C α H resonance of M57 was also present in the NOESY spectrum of *M. elsdenii* flavodoxin as expected from the *Clostridium MP* flavodoxin crystal structure.

The C(9)H resonance exhibited NOE connectivities to the C(1')H and C(2')OH resonances (Table 2) as is consistent with the structure of *Clostridium MP* flavodoxin. Several resonances of the ribityl side chain of the FMN molecule were unambiguously assigned using modified flavins selectively ¹³C enriched in the ribityl side chain. We used 1'-¹³C-, 2'-¹³C- and 5'-¹³C- enriched FMN molecules with an isotopic enrichment of >90 atom % and the natural prosthetic group of *M. elsdenii* flavodoxin was then replaced by these molecules using standard procedures [37]. By irradiating at the proton frequency in addition to applying a systematic increase of this frequency in steps of 10 Hz and detecting the changes in the fine structure of the ¹³C resonances, we were able to detect the resonance positions of the protons attached to the C(1')-, C(2')- and C(5')-atoms of the side chain of FMN. Combining the Cosy, HoHaHa and NOESY spectra we were able to detect the remaining proton resonances of the ribityl side chain with the exception of the C(3')OH resonance. The observed NOE connectivities of the ribityl side chain with the apoprotein were consistent with the three dimensional structure of *Clostridium MP* flavodoxin. The C₃'OH proton is therefore expected to be on the surface of the protein and a rapid exchange with solvent molecules would thus prevent detection of this proton. This interpretation is in agreement with experiments performed by Vervoort et al. [58] replacing FMN in *M. elsdenii* flavodoxin by riboflavin 3',5'-bisphosphate. In this study it was shown that the apoprotein binds the riboflavin 3',5'-bisphosphate molecule very tightly (K_D= 10 nM) with almost no disturbance of the specific interactions between the flavin molecule and the apoprotein. This implicates that the 3'-phosphate must be located at or very close to the surface of the protein with almost no interactions with

neighbouring amino acid residues [58]. This has indeed been demonstrated by its accessibility to Mn^{2+} [58].

Table 2: 1H and some ^{13}C resonances (in ppm) of FMN bound to apoflavodoxin from *M. elsdenii*.

1H resonances			^{13}C resonances	
N_3H	9.39		C_1'	46.50
N_5H	5.61		C_2'	66.09
C_6H	6.48		C_5'	65.15
$CH_3(7\alpha)$	2.04			
$CH_3(8\alpha)$	2.10			
C_9H	6.09			
$C_1'H$	2.82	3.36		
$C_2'H$	3.74			
$C_2'OH$	6.86			
$C_3'H$	3.01			
$C_3'OH$	n.o.			
$C_4'H^{**}$	3.99			
$C_4'OH^{**}$	5.96			
$C_5'H$	3.38	3.38		

- Several flavin 1H resonances were previously assigned by Moonen and Müller [10]. The $C_1'H$, $C_2'H$ and $C_5'H$ resonances were assigned using selectively ^{13}C enriched FMN molecules.

Resonances labeled with asterisks were assigned on the basis of NOESY spectra using the tertiary structure information we had gathered that time.

- Flavin ^{13}C resonances were determined using selectively ^{13}C enriched flavins.

The $N(3)H$ and the already-mentioned $N(5)H$ resonance positions were unambiguously determined by Moonen and Müller [10]. The resonance position of $N(3)H$ coincides with the amide resonance of E60 at 41 $^\circ C$. In addition, $N(3)H$ is expected to be in the neighbourhood of the side chain of E60 according to the crystallographic data on *Clostridium MP* flavodoxin. Because of these coinciding resonance positions it was not possible, starting at the $N(3)H$ resonance position, to detect NOE connectivities to side chain protons of E60. The $N(5)H$ resonance showed a clear NOE connectivity to the $H(7)$ proton resonance of W91 as expected. Despite the predicted structural homology between the flavin domains of *M. elsdenii* and *Clostridium MP* flavodoxins, the NOESY spectra of *M. elsdenii*

flavodoxin in the reduced state did not show strong NOE connectivities between N(5)H-60NH and N(3)H-92NH as would have been expected based on the crystallographic data of the semiquinone state of *Clostridium MP* flavodoxin. We will deal with this property in the near future when presenting the three-dimensional structure of *M. elsdenii* flavodoxin in the reduced state generated by using the NOE's between the different protons of flavodoxin as the primary source of information.

A clear difference is observed in the assignment of Y89 in our study compared to that of Moonen et al. [11]. These authors observed two nonequivalent C(2,6)H protons at 7.06 and 7.42 ppm and two overlapping C(3,5)H proton resonances at 6.59 ppm for Y89 at 33 °C, whereas we observed that Y89 has two equivalent C(2,6)H at 7.08 ppm and C(3,5)H protons at 6.60 ppm at 41 °C. Using a NOESY spectrum acquired at 37 °C where the aromatic resonances of Y89 and W96 are separated it can be deduced that the proton resonance at 7.42 ppm of reduced flavodoxin at 33 °C corresponds to the C(4)H proton of W96. This proton has a Cosy and NOESY cross peak with the C(5)H proton resonance of W96, the latter resonance coinciding with the C(3,5)H resonances of Y89 thus explaining the wrong assignment. The C(4)H and C(5)H protons of W96 are in the neighbourhood of the C_βH protons of A56 according to the three-dimensional structure of *Clostridium MP* flavodoxin and in *M. elsdenii* flavodoxin this will also be the case because clear NOE connectivities can be observed from the C_βH resonance of A56 to the C(4)H and C(5)H resonances of W96. No NOE connectivities between the C_βH protons of A56 and the ring protons of Y89 were observed, in agreement with the crystal structure of *Clostridium MP* flavodoxin. The intensities of the NOE connectivities between the C_αH and both C_βH resonances of Y89 are approximately equal as is compatible with the crystal structure of *Clostridium MP* flavodoxin. We did not observe large differences between both NOE connectivities as indicated in a previous study [11]. The suggestion by Moonen et al. [11] that a different relative position of A56 to the side chain of Y89 as compared to the position in crystals of *Clostridium MP* flavodoxin is largely based on the wrong assignment of a ring proton of Y89. This was caused by a lack of knowledge of the majority of the proton resonances of *M. elsdenii* flavodoxin, thereby demonstrating the importance of making an almost complete assignment of the proton resonances of a protein before making a detailed analysis of the protein structure. In the case of the oxidized state of *M. elsdenii* flavodoxin the assignments of the ring protons of Y89 by Moonen et al. [11] were consistent with our study demonstrating equivalence of the C(3,5)H and C(2,6)H protons of Y89, so no indication was found for a difference in "flipping rate" around the C_β-C_γ axis of the ring of Y89 between the two redox states of the protein.

We have demonstrated that the sequence specific resonance assignment procedure can be successfully applied to a relatively large protein consisting of 137 amino acid residues. All backbone proton resonances of *M. elsdenii* flavodoxin in the reduced state and all proton resonances of the prosthetic group FMN have been assigned with the exception of M1 NH. Full side chain assignments could be made for 119 residues and for the other amino acid residues partial side chain assignments have been made. Relay connectivities observed in the HoHaHa spectra were extensively useful to obtain correlations between protons separated by more than three chemical bonds within one particular spin system thereby characterizing these spin systems. Once the secondary structure of this protein became apparent, this was used to confirm assignments and solve numerous ambiguities in assigning the wealth of resonances. All fingerprint-region Cosy cross peaks could be assigned; in the case of the HoHaHa spectra 4 $^2\text{H}_2\text{O}$ exchangeable protons not showing Cosy connectivities but showing relay connectivities in the amide region could not be assigned. We expect that these protons belong to the side chains of either Asp, Glu, Arg or Lys; these resonances could not be connected with any of the assigned spin systems. During the assignment procedure we had the great benefit of the special properties of this flavin-containing protein, especially the paramagnetic one-electron reduced semiquinone state of the protein giving rise to considerably simplified 2D-NMR spectra.

The assignments presented in this paper provide the starting point for a variety of important studies on this flavin containing protein. The proton resonance assignments of *M. elsdenii* flavodoxin in the reduced state were the basis for assigning the proton resonances of *M. elsdenii* flavodoxin in the oxidized state as will be presented in a forthcoming paper. The wealth of observed NOE connectivities contain detailed information about the secondary structure of the protein as well as providing the input for the tertiary structure determination of flavodoxin. In the near future it will be possible to compare the "solution-structure" of *M. elsdenii* with the crystal structure of *Clostridium MP* flavodoxin. In addition, it will be possible to study the structure and dynamics of the flavin domain of *M. elsdenii* flavodoxin on going from the oxidized to the reduced state. NMR has proven to be a valuable tool for studying a protein of this relatively large size.

Acknowledgement

We are indebted to Dr. R. Hall for carefully reading the manuscript and M.C. Snoek for isolating the protein. We would like to thank Bruker Karlsruhe (F.R.G) for giving us measuring time for a few experiments. We especially thank the HF-SON NMR- Facility Nijmegen (The Netherlands) where the large majority of the

experiments was performed under ideal conditions. This study was carried out under the auspices of the Netherlands Foundation for Chemical Research (SON) with financial aid from the Netherlands Organization for the Advancement of Pure Research (NWO).

References

1. Mayhew, S.G. & Ludwig, M.L. (1975) *Enzymes 3rd Ed.* 12, 57-118.
2. Moonen, C.T.W. & Müller, F. (1982) *Biochemistry* 21, 408-414.
3. Moonen, C.T.W. & Müller, F. (1984) *Eur. J. Biochem.* 140, 303-309.
4. Tanaka, M., Haniu, M., Yasunobu, K., Mayhew, S. & Massey, V. (1973) *J. Biol. Chem.* 248, 4354-4366.
5. Tanaka, M., Haniu, M., Yasunobu, K., Mayhew, S. & Massey, V. (1974) *J. Biol. Chem.* 249, 4397.
6. Anderson, R.F. (1983) *Biochem. Biophys. Acta* 723, 78-82.
7. Schagen van, C.G. & Müller, F. (1981) *FEBS Lett.* 136, 75-79.
8. Vervoort, J., Müller, F., Mayhew, S.G., van den Berg, W.A.M., Moonen, C.T.W. & Bacher, A. (1986) *Biochemistry* 25, 6789-6799.
9. Franken, H.D., Rüterjans, H. & Müller, F. (1984) *Eur. J. Biochem.* 138, 481-489.
10. Moonen, C.T.W. & Müller, F. (1984) *Eur. J. Biochem.* 140, 311-318.
11. Moonen, C.T.W., Scheek, R.M., Boelens, R. & Müller, F. (1984) *Eur. J. Biochem.* 141, 323-330.
12. Wüthrich, K., Wider, G., Wagner, G. & Braun, W. (1982) *J. Mol. Biol.* 155, 311-319.
13. Wagner, G. & Wüthrich, K. (1982) *J. Mol. Biol.* 155, 347-366.
14. Wider, G., Lee, K.H. & Wüthrich, K. (1982) *J. Mol. Biol.* 155, 367-388.
15. Neuhaus, D., Wagner, G., Vasák, M., Kägi, J.H.R. & Wüthrich, K. (1985) *Eur. J. Biochem.* 151, 257-273.
16. Zuiderweg, E.R.P., Mollison, K.W. & Carter, G.W. (1988) *Biochemistry* 27, 3568-3580.
17. Kline, A.D. & Wüthrich, K. (1986) *J. Mol. Biol.* 192, 869-890.
18. Wagner, G., Neuhaus, D., Wörgötter, E., Vasák, M., Kägi, J.H.R. & Wüthrich, K. (1986) *Eur. J. Biochem.* 157, 275-289.
19. Zuiderweg, E.R.P., Kaptein, R. & Wüthrich, K. (1983) *Eur. J. Biochem.* 137, 279-292.
20. Otting, G., Steinmetz, W.E., Bougis, P.E., Rochat, H. & Wüthrich, K. (1987) *Eur. J. Biochem.* 168, 609-620.
21. Bach, A.C., Selsted, M.E. & Pardi, A. (1987) *Biochemistry* 26, 4389-4397.

22. Klevit, R.E., Drobny, G.P. & Waygood, E.B. (1986) *Biochemistry* 25, 7760-7769.
23. Sukumaran, D.K., Clore, G.M., Preuss, A., Zarbock, J. & Gronenborn, A.M. (1987) *Biochemistry* 26, 333-338.
24. Van de Ven, F.J.M. & Hilbers, C.W. (1986) *J. Mol. Biol.* 192, 389-417.
25. Van de Ven, F.J.M. & Hilbers, C.W. (1986) *J. Mol. Biol.* 192, 419-441.
26. Basus, V.J., Billeter, M., Love, R.A., Stroud, R.M. & Kuntz, I.D. (1988) *Biochemistry* 27, 2763-2771.
27. Montelione, G.T., Wüthrich, K. & Scheraga, H.A. (1988) *Biochemistry* 28, 195-203.
28. Robertson, A.D., Westler, W.M. & Markley J.L. (1988) *Biochemistry* 27, 2519-2529.
29. Chazin, W.J., Hugli, T.E. & Wright, P.E. (1988) *Biochemistry* 27, 9139-9148.
30. Driscoll, P.C., Hill, H.A.O. & Redfield, C. (1987) *Eur. J. Biochem.* 170, 279-292.
31. Redfield, C. & Dobson C. (1988) *Biochemistry* 27, 122-136.
32. Feng, Y., Roder, H. & Englander, S.W. (1988) *Biochemistry* 28, 195-203.
33. Wand, A., Di Stefano, D.L., Feng, Y., Roder, H. & Englander, S.W. (1988) *Biochemistry* 28, 186-194.
34. LeMaster, D.M. & Richards, F.M. (1988) *Biochemistry* 27, 142-150.
35. Moore, J.M., Chazin, W.J., Powls, R. & Wright, P.E. (1988) *Biochemistry* 27, 7806-7816.
36. Mayhew, S.G. & Massey, V. (1969) *J. Biol. Chem.* 244, 794-802.
37. Wassink, J.H. & Mayhew, S.G. (1975) *Anal. Biochem.* 68, 609-616.
38. Le Van, Q., Keller, P.J., Bown, D.H., Floss, H.G. & Bacher, A.J. (1985) *J. Bacteriol.* 162, 1280-1284.
39. Marion, D. & Wüthrich, K. (1983) *Biochem. Biophys. Res. Commun.* 113, 967-974.
40. Rance, M., Sörenson, O.W., Bodenhausen, G., Wagner, G., Ernst, R.R. & Wüthrich, K. (1983) *Biochem. Biophys. Res. Commun.* 117, 479-485.
41. Macura, S. & Ernst, R.R. (1980) *Molec. Phys.* 41, 95-117.
42. Mareci, T.H. & Freeman, R. (1983) *J. Magn. Reson.* 51, 531-535.
43. Wagner, G. & Zuiderweg, E.R.P. (1983) *Biochem. Biophys. Res Commun.* 113, 854-860.
44. Bax, A. & Davis, D.G. (1985) *J. Magn. Res.* 65, 355-360.
45. Pearson, G.A. (1977) *J. Magn. Reson.* 27, 265-272.
46. Billeter, M., Braun, W. & Wüthrich, K. (1982) *J. Molec. Biol.* 155, 321-346.
47. Wüthrich, K. (1986) *NMR of Proteins and Nucleic Acids*, Wiley, New York.
48. Müller, F. (1983) *Curr. Top. Chem.* 108, 71-107.
49. Wüthrich, K., Billeter, M. & Braun, W. (1984) *J. Mol. Biol.* 180, 715-740.

50. Mayhew, S.G. (1978) *Eur. J. Biochem.* 85, 535-547.
51. Wüthrich, K. & Wagner, G. (1979) *J. Mol. Biol.* 130, 1-18.
52. Moonen, C.T.W., Hore, P.J., Müller, F., Kaptein, R. & Mayhew, S.G. (1982) *FEBS Lett.* 149, 141-146.
53. Bundi, A. & Wüthrich, K. (1979) *Biopolymers* 18, 285-297.
54. Groß, K.H. & Kalbitzer, H.R. (1988) *J. Magn. Reson.* 76, 87-99.
55. Burnett, R.M., Darling, G.D., Kendall, D.S., LeQuesne, M.E., Mayhew, S.G., Smith, W.W. & Ludwig, M.L. (1974) *J. Biol. Chem.* 249, 4383-4392.
56. Smith, W.W., Burnett, R.M., Darling, G.D. & Ludwig, M.L. (1977) *J. Mol. Biol.* 117, 195-225.
57. Ludwig, M.L., Burnett, R.M., Darling, G.D., Jordan, S.R., Kendall, D.S. & Smith, W.W. (1976) in *Flavins and Flavoproteins* (Singer, T.P., ed.) pp. 393-404, Elsevier, Amsterdam.
58. Vervoort, J., van Berkel, W.J.H., Mayhew, S.G., Müller, F., Bacher, A., Nielsen, P. & LeGall, J. (1986) *Eur. J. Biochem.* 161, 749-756.

Chapter 3

Secondary and tertiary structure characteristics of *Megasphaera elsdenii* flavodoxin in the reduced state as determined by two-dimensional ^1H NMR

Carlo P.M. van Mierlo, Franz Müller¹ and Jacques Vervoort

Department of Biochemistry, Agricultural University, Wageningen, The Netherlands.

1. Present address: Sandoz, Agro Ltd., Department of Toxicology, Basle Switzerland.

Summary

The secondary structure of two-electron reduced *M. elsdenii* flavodoxin has been determined by visual, qualitative inspection of the sequential connectivities involving C α H, C β H and NH protons observed in NOESY spectra. Results from an amide proton exchange experiment were used to confirm the secondary structure assignment and to demonstrate the compactness and stability of the protein. After the secondary structure elements were established, the global fold of the protein and the flavin binding site have been determined using nonsequential interresidual NOE connectivities as primary source of information. The secondary structure and the global fold of *Megasphaera elsdenii* and *Clostridium MP* flavodoxin appeared to be very similar, differences are observed however. *M. elsdenii* flavodoxin consists of a central parallel β -sheet including 5 strands surrounded on both sides by a pair of α -helices.

Introduction

The flavodoxin from *Megasphaera elsdenii* is a non-crystallizable protein which contains riboflavin-5'-monophosphate as a prosthetic group and functions as an electron carrier in biological reactions. The FMN molecule is noncovalently but very tightly bound to the apoprotein [1]. The protein-bound flavin can occur in the oxidized, one-electron reduced (semiquinone) and the two-electron reduced (hydroquinone) state. Under iron-deficient conditions the protein is produced in large quantities by *M. elsdenii* as a replacement for ferredoxin [1].

In vivo the flavodoxin shuttles between the semiquinone and the hydroquinone states owing to a high activation barrier occurring between the oxidized and the semiquinone state and the absence of an activation barrier for the semiquinone/hydroquinone transition [2]. It is this activation barrier that predestinates the protein for one-electron transfer reactions [2]. The flavodoxin from *M. elsdenii* represents a small protein which has a molecular mass of 15 kDa and consists of 137 amino acid residues the sequence of which is known [3,4]. Upon binding of FMN to the apoprotein the redox potential of the prosthetic group is strongly altered as compared to free FMN [1].

M. elsdenii flavodoxin, due to its easy availability in large quantities, its high solubility and high stability, has been subjected to various NMR techniques. The electronic and conformational structure of the protein-bound flavin has been probed, it has been shown that the flavin binding regions of *M. elsdenii* and *Clostridium MP* flavodoxin are very similar [5-7]. In addition a full assignment of the carbon and nitrogen atoms of the protein-bound prosthetic group has been done

using ^{13}C - and ^{15}N - enriched flavins and a few amino acid residues in the immediate neighbourhood of the isoalloxazine moiety of the flavodoxin have been assigned using one-dimensional ^1H NMR techniques [5,8]. In an initial two-dimensional NMR study it appeared possible to assign (partly) four amino acid residues in the immediate neighbourhood of the flavin and to confirm the one-dimensional assignments [9]. It was also shown that W-91 in *M. elsdenii* flavodoxin is in close proximity to the flavin as is the case for W-90 in *Clostridium MP* flavodoxin. A56 and Y89 showed identical relative positions and dihedral angles in both the oxidized and the reduced state of *M. elsdenii* flavodoxin whereas W91 appeared to be slightly displaced on going from the oxidized to the reduced state [9].

Very recently assignments for the 137 amino acid residues of *M. elsdenii* flavodoxin in the reduced state have been made [10] using the sequential resonance assignment procedure [11-14]. In this paper we will deal with the structure characteristics of reduced *M. elsdenii* flavodoxin.

The aim of our 2D-NMR studies on *M. elsdenii* flavodoxin is to get a better insight in the parameters which determine the biological function of this flavoprotein. As NMR reveals detailed information concerning both the structure of a protein in solution in addition to dynamical parameters it will be possible to obtain a solution structure of the protein. This in turn will allow to compare the structure of *M. elsdenii* flavodoxin with that of the closely related protein from *Clostridium MP* for which a X-ray structure is known [15].

Materials and methods

Flavodoxin from *M. elsdenii* was isolated and purified as previously described [16]. Reduction and reoxidation experiments were conducted by the addition of the desired amount of a dithionite solution to the anaerobic solution of flavodoxin in the oxidized state. Anaerobic solutions were achieved by carefully flushing the flavodoxin solution in the NMR tube with argon for about 20 min. The desired degree of reoxidation was obtained by injecting small volumes of air into the NMR tube containing the flavohydroquinone solution followed by gentle mixing.

All samples contained 6 to 10 mM flavodoxin in solutions consisting of a mixture of 20% potassium pyrophosphate and 80% potassium phosphate with a total concentration ranging from 75 to 200 mM, pH 8.3.

All measurements were done in a mixture of 10% $^2\text{H}_2\text{O}$ /90% H_2O . The amide exchange experiment was performed by dissolving the freeze-dried protein in $^2\text{H}_2\text{O}$, pH 8.3, followed by reduction of the solution just prior to acquiring the 2D-NMR spectrum. The NMR sample tube with the protein solution was kept on ice

before the sample was inserted into the magnet. The exchange experiment was performed at 41 °C, the corresponding NOESY experiment took 19.4 h.

The phase sensitive NOESY spectra were acquired on a Bruker AM600 operating at 600 MHz using Time Proportional Phase Increments [17,18], no zero quantum filter was applied. Mixing times of 50, 100 and 150 ms were used; the NOESY spectrum corresponding to a mixing time of 150 ms has been the basic spectrum for making sequential resonance assignments [10]. The carrier frequency was positioned at the middle of the spectrum coinciding with the water resonance. Specific irradiation of the water resonance took place at all times, except during the data acquisition period. Irradiation of the water protons for 2.5 s with 20-38 dB attenuation from 0.2 Watt was sufficient to saturate the protons, the power of irradiation depended on the solvent used (H₂O or ²H₂O).

Experiments were done at 33 °C and 41 °C. The number of scans varied between 16 and 112 whereas the number of increments varied between 377 and 519, the total acquisition time varied between 7.9 and 35.1 h. After data acquisition all further data handling was performed on a Microvax II computer and a Vaxstation 2000 using software obtained from Dr. R. Boelens, modified to our specific requirements. The data were digitally filtered using sine bell or squared sine bell window functions shifted by various amounts as described in the Fig. legends. After zero filling, spectra with a digital resolution of 4.1 Hz per point in ω_2 direction and 8.1 Hz per point in ω_1 direction were obtained. After the double Fourier transformation of the data of the 2D-NMR experiment baseline corrections with a fourth order polynomial were performed according to Pearson in both frequency directions [19]. The 2D-NMR spectra are presented as contour plots with levels increasing by a factor of 1.3.

Results and discussion

Secondary structure

Based on the previous assignments of the individual amino acid residues of *M. elsdenii* flavodoxin [10] the secondary and tertiary structure of the protein is presented in this paper. In addition the data have also been extensively exploited to confirm assignments and to search for "missing" amino acid residues. By visual qualitative inspection of the patterns of sequential connectivities in the NOESY spectra it is possible to identify regular secondary structure elements within the primary sequence of a protein [14,20].

Fig. 1 shows part of the 150 ms NOESY spectrum of reduced *M. elsdenii* flavodoxin and is an illustration of the sequential connectivities observed in two

regions of the protein showing β -sheet characteristics. Strong $d_{\alpha N}$ connectivities are observed between neighbouring amino acid residues, one starting at the $C_{\alpha}H$ resonance of V2 and ending at the amide resonance of W7, and the other starting at the $C_{\alpha}H$ resonance of V49 and extending to the amide resonance of G53, both are typical for β -sheet structures. In Fig. 1 one can in addition observe long-range interstrand NOE connectivities, e.g. 2/31, 4/33, 5/52, 7/54, 32/3, 34/5, 50/3, 51/4 and 53/6 (representation: $NH(i)/C_{\alpha}H(j)$, i and j are non-sequential neighbours).

Fig. 2 is an illustration of the observation of strong d_{NN} connectivities in the region D64 to K79 in a 50 ms NOESY spectrum of reduced *M. elsdenii* flavodoxin. This region of the primary sequence of the protein will therefore have helical characteristics.

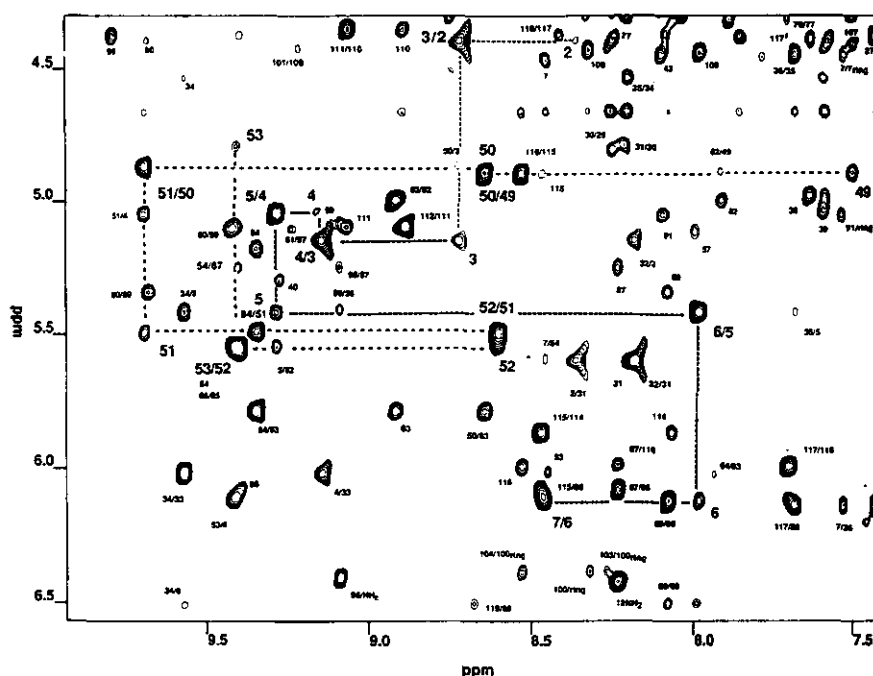


Fig. 1 Part of a 600 MHz NOESY spectrum of reduced *M. elsdenii* flavodoxin in 90% H_2O /10% D_2O , pH 8.3, 41 $^{\circ}C$, illustrating two sequential pathways. The mixing time was 150 ms, the spectral resolution is 4.1 Hz/point in ω_2 direction and 8.1 Hz/point in ω_1 direction. The cross peaks are labeled ω_2/ω_1 . The spectrum was processed with a sine-bell shifted by 15 $^{\circ}$ in t_2 and a squared sine-bell shifted by 22.5 $^{\circ}$ in t_1 dimension.

Use has been made of the individual amide exchange rates against $^2\text{H}_2\text{O}$ of reduced *M. elsdenii* flavodoxin to acquire supporting evidence for the regular secondary structures as determined by interresidual NOE [14,21].

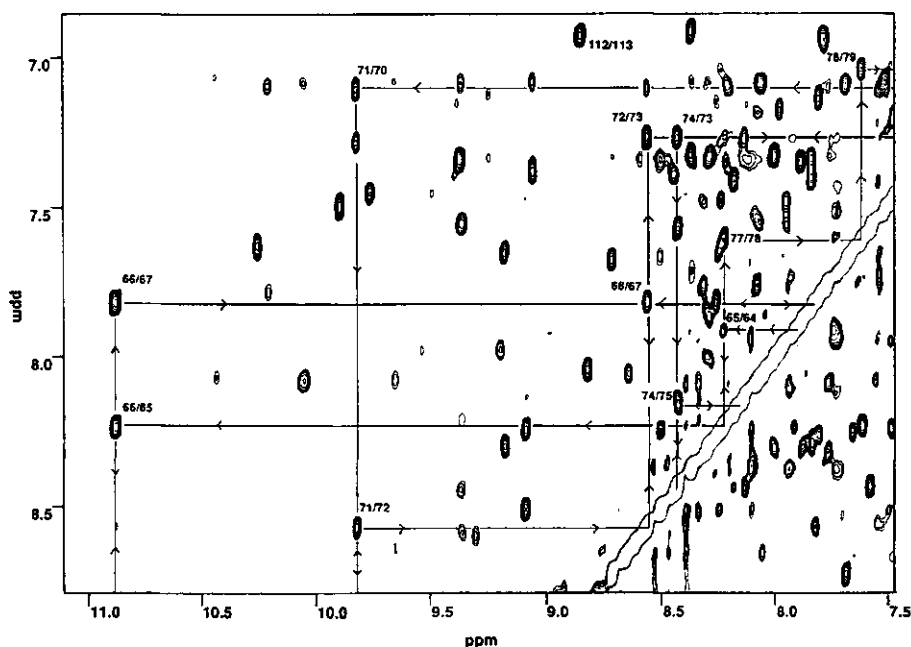


Fig. 2 Part of a 600 MHz NOESY spectrum of reduced *M. elsdenii* flavodoxin in 90% H_2O /10% $^2\text{H}_2\text{O}$, pH 8.3, 41 $^\circ\text{C}$, illustrating the sequential pathway for an helical region in the protein (the d_{NN} connectivities going from K77 to K79 correspond to a turn-like region of the protein (see text)). The mixing time was 50 ms. Cross peaks are labeled $\text{NH}(\omega_2)/\text{NH}(\omega_1)$. The amide resonances of E68 and T72 are coinciding as is the case for the amide resonances of K77 and S65. The processing and the spectral resolution of the spectrum are as in Fig. 1. Interruptions of the d_{NN} connectivities are occurring at the positions of P69 and P76. The cross peak 112/113 has been labeled to illustrate the connectivity corresponding to an irregularity in β -strand no. 5 (see text).

Fig. 3 is an illustration of the amide exchange experiment and depicts the same region of the 150 ms NOESY spectrum of reduced *M. elsdenii* flavodoxin as in Fig. 1, except that the flavodoxin has been dissolved in $^2\text{H}_2\text{O}$, pH 8.3, and recorded at 41 $^\circ\text{C}$. This NOESY spectrum was acquired in 19.4 h. Amide protons which are still present in the NOESY spectrum of Fig. 3 are therefore very persistent (strongly hydrogen bonded). For instance on going from E3 to W7 and from I50 to G53 the latter is consistent with the NOE contact analysis indicating that this region is being part of an β -sheet. Both strands are expected to be not peripheral as the amide

protons of both strands are persistent. The amide protons of V2 and V49 are not persistent so they are expected to be at the beginning of the β -sheet structure (less stabilized by hydrogen bonding). Fig. 4 depicts the fingerprint region of the protein during the amide exchange experiment and is another illustration of the many persistent amide protons of flavodoxin. Fig. 4 presents the same region of the NOESY spectrum of flavodoxin as in Fig. 5 which has been acquired with water as solvent.

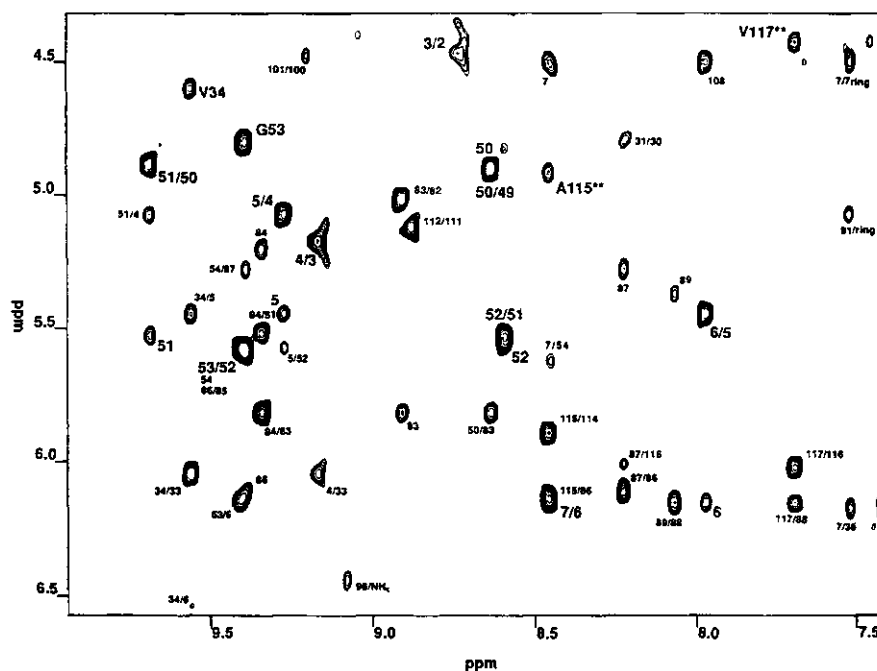


Fig 3. The same spectral region of a 600 MHz NOESY spectrum as presented in Fig. 1 but the reduced *M. elsdenii* flavodoxin has been dissolved in 100% $^2\text{H}_2\text{O}$. Cross peaks which persisted during the amide exchange experiment have been labeled by numbers using the same presentation as in Fig. 1. Note the increased intensities of the cross peaks corresponding to the $\text{NH}/\text{C}_\alpha\text{H}$ connectivities of respectively V34 and G53 and A115 and V117 as compared to Fig. 1. The latter two cross peaks have been labeled by asterisks (see text). Cross peaks belonging to amides having intermediate exchange rates with the solvent (e.g. the $\text{NH(i)}/\text{C}_\alpha\text{H(i)}$ connectivity of D43) can be observed at lower contour levels.

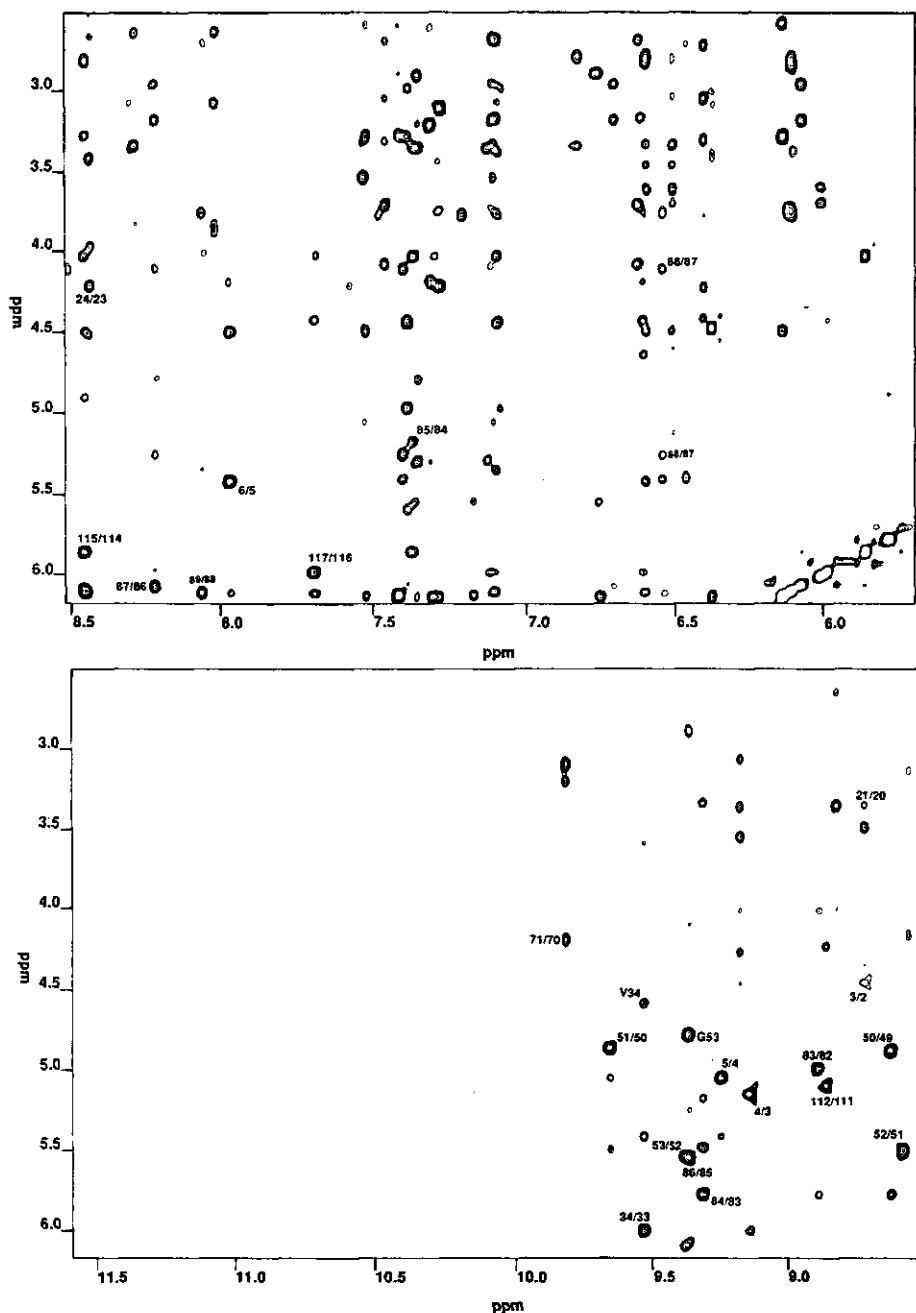


Fig. 4(A+B) The fingerprint region of a 600 MHz NOESY spectrum (150 ms mixing time) of reduced *M. elsdenii* flavodoxin in 100% $^2\text{H}_2\text{O}$, pH 8.3 (uncorrected for isotope effects), 41 $^\circ\text{C}$. Cross peaks which persisted during the amide exchange experiment have been labeled by numbers using the same presentation as in Fig. 5. Several cross peaks which are not observed in this figure, like 68/67, 124/123, 119/118 etc., as a result of intermediate exchange with the solvent (see Fig. 6) can be observed at deeper contour levels.

Two-dimensional amide exchange experiments are an elegant way of simplifying spectra and thereby facilitating the sequential resonance assignment in 2D-NMR spectra of relatively large proteins by revealing the typical connectivity patterns of resonances being part of regular secondary structures.

Fig. 3 and Fig. 4 also illustrate some other beneficial aspects of acquiring spectra of partly deuterated protein samples. The irradiation power needed to saturate the residual water resonance in an amide exchange experiment is much lower than that needed when spectra are acquired with water as solvent. In addition there is a slight shift of the water resonance leading to a better signal to noise ratio of cross peaks which are close to or lie on the water resonance position. However the corresponding amide proton has to be persistent to benefit from this advantage. This is demonstrated for the NH- $C_{\alpha}H$ cross peaks belonging to V34 and G53 in Figs. 1 and 3, these cross peaks can be clearly observed in Fig. 3. Another advantage is the substantial increase in peak heights of several cross peaks, which do not coincide with the water resonance in the NOESY spectrum of flavodoxin. Two examples are illustrated in Fig. 3, the NH(i)/ $C_{\alpha}H$ (i) cross peaks of A115 and V117 are stronger in Fig. 3 than in Fig. 1. The amide protons of A115 and V117 are persistent, the $C_{\alpha}H$ resonances do not coincide with the water resonance. In contrast to the NH(i)/ $C_{\alpha}H$ (i) cross peaks of A115 and V117 the strong cross peaks of NH(A115)/ $C_{\alpha}H$ (T114) and NH(V117)/ $C_{\alpha}H$ (I116) are virtually identical in both spectra (see Fig. 1). The observed intensity increase of the NH(i)/ $C_{\alpha}H$ (i) cross peaks can be the result of several effects. Firstly, as the power of irradiation has been strongly reduced in the amide exchange experiment using 2H_2O , a negative NOE of a relatively rapid exchange of neighbouring protons of the $C_{\alpha}H$ of A115 and V117 with saturated solvent molecules will be diminished which can cause the increase of a NH(i)/ $C_{\alpha}H$ (i) cross peak [22]. This is a likely explanation for the intensity increase of the NH(i)/ $C_{\alpha}H$ (i) cross peak of V117 as the amide proton of V117 is persistent and the nearest exchangeable neighbour of the C_{α} proton of V117, being part of a peripheral β -strand (see following), is the amide proton of N118 which is rapidly exchanging on the NMR timescale (pH 8.3, 41 °C). The amide resonance position of N118 has been determined using the one-electron reduced and the oxidized protein in solutions buffered at lower pH values (slower exchange). This lowering of pH would not have been possible for the two-electron reduced protein [10], in which the amide resonance is almost absent. The intensity of the NH(i)/ $C_{\alpha}H$ (i) cross peak of V117 is higher in the oxidized than in the reduced state, as would be expected (unpublished observation). Secondly, the intensity increase of a NOESY cross peak can be caused by the replacement of exchangeable protons of the protein located in the immediate neighbourhood of a specific proton, e.g. the $C_{\alpha}H$ of A115, by deuterons and/or by exchange of

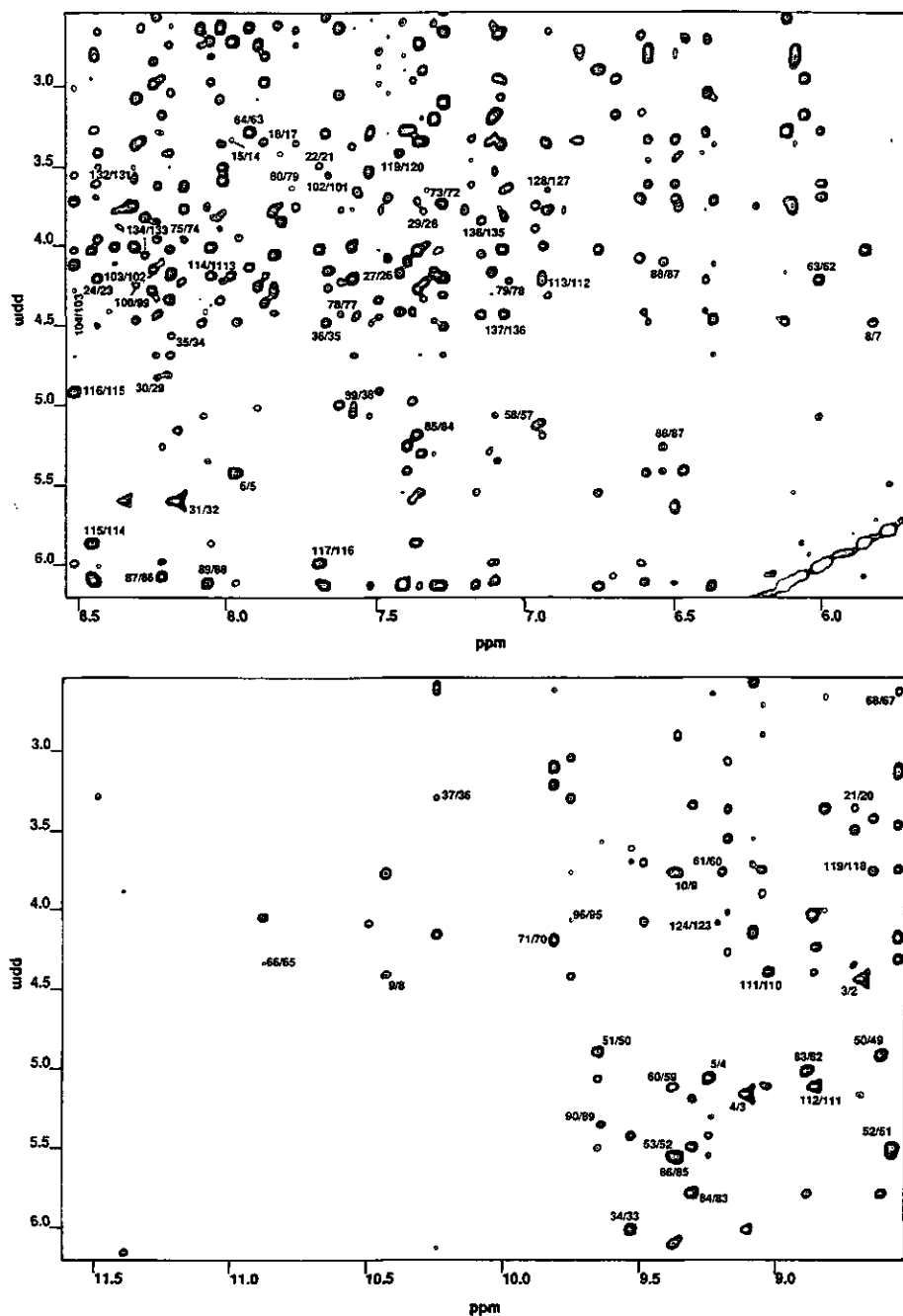


Fig. 5(A+B) The same spectral region of the 600 MHz NOESY spectrum (150 ms mixing time) as presented in Fig. 4 but acquired with reduced *M. elsdenii* flavodoxin in 90% H_2O /10% D_2O , pH 8.3, 41 $^{\circ}\text{C}$. In this figure the major $d_{\alpha\text{N}}$ connectivities are labeled $\text{NH}(\omega_2)/\text{C}_{\alpha}\text{H}(\omega_1)$, the figure was taken from reference [10]. Processing and resolution as in Fig. 1.

structurally bound water against $^2\text{H}_2\text{O}$ molecules. A115 is positioned in a peripheral β -sheet strand of the protein accessible to solvent molecules (see below), although no rapidly exchanging proton(s) on the NMR timescale have been detected in the immediate neighbourhood ($< 4 \text{ \AA}$) of the C_αH . For a specific proton this exchange can result in a less efficient relaxation mechanism through dipolar interaction (dominant relaxation mechanism in proteins) with the structurally bound solvent molecules and/or the neighbouring exchangeable protons, resulting in an increase of T_2 of this proton and thereby in an intensity increase of the corresponding cross peaks in the 2D spectrum. In addition spin-diffusion routes via the bound $^2\text{H}_2\text{O}$ molecules and/or via the neighbouring exchangeable deuterons, diminishing the intraresidual cross peak intensities, will be blocked. Similar effects have been observed by LeMaster and Richards [23] for *Escherichia coli* thioredoxin. They observed these effects by making use of random fractional deuteration of the protein resulting in a narrowing of resonances of the protein dissolved in H_2O . The proton attached to the nitrogen atom of I116, which is being replaced by a deuteron, is in the immediate neighbourhood of the C_αH of A115. This could explain the intensity increase of the $\text{NH(i)}/\text{C}_\alpha\text{H(i)}$ cross peak of A115. In addition the possibility that structurally bound, exchangeable water molecules are present in this region of the protein cannot be excluded. When the detailed tertiary structure of *M. elsdenii* flavodoxin will be known then it will be possible to elucidate if the increased intensities of the NOESY cross peaks is solely a result of the replacement of structurally bound water molecules by $^2\text{H}_2\text{O}$ molecules.

The double-quantum filtered Cosy spectra of reduced *M. elsdenii* flavodoxin contain an overwhelming amount of partially overlapping cross peaks. Therefore the vicinal coupling constant $^3J_{\text{HN}\alpha}$ could not be determined from our spectra, although such coupling constants have been used as supporting evidence for the secondary structure determination of relatively small proteins [14].

Fig. 6 gives an overview of the observed sequential connectivities of the two-electron reduced *M. elsdenii* flavodoxin in a 50 ms NOESY spectrum at 41°C , pH 8.3. A NOESY spectrum with a mixing time of 50 ms was used in order to avoid effects of spin diffusion in the determination of the secondary structure elements of *M. elsdenii* flavodoxin. Only in case of the $d_{\alpha\beta i+3}$ connectivities a 150 ms NOESY spectrum was used because we had to deal with t_1 -noise in the corresponding part of the 50 ms NOESY spectrum and $d_{\alpha\beta i+3}$ connectivities are weak in a 50 ms NOESY spectrum [14]. In context with Fig. 6 several problems need to be discussed. When amide resonance positions are in close proximity of one another no d_{NN} connectivity will be found, as in case of e.g. N12-T13, A15-M16, I20-E21 etc. Moreover when the C_αH resonance coincides with the water resonance no $d_{\alpha\text{N}}$, $d_{\alpha\text{Ni}+3}$ and $d_{\alpha\beta i+3}$ connectivities are observed. In case of $d_{\alpha\text{Ni}+3}$ and $d_{\alpha\beta i+3}$ medium

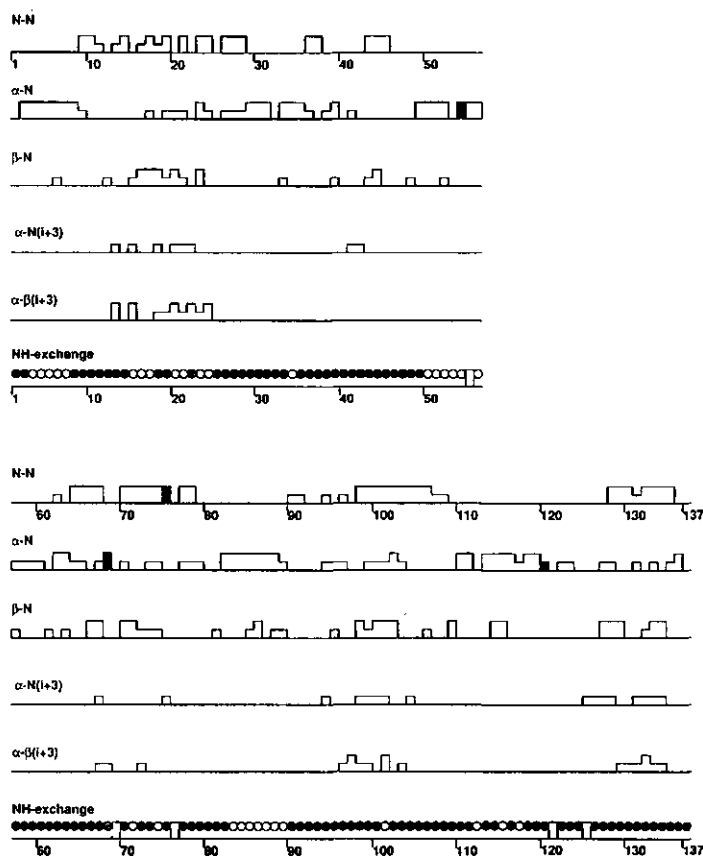


Fig. 6 Sequential and medium-range NOE contacts, used to characterize the secondary structure, observed in a NOESY spectrum of reduced *M. elsdenii* flavodoxin with a mixing time of 50 ms, pH 8.3, 41 °C. Distinction has been made between strong NOE connectivities on one hand and medium and weak NOE connectivities on the other hand. The grey boxes represent respectively $d_{\alpha\delta}$, $d_{N\delta}$, $d_{N\delta}$ and $d_{\alpha\delta}$ connectivities involving proline residues. In case of doubts whether a connectivity existed (overlapping cross peaks) no connectivity is given. The α - β_{i+3} connectivities are taken from a 150 ms NOESY spectrum, see text. No use has been made of the oxidized state of flavodoxin. Black-filled, grey-filled and open circles indicate amide protons with fast, intermediate and slow exchange rates, respectively. Amide proton resonances with slow exchange rates were present during the 19.4 h amide exchange experiment, pH 8.3, 41 °C. Amide proton resonances corresponding to the black-filled circles had no detectable intensity in the amide exchange experiment.

range NOE connectivities, characteristic for α -helices, several overlapping cross peaks are observed. This is not surprising considering the size of *M. elsdenii* flavodoxin. In case of (possible) overlap no connectivity is given explaining the absence of several of these connectivities in the α -helical regions of the protein (see Fig. 6).

Table 1: Amide and C α proton resonance positions (in ppm) of amino acid residues of β -sheet strands in reduced *M. elsdenii* flavodoxin as determined by 2D-NMR. The resonance positions were taken from van Mierlo et al. [10], (pH 8.3; 41°C). The water resonates at 4.68 ppm under these conditions, C α H's resonating at lower field positions are in bold letter type. Amino acid residues labeled with one asterisk are moderately and those labeled with two asterisks are strongly influenced by the paramagnetism of the flavin moiety (see text).

Strand 1			Strand 2			Strand 3		
	NH	C α H		NH	C α H		NH	C α H
V2	8.33	4.40	V31	8.17	5.60	V49	7.48	4.89
E3	8.69	5.15	E32	8.15	4.66	I50	8.61	4.87
I4	9.11	5.05	S33	8.43	6.01	L51	9.65	5.49
V5	9.25	5.42	V34	9.53	4.53	L52	8.57	5.54
Y6	7.95	6.11	R35	8.17	4.45	G53*	9.37	4.79;1.80
W7*	8.43	4.46	F36	7.65	3.25	C54*	9.36	5.60
						P55*	-----	5.40
						A56**	6.46	2.67
Strand 4			Strand 5					
K82	7.88	5.00	T110	8.86	4.37			
V83	8.88	5.79	V111	9.03	5.09			
G84	9.31	5.18	I112	8.85	4.21			
L85	7.35	5.54	G113	6.93	4.15;3.97			
F86	9.29	6.08	T114	8.03	5.86			
G87*	8.20	5.25;4.06	A115	8.44	4.90			
S88*	6.53	6.11	I116*	8.50	5.99			
Y89**	8.05	5.34	V117*	7.67	4.38			
			N118*	8.33	3.70			
			E119*	8.65	3.39			

Based mainly on stretches of strong d α N connectivities, we conclude that *M. elsdenii* flavodoxin contains 5 β -sheet strands: strand 1: V2-W7; strand 2: V31-F36; strand 3: V49-A56; strand 4: K82-Y89 and strand 5: T110-E119. Strand 4 might

extend to G80. The amide resonance of G80 has a low intensity because it is influenced by the high pH of the solution [10]. For this reason we could not detect d_{NN} connectivities in the 50 ms NOESY spectrum and hence exclude G80 as a β -sheet amino acid residue. The $C_{\alpha}H$ resonance of K81 and of A109 coincide with the water resonance so we cannot exclude these amino acid residues as being part of respectively, β -sheet strands no. 4 and no. 5. Strand 2 and strand 5 are peripheral. The majority of the amide protons of strand 2 exchange completely with 2H_2O , the expected alternating exchange pattern is therefore not observed. This is a consequence of the experimental conditions (19.4 h at pH 8.3 and 41 $^{\circ}C$). The results indicate that strand 2 is not as strongly hydrogen bonded as strand 5. For strand 5 the expected alternating amide exchange pattern is observed on going from E119 to T114, then an irregularity in the exchange pattern is observed: G113 is exchanging against expectation and I112 is persistent. The irregularity in this β -strand might be caused by the existence of a β -bulge as was more often observed in β -sheet structures [21]. This aspect will be treated in the next section. Strands 1, 3 and 4 are internal strands as indicated by the observation of many persistent amides, only a few amides at the extremes of these strands are exchanging with the solvent. Regarding the chemical shifts of the amide and $C_{\alpha}H$ protons being part of the β -sheet, see Table 1, we can conclude that a $C_{\alpha}H$ resonating at lower field than water is a strong indication for the corresponding amino acid residue being part of a β -sheet structure. 64.3% of the β -sheet C_{α} protons in *M. elsdenii* flavodoxin resonate at lower field than water (in case of glycines the $C_{\alpha}H$ resonating at the lowest field was used), whereas only 9.5% of the $C_{\alpha}H$ resonances being part of other secondary structure elements of flavodoxin are resonating at lower field than water.

Our observation concerning the $C_{\alpha}H$ resonances is consistent with previous observations by Wagner et al. [24] and Pardi et al. [25] on BPTI. In these studies the ring current effects resulting from aromatic amino acid residues and the random coil chemical shifts were subtracted from the overall conformation-dependent chemical shifts of amino acid residues being part of an anti-parallel β -sheet structure. A d^{-3} distance dependence of the chemical shifts of amide and β -sheet C_{α} proton resonances was found, d being the distance between a carbonyl (or water) oxygen and the amide or C_{α} proton [24,25]. For flavodoxin such a calculation is not yet possible as the detailed structure of the protein is not known. Our data show that finding a $C_{\alpha}H$ resonance at lower field than the water resonance, without knowing the tertiary structure of the protein, is already an indication that the corresponding amino acid residue is part of a β -sheet. The observed amide resonances of flavodoxin do not allow for a clear distinction between general resonances of amino acid residues being or not being part of a β -sheet structure. In other studies [24,25]

the conformation-dependent downfield chemical shift of the β -sheet amide protons appeared to be larger than those for C_{α} protons. This trend was not observed for flavodoxin. The presence of the relatively large aromatic prosthetic group FMN in flavodoxin which is tightly hydrogen bonded to amino acid residues [7] not involved in β -sheet structures (see following) could explain this difference. A more detailed inspection of correlations between the protein conformation and the chemical shifts of backbone hydrogen atoms must await the solution structure of flavodoxin.

There are four regions of helicity in the two-electron reduced *M. elsdenii* flavodoxin as recognized by stretches of d_{NN} connectivities, helix 1: approximately N12-A26; helix 2: approximately D64-A75; helix 3: approximately G94-E105 and helix 4: approximately C127-A135. These helical regions are further confirmed by $d_{\beta N}$ and medium range $d_{\alpha N i+3}$ and $d_{\alpha \beta i+3}$ connectivities. The amides in the α -helices of *M. elsdenii* flavodoxin, with the exception of helix 1, appear to be not as persistent as the amides which are hydrogen bonded in the β -sheets of flavodoxin, at least under the experimental conditions used.

The identification of classical tight turns [21], solely based on the information contained in Fig. 6, is not very reliable. Tight turns consist of four amino acid residues characterized by isolated short d_{NN} connectivities, type II- and half turns by isolated short $d_{\alpha N}$ connectivities [14]. As a turn consists of a small number of amino acid residues, the uniqueness of turn identification is small. Moreover distinguishing between the types of classical turns solely based on NOE constraints is not possible [14]. When the three-dimensional orientation of the known secondary structure elements will be known, the position of tight turns will become evident. We will therefore locate the tight turns in flavodoxin during the determination of the global fold of the protein.

Tertiary structure

The main secondary structural elements have been determined using nearest neighbour NOE contacts between amino acid residues as primary source of information. However the NOESY spectra contain an overwhelming amount of extra information as is seen in Fig. 1. This becomes even more evident when studying the complete NOESY spectrum of a protein of the size of flavodoxin. The additionally observed non-sequential interresidual cross peaks connect resonances of protons from amino acid residues which are, as a result of the tertiary folding of the protein, far apart in the primary sequence. Based on these long-range NOE's [14,26] it is possible to determine the global fold of flavodoxin. In case of *M. elsdenii* flavodoxin we can also make use of the special properties of this protein concerning the fast electron exchange between the one-electron (paramagnetic)

and the two-electron (diamagnetic) reduced state thereby revealing tertiary structure information in the vicinity of the prosthetic group [6,10].

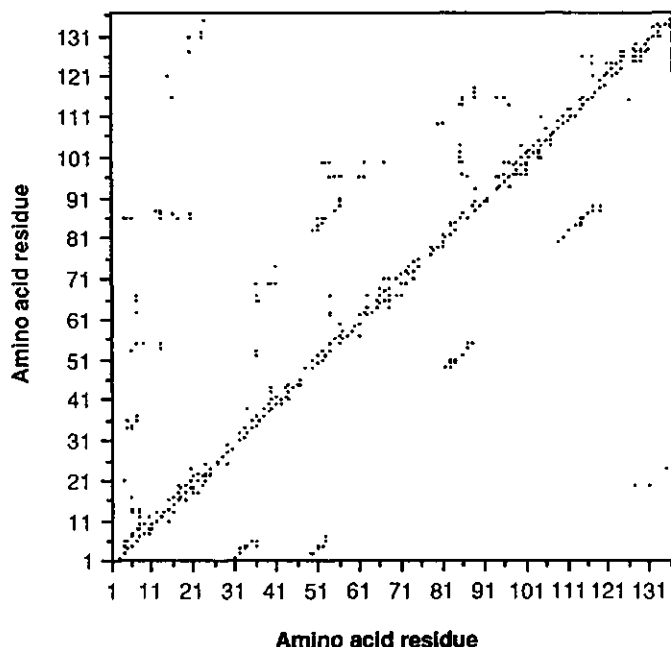


Fig. 7 Plot of the observed NOE's in a 150 ms NOESY spectrum between amino acid residues of reduced flavodoxin. A point below the diagonal indicates a NOE connectivity between respectively NH and NH, NH and C α H or C α H and C α H. A point above the diagonal indicates connectivities between an NH proton and a side chain proton or between side chain and side chain protons (side chain protons are C β H, C γ H etc.). The parallel β -sheet elements and their relative positions can be easily recognized below the diagonal.

Fig. 7 represents the 642 interresidual distance constraints detected in the 150 ms NOESY spectrum of the two-electron reduced *M. elsdenii* flavodoxin. Fig. 7 comprises a compact presentation of the many NOE contacts observed in the NOESY spectrum and depicts the secondary and tertiary structure characteristics of flavodoxin.

The β -sheet structure

NOE contacts between amino acid residues on the right-hand side of Fig. 7 give a clear indication of the secondary structure of flavodoxin. The 5 β -sheet strands are clearly of a parallel fashion because the corresponding parallel lines of contacts between amino acid residues are observed. In case of an antiparallel β -sheet a line of contacts perpendicular to the diagonal would be expected. Several long-range NOE's between adjacent β -sheet strands are observed in Figs. 1 and 7.

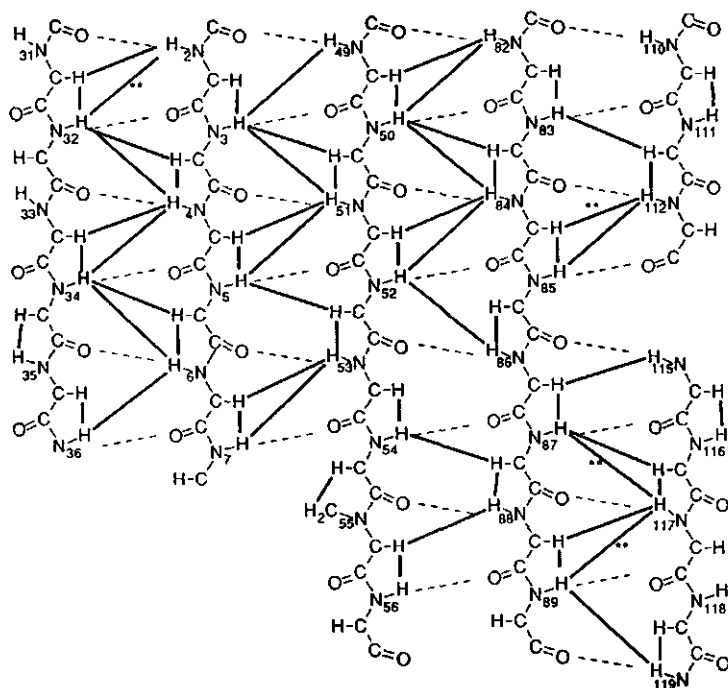


Fig. 8 Parallel β -sheet of *M. elsdenii* flavodoxin. Dashed lines indicate hydrogen bonds as expected on the basis of the relative position of the strands and the amide exchange characteristics. Solid bold lines indicate the NOE connectivities between protons observed in a 150 ms NOESY spectrum. Bold lines with asterisks represent NOE connectivities observed after building the β -sheet. The irregularity in β -sheet strand no. 5 at amino acid residue number 113 and 114, expected to represent a β -bulge (see text), has not been depicted. To present the irregularity properly a stereo drawing would be necessary.

The unique way to align the 5 β -sheet strands consistent with the observed NOE's is shown in Fig. 8. The 5 β -strands form a single β -sheet with the connectivity 2-1-3-4-5, the β -sheet strands 2 and 5 being peripheral as already suggested on the

basis of the amide proton exchange experiment. After constructing the parallel β -sheet structure, which is generally more regular than an anti-parallel β -sheet [21], it appeared possible to detect several "not yet observed" but now predicted NOE cross peaks in the 150 ms NOESY spectrum consistent with the generated secondary structure. These "new" distance constraints are shown in Fig. 8. An irregularity is observed in strand 5, already indicated in the amide exchange experiment, which is characterized by a strong d_{NN} connectivity (between the amide protons of I112 and G113, see Fig. 2 and Fig. 6). This connectivity is unusual for an regular β -sheet strand. It is therefore very likely that we have to deal with an β -bulge in strand 5 which is known to occur rarely in parallel β -sheets [21].

The position of the α -helices

The four regions of helicity in flavodoxin can be recognized at the right-hand side of Fig. 7 by stretches of contacts close to the diagonal. These stretches are a result of medium range NOE contacts between backbone protons characteristic for α -helical structures. For positioning the helices in the tertiary structure of the protein the left-hand side of Fig. 7 is useful showing the many nonsequential interresidual NOE contacts observed between several amino acid residues. For determining the global fold of the protein the helices are treated as solid structures whereas the β -sheet is treated as a planar structure. In practice, however, most parallel β -sheet structures are exhibiting a typical twist [21], which is consistent with several observed NOE contacts (unpublished observation). A few NOE contacts determining the global fold of the protein as observed in Fig. 7 have been further specified in Table 2. Using Fig. 7 and Table 2 it is clear that helices no. 1 and no. 4 are in close proximity of each other resulting in many interhelical connectivities. Helix no. 1 is exhibiting several NOE contacts with β -sheet strands no. 1, 3, and 4 and can be placed in space taking into account that the parallel β -sheet strands no. 1 and no. 2 must be interconnected by helix no. 1 as a result of primary structure restrictions. Helix no. 4 can be positioned in space via its C-terminal NOE connectivities with the C-terminus of helix no. 1; several amino acid residues between the C-terminus of β -sheet no. 5 and the N-terminus of helix no. 4 are exhibiting NOE connectivities with the C-terminus of β -sheet no. 5 (see Fig. 8), consistent with a turn folding helix 4 in close position to helix no. 1. No NOE contacts have been observed between, on the one hand, helices no. 1 and no. 4 and, on the other hand, the other two helices no. 2 and no. 3. As the latter helices have, in addition to an interhelical NOE contact, clear NOE contacts with the β -sheet structure, both couples of helices must be placed on opposite sites of the β -sheet of the flavodoxin. The β -sheet therefore comprises the central part of the molecule. The C-terminal end of helix no. 4 is not in close proximity of the β -sheet as no NOE connectivities to the β -sheet have been observed. This could be due to

a twist in the central β -sheet. This aspect has not been depicted in the simple global fold presentation of the protein in Fig. 9. In order to position helices precisely in the tertiary structure of the protein, side chain-side chain NOE's of amino acid residues being part of the helices are needed, these NOE's are in practice difficult to obtain because many overlapping NOE cross peaks are occurring in the high field part of the NOESY spectra. In addition this region of the spectrum is suffering from t_1 -noise. The determination of the tertiary structure of a protein via 2D-NMR is therefore mainly based on backbone-backbone and backbone-side chain connectivities.

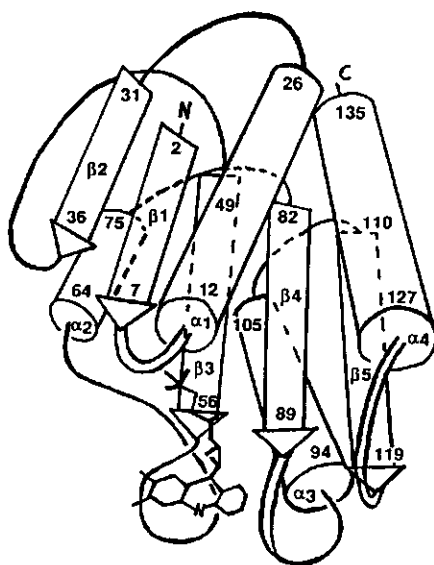


Fig. 9 Global fold of *M. elsdenii* flavodoxin as determined by 2D-NMR. The α -helices and β -sheet strands including the N- and C-terminal ends are depicted. The FMN moiety has also been included. (In preparing this figure, use has been made of the global fold presentation of *Clostridium MP* flavodoxin by Adman [27].)

Helix no. 2 is showing NOE contacts with β -sheet strands no. 1, no. 2 and no. 3. The N-terminus of this helix is in close proximity of amino acid residues W7, C54 and E37. The C-terminal part of the helix is not showing NOE contacts to the central β -sheet, so the helix must point away from the central β -sheet, on going from the N- to the C-terminal part of the helix. Knowing in addition that amino acid residues K82 to Y89 are again part of the central β -sheet we can place helix no 2. This helix

shows many NOE contacts to the part of the protein roughly lying between amino acid residues 36 and 46, not yet fully characterized. Helix no. 3 is showing several NOE connectivities to β -sheet strands no. 3, 4 and 5 and is connecting strand 4 and 5. NOE connectivities between W100 of helix no. 3 and V67 of helix no 2 are being observed. Using this information helix no. 3 can be positioned into the tertiary structure of the protein.

Table 2: Several specific NOE contacts observed in two-electron reduced *M. elsdenii* flavodoxin specifying the global fold of the protein in solution. For NOE connectivities observed in the β -sheet see Fig. 8.

Helix 1	NOE's to		Helix 3	NOE's to	
(NH)E14	(C β H)S8	strand 1	(ring)W96	(C γ H)A56	strand 3
(C γ H)A17	(ring)Y6	strand 1	(ring)W100	(C δ H)L52	strand 3
(C δ H)I20	(ring)F86	strand 4	(ring)W96	(C α H)G87	strand 4
(NH)I20	(C α H)C127	helix 4	(ring)W100	(C δ H)L85	strand 4
(C γ H)V24	(NH)A115	strand 5	(NH)K101	(C δ H)L85	strand 4
(C δ H)I20	(NH)G131	helix 4	(OH)T104	(C δ H)L85	strand 4
(NH)V24	(NH)A135	helix 4	(NH)G94	(C δ H)I116	strand 5

helix 2	NOE's to	
(C γ H)V66	(ring)W7	strand 1
(C γ H)V67	(ring)F36	strand 2
(C γ H)V67	(C α H)C54	strand 3
(C γ H)V67	(ring)W100	helix 3

Placing the FMN moiety

During the sequential resonance assignment procedure several NOE connectivities were observed between the apoprotein and the prosthetic group FMN. Fig. 10 depicts the prosthetic group and Table 3 gives an overview of observed connectivities of the flavin with the apoprotein. Using the fast electron shuttle between the paramagnetic one-electron reduced and the diamagnetic two-electron reduced state and varying the percentage semiquinone in the sample it appeared possible to create a varying sphere of protons (affected by the paramagnetism of the flavin [6,10]) around the flavin. This property of flavodoxin reveals tertiary structure information with respect to the position of the flavin and as a check of the correct placement of secondary structure elements. Proton resonances of the amino acid residues A56, M57, G58, S59, E60, E61, Y89, G90, W91 and G92 disappear almost immediately on slight oxidation of a reduced

flavodoxin solution. These amino acid residues must therefore be in the immediate neighbourhood of the flavin [10]. A56 and Y89 are part of the central β -sheet, so the isoalloxazine ring must be in close contact with the C-terminal parts of strand 3 and strand 4. This is confirmed by several NOE connectivities of the isoalloxazine moiety to these strands (Table 3). Strand 2 is exhibiting the largest distance of all β -sheet strands to the isoalloxazine moiety as no amino acid residue of this strand is influenced by the paramagnetic flavin.

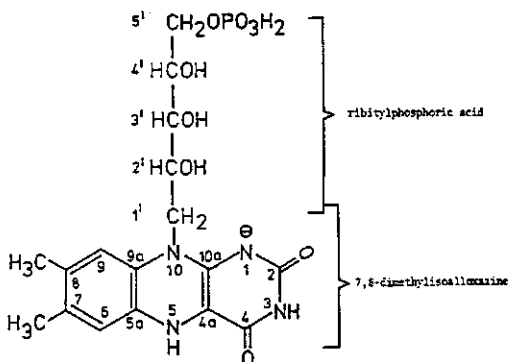


Fig 10 Structure of two-electron reduced riboflavin 5'-phosphate (FMNH⁻).

The helices are further apart from the isoalloxazine moiety than the C-terminal ends of β -sheet strand 3 and 4 because none of the resonances of the amino acid residues of the helices are disappearing in the NOESY spectra on formation of a small amount of semiquinone. Proton resonances of amino acid residues W7, S8, T10, N12, T13, G53, C54, P55, L62, E63, G87, S88, S93, G94, E95, W96, M97, D98, A99, I116, V117, N118 and E119 disappear with higher percentages semiquinone in the samples [10]. Therefore helices no. 2 and no. 4 are not being influenced by the paramagnetism of the flavin and will, as a result, not be in the direct vicinity of the flavin. On the other hand the N-terminal parts of helices no. 1 and no. 3 must be in the neighbourhood of the flavin. This is also the case for the C-terminal part of strand no. 5 and the C-terminal parts of strand 3 and 4 as already discussed. The majority of the amino acid residues being strongly influenced by the paramagnetism of the flavin are not categorized as helical or β -sheet structure elements but possess coil structure. All the previous information is in good agreement with the results obtained from other studies in which it was shown that the flavin binding regions of *M. elsdenii* and *Clostridium MP* flavodoxin are similar

[5-7]. This information was used for positioning the flavin moiety into the tertiary structure of the protein (Fig. 9).

Table 3: NOE connectivities of FMN to the apoprotein as observed in the 150 ms NOESY spectrum of two-electron reduced *M. elsdenii* flavodoxin at 41 °C, pH 8.3.

flavin proton	NOE connectivity with
N(5)H	(C $_{\alpha}$ H)M57; (NH)G58; (ring)W91
C(6)H	(C $_{\alpha}$ H)M57; (NH)G58
CH ₃ (7 α)	(C $_{\alpha}$ H)M57; (NH)G58
CH ₃ (8 α)	(NH)G58
C(1')H	(C $_{\alpha}$ H)Y89
C(2')H	(NH)A56; (C $_{\alpha}$ H)Y89; (NH)G90
C(3')H	(C $_{\alpha}$ H)Y89
C(4')H	(C $_{\alpha}$ H)Y89

The remaining structure

Now the major structure elements have been positioned in space the remaining stretches of the backbone can also be placed.

As helix no. 1 (N12-A26) is in close proximity to the β -sheet and is continuing in parallel β -sheet strand no. 2 (V31-F36) there must be turns in the regions S8-N12 and A26-V31, the NOE connectivities are consistent with this (Fig 6). Helix no. 2 is connecting strand 3 with strand 4, therefore in the region M57-E63, the neighbourhood of the flavin, a coil like structure exists. In the region P76-K81 a turn is present which is confirmed by d_{NN} connectivities in the region K77-K79 (see Fig. 2). Helix no. 3 is connecting strand 4 and strand 5. A coil kind of region is expected in the region G90-E94, this region is in the immediate neighbourhood of the flavin and is closely similar to the identical region in the structure of *Clostridium MP* flavodoxin, as expected. In the region D106-A109 a turn has to be present to connect the helix with strand no. 5. As a consequence of helix no. 4 being parallel to helix no. 1, the tertiary position of which is known, there must be a turn in the region M120-E126 of the protein.

The region F36-D48 has not yet been assigned to a secondary structure element, we define it therefore as a coil region. A coil region is not the same as a randomly organized region [21], it has a strong organization as evidenced by clear NOE contacts in this region. This region may contain a small helix involving residues 43-45 (see Figs. 6 and 9) causing a turn in the coil in order to connect the coil with β -sheet strand no. 3. Amino acid residue E37 to V41 are exhibiting many NOE contacts with helix no. 2 (see Fig. 7), so these regions of the protein will be

parallel. As the coil region in addition is connecting β -sheet strands no. 2 and no. 3 there must be a turn in the region F36-D38 (as is consistent with d_{NN} connectivities observed in this region). Fig. 9 is showing the global fold of *M. elsdenii* flavodoxin based on the determination of secondary structure elements and their relative positions. The central β -sheet is being surrounded by four α -helices. As the central β -sheet is shielded more from solvent molecules than the α -helices this might explain the observed greater persistence of the amide protons being part of the β -sheet as compared to the amide protons of an α -helix (Fig. 6). In addition the α -helices might be more flexible than the β -sheet explaining the higher exchange rate of the former amide protons.

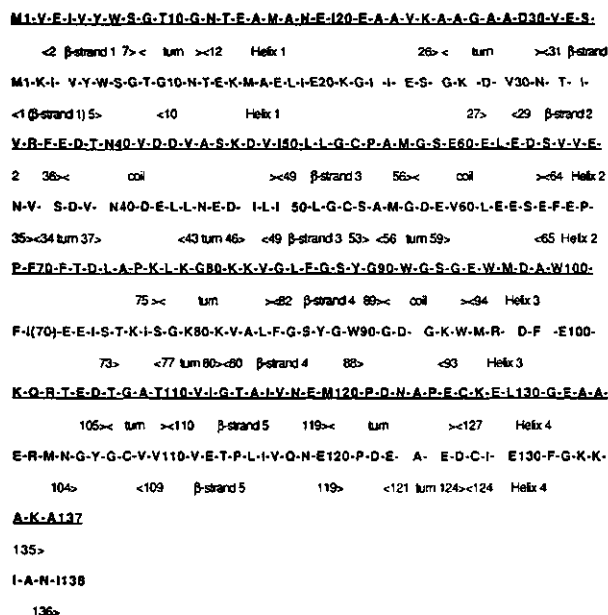


Fig. 11 Secondary structure of *M. elsdenii* flavodoxin as determined by short-range and medium-range NOE connectivities (the N- and C-terminal points of the turns and coils in case of *M. elsdenii* flavodoxin have been roughly determined, see text). The amino acid residues of *M. elsdenii* flavodoxin have been underlined. In normal letter type the amino acid residues of *Clostridium MP* flavodoxin have been depicted including the secondary structure elements as determined by crystallography [15].

In Fig. 11 the secondary structure elements of *M. elsdenii* flavodoxin as determined by 2D-NMR and of the related flavodoxin from *Clostridium MP* as determined by crystallography are depicted. The figure clearly demonstrates the high similarity between both flavodoxins concerning the secondary structure. It was

already known that the tertiary structure of the flavin binding region of both proteins must be very similar. The same also holds for the rest of the tertiary structure (Fig. 9) which is very similar to that of *Clostridium MP* flavodoxin [15,28,29].

By qualitative visual inspection of NOE cross peak connectivities it was possible to compare the secondary structure characteristics and the global fold of a noncrystallizable flavodoxin with a crystallizable one. During the sequential resonance assignments in several regions of the protein, knowing the secondary and global tertiary fold as determined by 2D-NMR, we could benefit from the crystal structure of *Clostridium MP* flavodoxin [10].

Conclusion

M. elsdenii flavodoxin consists of five parallel β -sheet strands and four α -helices and is therefore classified as a protein consisting of parallel α/β domains [21]. The central β -sheet of the protein is surrounded by four helices and is compact and very stable as demonstrated by the extremely slow exchange of several amide protons of the β -sheet. An irregularity exists in β -sheet strand no. 5.

The flavin is noncovalently bound at the surface of the protein. Using the 642 NOE constraints gathered at this moment it will be possible to generate an even more detailed presentation of the tertiary structure of the protein in the near future. Using the structure of the two-electron reduced *M. elsdenii* flavodoxin a comparison of the flavin binding region of *M. elsdenii* flavodoxin with that of *Clostridium MP* flavodoxin will be possible. Differences in the isoalloxazine binding region must occur as several NOE connectivities, expected on the basis of the crystal structure of *Clostridium MP* flavodoxin, are not present in the NOESY spectra of *M. elsdenii* flavodoxin [10].

Acknowledgement

We would like to thank the HF-SON NMR-facility Nijmegen (The Netherlands) where the majority of the experiments were performed. This study was carried out under the auspices of the Netherlands Foundation for Chemical Research (SON) with financial aid from the Netherlands Organization for the Advancement of Pure Research (NWO).

References

1. Mayhew, S.G. & Ludwig, M.L. (1975) *The Enzymes* 12, 57-118.

2. Moonen, C.T.W. & Müller, F. (1982) *Biochemistry* 21, 408-414.
3. Tanaka, M., Haniu, M., Yasunobu, K. Mayhew, S. & Massey, V. (1973) *J. Biol. Chem.* 248, 4354-4366.
4. Tanaka, M., Haniu, M., Yasunobu, K., Mayhew, S. & Massey, V. (1974) *J. Biol. Chem.* 249, 4397.
5. Moonen, C.T.W., Hore, P.J., Müller, F., Kaptein, R. & Mayhew, S.G. (1982) *FEBS Lett.* 149, 141-146.
6. Moonen, C.T.W. & Müller, F. (1984) *Eur. J. Biochem* 140, 303-309.
7. Vervoort, J., Müller, F., Mayhew, S.G., van den Berg, W.A.M., Moonen, C.T.W. & Bacher, A. (1986) *Biochemistry* 25, 6789-6799.
8. Schagen van, C.G. & Müller, F. (1981) *FEBS Lett.* 136, 75-79.
9. Moonen, C.T.W., Scheek, R.M., Boelens, R. & Müller, F. (1984) *Eur. J. Biochem.* 141, 323-330.
10. Mierlo van, C.P.M., Vervoort, J., Müller, F. & Bacher, A. (1990) *Eur. J. Biochem.* 187, 521-541.
11. Wüthrich, K., Wider, G., Wagner, G. & Braun, W. (1982) *J. Mol. Biol.* 155, 311-319.
12. Wagner, G. & Wüthrich, K. (1982) *J. Mol. Biol.* 155, 347-366.
13. Billeter, M., Braun, W. & Wüthrich, K. (1982) *J. Mol. Biol.* 155, 321-346.
14. Wüthrich, K. (1986) *NMR of proteins and Nucleic Acids*, Wiley, New York.
15. Smith, W.W., Burnett, R.M., Darling, G.D. & Ludwig, M.L. (1977) *J. Mol. Biol.* 117, 195-225.
16. Mayhew, S.G. & Massey, V. (1969) *J. Biol. Chem.* 244, 794-802.
17. Marion, D. & Wüthrich, K. (1983) *Biochem. Biophys. Res. Commun.* 113, 967-974.
18. Rance, M., Sörenson, O.W., Bodenhausen, G., Wagner, G., Ernst, R.R. & Wüthrich, K. (1983) *Biochem. Biophys. Res. Commun.* 117, 479-485.
19. Pearson, G.A. (1977) *J. Magn. Res.* 27, 265-272.
20. Wüthrich, K., Billeter, M. & Braun, W. (1984) *J. Mol. Biol.* 180, 715-740.
21. Richardson, J. (1981) *Adv. Protein Chem.* 34, 167-339.
22. Dubs, A., Wagner, G. & Wüthrich, K. (1979) *Biochim. Biophys. Acta.* 577, 177-194.
23. LeMaster, D.M. & Richards, F.M. (1988) *Biochemistry* 27, 142-150.
24. Wagner, G., Pardi, A. & Wüthrich, K. (1983) *J. Am. Chem. Soc.* 105, 5948-5949.
25. Pardi, A, Wagner, G. & Wüthrich, K. (1983) *Eur. J. Biochem.* 137, 445-454.
26. Klevit, R.E. & Waygood, E.B. (1986) *Biochemistry* 25, 7774-7781.
27. Adman, E.T. (1979) *Biochim. Biophys. Acta.* 549, 107-144.

28. Burnett, R.M., Darling, G.D., Kendall, D.S., LeQuesne, M.E., Mayhew, S.G., Smith, W.W. & Ludwig, M.L. (1974) *J. Biol. Chem.* 249, 4383-4392.
29. Ludwig, M.L., Burnett, R.M., Darling, G.D., Jordan, S.R., Kendall, D.S. & Smith, W.W. (1976) in *Flavins and Flavoproteins* (Singer, T.P., ed.) pp. 393-404, Elsevier, Amsterdam.

Chapter 4

Tertiary structure of two-electron reduced *Megasphaera elsdenii* flavodoxin and some implications, as determined by two-dimensional ^1H NMR and restrained molecular dynamics

Carlo P. M. van Mierlo¹, Philip Lijnzaad¹, Jacques Vervoort¹, Franz Müller²,
Herman J. C. Berendsen³ and Jacob de Vlieg⁴

1. Department of Biochemistry, Agricultural University, Wageningen, The Netherlands.

2. Present address: Sandoz, Agro Ltd, Department of Toxicology, Basle, Switzerland.

3. Laboratory of Physical Chemistry, University of Groningen, The Netherlands.

4. European Molecular Biology Laboratory, Heidelberg, Federal Republic of Germany.

Summary

Of the non-crystallizable two-electron reduced *Megasphaera elsdenii* flavodoxin (15 kDa, 137 amino acid residues) the tertiary structure has been determined using nuclear Overhauser enhancement (NOE) restraints extracted from two-dimensional ^1H NMR spectra. A tertiary structure satisfying the experimental restraints very well (maximum NOE violation of 0.66 Å) was obtained with use of restrained molecular dynamics, using 509 distance restraints (including one *non*-NOE) on a starting structure modeled from the crystal structure of one-electron reduced *Clostridium MP* flavodoxin. The protein consists of a central parallel β -sheet surrounded on both sides by two α -helices. The flavin is positioned at the periphery of the molecule. The tertiary structure of the protein is highly defined with the exception of the flavin. The latter is expected to result from performing the RMD simulation without water molecules and without proper charges on the flavin. The flavin, including the phosphate, the ribityl side chain and the isoalloxazine ring, is solvent accessible under the experimental conditions used and evidenced by a two-dimensional amide exchange experiment. This accessibility is expected to be important in the redox potential regulation of the semiquinone/hydroquinone couple of the protein. The amide exchange against deuterons and several typical line shapes in the 2D-NMR spectra are consistent with the structure generated. The structure is discussed in detail.

Introduction

Flavodoxins are low-potential electron-transfer proteins which have been found in several strains of bacteria and algae. The flavodoxins comprise a group of small monomeric proteins with a molecular mass ranging from 14 to 23 kDa containing non-covalently bound riboflavin-5'-phosphate (FMN) as prosthetic group. The chemical and physical properties have been intensively studied (for a review see ref. [1]).

The crystal structures of three flavodoxins have been determined: *Clostridium MP* flavodoxin in the oxidized (1.9 Å resolution) and the one-electron reduced state (1.8 Å resolution, 138 amino acid residues) [2-4], *Desulfovibrio vulgaris* flavodoxin in the oxidized state (2.0 Å resolution, 148 amino acid residues) [5] and *Anacystis nidulans* flavodoxin in the oxidized state (2.5 Å resolution, 169 amino acid residues) [6-8]. These three proteins are typical α/β proteins having a parallel β -sheet consisting of 5 strands as a core. The three-dimensional structures are quite similar, *A. nidulans* flavodoxin having an insertion of 20 residues in the fifth strand of the parallel β -sheet distinguishing it from the other two flavodoxins [8]. The

conformation of the flavin binding region in these three flavodoxins, the main region of interest concerning the tuning of the redox potential, differs however significantly [6]. The flavin is positioned at the periphery of the three flavodoxins. Some results regarding the shape of the dihydro-isoalloxazine, the positions of three atoms (Ser7 OH, Ser87 OH and the carbonyl group of Gly57) and the sidechain positions of Glu59, Met56 and Trp90 of two-electron reduced *Clostridium MP* flavodoxin have also been published [4].

We have devoted a program to the study of the noncrystallizable flavodoxin of *Megasphaera elsdenii* using various NMR techniques. In vivo *M. elsdenii* flavodoxin shuttles between the semiquinone (one-electron reduced) and the hydroquinone (two-electron reduced) states as a result of the absence of an high activation barrier between these two redox states [9]. It is the absence of this activation barrier that predestinates the protein for one-electron transfer reactions.

One-dimensional NMR results using ^{13}C - and ^{15}N - enriched flavins, probing the electronic and conformational structure of the flavin, showed that the flavin binding regions of *M. elsdenii* and *Clostridium MP* flavodoxin are very similar [10-12]. In an initial two-dimensional NMR study on *M. elsdenii* flavodoxin it appeared possible to assign (partly) four amino acid residues in the immediate neighbourhood of the flavin, thereby confirming earlier one-dimensional ^1H NMR assignments [10,13,14]. Recently, we have described the sequential assignments of the ^1H NMR spectrum of two-electron reduced *M. elsdenii* flavodoxin (137 amino acid residues, 15 kDa) [15]. The secondary structure and the global fold of *M. elsdenii* flavodoxin were recently deduced from 2D-NMR data [16]. In this paper we describe the tertiary solution structure of two-electron reduced *M. elsdenii* flavodoxin based on the previously gathered structure information [15,16] and restrained molecular dynamics (RMD) [17-19] with interresidual distance restraints extracted from NOESY spectra. We did not make use of distance geometry methods [20-22] to arrive at a starting structure for the RMD calculations, but followed a different procedure.

For a few proteins of which no crystal structure is known the tertiary structure has been determined by NMR techniques. These include lac repressor headpiece [18], insectotoxin I₅A [23], proteinase inhibitor II from bull seminal plasma [24], phoratoxin [25], hirudin [26], human epidermal growth factor [27], the globular domain of histone H5 [28], acyl carrier protein from *Escherichia coli* [29] and human complement protein C5a [30]. All of these proteins have a molecular weight below 10 kDa. The determination of the tertiary structure of two-electron reduced *M. elsdenii* flavodoxin with a molecular mass of 15 kDa therefore represents an important progress in the determination of protein structures by NMR.

Materials and methods

NMR spectroscopy

The NMR studies were done on *M. elsdenii* flavodoxin which was isolated and purified as previously described [31]. The NMR samples contained 6 to 10 mM flavodoxin in solutions consisting of a mixture of 20% potassium pyrophosphate and 80% potassium phosphate with concentrations ranging from 75 to 200 mM, pH 8.3. For the tertiary structure determination phase sensitive NOESY spectra of the protein dissolved in a mixture of 10% $^2\text{H}_2\text{O}$ /90% H_2O , using time proportional phase increments [32,33], were acquired at 41 $^\circ\text{C}$ with mixing times of 50, 100 and 150 ms. The NOESY spectra were acquired on a Bruker AM600 operating at 600 MHz; no zero quantum filters were applied. Selective irradiation of the water resonance took place at all times, except during the data acquisition period; a relaxation delay of 2.5 s was used.

After data acquisition all further data handling was performed on a MicroVAX II computer and a VAXstation 2000 using software obtained from Dr. R. Boelens, modified to our specific requirements. The NOESY data were digitally filtered using a sine bell shifted by 15.0 $^\circ$ in t_2 dimension and a squared sine bell shifted by 22.5 $^\circ$ in t_1 dimension. After zero filling the spectral resolution of the NOESY spectra was 4.1 Hz per point in ω_2 direction and 8.1 Hz per point in ω_1 direction. Baseline corrections in both frequency directions were applied to the spectra using a fourth order polynomial according to Pearson [34]. The spectra were plotted as contour plots (0.13 ppm per cm) with levels increasing by a factor of 1.3. Details concerning the 2D-NMR experiments for the sequential resonance assignments [35-38], in addition to the NOESY experiments described here, have been published previously [15,16].

Reduction of the protein was achieved by the addition of the desired amount of a dithionite solution to the anaerobic solution of oxidized flavodoxin. Anaerobic solutions were obtained by carefully flushing the flavodoxin solution in the NMR tube with argon for about 20 min. The desired degree of reoxidation was obtained by injecting small volumes of air into the NMR tube containing the flavohydroquinone solution followed by gentle mixing.

Computational methods

a. Distance restraints

The 150 ms NOESY spectrum of two-electron reduced *M. elsdenii* flavodoxin has been the basis for estimating interproton distances. NOE intensities were visually classified in three distance ranges, 0-2.7 Å, 0-3.3 Å and 0-4.2 Å,

corresponding to strong, medium and weak NOE's [24,38,39]. For NOE's involving methyl groups an additional 0.5 Å was added to the upper distance limit to correct for the higher apparent intensity of the methyl resonance [26,40]. The initial list of 684 restraints was corrected after failure of the first RMD run, resulting in 619 restraints. For the final run, the NOE's have been thoroughly checked in the 50 ms NOESY spectrum to avoid restraints resulting purely from spin diffusion [41]. 133 restraints had to be discarded, resulting in a final list of 508 interresidual restraints. One repulsive *non*-NOE restraint [42] in the flavin binding region was considered to be relevant, and included. No intraresidual NOE restraints or dihedral angle restraints were used. Attractive restraints between amide protons and carbonyl oxygens have also not been used in order to preserve the secondary structure.

For some proton-proton pairs, corrections have to be applied to the upper distance limit. This may arise in cases where protons cannot be distinguished in the NMR spectra, either because of the lack of stereo specific assignments or because of rapid dynamic processes. In these cases the distance restraint must be applied to the average position (pseudo-atom) and the upper limit bound is corrected for the difference between the proton position and the actual pseudo position [43]. A full description of the concept of the use of pseudo-atoms as used in our calculations was published previously [44].

b. Molecular model

A starting structure was modeled from the crystal structure of *Clostridium MP* flavodoxin in the semiquinone state by amino acid residue replacement, using the interactive graphic programs WHATIF [45] and FRODO [46]. These programs were also used when the structure was manually adjusted. Insertion of E3 in, and deletion of L115 and D126 from the structure of *Clostridium MP* flavodoxin has been done to generate the starting structure of *M. elsdenii* flavodoxin. In order to remove high potential energies resulting from the model building on a graphics display system, the starting structure was relaxed by performing steepest descent energy minimization (EM) while the backbone atom positions were positionally restrained (in order to preserve the global fold). Every RMD run was preceded by EM without restraining positions, but using the distance restraints obtained from NMR with a distance restraint force constant of 250 kJ mol⁻¹nm⁻².

c. Molecular dynamics using distance restraints

RMD calculations, solving the classical Newtonian equations of motion of all atoms, are applied to the protein structure using a force field [44,47,48] of the form:

$$V(r_1, r_2, \dots, r_N) = \\ = \sum_{\text{angles}} 1/2 \cdot K_\theta [\theta - \theta_0]^2 + \sum_{\text{torsions}} 1/2 \cdot K_\zeta [\zeta - \zeta_0]^2 + \sum_{\text{dihedrals}} K_\phi [1 + \cos(n\phi - \delta)] \\ + \sum_{\text{pairs}(i,j)} [C_{12}(i,j)/r_{ij}^{12} - C_6(i,j)/r_{ij}^6 + q_i q_j / (4\pi\epsilon_0\epsilon_r r_{ij})] + \sum_{\text{restraints}(i,j)} V_{dc}(r_{ij}, r_{ij}^0)$$

describing the potential energy of the molecular system as a function of the positions r_i of the N atoms labeled by the index i . The usual term for harmonic bond-stretching was omitted as all bonds were artificially constrained to constant length for efficient computing; this was done by use of the SHAKE-procedure [49,50]. The first term in the above equation describes the harmonic bond-angle bending θ around the optimal angle θ_0 with force constant K_θ . The second two terms describe the torsional or dihedral-angle interactions comprising a harmonic term for so called improper dihedrals (ζ) that preserve planarity and chirality (aromatic rings, C_α carbons) and a term for dihedrals (ϕ) that are allowed to make transitions. The fourth term represents the non-bonded interactions between pairs of atoms i and j with charges q_i and q_j at distances r_{ij} , containing the Van der Waals and the Coulomb interactions.

The last term in the force field represents the 'non-physical' distance restraints resulting in forces that pull the atoms to the specified distance r_{ij}^0 . The term has the following form [44]:

$$\begin{aligned} V_{dc}(r_{ij}, r_{ij}^0) &= 0 & \text{if } 0 \leq r_{ij} \leq r_{ij}^0 \\ V_{dc}(r_{ij}, r_{ij}^0) &= 1/2 \cdot K_{dc} [r_{ij} - r_{ij}^0]^2 & \text{if } r_{ij}^0 \leq r_{ij} \leq r_{ij}^1 \\ V_{dc}(r_{ij}, r_{ij}^0) &= 1/2 \cdot K_{dc} [2r_{ij} - r_{ij}^0 - r_{ij}^1] [r_{ij}^1 - r_{ij}^0] & \text{if } r_{ij}^1 \leq r_{ij} \end{aligned}$$

The potential energy term V_{dc} is taken linear beyond r_{ij}^1 to avoid very strong restraining forces (which can easily lead to a distortion of the structure [44]). Here a value of $r_{ij}^1 = r_{ij}^0 + 0.1$ nm is used. The value of K_{dc} was changed during the refinement. We started with a relatively low value of $250 \text{ kJ mol}^{-1}\text{nm}^{-2}$ in order not to disrupt the global fold of the protein and to use the flexibility of the molecule for a proper search in conformation space. When the NOE restraints were no longer strongly violated, K_{dc} was gradually increased to a high value of $4000 \text{ kJ mol}^{-1}\text{nm}^{-2}$.

Initial velocities of the atoms were taken from a Maxwellian distribution at 314 K. Translational and rotational motion of the flavodoxin were "frozen". During the RMD calculations the system was coupled to a thermal bath with a temperature of 314 K, the coupling constant was 0.1 ps [51]. The RMD time step was 1 fs; the list of non-bonded neighbouring atom pairs was updated every 10 fs; a cut-off radius of 8 Å was used beyond which no non-bonded interactions were evaluated. Solvent was not included in the calculations.

The simulations were performed on a CONVEX-C1-XP and a VAX8650 computer using the GROMOS software package [47].

Results and discussion

Generating the tertiary structure

The NOESY spectra of *M. elsdenii* flavodoxin contain an overwhelming amount of NOE connectivities. The majority of the protons has, beside the many intraresidual contacts, several interresidual NOE connectivities to other spin systems. About 4500 cross peaks are observed at the left hand side of the water resonance in the 150 ms NOESY spectrum.

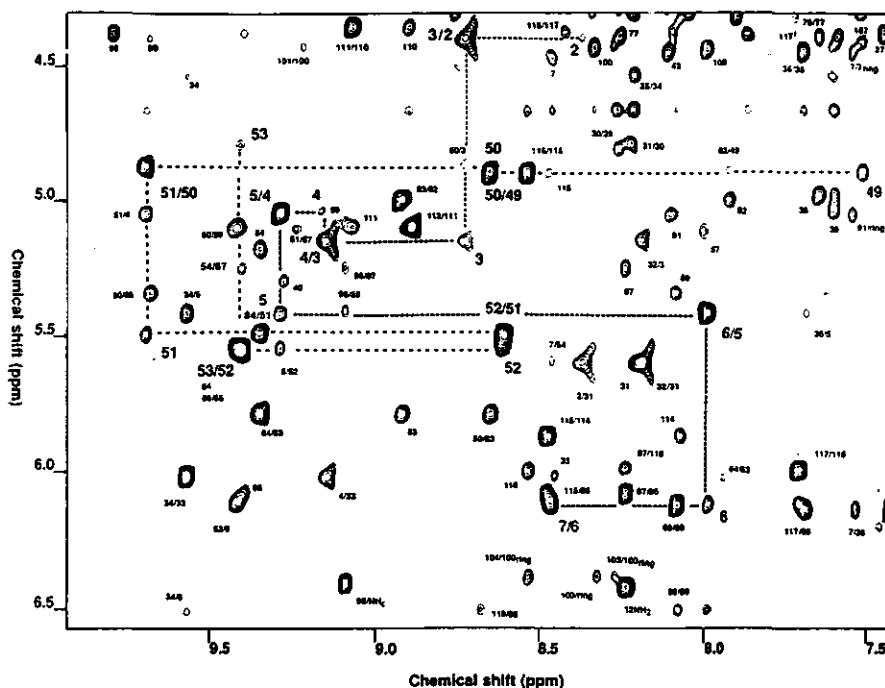


Fig. 1 Part of a 600 MHz NOESY spectrum of two-electron reduced *M. elsdenii* flavodoxin in 90% H_2O /10% D_2O , pH 8.3, 41 $^{\circ}\text{C}$. Two sequential pathways are illustrated. The mixing time is 150 ms. Cross peaks are labeled ω_2/ω_1 . Note the typical line shape of several cross peaks (e.g., 3/2, 4/3, 2/31, etcetera).

The global fold (Fig. 9 in [16]) of *M. elsdenii* flavodoxin has been determined using non-sequential interresidual NOE's connecting protons far apart in the

primary structure but in close proximity of each other as a result of the tertiary folding of the protein. The main secondary structure elements as determined by NMR have been positioned relative to each other using these long-range NOE's. These elements are: four regions of helicity, helix 1 extending from N12 to A26, helix 2 extending from D64 to A75, helix 3 extending from G94 to E105 and helix 4 extending from C127 to A135, and five β -sheet strands, strand 1: V2-W7, strand 2: V31-F36, strand 3: V49-A56, strand 4: K82-Y89 and strand 5: T110-E119 [16]. Fig. 1 illustrates several NOE connectivities determining the secondary structure elements and their relative spatial positions for a selected part of a NOESY spectrum. *M. elsdenii* flavodoxin appeared to contain a central parallel β -sheet consisting of the five already mentioned strands with the connectivity pattern 2-1-3-4-5. The β -sheet forms the core of the protein, and is surrounded by two α -helices on both sides, respectively helix no. 1 and no. 4 on one side and helix no. 2 and no. 3 on the opposite side of the sheet. The flavin could be positioned using several NOE connectivities between the prosthetic group and the apoprotein. During every stage of the analysis of the 150 ms NOESY spectrum of two-electron reduced *M. elsdenii* flavodoxin extensive use has been made of structural information already gathered. Interresidual NOE connectivities consistent with this structural information could then be assigned unambiguously.

Comparing the secondary structure elements and the global fold of two-electron reduced *M. elsdenii* flavodoxin with the crystal structures of *Clostridium MP* flavodoxin (oxidized as well as one-electron reduced), it became clear that there is a high structural similarity between both flavodoxins [16]. It was already concluded from previous ^{13}C and ^{15}N NMR studies that the FMN binding regions of *M. elsdenii* and *Clostridium MP* flavodoxin are remarkably similar [10-12]. Moreover, the amino acid sequence homology between *M. elsdenii* and *Clostridium MP* flavodoxin is 44%. The crystal structure of the one-electron reduced *Clostridium MP* flavodoxin is assumed to be virtually identical to its two-electron reduced structure. Therefore the crystal structure of the semiquinone state of *Clostridium MP* flavodoxin was used to build a plausible starting structure for the RMD calculations on two-electron reduced *M. elsdenii* flavodoxin. Following this procedure we circumvented the already for small proteins time consuming [30] procedure of distance geometry methods [20-22].

A RMD run was performed on the starting structure using 684 interresidual distance restraints, divided into three distance ranges corresponding to strong, medium and weak NOE's, obtained from the 150 ms NOESY spectra of flavodoxin. We aborted this RMD run after 30 ps simulation since no convergence to a structure

acceptably satisfying the restraints was obtained: 57 violations exceeding the NOE distance restraint with at least 1.4 Å were still present (Fig. 2).

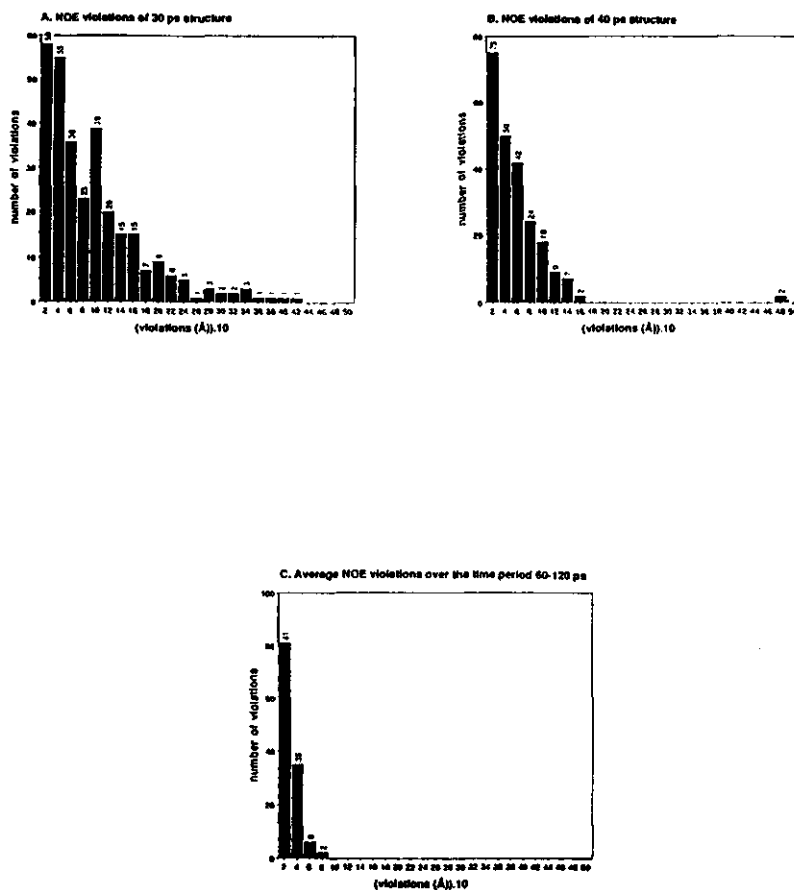


Fig. 2 Number of distance restraint violations as a function of the size (in Å) of the violations. Each bar corresponds to violations in the region given by the horizontal number and the horizontal number-0.2 Å. The *non*-NOE between NH(E60) and N5H is violated by 0.11 Å in the average structure (60-120 ps); see text.

Checking all NOE restraints which give rise to violations exceeding 0.8 Å after 30 ps of RMD revealed the primary source of these violations: human mistakes. In tabulating a few thousand NOE cross peaks (including both inter- and intraresidual connectivities) several correctly observed connectivities were wrongly labelled (e.g. tabelling a $d_{\alpha N}$ connectivity as a $d_{N\alpha}$ connectivity results in a NOE distance restraint violation), or their intensities were estimated poorly. The RMD results appeared to

function as a convincing indicator for this type of mistakes, made in assigning the NOESY spectrum of a protein the size of flavodoxin. There is evidently a need for automated 'bookkeeping' of assignments, automated peak integration procedures should be part of this. Assigning NMR spectra of a protein of this size by hand presumably represents the limits of what is feasible.

A new RMD run was performed using the corrected NOE restraint list of 619 restraints, resulting in a considerable decrease of violations. After 40 ps RMD only 20 distance restraints of the total number of 619 restraints were violated with more than 1.0 Å, including two serious violations of 4.6 and 4.8 Å (see Fig. 2). The serious violations involved NOE's connecting the amide resonance of I20 with the C α H and one C β H resonance of E126. The NOE's between protons of amino acid residues in the immediate neighbourhood of I20 and E126 were consistent with the global fold of that part of the protein, and were not showing serious violations after the RMD run. Thorough inspection of several 2D spectra resulted in the conclusion that the assignment of amino acid residues E126 and C127 should be interchanged, resulting in the loss of the two serious NOE violations. In fact the assignments of E126 and C127 by van Mierlo et al. [15] has been done this way. This illustrates the value of RMD as an aid in interpreting spectra.

In the list for the final RMD run NOE restraints resulting from spin diffusion [41] were not incorporated. These restraints have been eliminated by checking a 50 ms NOESY spectrum. The large majority of the NOE's indicative for secondary structure were observed in the 150 ms, the 100 ms as well as in the 50 ms NOESY spectra. Spindiffusive NOE's appeared to be homogeneously distributed among the amino acid residues of flavodoxin, as expected for a compact globular protein.

It was noted that a 180° rotation of the peptide bond between P121 and D122, and between D122 and N123 would fit the NOE restraints better. As RMD appeared to be unable to perform this transition, we decided to do this manually. Torsion angles of V44, I50 and V67 (χ), and of L85 (χ) were adjusted for the same reason.

In the final distance restraint list one repulsive restraint (*non*-NOE) [42] has been included between N $_5$ H of the flavin and the amide proton of E60, as clearly no NOE has been observed between these protons in the 50, 100 and 150 ms NOESY spectra (see Fig. 1, N $_5$ H=5.61 ppm, NH(60)= 9.39 ppm) [15]. We do not expect that the absence of this NOE is a result of local mobility larger than that of the rest of the protein, because the amide resonance of E60 has several manifest intra- and interresidual NOE connectivities as is the case with the other amino acid residues, e.g. the amino acid residues being part of the central β -sheet of the protein. The β -sheet region will be the most rigid part of the molecule as a consequence of packing restraints [52].

Clear intense NOE cross peaks between the flavin and the apoprotein have been observed [15,16], consistent with the observation that the flavin is tightly bound to the apoprotein [9,12,53]. The protein-bound isoalloxazine ring and the phosphate do not exhibit large fluctuations on the (sub)nanosecond timescale [9,12,53]. Limited flexibility of the flavin on the picosecond time scale however cannot be excluded based on NMR results. It has been demonstrated for globular proteins that when the structures are treated as rigid the analysis of the structures of these proteins based on NOE measurements is meaningful [54-56]. The decrease in NOE intensity as a result of picosecond motions is in general too small to produce a significant change in the distance dependence of the NOE's [57]. We therefore consider the *non*-NOE restraint as meaningful.

For the four yet unassigned exchangeable side chain protons observed in the two-dimensional homonuclear Hartmann Hahn transfer spectra [58], but not in the NOESY spectra [15], we expect that the lack of NOE's is due to fast motions of these protons being part of flexible side chains at the surface of the protein.

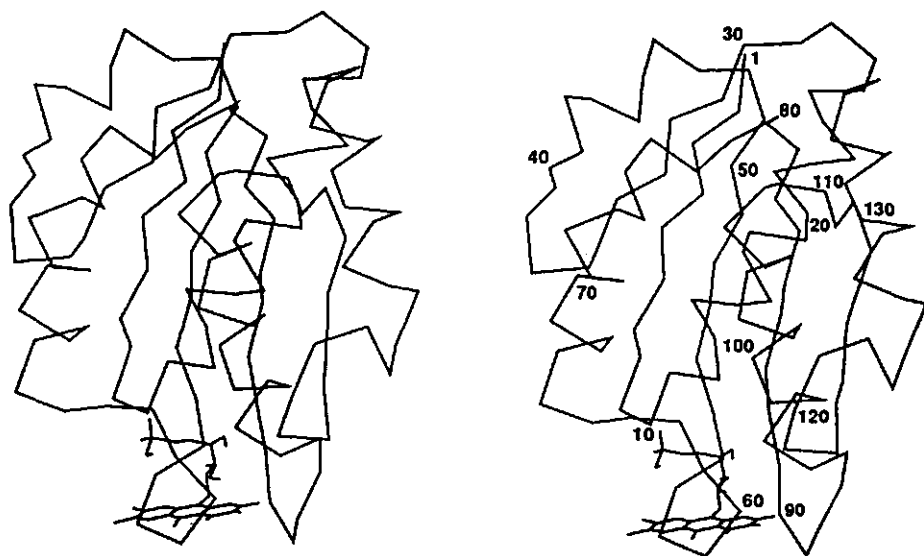
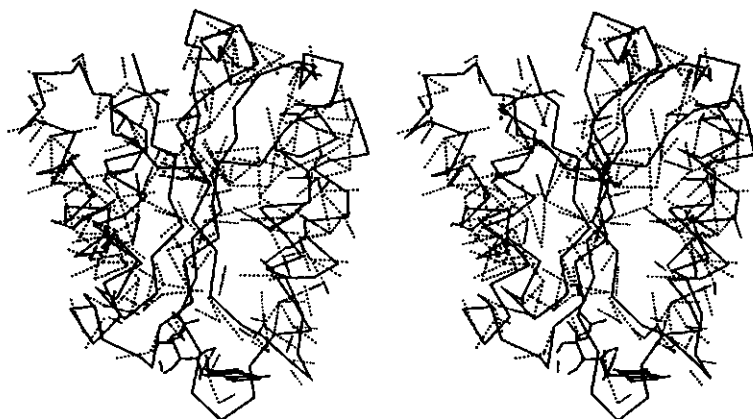


Fig. 3 Stereo drawing showing the C_{α} and FMN atoms of two-electron reduced *M. elsdenii* flavodoxin. The structure has been generated by averaging the RMD trajectory in the range of 60 to 120 ps (see text).

The final distance restraint list of 509 restraints comprised 293 sequential and medium-range distances and 216 long-range distances (amino acid residues at least 4 positions apart in the primary sequence [30]). Subsequently, a RMD run of

120 ps was done. During the first 50 ps the force constant was gradually increased to a high value of 4000 kJ mol⁻¹nm⁻². From 50 ps on the potential energy and distance restraint energy stabilizes to low values, and we decided to keep the force constant at this value. The time span from 60-120 ps, at a time resolution of 0.02 ps, was used for calculating time averages of various quantities and obtaining an average structure.

A



B

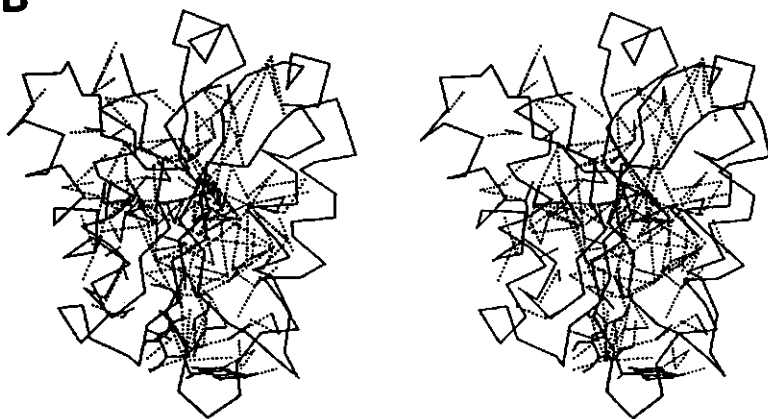


Fig. 4 Representation of the sequential and medium-range NOE's (Fig. 4A) and of the long-range NOE's (amino acid residues at least four residues apart in the primary sequence, Fig. 4B) in the structure of flavodoxin (the structure has been generated by averaging the RMD trajectory in the range of 60 to 120 ps). C_α and FMN atoms are shown, NOE's are depicted by dashed lines to the positions of atoms involved. Fig. 4A comprises 293 restraints and Fig. 4B comprises 215 restraints.

This resulted in a structure of two-electron reduced *M. elsdenii* flavodoxin that satisfies the experimental restraints very well (Figs. 2 and 3). The structure has a low potential energy (-2278 ± 122 kJ mol⁻¹) and essentially satisfies the experimental distance restraints (time averaged sum of all violations is 2.27 nm, largest occurring violation is 0.07 nm). In the following we will refer to this as the averaged structure.

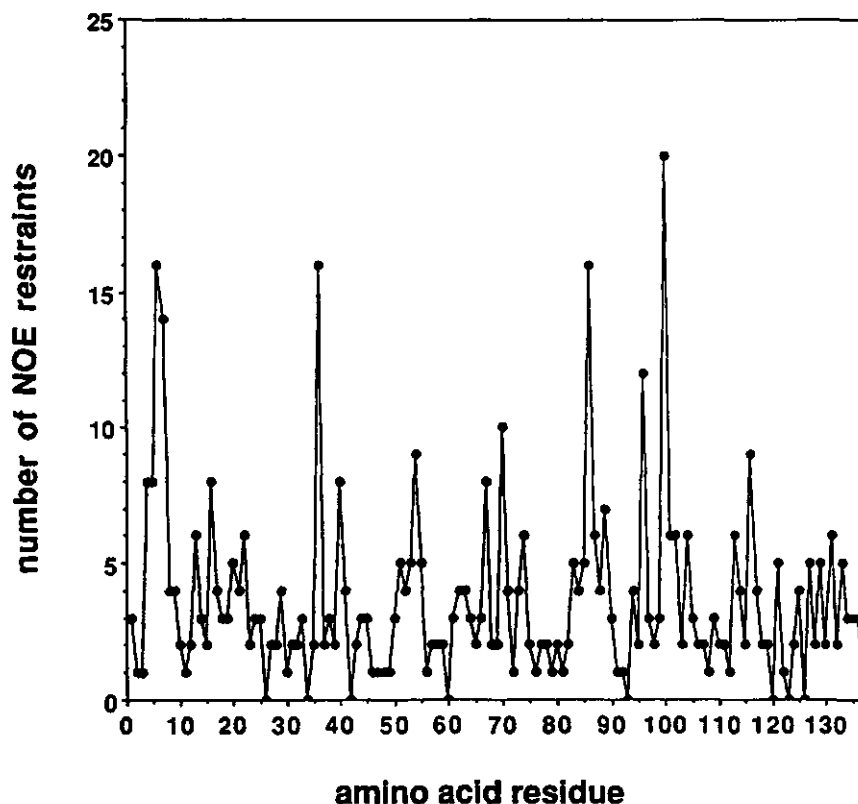


Fig. 5 Number of NOE restraints per amino acid residue as used in the final RMD calculations. NOE contacts resulting from spin-diffusion have not been incorporated; no difference has been made between short- and medium-range NOE's and long-range NOE's.

A pictorial representation of sequential and medium-range NOE's and the long-range NOE's is given in Fig. 4. There is a very good spreading of restraints over the molecule. The compactness of flavodoxin is reflected in a large number of long-range NOE's resulting in a high definition of the tertiary structure (Fig. 4). Fig. 5 shows the number of restraints per amino acid residue; only a few residues, all at

the surface of the molecule, are unrestrained. Fig. 6 shows a superposition of 7 structures of flavodoxin generated in the range 60-120 ps with a 10 ps time-interval, all satisfying the NOE restraints. As can be seen, the flexibility of the β -strand is low. The helices of the protein exhibit higher positional flexibility, whereas turn and coil regions have the highest flexibility, as expected. However, the flexibility, even for the turn and coils, is still rather low. The average RMSD for an ensemble of structures with 5 ps time-spacing in the range from 60 to 120 ps is 0.57 Å for the main chain atoms and 0.85 Å for the side chain atoms. Fig. 7 depicts the root mean square variations for main chain and side chain atoms in this ensemble. It should be noted that the RMD run has been performed in vacuo. Calculations in the presence of water are expected to result in smaller fluctuations. The relatively high main chain fluctuations of W91 and N123 (respectively 1.4 and 1.1 Å) and side chain fluctuations of R35, E61, E95, E119 and M120 (respectively 1.8, 2.0, 2.1, 1.9 and 1.8 Å) will be the result of the in vacuo calculations, as all these residues are on the surface of the molecule.

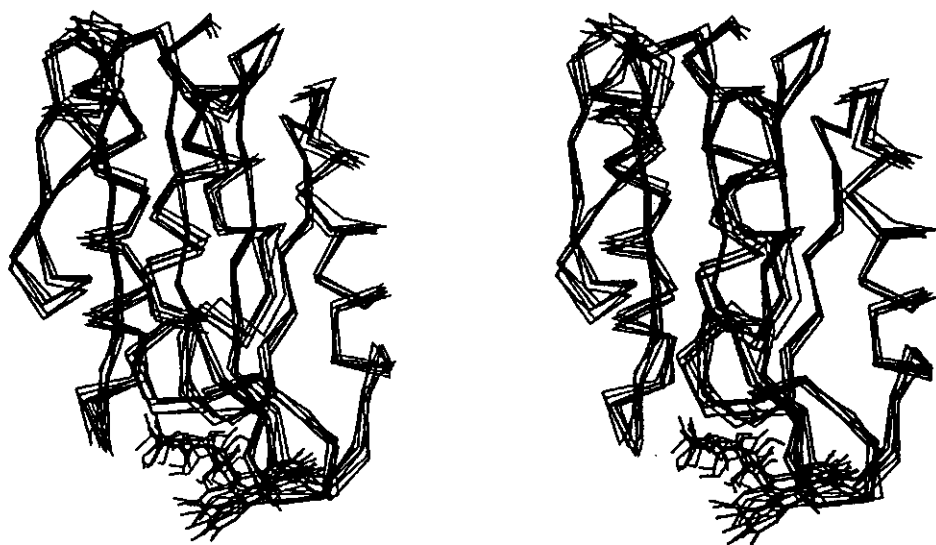
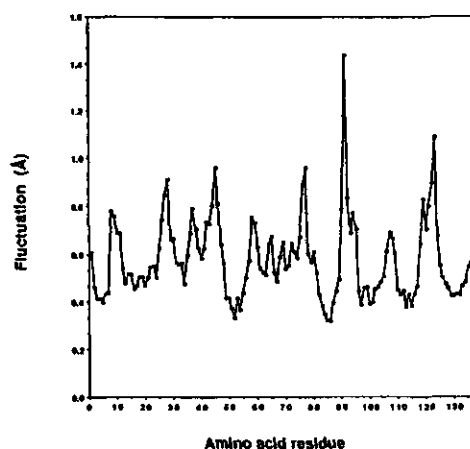


Fig. 6 Superposition of 7 flavodoxin structures showing the C_{α} positions. Time-spacing between the structures is 10 ps, starting with the structure after 60 ps RMD using 509 distance restraints (see text).



B. Average side chain fluctuation

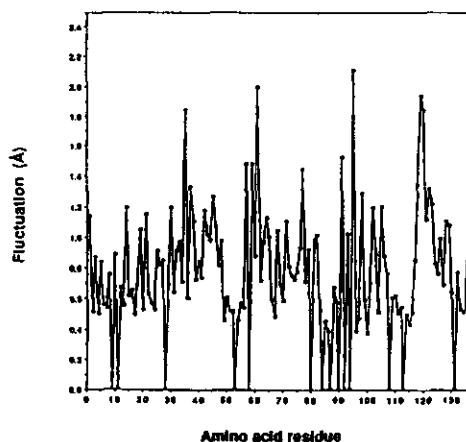


Fig. 7 Main chain (Fig. 7A) and side chain fluctuations (Fig. 7B) of two-electron reduced *M. elsdenii* flavodoxin as calculated from the RMD trajectory in the range of 60 to 120 ps. Amino acid residues having no side chain fluctuations in Fig. 7B are glycines.

Figure 8 depicts the Ramachandran (ϕ, ψ)-plot [59] of the averaged structure of the flavodoxin molecule. The majority of the amino acid residues having unfavorable (ϕ, ψ) combinations are glycine residues which are known to have a greater freedom in dihedral angles.

We can conclude that the obtained tertiary structure of two-electron reduced *M. elsdenii* flavodoxin satisfies the NMR restraints very well. The structure will be further analyzed in the following sections.

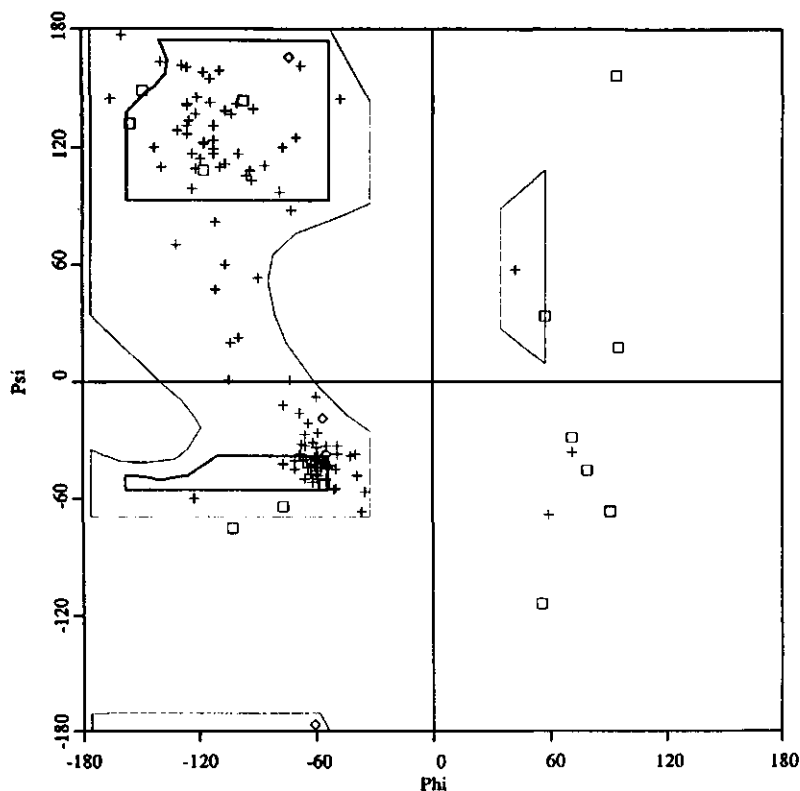


Fig. 8 Ramachandran (ϕ, ψ)-plot of the averaged structure of two-electron reduced *M. elsdenii* flavodoxin. The 'fully allowed' conformation boundary for the NCC' angles $\tau(C_\alpha)=110^\circ$ (bold line) and 'outer limit' boundary for $\tau(C_\alpha)=115^\circ$ (thin line) were taken from [59]. (\square) glycine, (\diamond) proline, (+) other amino acid residues.

Discussion of the tertiary structure

a. secondary structure elements and exchange characteristics

The secondary structure of the averaged protein structure (Fig. 3) has been analyzed using the criteria of Kabsch and Sander [60]. Secondary structure elements are recognized by their specific hydrogen bonding patterns. The secondary structure is summarized in Table 1. In addition to this, the computed water accessibility of amino acid residues has been indicated, as well as the individual amide exchange rates against $^2\text{H}_2\text{O}$ determined via a 2D-NMR exchange experiment [15,16]. Amides with slow exchange rates were present during the $^2\text{H}_2\text{O}$ exchange NOESY experiment which lasted 19.4 h (pH 8.3, 41 $^\circ\text{C}$). Amide protons with fast exchange rates had no detectable resonance intensity in the exchange experiment [15,16]. *M. elsdenii* flavodoxin is clearly a parallel α/β -

protein [61]. Five regions of helicity are recognized: N12-A26; V41-A45; D64-L74; E95-D106 and E126-A135 and five regions showing β -sheet characteristics: V2-Y6; V31-R35; V49-G53; K82-Y89 and T110-N118. The small α -helix from V41 to A45 has been predicted [16]. β -sheet strand no. 3 extends from residue V49 to A56 as judged from $d_{\alpha N}$ connectivities, and from V49 to G53 based on hydrogen bonding patterns [60]; this is the result of P55 disturbing the hydrogen bonding pattern.

The water accessibility of amino acid residues being part of the internal β -sheet strands of the flavodoxin molecule is low, many of them are even inaccessible to water molecules (Table 1). This property, combined with hydrogen bonding of the corresponding amide protons, results in the strong persistence of these amides against $^2\text{H}_2\text{O}$ exchange at pH 8.3 and 41 $^\circ\text{C}$ [15,16]. Every second amide proton of the peripheral strands of the β -sheet (V31-R35 and T110-N118) is not hydrogen bonded, and will exchange relatively rapidly with the solvent [38]. This is indeed observed for strand T110-N118, although it exhibits an irregularity in the exchange pattern that is consistent with a β -bulge (Fig. 9).

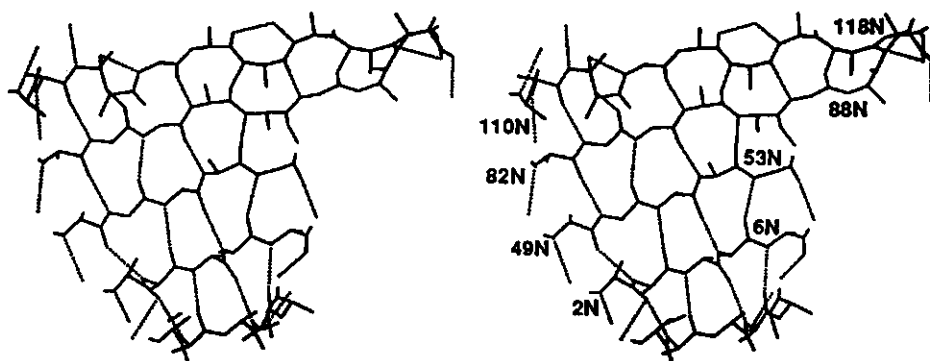


Fig. 9 Stereo drawing showing the C_{α} plot of the central β -sheet of *M. elsdenii* flavodoxin (taken from the structure averaged over 60-120 ps). Hydrogen bonds are indicated by dotted lines. Note the irregularity at residues 112 and 113. In some cases the hydrogen bonding partner has not been depicted as it does not belong to the β -sheet.

Only one amide proton of the other peripheral strand V31-R35 shows slow exchange with the deuterated solvent. This strand is particularly accessible to solvent molecules.

In some cases hydrogen bonding between residues in the calculated structure may result from doing the simulations in the absence of solvent. This could be the case for the hydrogen bond observed between NH(116) and an O_{ϵ} atom of E126 (Fig. 9 shows the hydrogen bond starting at NH(116), the O_{ϵ} atoms of E126 have not been depicted). The amide proton of I116 is exchanging relatively rapidly with

deuterium oxide. Both groups are on the surface of the molecule and accessible to solvent molecules. When water will be included in the calculations, it is very likely that both groups will be stabilized by hydrogen bonding to solvent molecules.

Residues which are part of helices appear to be more accessible to solvent than residues which are part of the β -sheet of the protein. This is in agreement with expectation because the α -helices do not form the core of the molecule but surround it. The majority of the amide protons, which are not part of α -helices or β -sheet strands, exhibits fast exchange with deuterium oxide (Table 1). Such amide protons take part in turns and bends which are less stabilized by hydrogen bonding, and are normally flexible and highly solvent accessible, as they occur most frequently at the surface of proteins [61]; as is also the case for *M. elsdenii* flavodoxin (Fig. 3). (In case an amino acid residue has no calculated solvent accessibility for the averaged structure but its corresponding amide proton does exchange (e.g. T13, Table 1) this must result from flexibility of the molecule.) It can be concluded that the tertiary structure of *M. elsdenii* flavodoxin as presented in this paper is consistent with the amide exchange characteristics.

Table 1: Secondary structure analysis according to Kabsch and Sander [60] of the structure of two-electron reduced *M. elsdenii* flavodoxin (averaged over 60-120 ps). Structure characterization: "H"= α -helix; "B"= residue in isolated β -bridge; "E"= extended strand, participates in β -ladder; "G"= 3-helix (3_{10} helix); "T"= H-bonded turn; "S"= bend. In case of structural overlaps, priority is given to the structure first appearing in the list. The accessibility of an amino acid residue for water molecules is given as an accessible surface (\AA^2), dividing the value by 10 roughly yields the number of water molecules that can be in contact with the amino acid residue. The exchange rate of the amide proton is denoted by the following signs: 0, + and ++, indicating slow, intermediate and fast exchange rates respectively. Amide protons with slow exchange rates were present during the 19.4 h lasting exchange NOESY experiment in $^2\text{H}_2\text{O}$ (pH 8.3, 41 $^\circ\text{C}$). Amide protons with fast exchange rates had no detectable resonance intensity in the exchange experiment [15,16]. The table lists the amino acid residue followed by its secondary structure characterization, accessibility and finally exchange rate.

M1	80	++	E37	T	113	++	D73	H	66	++	A109	3	+
V2	E 1	++	D38	S	94	++	L74	H	1	0	T110	E 57	++
E3	E 6	0	T39		30	++	A75	G	25	++	V111	E 26	++
I4	E 0	0	N40		56	++	P76	G	83		I112	E 39	0
V5	E 0	0	V41	H	17	++	K77	G	87	++	G113	E 27	++
Y6	E 23	0	D42	H	109	++	L78		0	++	T114	E 44	++
W7	40	0	D43	H	78	+	K79	S	126	++	A115	E 0	0
S8	10	++	V44	H	0	+	G80	S	56	++	I116	E 43	++
G9	S 44	++	A45	H	38	+	K81		42	++	V117	E 0	0
T10	S 86	++	S46	T	79	++	K82	E	73	++	N118	E 84	++
G11	S 45	++	K47		24	++	V83	E	0	0	E119	S 84	+
N12	H 1	++	D48	S	79	++	G84	E	0	0	M120	S 101	++
T13	H 0	++	V49	E	0	0	L85	E	0	0	P121	S 9	
E14	H 68	+	I50	E	0	0	F86	E	0	0	D122	S 99	++
A15	H 40	0	L51	E	0	0	G87	E	0	0	N123	S 117	+
M16	H 0	0	L52	E	2	0	S88	E	0	0	A124	15	+
A17	H 0	0	G53	E	0	0	Y89	E	30	0	P125	T 70	
N18	H 76	+	C54		0	0	G90	S	32	++	E126	H 68	++
E19	H 22	+	P55		2		W91	S	198	++	C127	H 0	++
I20	H 0	0	A56		0	0	G92		17	++	K128	H 85	++
E21	H 18	0	M57	B	46	++	S93		54	++	E129	H 101	++
A22	H 59	+	G58	T	51	++	G94	S	19	++	L130	H 7	+
A23	H 19	0	S59	T	96	++	E95	H	124	++	G131	H 0	++
V24	H 0	0	E60	T	22	++	W96	H	2	++	E132	H 88	++
K25	H 126	++	E61	B	103	++	M97	H	11	+	A133	H 31	+
A26	H 91	+	L62		8	++	D98	H	108	++	A134	H 3	++
A27	T 60	++	E63		3	++	A99	H	32	+	A135	H 23	+
G28	T 74	++	D64	H	91	++	W100	H	2	+	K136	T 151	++
A29	21	++	S65	H	82	++	K101	H	90	0	A137	33	++
D30	96	++	V66	H	26	++	Q102	H	103	++	FMN*	134	++
V31	E 29	+	V67	H	3	+	R103	H	74	+			
E32	E 39	++	E68	H	45	+	T104	H	0	+			
S33	E 36	++	P69	H	72		E105	H	82	+			
V34	E 40	0	F70	H	15	++	D106	T	111	++			
R35	E 70	++	F71	H	29	0	T107	T	32	+			
F36	T 7	++	T72	H	97	+	G108	T	51	+			

* N₃H and N₅H of the flavin do exchange rapidly with deuterons.



Fig. 10 Superposition of the 'solution' structure of two-electron reduced *M. elsdenii* flavodoxin (averaged over 60-120 ps RMD) and the crystal structure of one-electron reduced *Clostridium MP* flavodoxin. The RMSD of the C_{α} atoms of both structures was minimized by translation and rotation. Bold line: *M. elsdenii* flavodoxin; thin line: *Clostridium MP* flavodoxin.

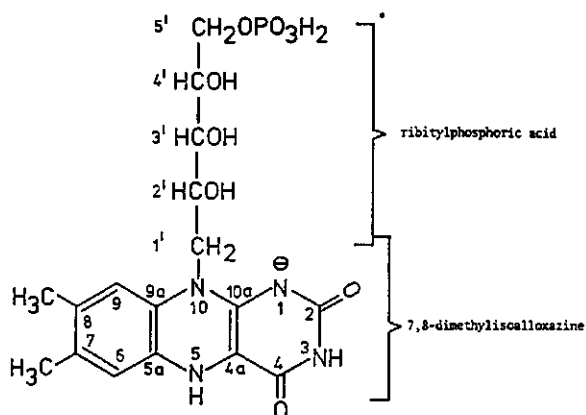


Fig. 11 Structure of two-electron reduced riboflavin 5'-phosphate (FMNH[•]).

The high structural similarity between flavodoxin from *Clostridium MP* and *M. elsdenii* has been visualized in Fig. 10. A striking difference is observed in the

position of the phosphate moiety of FMN (Fig. 11). Investigation of 'snap shot' structures from the 60-120 ps interval showed torsional fluctuations around the C5'-O5' axis, as well as flipping motions of the benzene part of the isoalloxazine.

b. the FMN binding region

Amino acid residues W7-T13, G53-E63, G87-A99 and I116-E119 form the flavin binding site of flavodoxin, as judged from disappearance or broadening of the corresponding proton resonances in a solution of flavodoxin molecules in the semiquinone state [15,16]. The amino acid residues A56-E61 and Y89-G92 are in the immediate neighbourhood of the isoalloxazine ring of the flavin molecule. This is in agreement with the observation of the instantaneous disappearance of the corresponding proton resonances in a solution of reduced flavodoxin containing a small amount semiquinone, the result of a fast electron transfer between the flavodoxin molecules [11,15].

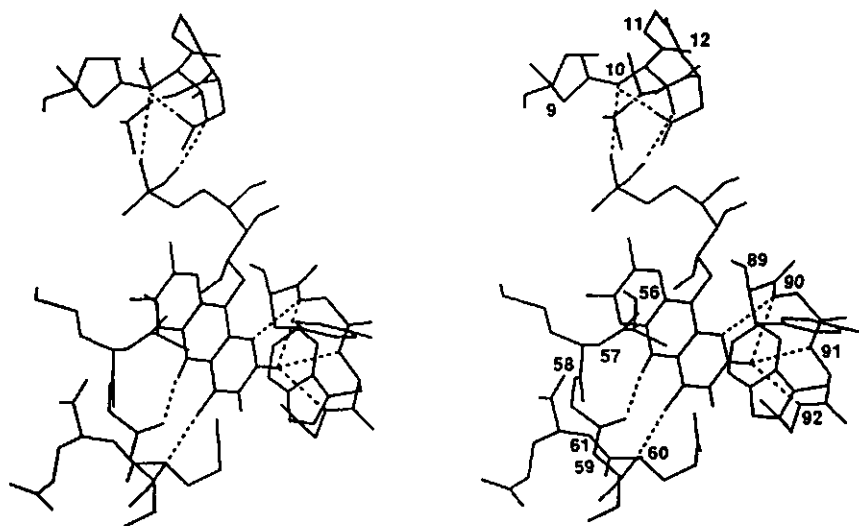


Fig. 12 Stereo drawing showing the environment of the isoalloxazine moiety and the phosphate group of two-electron reduced *M. elsdenii* flavodoxin (structure averaged over 60-120 ps RMD). The region includes S8-T13, A56-E61 and Y89-G92. Hydrogen bonds (existing at least 30% of the time in the trajectory 60-120 ps) are shown by dashed lines connecting the donor and acceptor. Amides have been labeled.

The phosphate group and C5'H, C4'H, C4'OH, C3'H and C3'OH do not have NOE restraints, whereas C1'H, C2'OH, C6H, CH₃(7 α) and C9H of the flavin do have NOE restraints. The phosphate group shows strong positional fluctuation during the

molecular dynamics simulation (1.18 Å RMSD fluctuation). Positions differ as much as 4 Å. We do not believe that such a high flexibility is realistic, but is a computational artefact resulting from two effects.

Firstly, the phosphate is bound in the dianionic form [9]. The negatively charged phosphate is expected, in analogy to *Clostridium MP* flavodoxin, to be strongly hydrogen bonded to the loop S8-T13. The phosphate is necessary for a strong binding of FMN to the apoprotein of *M. elsdenii* ($K_a=1.1 \times 10^8 \text{ M}^{-1}$ in the reduced state) and *Clostridium MP* flavodoxin, riboflavin does not bind to a detectable extent ($K_a < 10^3 \text{ M}^{-1}$) [1]. The hydrogen bonding capacity of the loop region can be observed in Fig. 12. However, in the RMD calculations the two negative charges on the phosphate could not properly be taken into account.

Secondly, water plays an important role in regions of the molecule accessible to solvent molecules and having a charge. The phosphate binding region is accessible to solvent molecules as observed in an amide exchange experiment (Table 1). The hydrogen bond between NH(10) and O_e(12), observed in the RMD run, might be the result of the absence of water molecules. Based on the high structural similarity between *M. elsdenii* and *Clostridium MP* flavodoxin we do expect the phosphate binding regions to be virtually identical. This implies, for the *M. elsdenii* protein, hydrogen bonds from the phosphate to the amides of G9, T10, N12 and T13 and to S8OH, T10OH and T13OH. The amide protons of G9, T10, N12 and T13 resonate at very low field, at 10.43, 9.35, 11.49 and 11.40 ppm respectively [15]. This is consistent with a low electron density on these protons as a result of strong hydrogen bonding to the negatively charged phosphate. The amides of T10, N12 and T13 are at least 5.0 Å away from the indole part of W7 which is the aromatic amino acid residue in closest proximity to the phosphate binding region. This suggests that the vicinity of the phosphate is the major cause for the anomalous chemical shifts. The resonance position of the amide of G9 might be influenced by the indole part of W7 which is in proximity. Quijcho et al. [62] proposed, based on detailed investigations of a few crystal structures of proteins, that isolated charges can be stabilized by peptide dipoles in the interior of a protein. Our NMR results suggest that the phosphate group is 'solvated' by the local dipolar components of the apoprotein. Local polarity of the protein is expected to play an important role in the stabilization of ionic groups [63]. The study on flavodoxin is to our knowledge the first support of such stabilizing peptide dipoles based on experimentally determined chemical shifts of amide protons and not based solely on distance information [62].

The amide proton of G11 is not expected to form a hydrogen bond to the phosphate. This is reflected in its chemical shift of 7.55 ppm [15]. Observation of the exchangeable protons S8OH, T13OH and NH_e(12) in the loop-like phosphate-

binding region at a relatively high pH of 8.3 and 41 °C [15] is strongly indicative for strong hydrogen bonding of these protons (as in the crystal structure of *Clostridium MP* flavodoxin [2-4]). The hydroxyl functions of S8 and T13 both resonate downfield shifted from their expected resonance positions. The hydroxyl group of T10 does not form a strong hydrogen bond to the phosphate group as its resonance has not been observed.

Despite the hydrogen bonding to the phosphate the amides of G9, T10, N12 and T13 exhibit fast exchange with the deuterated solvent on the time scale of a two-dimensional NOESY exchange experiment (Table 1); the amino acid residues are clearly solvent accessible. This is in contradiction with the results of Moonen and Müller [9] who showed that "the phosphate group is deeply buried in the apoenzyme and inaccessible to the solvent". They based their conclusions on the pH-independence of the ^{31}P chemical shift in the pH range 6.0-9.2 of the flavodoxin solution, and on the constant linewidth of the phosphorus resonance on redissolving the flavodoxin in water after it had been dissolved in deuterium oxide (at pH 8.2, 26 °C [9]). In the 2D- ^1H NMR spectra the chemical shifts of the amide protons involved in phosphate binding of *M. elsdenii* flavodoxin appear to be almost independent (0.1 ppm variation) of the pH in the region 7.0-8.3 in samples containing varying percentages semiquinone/hydroquinone. This is in agreement with and complementary to the results of Moonen and Müller [9]. The hydrogen bonding to the phosphate group overshadows the pH effect as is also the case for the phosphorus resonance. The amide protons hydrogen bonding to the phosphate exchange relatively rapidly with the deuterated solvent. In the first scan of a two-dimensional NOESY exchange experiment they are already exchanged (the sample was kept on ice during dissolving the protein in deuterium oxide, the first scan was taken approximately an half hour after the sample was put into the magnet at 41 °C, unpublished observation). This explains the constant linewidth of the phosphorus resonance after redissolving the flavodoxin in water, as every deuterium has already been replaced by a proton before the first NMR scan had been acquired by Moonen and Müller [9]. The solvent accessibility of the phosphate as determined by NMR demonstrates the need for additional RMD calculations of the three-dimensional structure of *M. elsdenii* flavodoxin in the presence of water.

C2'OH of the ribityl side chain forms a hydrogen bond with the carbonyl of A56 and C3'OH with O_e of E119. The latter hydrogen bond is not expected, as the resonance of C3'OH is absent in the 2D-NMR spectra caused by too rapid exchange with the solvent [15]. In *Clostridium MP* and *D. Vulgaris* flavodoxin, the C3'OH is accessible to the solvent as deduced from X-ray [2-5] and ^{31}P NMR data [64] on the native and with riboflavin 3',5'-bisphosphate reconstituted proteins. The hydrogen bond observed for *M. elsdenii* flavodoxin is therefore expected to be an

artefact resulting from calculation without water. C₄'OH also has a hydrogen bond to an O_e atom of E119 in the averaged structure (60-120 ps). This hydrogen bond is real and is reflected by the observation of C₄'OH by NMR despite its position on the periphery of the molecule.

Table 2: Short contacts involving hydrogen bonds between the isoalloxazine moiety and the apoproteins of two-electron reduced *M. elsdenii* flavodoxin and one-electron reduced *C. MP* flavodoxin [3]. Hydrogen bond criteria: hydrogen-acceptor distance ≤ 0.25 nm; donor-hydrogen-acceptor angle $\geq 135^\circ$.

FMN atom	<i>Clostridium MP</i> flavodoxin	distance (Å)	<i>M. elsdenii</i> flavodoxin	distance (Å)
N(1)	G89(NH)	3.0	G90(NH)	2.3
N(3)H	E59(O _e)	2.7	E60(O _e)	3.4
N(5)H	G57(O)	2.8	G58(O)	2.1
O(2)	G91(NH)	2.9	G92(NH)	1.9
O(2)	G89(NH)	3.0	G90(NH)	2.2
O(2)	W90(NH)	3.2	W91(NH)	2.3
N(1)			W91(NH)	2.9
O(4)	E59(NH)	2.8	E60(NH)	2.0

In Fig. 12 the hydrogen bonding of the isoalloxazine moiety with the apoprotein is depicted, the situation is very similar to *Clostridium MP* flavodoxin [3]. Distances between the hydrogen bonding partners as determined for *Clostridium MP* flavodoxin [3] and *M. elsdenii* flavodoxin are given in Table 2. Differences between both proteins are observed in the distances between N₁ and O₂ of the flavin and the neighbouring amides. In the two-electron reduced *M. elsdenii* flavodoxin (having a negative charge on N₁ [12]) the NOE restraints lead to a structure that is more compact around N₁ and O₂ than in one-electron reduced *Clostridium MP* flavodoxin. It is not yet clear whether this is a consequence of introducing an negative charge on N₁ (reflected in the NOE restraints) as compared to the one-electron reduced state of *Clostridium MP* flavodoxin, or whether this results from omitting water molecules from the calculations.

Part of the isoalloxazine binding region is accessible to solvent molecules, evidenced by the computed solvent accessibility of many of the constituting residues, and by the exchange characteristics of the amide protons in this region in a NOESY exchange experiment at 41 °C, pH 8.3 (Table 1). The majority of the amide protons in this region shows a rapid exchange with the deuterated solvent. The amino acid residues P55, A56 and S88 are however, inaccessible to solvent

molecules. The accessibility does not imply that exchangeable protons of flavodoxin do exchange rapidly with solvent on the **NMR time scale**. Such a rapid exchange would result in saturation transfer from the irradiated water to these exchangeable protons, as observed for the amide protons of V41, D48, G80, N118, D122 and E126 of two-electron reduced flavodoxin [15]. All other exchangeable protons are detected in a NMR experiment with water as solvent [15] implying that these protons do not rapidly exchange within a time span of a few seconds. This is also consistent with previous ^{15}N NMR results showing that N_3H and N_5H of the flavin do exchange slowly on the NMR time scale [12], and with the indifference of the 5'-phosphate group on addition of Mn^{2+} to the solvent [64], as Mn^{2+} will not come in close contact with the phosphate group on the time scale of seconds. The possibility of measuring exchange characteristics of individual protons by NMR signifies important additional information on protein tertiary structure. In the crystallographic study on one-electron reduced *Clostridium MP* flavodoxin one water molecule has been observed in the immediate vicinity of the isoalloxazine moiety and three water molecules in the vicinity of the ribityl side chain. Contact of the isoalloxazine moiety with the solvent was regarded as severely restricted [3], the benzene part of the isoalloxazine appeared solvent accessible.

Moonen et al. [65] proposed electrostatic interactions as the main factor determining the redox potential for the semiquinone/hydroquinone transition in flavodoxins. Entropy changes between one- and two-electron reduced *M. elsdenii* flavodoxin will not contribute significantly to the free energy change, hence to its redox potential, because there is no large conformational difference between the two redox states as judged by kinetic exchange experiments [11]. The electrostatic interaction energy between the negative charge on the N_1 of the protein-bound two-electron reduced FMN and the two negative charges on the phosphate group of FMN, separated by a distance of approximately 8 Å, were postulated to represent the dominant contribution to the corresponding redox potential of the flavodoxins, assuming a relative dielectric constant of 20 [65]. Also the monopole-monopole interaction between N_1 and the negative charges of the protein, and the monopole-dipole interaction between N_1 and the dipole moment of the protein were considered to contribute to the redox potential, but both to a lesser extent than the N_1 -phosphate interaction. The phosphate group and the isoalloxazine ring were considered to be tightly bound and buried in the protein. The present study however indicates that the phosphate-binding region and part of the isoalloxazine binding region are accessible to the solvent. Recent insights in the importance of electrostatic interactions in proteins [63, 66-68] show that charges can be effectively stabilized, especially in solvent accessible regions of the protein, resulting in large effective dielectric constants in these regions (ϵ_r between 30 and 60 in most cases

[63]), thus rendering long-range electrostatic interactions less determining. Based on charge stabilization and solvent accessibility it could be imagined that the role of the negatively charged phosphate group on the redox potential of the flavodoxin will be less dominant than proposed [65]. Short-range electrostatic interactions ($R < 4 \text{ \AA}$) caused by local polarities were reported to be very important, e.g. in the case of the control of the redox potential of cytochrome *c* (103 amino acid residues) as compared to a reference octapeptide system with a methionine-histidine ligated heme, having the same heme-ligand complex as cytochrome *c* [67]. The difference in redox potential between these systems is about 300 mV. In this study, interactions between the heme charges and the protein permanent dipoles (e.g., the N-H and C=O dipoles of the peptide bonds), the protein induced dipoles and the water molecules were calculated as were the monopole-monopole interactions between charges. The polarization of water molecules around cytochrome *c* appeared to compensate largely the electrostatic interactions between the charge center of the oxidized heme and the propionate O^- , being at a distance of 8 Å of the heme center. This corresponds to a large dielectric constant. The major contribution to the redox potential of cytochrome *c* as compared to the octapeptide appeared to be the destabilization of the heme charge in the oxidized state (relative to its energy in water) by its local microenvironment as compared to the reduced heme. The microenvironment can be considered as a medium of low dielectric constant [67]. For *M. elsdenii* flavodoxin we are dealing with a comparable situation: a charged N_1 of the isoalloxazine ring in case of two-electron reduction and an uncharged N_1 in case of one-electron reduction. The electrostatic interaction between the charge on N_1 and the phosphate is expected to be, as for cytochrome *c*, largely compensated as a result of polarization of water molecules present in the immediate neighbourhood of both groups.

The NMR results concerning the water accessibility of amino acid residues in the flavin binding region will be essential in understanding the redox properties of this protein. We think, related to the situation described for cytochrome *c*, that the charged N_1 is destabilized by its nonpolar microenvironment in which no charged group is present within a distance of 6 Å of the N_1 as is deduced from the tertiary structure, as compared to the uncharged situation (both relative to their energies in water) resulting in a major contribution to the redox potential. The presence of water molecules in the vicinity of the isoalloxazine moiety, as evidenced by the amide exchange characteristics, does not imply that a water molecule is present at the N_1 position, no space is present at that position for such a molecule as is also the case for *Clostridium MP* flavodoxin [69]. Such a water molecule would result in protonation of the N_1 , which is not observed in *M. elsdenii* flavodoxin [12]. The electrostatically destabilized (relative to water), negatively charged N_1 is expected

to be crucial in the explanation of the redox potential of this flavodoxin. A calculation of the overall free energy change associated with the change in N_1 charge on going from the semiquinone to the hydroquinone state, in which the electrostatic solvent effects are properly taken into account, will reveal the roles of the various electrostatic interactions in determining the redox potential. To gain more insight in the role water is expected to play in the flavin-binding region of flavodoxin additional simulations taking water molecules into account will be performed. Such calculations are expected to result in a tertiary structure slightly different from the one presented here, but nevertheless important in view of the function of flavodoxin. For example the distance between the amides of E60 and E61, which are both close to the isoalloxazine, is 3.0 Å in the structure presented here (the corresponding amides are separated by 2.9 Å in the crystal structure of *Clostridium MP* flavodoxin). No d_{NN} contact between both amino acid residues is observed however.

c. NMR parameters and tertiary structure

Knowing a tertiary structure consistent with the NOE distance restraints of *M. elsdenii* flavodoxin, it is possible to have a closer view at some features of this molecule, notably typical NH chemical shifts. Amide backbone protons exhibiting a chemical shift that exceeds 9.50 ppm are expected to reflect specific properties of the flavodoxin molecule; these include the amides of G9, N12, T13, V34, E37, L51, V66, F71, G90, G92, S93, W96, N123 and E126 [15]. The large majority of the amide proton resonances of proteins reported so far have chemical shifts below 9.5 ppm [70]. The typical chemical shifts of G9, N12 and T13 are expected to result from the strong hydrogen bonding to the dianionic phosphate of the FMN molecule as already described. The amide protons of G90, G92 and S93 are in the plane of the flavin molecule, their down-field shifts result from ring currents in the aromatic part of the prosthetic group. The amide proton resonances of V34, E37, V66, F71 and W96 are shifted downfield, probably as a result of local magnetic fields caused by aromatic groups in the immediate vicinity of these protons.

There are no aromatic groups in the immediate vicinity of the amide protons of L51, N123 and E126, nor are these protons significantly stronger hydrogen bonded than the other amide protons. Presently we have no explanation for the extreme resonance positions of these amide resonances (9.65, 10.49 and 10.32 ppm respectively [15]). In the immediate neighbourhood of N123 and E126 are proline residues, respectively P121 and P125, which are known as 'structure breakers'; this might exert an effect on the chemical shift of these amides [71].

Another typical property of two-electron reduced flavodoxin is the unusual line shape of several cross peaks in the two-dimensional NMR spectra (Fig. 1, cross

peaks labeled 3, 3/2, 4/3, 32/3, 2/31, 31/32, 4/33, 51/50, 112/111; the residues concerned are all part of the central parallel β -sheet of flavodoxin). The wing shaped line shape is also observed for these cross peaks in the two-dimensional amide exchange experiment against deuterons as they do not disappear [16]. The wing shape is enhanced when the temperature of the sample is increased (unpublished observation). The resonances of amino acid residues V2, E3, I4, E32, L51, K82, G84 and I112 are exhibiting these lineshapes. The effect is strongest for the NOESY cross peaks involving the amide resonances of V2, E3, I4 and E32 (see Fig. 1). The extraordinary line shape immediately disappears on slight oxidation of the two-electron reduced flavodoxin sample, normal lineshapes are then observed (Fig. 7 and Fig. 8 in [15]).

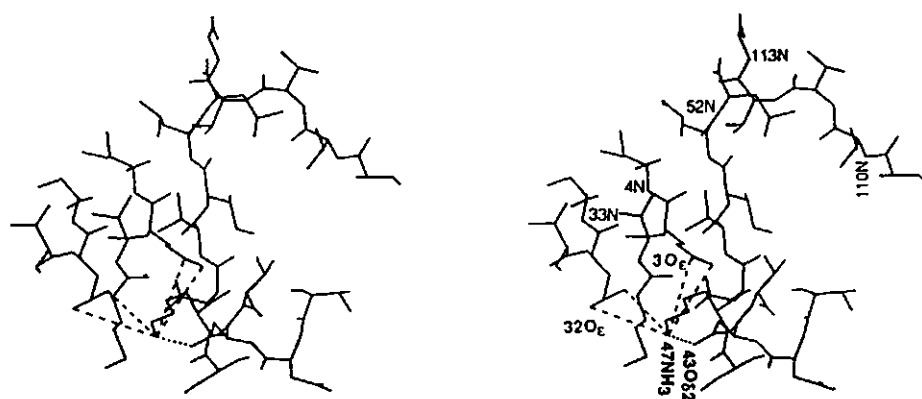


Fig. 13 Stereo picture showing a saltbridge between the polar head groups of E3, E32, D43 and K47. The region shown includes M1-I4, V31-S33, V41-V44, S46-L52 and A109-G113, residues mainly belonging to the central β -sheet of *M. elsdenii* flavodoxin. The polar parts, involved in the saltbridge are solvent accessible.

We have demonstrated using NOESY difference spectra [15] that a pH drop of approximately 0.5 unit occurs on slight oxidation of a completely reduced flavodoxin sample. On basis of the local structure around V2, E3, I4 and E32 (Fig. 13) we now tentatively explain these typical lineshapes as a result of instability of a saltbridge between the polar groups of the side chains of E3, E32, D43 and K47. The majority of the flavodoxin molecules has a saltbridge in this region of the protein, these molecules are characterized by a normal symmetric lineshape at the central position of the corresponding cross peaks. As a consequence of the high pH (pH=8.3) and temperature (41 °C) this saltbridge is not present anymore in a fraction of the molecules. We think a small structural rearrangement of the side chains is responsible for the existence of two slightly different structures, with

slightly different resonance positions. These two structures do not interconvert on the NMR timescale but can both return to the original saltbridge conformation with an intermediate exchange rate on the NMR timescale. Both structures exhibit the same decreased resonance position of the corresponding backbone amide resonances and different aliphatic resonance positions resulting in the typical line shape as observed in Fig. 1. On slight oxidation of the sample the pH drops immediately, the saltbridge is then stabilized and all flavodoxin molecules have the same conformation again, evidenced by the normal line shape then observed. It is remarkable that the disruption of this saltbridge not only results in a local rearrangement of amino acid residues, but that its influence is extended over a large part of the central β -sheet structure (e.g. the amide resonance of I112, roughly 20 Å separated from the saltbridge, is exhibiting the same typical line shape) of the flavodoxin molecule. This is a nice illustration of the influence of dynamic phenomena on line shape; it is, to our knowledge, the first time such local rearrangements are observed within proteins by use of NMR. There are no indications for any change in the structure of the flavin binding region.

Concluding remarks

A tertiary structure of two-electron reduced *M. elsdenii* flavodoxin has been determined that satisfies the NOE restraints very well (0.66 Å maximum NOE violation). The definition of the structure of the apoprotein is high. FMN was found to be very flexible. We expect this to be an artefact of calculations without solvent, and without proper charges on the phosphate and N₁ position. The flavin binding region, being the interesting part of the molecule, is largely solvent accessible as determined by a two-dimensional NOESY exchange experiment (this does not imply rapid amide proton exchange on the NMR time scale). We expect the presence of water in the neighbourhood of the flavin to be important in the redox potential regulation of the semiquinone/hydroquinone couple of flavodoxin. Beside satisfying the NOE restraints, the structure of *M. elsdenii* flavodoxin obtained is largely consistent with other NMR parameters such as amide exchange characteristics. Based on the high structural similarity between *M. elsdenii* and *Clostridium MP* flavodoxin, we think that water plays virtually the same role in both proteins.

Using the structure information gathered now it is possible to have a closer view at *M. elsdenii* flavodoxin in the oxidized state, as will be presented in the near future. The still remaining unassigned NOE cross peaks for the two-electron reduced state of the protein can be assigned using the detailed tertiary structure as presented in this paper and these can then be used as additional NOE restraints for

refining the tertiary structure of this protein. In addition to this it will be possible to make a number of stereospecific assignments by comparing distances in the obtained structure with intensities; this leads to better definition of the structure [38]. Molecular dynamics simulations of the structure of *M. elsdenii* flavodoxin taking the solvent into account are planned and will be required for more accurate results.

Acknowledgements

We would like to thank Gert Vriend for his kind and expert assistance at using WHATIF. All 2D-NMR experiments have been performed at the HF-SON NMR-Facility, Nijmegen, the Netherlands. This study was carried out under the auspices of the Netherlands Foundation for Chemical Research (SON) with financial aid from the Netherlands Organization for the Advancement of Pure Research (NWO). The EMBL (Heidelberg, Federal Republic of Germany) and the BIOSON institute (Groningen, the Netherlands) kindly supplied us with computer facilities which is gratefully acknowledged.

References

1. Mayhew, S.G. & Ludwig, M.L. (1975) *Enzymes 3rd Ed.* 12, 57-118.
2. Burnett, R.M., Darling, G.D., Kendall, D.S., LeQuesne, M.E., Mayhew, S.G., Smith, W.W. & Ludwig, M.L. (1974) *J. Biol. Chem.* 249, 4383-4392.
3. Smith, W.W., Burnett, R.M., Darling, G.D. & Ludwig, M.L. (1977) *J. Mol. Biol.* 117, 195-225.
4. Ludwig, M.L., Burnett, R.M., Darling, G.D., Jordan, S.R., Kendall, D.S. & Smith, W.W. (1976) in *Flavins and Flavoproteins* (Singer, T.P., ed.) pp. 393-404, Elsevier, Amsterdam.
5. Watenpaugh, K.D., Sieker, L.C. & Jensen, L.H. (1973) *Proc. Nat. Acad. Sci. Us* 70, 3857-3860.
6. Smith, W.W., Patridge, K.A., Ludwig, M.L., Petschko, G.A., Tsernoglou, D., Tanakar, M. & Yasanobu, K.T. (1983) *J. Mol Biol.* 165, 737-755.
7. Ludwig, M.L., Patridge, K.A. & Tarr, G. (1984) in *Flavins and Flavoproteins* (Bray, R.C., Engel, P.C. & Mayhew, S.G. eds.) pp. 253-259, Walter de Gruyter & Co., Berlin-New York.
8. Laudenbach, D.E., Straus, N.A., Patridge, K.A. & Ludwig, M.L. (1987) in *Flavins and Flavoproteins* (Edmondson, D.E. & McCormick, D.B. eds.) pp. 249-260, Walter de Gruyter & Co., Berlin-New York.
9. Moonen, C.T.W. & Müller, F. (1982) *Biochemistry* 21, 408-414.

10. Moonen, C.T.W., Hore, P.J., Müller, F., Kaptein, R. & Mayhew, S.G. (1982) *FEBS Lett.* **149**, 141-146.
11. Moonen, C.T.W. & Müller, F. (1984) *Eur. J. Biochem.* **140**, 303-309.
12. Vervoort, J., Müller, F., Mayhew, S.G., van den Berg, W.A.M., Moonen, C.T.W. & Bacher, A. (1986) *Biochemistry* **25**, 6789-6799.
13. Schagen van, C.G. & Müller, F. (1981) *FEBS Lett.* **136**, 75-79.
14. Moonen, C.T.W., Scheek, R.M., Boelens, R. & Müller, F. (1984) *Eur. J. Biochem.* **141**, 323-330.
15. Mierlo van, C.P.M., Vervoort, J., Müller, F. & Bacher, A. (1990) *Eur. J. Biochem.* **187**, 521-541.
16. Mierlo van, C.P.M., Müller, F. & Vervoort, J. (1990) *Eur. J. Biochem.*, (in press).
17. Van Gunsteren, W.F., Kaptein, R. & Zuiderweg, E.R.P. (1983) in *Nucleic Acid Conformation and Dynamics* (Olson, W.K., ed.) Report of NATO/CECAM Workshop, pp. 79-92, Orsay, France.
18. Kaptein, R., Zuiderweg, E.R.P., Scheek, R.M., Boelens, R. & van Gunsteren, W.F. (1985) *J. Mol. Biol.* **182**, 179-182.
19. Clore, G.M., Brünger, A.T., Karplus, M. & Gronenborn, A.M. (1986) *J. Mol. Biol.* **191**, 523-551.
20. Havel, T.F., Crippen, G.M. & Kuntz, I.D. (1979) *Biopolymers* **18**, 73-81.
21. Havel, T.F., Kuntz, I.D. & Crippen, G.M. (1983) *Bull. Math. Biol.* **45**, 665-720.
22. Braun, W. & Go, N. (1985) *J. Mol. Biol.* **186**, 611-626.
23. Arseniev, A.S., Kondakov, V.I., Maiorov, V.N. & Bystrov, V.F. (1984) *FEBS Lett.* **165**, 57-62.
24. Williamson, M.P., Havel, T.F. & Wüthrich, K. (1985) *J. Mol. Biol.* **196**, 611-639.
25. Clore, G.M., Sukumaran, D.K., Nilges, M. & Gronenborn, A.M. (1987) *Biochemistry* **26**, 1732-1745.
26. Clore, G.M., Sukumaran, D.K., Nilges, M., Zarbock, J. & Gronenborn, A.M. (1987) *EMBO J.* **6**, 529-537.
27. Cooke, R.M., Wilkinson, A.J., Baron, M., Pastore, A., Tappin, M.J., Campbell, I.D., Gregory, H. & Sheard, B. (1987) *Nature* **327**, 339-341.
28. Clore, G.M., Gronenborn, A.M., Nilges, M., Sukumaran, D.K. & Zarbock, J. (1987) *EMBO J.* **6**, 1833-1842.
29. Holak, T.A., Kearsley, Y.K. & Prestegard, J.H. (1988) *Biochemistry* **27**, 6135-6142.
30. Zuiderweg, E.R.P., Nettesheim, D.G., Mollison, K.W. & Carter, G.W. (1989) *Biochemistry* **28**, 172-185.
31. Mayhew, S.G. & Massey V. (1969) *J. Biol. Chem.* **244**, 794-802.
32. Marion, D. & Wüthrich, K. (1983) *Biochem. Biophys. Res. Commun.* **113**, 967-974.

33. Rance, M., Sörenson, O.W., Bodenhausen, G., Wagner, G., Ernst, R.R. & Wüthrich, K. (1983) *Biochem. Biophys. Res. Commun.* 117, 479-485.
34. Pearson, G.A. (1977) *J. Magn. Res.* 27, 265-272.
35. Wüthrich, K., Wider, G., Wagner, G. & Braun, W. (1982) *J. Mol. Biol.* 155, 311-319.
36. Billeter, M., Braun, W. & Wüthrich, K. (1982) *J. Mol. Biol.* 155, 321-346.
37. Wagner, G. & Wüthrich, K. (1982) *J. Mol. Biol.* 155, 347-366.
38. Wüthrich, K. (1986) *NMR of Proteins and Nucleic Acids*, Wiley, New York.
39. Clore, G.M., Nilges, M., Sukumaran, D.K., Brünger, A.T., Karplus, M. & Gronenborn, A.M. (1986) *EMBO J.* 5, 2729-2735.
40. Wagner, G., Braun, W., Havel, T.F., Schaumann, T., Go, N. & Wüthrich, K. (1987) *J. Mol. Biol.* 196, 611-639.
41. Kalk, A. & Berendsen, H.J.C. (1976) *J. Magn. Res.* 24, 343-366.
42. De Vlieg, J., Boelens, R., Scheek, R.M., Kaptein, R. & van Gunsteren, W.F. (1986), *Isr. J. Chem.* 27, 181-188.
43. Wüthrich, K., Billeter, M. & Braun, W. (1983) *J. Mol. Biol.* 169, 949-961.
44. Van Gunsteren, W.F., Boelens, R., Kaptein, R., Scheek, R.M. & Zuiderweg, E.R.P. (1985) in *Molecular Dynamics and Protein Structure* (J. Hermans, ed.), Polycrystal Book service, Western Springs, USA, 92-99.
45. Whatif: A molecular modelling and drug design program.,(1990)*Journ. of Molec. Graphics*,(in press).
46. Jones, T.A. (1978) *J. Appl. Crystallogr.* 11, 268-272.
47. Van Gunsteren, W.F. & Berendsen, H.J.C.(1987) *GROningen MOlecular Simulation (GROMOS) library manual*, Biomos B.V., Nijenborgh 16, Groningen, The Netherlands, 1-229.
48. Van Gunsteren, W.F. (1988) *Protein Engineering* 2, 5-13.
49. Ryckaert, J.P., Cigotti, G. & Berendsen, H.J.C. (1977) *J. Comput. Phys.* 23, 327-341.
50. Van Gunsteren, W.F., Boelens, R., Kaptein, R., Scheek, R.M. & Zuiderweg, E.R.P. (1985) in *Molecular Dynamics and Protein Structure* (J. Hermans, ed.), Polycrystal Book service, Western Springs, USA, 5-14.
51. Berendsen, H.J.C., Postma, J.P.M., van Gunsteren, W.F., Di Nola, A. & Haak, J.R. (1984) *J. Chem. Phys.* 81, 3684-3690.
52. McGammon, J.A. & Harvey, S. C. (1987) *Dynamics of proteins and nucleic acids*, Cambridge University Press, Cambridge, Great-Britain.
53. Moonen, C.T.W. & Müller, F. (1983) *Eur. J. Biochem.* 133, 463-470.
54. Olejniczak, E.T., Poulsen, F.M. & Dobson, C.M. (1984) *J. Magn. Res.* 59, 518-523.

55. LeMaster, D.M., Kay, L.E., Brünger, A.T. & Prestegard, J.H. (1988) *FEBS Lett.* **236**, 71-76.
56. Madrid, M. & Jardetzky, O. (1988) *Bioch. Bioph. Acta* **953**, 61-69.
57. Olejniczak, E.T., Dobson, C.M., Karplus, M. & Levy, R.M. (1988) *J. Am. Chem. Soc.* **106**, 1923-1930.
58. Bax, A. & Davis, D.G. (1985) *J. Magn. Res.* **65**, 355-360.
59. Ramakrishnan, C. & Ramachandran, G.N. (1965) *Biophys. J.* **5**, 909-933.
60. Kabsch, W. & Sander, C. (1983) *Biopolymers* **22**, 2577-2637.
61. Richardson, J. (1981) *Adv. Protein Chem.* **34**, 167-339.
62. Quijcho, F.A., Sack, J.S. & Vyas, N.K. (1987) *Nature* **329**, 561-564.
63. Warshel, A. (1987) *Nature* **330**, 15-16.
64. Vervoort, J., van Berkel, W.J.H., Mayhew, S.G., Müller, F., Bacher, A., Nielsen, P. & LeGall, J. (1986) *Eur. J. Biochem.* **161**, 749-756.
65. Moonen, C.T.W., Vervoort, J. & Müller, F. (1984) in *Flavins and Flavoproteins* (Bray, R.C., Engel, P.C. & Mayhew S.G., eds.) pp. 493-496, Walter de Gruyter & Co., Berlin.
66. Warshel, A. & Russel, S.T. (1984) *Q. Rev. Biophys.* **17**, 283-422.
67. Churg, A.K. & Warshel, A. (1986) *Biochemistry* **25**, 1675-1681.
68. Mehler, E.L. & Eichele, G. (1984) *Biochemistry* **23**, 3887-3891.
69. Laudenbach, D.E., Straus, N.A., Patridge, K.A. & Ludwig, M.L. (1987) in *Flavins and Flavoproteins* (Edmondson, D.E. & McCormick, D.B., eds.), pp. 249-260, Walter de Gruyter & Co., Berlin.
70. Groß, K.H. & Kalbitzer, H.R. (1988) *J. Magn. Reson.* **76**, 87-99.
71. Szilágyi, L. & Jardetzky, O. (1989) *J. Magn. Reson.* **83**, 441-449.

Supplementary material:

NOE restraint list of two-electron reduced *M. elsdenii* flavodoxin as determined from a 150 ms NOESY spectrum (pH 8.3, T=41 °C). Cross peaks resulting from spin diffusion, as judged from a 50 ms NOESY spectrum, were omitted from this list.

Symbols used: HA=C α H; HB=C β H; HG=C γ H; HN=NH; HZ=C δ H of Phe; QA=pseudo atom for C α H $_2$; QB= pseudo atom for C β H $_2$; QG= pseudo atom for C γ H $_3$'s or C γ H $_2$'s, QD= pseudo atom for C δ H $_3$'s or C δ H $_2$'s and C δ H's of aromatic amino acid residues; QE= pseudo atom for C ϵ H $_2$'s and C ϵ H's of aromatic amino acid residues; MG, MD, ME= pseudo atoms for methyl groups at respectively γ , δ or ϵ position of an amino acid residue; HE1=NH $_\epsilon$ proton of tryptophan residues; H2, H4, H5 and H6= corresponding protons of indole part of a tryptophan residue; HOB= C $_2$ 'OH of FMN.

Residue	NOE restraint with		upper limit (Å)	
1MET	HA	2VAL	HN	2.7
	HA	31VAL	HA	4.2
	QG	31VAL	HA	4.2
2VAL	HA	3GLU	HN	3.3
3GLU	HN	50ILE	HA	3.3
4ILE	HN	33SER	HA	3.3
	HN	32GLU	HN	3.3
	HN	3GLU	HA	3.0
	HA	6TYR	QD	4.2
	MG	86PHE	QD	3.3
	MG	86PHE	QE	3.3
	MG	86PHE	H4	3.3
	MD	21GLU	HN	4.0
5VAL	HN	4ILE	HA	3.0
	HA	34VAL	HN	2.7
	HA	6TYR	HN	2.7
	HA	33SER	HA	4.2
	HA	36PHE	HN	4.2
	QG	6TYR	HN	3.3
	QG	34VAL	HN	4.0
	QG	36PHE	HA	3.3
6TYR	HN	36PHE	HN	3.3
	HA	53GLY	HN	3.3
	HA	53GLY	QA	3.3
	QB	7TRP	HN	2.7
	QB	53GLY	HN	3.3
	QB	86PHE	QD	2.7
	QD	35ARG	HA	2.7
	QE	35ARG	HA	2.7
	QE	14GLU	HA	2.7
	QD	17ALA	MB	3.3
	QE	17ALA	MB	3.3
	QD	34VAL	HN	2.7

7TRP	QE	34VAL	HN	2.7
	QD	13THR	MG	3.3
	QD	5VAL	HA	3.3
	QD	4ILE	MG	3.3
8SER	HN	6TYR	QD	2.7
	HN	53GLY	HN	3.3
	HN	6TYR	HA	3.0
	HN	36PHE	QE	4.2
	HE1	66VAL	MG1	3.3
	HE1	66VAL	MG2	3.3
	HE1	66VAL	HB	3.3
	H2	67VAL	QG	4.0
	H2	66VAL	QG	4.0
	H2	66VAL	HB	3.3
	H2	36PHE	QD	3.3
	H6	9GLY	QA	3.3
	H5	55PRO	QD	3.3
	H4	55PRO	QD	3.3
9GLY	HN	7TRP	HA	3.0
	HA	9GLY	HN	2.7
	QB	6TYR	QD	3.3
	QB	6TYR	QE	3.3
10THR	HN	7TRP	H5	4.2
	HN	8SER	HG	4.2
	HN	55PRO	QG	4.2
	QA	10THR	HN	3.3
11GLY	HN	8SER	HA	4.2
	HN	9GLY	HN	3.3
12ASN	HN	10THR	HN	3.3
13THR	HN	11GLY	HN	3.3
	HN	8SER	HG	4.2
	HN	12ASN	QB	3.3
14GLU	HN	8SER	HG	3.3
	HN	12ASN	HN	3.3
	MG	88SER	HN	4.0
	MG	86PHE	QD	4.0
	MG	54CYS	HA	4.0
	HN	8SER	QB	3.3
15ALA	HN	13THR	HN	3.3
	HA	6TYR	QD	3.3
	HN	14GLU	HA	3.3
16MET	HN	14GLU	HN	3.3
17ALA	HN	17ALA	HN	3.3
	HN	15ALA	QB	3.3
	HN	15ALA	HA	4.2
	HN	13THR	HA	3.3
	HA	19GLU	HN	3.3
	QB	17ALA	HN	2.7
	ME	116ILE	HA	3.3
	ME	87GLY	HN	4.0
	HN	86PHE	QD	3.3
18ASN	HA	18ASN	HN	3.3
	MB	18ASN	HN	3.3
	MB	86PHE	QD	3.3
	HN	17ALA	HN	3.0
19GLU	HA	19GLU	HN	3.3
	QB	19GLU	HN	3.3
	HN	18ASN	HN	3.0

20ILE	HA	20ILE	HN	3.3
	QB	20ILE	HN	3.3
21GLU	HN	19GLU	HN	3.3
	HA	23ALA	HN	3.3
	QG	131GLY	HN	3.3
	QG	21GLU	HN	3.3
	MD	127CYS	HA	3.3
22ALA	HN	20ILE	HA	3.3
	HN	20ILE	HB	2.7
	HN	18ASN	HA	3.3
	HN	20ILE	HN	3.3
23ALA	HN	21GLU	QB	3.3
	HN	21GLU	HA	3.3
	HN	21GLU	HN	3.3
	HN	24VAL	HN	4.2
	HN	25LYS	HN	4.2
	HA	25LYS	HN	3.3
24VAL	HN	22ALA	MB	3.3
	HN	22ALA	HN	4.2
25LYS	HN	23ALA	HA	3.3
	HN	23ALA	HN	3.3
	HN	21GLU	HA	3.3
27ALA	HN	24VAL	HA	4.2
	HN	24VAL	QG	4.0
	HN	24VAL	HN	3.0
28GLY	HN	26ALA	HA	3.3
	HN	26ALA	HN	3.0
29ALA	HN	27ALA	HA	3.3
	HN	27ALA	HN	3.0
30ASP	HN	28GLY	QA	3.3
	HN	25LYS	HA	3.3
	HN	28GLY	HN	3.3
	MB	30ASP	HN	3.3
31VAL	HN	29ALA	HA	3.3
32GLU	HA	32GLU	HN	2.7
	HA	2VAL	HN	2.7
33SER	HN	3GLU	HA	2.7
	QB	33SER	HN	4.2
34VAL	HN	32GLU	HA	2.7
	HA	34VAL	HN	2.7
	QB	34VAL	HN	2.7
35ARG				
36PHE	HN	34VAL	HA	3.3
	HA	6TYR	HN	3.3
	HN	35ARG	HA	3.3
	HA	37GLU	HN	3.3
	QB	37GLU	HN	3.3
	QD	5VAL	QG	3.3
	QD	35ARG	HA	3.3
	QE	5VAL	QG	3.3
	QE	53GLY	HN	3.3
	QE	7TRP	QB	4.2
	HZ	5VAL	QG	4.0
	HZ	52LEU	HA	3.3

	HZ	53GLY	HN	3.3
	OD	67VAL	QG	3.3
	OD	66VAL	QG	3.3
	QE	67VAL	QG	3.3
	QE	66VAL	QG	3.3
	H4	67VAL	QG	3.3
37GLU				
	HN	36PHE	HN	3.3
	HN	66VAL	QG	3.3
38ASP				
	HN	39THR	MG	4.0
	HN	37GLU	HN	3.3
	QB	39THR	HN	3.3
39THR				
	HN	38ASP	HA	2.7
	HB	40ASN	HN	3.3
40ASN				
	HN	43ASP	QB	3.3
	HN	44VAL	QG	4.0
	HN	70PHE	HZ	3.3
	HN	70PHE	OD	3.3
	HN	39THR	HA	2.7
	HN	39THR	MG	3.3
	HA	39THR	MG	4.0
	HA	41VAL	QG	4.0
41VAL				
	HN	40ASN	HA	3.3
	HA	42ASP	HN	3.3
	HB	42ASP	HN	4.2
	QG	42ASP	HN	3.3
42ASP				
43ASP				
	HN	44VAL	HB	4.2
	HN	44VAL	QG	4.0
44VAL				
	HN	43ASP	QB	3.3
	HN	41VAL	HA	3.3
	HN	43ASP	HN	3.3
45ALA				
	HN	44VAL	QG	3.3
	HN	44VAL	HB	3.3
	HN	44VAL	HN	3.3
46SER				
	HN	45ALA	HN	3.3
47LYS				
	HN	45ALA	HA	4.2
48ASP				
	QB	49VAL	HN	3.3
49VAL				
	HA	82LYS	HN	3.3
50ILE				
	HN	83VAL	HA	2.7
	HN	49VAL	HA	3.3
	HN	84GLY	HN	4.2
51LEU				
	HN	50ILE	MG	3.3
	HN	4ILE	HA	2.7
	HN	50ILE	HA	3.3
	HA	83VAL	HA	3.3
	OD	52LEU	HN	4.0
52LEU				
	HN	86PHE	HN	3.3
	HN	51LEU	HA	3.3
	HN	85LEU	OD	3.3
	HA	5VAL	HN	3.3
53GLY				
	HN	52LEU	QB	2.7
	HN	52LEU	HA	3.3
	HN	86PHE	OD	3.3

54CYS	QA	100TRP	H6	3.3
	QA	86PHE	H4	3.3
	HN	13THR	MG	4.0
	HN	53GLY	QA	3.3
	HA	67VAL	QG	4.0
	HA	55PRO	QD	2.7
	HG	67VAL	QG	4.0
	HG	62LEU	QD	3.3
	HG	63GLU	HN	3.3
	HG	63GLU	QB	3.3
55PRO	HG	96TRP	H2	4.2
56ALA	HA	56ALA	MB	4.0
	HA	87GLY	QA	3.3
	HA	96TRP	HE1	3.3
	QB	56ALA	HN	3.3
	QB	88SER	HN	3.3
57MET	HN	55PRO	HA	2.7
58GLY	HN	56ALA	HA	3.3
	HA	58GLY	HN	3.3
59SER	HN	57MET	QB	2.7
	HN	57MET	QG	2.7
60GLU	HN	58GLY	QA	3.3
	HA	60GLU	HN	3.3
61GLU	-			
62LEU	HN	60GLU	HA	3.3
	HN	57MET	HN	3.3
	HN	96TRP	QB	4.2
63GLU	HN	61GLU	QB	3.3
	HA	96TRP	H2	3.3
	QD	63GLU	HN	4.0
	QD	96TRP	HE1	4.0
64ASP	HN	67VAL	HB	3.3
	HN	62LEU	HA	2.7
	QG	7TRP	H7	3.3
	QG	7TRP	H6	3.3
65SER	HN	63GLU	HA	3.3
	HN	63GLU	QG	3.3
	HA	65SER	HN	3.3
66VAL	HN	64ASP	HN	3.3
	HA	66VAL	HN	3.3
67VAL	HN	68GLU	HN	3.3
	HN	65SER	HN	3.3
	QG	7TRP	HE1	4.0
68GLU	HN	66VAL	HB	2.7
	HN	66VAL	QG	3.3
	HN	66VAL	HN	3.3
	HA	68GLU	HN	3.3
	HA	70PHE	HN	3.3
	HB	68GLU	HN	3.3
	QG	66VAL	HN	4.0
	QG	68GLU	HN	3.3
69PRO	HN	64ASP	HA	3.3
	HN	67VAL	HN	3.3
	QD	68GLU	HN	3.3
	QD	66VAL	HN	4.2

70PHE	HN	72THR	HN	4.2
	HA	71PHE	HN	3.3
	QD	40ASN	HA	3.3
	QD	41VAL	QG	4.0
	QD	36PHE	QD	3.3
	QE	40ASN	HA	3.3
	QE	36PHE	QE	3.3
	QE	41VAL	QG	4.0
	HZ	40ASN	HA	3.3
71PHE	HZ	39THR	MG	3.3
	HN	70PHE	QB	2.7
	HN	67VAL	QG	3.3
	HN	67VAL	HA	3.3
72THR	QD	68GLU	HA	3.3
	HN	71PHE	QB	3.3
73ASP	HN	72THR	HN	3.3
	HN	74LEU	HN	3.3
	HN	72THR	HB	3.3
	HN	72THR	HA	3.3
74LEU	HN	41VAL	QG	4.0
	HN	73ASP	QB	3.3
	HN	71PHE	HA	3.3
	HN	75ALA	HN	3.3
	HA	75ALA	HN	3.3
	HA	41VAL	QG	3.3
	HA			
75ALA	HN	74LEU	QB	3.3
	HN	76PRO	QD	3.3
76PRO	QD	75ALA	MB	4.0
77LYS	HN	78LEU	HN	3.3
	HA	78LEU	HN	3.3
78LEU	HN	79LYS	HN	3.3
	QD	79LYS	HN	4.2
79LYS	HN	78LEU	HA	3.3
	HN	81LYS	HN	3.3
80GLY	HN	79LYS	HA	2.7
	HN			
81LYS	HN	109ALA	MB	4.0
	HN	81LYS	QB	3.3
82LYS	HN	81LYS	HA	3.3
	HN			
83VAL	HN	111VAL	HA	3.3
	HA	51LEU	QD	4.0
	HA	50ILE	HB	3.3
	HA	84GLY	QA	3.3
	QG	85LEU	QD	4.0
84GLY	HN	51LEU	QD	4.0
	HN	83VAL	QG	3.3
	HN	51LEU	HA	2.7
	QA	113GLY	HN	3.3
85LEU	HN	114THR	HA	2.7
	QB	86PHE	HN	2.7
	QD	104THR	HN	3.3
	QD	86PHE	HN	4.0
	QD	104THR	HG	4.0
86PHE	HN	87GLY	HN	4.2

	HA	115ALA	HN	3.3
	HA	115ALA	MB	3.3
	HA	97MET	ME	3.3
	QB	87GLY	HN	3.3
	QB	115ALA	HN	3.3
	QD	20ILE	MD	3.3
	QD	51LEU	QD	2.7
	QE	20ILE	MD	4.0
	QE	53GLY	HN	3.3
	QE	17ALA	MB	4.0
	QE	13THR	MG	4.0
	HZ	6TYR	QB	3.3
	HZ	20ILE	MD	4.0
	HZ	17ALA	MB	3.3
	HZ	6TYR	HA	4.2
87GLY				
	HN	116ILE	HA	3.3
	QA	13THR	MG	3.3
	QA	54CYS	HN	3.3
	QA	96TRP	HE1	3.3
	QA	96TRP	H6	3.3
	QA	96TRP	H7	3.3
88SER				
	HN	55PRO	HA	3.3
	HA	89TYR	HN	3.3
	QB	89TYR	HN	3.3
	HG	12ASN	QB	3.3
89TYR				
	HN	119GLU	HN	3.3
	HN	117VAL	HA	4.2
	HA	56ALA	MB	3.3
	QE	93SER	HA	3.3
	QE	116ILE	HB	3.3
	QE	116ILE	MD	3.3
	QE	116ILE	QG	2.7
90GLY				
	HN	89TYR	QB	3.3
	HN	89TYR	QD	2.7
	HN	89TYR	HA	3.3
91TRP				
	HN	90GLY	HN	3.3
92GLY				
	HN	91TRP	HN	3.3
93SER				
94GLY				
	HN	96TRP	H4	3.3
	HN	96TRP	H5	3.3
	QA	97MET	HN	3.3
	QA	96TRP	H4	3.3
95GLU				
	HN	94GLY	QA	3.3
	HA	96TRP	HN	3.3
96TRP				
	HN	95GLU	QB	3.3
	QB	56ALA	MB	4.0
	HE1	54CYS	QB	3.3
	HE1	100TRP	H4	3.3
	H2	62LEU	QD	3.3
	H2	62LEU	HG	3.3
	H2	56ALA	HA	3.3
	H7	55PRO	HA	3.3
	H7	97MET	ME	4.0
	H4	56ALA	MB	4.0
	H4	97MET	HN	3.3
	H4	97MET	QB	3.3
97MET				
	HN	96TRP	HA	3.3
	HN	99ALA	HN	4.2
	HN	96TRP	HN	3.3
98ASP				
	HN	97MET	HN	3.3

99ALA	QB	99ALA	HN	3.3
	HN	98ASP	HN	3.3
	HA	100TRP	HN	3.3
100TRP	MB	100TRP	HN	4.0
	HN	99ALA	HN	3.3
	HA	101LYS	HN	3.3
	QB	101LYS	HN	3.3
	HE	185LEU	QD	4.0
	HE	162LEU	QD	4.0
	HE	152LEU	QD	4.0
	H2	104THR	HO	3.3
	H2	85LEU	QD	4.0
	H7	85LEU	QD	4.0
	H7	52LEU	QD	4.0
	H7	67VAL	QG	3.3
	H7	62LEU	QD	3.3
	H7	86PHE	HN	3.3
	H7	54CYS	QB	2.7
	H7	85LEU	HA	3.3
	H7	52LEU	QB	2.7
	H6	62LEU	QD	4.0
	H4	85LEU	QD	4.0
	H4	62LEU	QD	3.3
101LYS	H4	97MET	HA	3.3
	HN	97MET	HA	3.3
	HN	85LEU	QD	4.0
	HN	98ASP	HA	3.3
	HN	100TRP	HN	3.3
	HA	85LEU	QD	3.3
	QB	85LEU	QD	4.0
102GLN				
	HN	101LYS	HA	3.3
	HN	101LYS	QB	3.3
	HN	101LYS	QG	3.3
	HN	101LYS	HN	3.3
	HA	103ARG	HN	3.3
	QB	103ARG	HN	3.3
103ARG				
	HN	102GLN	HN	3.3
	HA	104THR	HN	3.3
104THR				
	HN	101LYS	HA	3.3
	HN	102GLN	HN	4.2
	HN	103ARG	HN	4.2
	HN	105GLU	QB	3.3
	HG	105GLU	HN	3.3
	MG	105GLU	HN	4.0
105GLU				
	HN	101LYS	HA	3.3
	HN	104THR	HN	3.3
	HN	111VAL	QG	2.7
106ASP				
	HN	105GLU	HA	3.3
	HN	105GLU	HN	3.3
107THR				
	HN	106ASP	HN	3.3
	HN	104THR	HA	4.2
108GLY				
	HN	107THR	HN	3.3
109ALA				
	HN	108GLY	HN	3.3
	HA	110THR	HN	2.7
	MB	110THR	HN	4.0
110THR				
	HN	111VAL	QG	4.0
	HA	111VAL	HN	2.7
111VAL				
	HN	110THR	MG	3.3

112ILE	HA	113GLY	HN	3.3
113GLY	HN	111VAL	HA	3.3
	HN	112ILE	MD	4.0
	HN	112ILE	MG	4.0
	HN	112ILE	HA	3.3
	HN	111VAL	QG	4.0
	HN	112ILE	QG	3.3
	HN	112ILE	HN	3.3
114THR				
	HN	113GLY	QA	3.3
	HA	115ALA	MB	4.0
	HA	97MET	ME	4.0
	HA	84GLY	QA	4.2
115ALA				
	HN	114THR	HA	3.3
	MB	116ILE	HN	3.3
116ILE				
	HN	115ALA	HA	2.7
	HA	89TYR	QE	3.3
	HB	89TYR	QD	3.3
	HB	96TRP	H6	3.3
	MG	96TRP	H5	4.0
	MG	96TRP	H7	4.0
	MG	89TYR	QD	4.0
	MG	89TYR	QE	4.0
	MD	96TRP	H5	4.0
117VAL				
	HN	89TYR	QD	3.3
	HN	89TYR	QE	3.3
	HN	88SER	HA	3.3
	HN	116ILE	HA	3.3
118ASN				
	HN	117VAL	HA	3.3
	HA	89TYR	QD	3.3
119GLU				
	HN	118ASN	HA	2.7
	HA	120MET	HN	3.3
120MET				
121PRO				
	HA	117VAL	QG	4.0
	HA	122ASP	HN	3.3
	HA	124ALA	MB	5.0
	QD	120MET	HA	3.3
	QD	122ASP	HN	4.2
122ASP				
	HA	123ASN	HN	2.7
123ASN				
124ALA				
	HN	123ASN	HA	3.0
	MB	117VAL	QG	4.0
125PRO				
	HA	128LYS	HN	3.3
	HA	129GLU	HN	4.2
	HA	127CYS	HN	4.2
	QD	124ALA	HA	3.3
126GLU				
127CYS				
	HN	129GLU	HN	4.2
	HA	130LEU	HN	4.2
	HA	20ILE	QG	4.2
	QB	20ILE	QG	4.2
	QB	20ILE	HN	3.3
128LYS				
	HN	127CYS	HA	3.3
	HN	127CYS	QB	3.3
129GLU				
	HN	128LYS	HA	3.3

130LEU	HN	128LYS	QB	3.3
	HN	128LYS	QG	3.3
	HN	126GLU	HA	3.3
	HN	128LYS	HN	3.3
130LEU	HN	129GLU	HN	3.3
	HA	131GLY	HN	3.3
131GLY	HN	128LYS	HA	3.3
	HN	20ILE	MG	4.0
	HN	20ILE	HA	3.3
	HN	23ALA	MB	5.0
	HN	130LEU	HN	3.3
	QA	132GLU	HN	3.3
132GLU	HN	23ALA	MB	4.0
	HN	131GLY	HN	3.3
133ALA	HN	132GLU	QG	3.3
	HN	132GLU	QB	3.3
	HN	131GLY	QA	4.2
	HN	132GLU	HN	3.3
	HN	134ALA	HN	3.3
134ALA	HN	133ALA	HA	3.3
	HN	136LYS	HN	4.2
	HN	135ALA	HN	3.3
135ALA	HN	24VAL	HA	3.3
	HN	24VAL	QG	3.3
	HN	136LYS	HN	3.3
136LYS	HN	135ALA	HA	3.3
	HN	133ALA	HA	3.3
	HA	137ALAH	N	3.3
137ALA	HN	134ALA	HA	3.3
138FMN	HOB	56ALA	HN	3.3
	H6	57MET	HA	3.3
	H6	58GLY	HN	2.7
	M7	58GLY	HN	4.0
	HOB	89TYR	HA	3.3
	QA	90GLY	HN	3.3
	H9	138FMN	HOB	4.2
	H9	138FMN	QA	3.3
non-NOE's:				
60GLU	HN	138FMN	H5	4.6

Chapter 5

A two-dimensional ^1H NMR study on *Megasphaera elsdenii* flavodoxin in the oxidized state and some comparisons with the two-electron reduced state

Carlo P.M. van Mierlo, Boudewijn P. J. van der Sanden, Peter van Woensel, Franz Müller¹ and Jacques Vervoort

Department of Biochemistry, Agricultural University, Wageningen, The Netherlands.

1. Present address: Sandoz AG, Agro Ltd., Department of Toxicology, Basle, Switzerland.

Summary

Assignments for the 137 amino acid residues of oxidized *Megasphaera elsdenii* flavodoxin have been made using the sequential resonance assignment procedure. Great benefit was experienced from assignments of the fully reduced protein. The secondary and tertiary structures of the typical α/β protein remain virtually identical on going from the oxidized to the two-electron reduced state as judged from NOESY spectra. However, functionally important conformation changes in the flavin binding region do occur on reduction. Considerable, reduction state dependent, chemical shift variations of protons in the immediate vicinity of the isoalloxazine moiety take place. From analysis of these shifts it can be concluded that ring current effects of the pyrazine part of the flavin diminish on two-electron reduction.

Introduction

Flavodoxins are a group of small flavoproteins (molecular mass ranging from 14 to 23 kDa) functioning as low-potential electron transfer proteins [1]. They contain non-covalently bound riboflavin-5'-phosphate (FMN) as prosthetic group and have been found in several strains of bacteria and algae [1].

In our laboratory we are studying the noncrystallizable flavodoxin from *Megasphaera elsdenii* using various NMR techniques. This protein is produced in large quantities under iron-deficient conditions by *M. elsdenii* and can occur in three redox states: the oxidized, the one-electron reduced semiquinone and the two-electron reduced hydroquinone state. FMN bound to the apoprotein has strongly altered redox potentials as compared to free FMN. The transition from the oxidized to the semiquinone state of flavodoxin ($E_2 = -115$ mV) has a more positive redox potential, whereas the redox potential for the transition of the semiquinone to the hydroquinone state ($E_1 = -375$ mV) is much more negative as compared to free FMN [1]. In vivo the flavodoxin from *M. elsdenii* shuttles between the semiquinone and the hydroquinone states as a result of the high activation barrier between the oxidized and the semiquinone state and the absence of such barrier for the semiquinone/hydroquinone transition [2]. It is this activation barrier that predestines the protein for one-electron transfer reactions.

Recently we have described the sequential assignments [3-6] of the ^1H NMR spectrum of the two-electron reduced *M. elsdenii* flavodoxin (137 amino acid residues, molecular weight 15 kDa) [7]. Based on these sequential assignments using interresidual NOE connectivities the secondary structure elements of two-electron reduced *M. elsdenii* flavodoxin were determined [8]. The tertiary structure

has been generated using restrained molecular dynamics [9-11] with 509 interresidual distance constraints which have been extracted from the NOESY spectra [12]. The solution structure has been compared with the strongly resembling crystal structure of the related *Clostridium MP* flavodoxin in the semiquinone state [13-15].

In this paper we describe the sequential assignments of the ^1H NMR spectrum of *M. elsdenii* flavodoxin in the oxidized state. A comparison of the oxidized to the semiquinone and hydroquinone states is made. Special attention is paid to conformational differences between the two redox states.

Materials and methods

Flavodoxin from *M. elsdenii* was isolated and purified as previously described [16]. For the removal of all exchangeable protons of the protein, the apoflavodoxin was prepared according to the method of Wassink & Mayhew [17]. The apoflavodoxin was then dissolved in $^2\text{H}_2\text{O}$ and freeze dried, this procedure was repeated at least two times. The reconstitution with FMN was done in $^2\text{H}_2\text{O}$ at room temperature. Reconstitution using isotope enriched FMN molecules were done in an analogous way. Excess FMN was removed from reconstituted flavodoxin by molecular sieve chromatography (Biogel P-6Dg).

Selectively ^{13}C enriched [$1',2'-^{13}\text{C}_2$] and [$5'-^{13}\text{C}$]riboflavin was synthesized by a known procedure using ^{13}C -labeled ribose (Omicron Biochemicals Inc., South Bend Indiana) to produce [$1',2'-^{13}\text{C}_2$] and [$5'-^{13}\text{C}$] 6,7-dimethyl-8-ribityllumazine as described by Vervoort et al. [18]. The lumazine derivative in turn was converted to riboflavin by treatment with riboflavin synthase from *Bacillus subtilis* [19]. The ^{13}C -labeled riboflavin was then converted to the respective 5'-phosphates by sequential treatment with FAD-synthetase and phosphodiesterase [20-22].

^{13}C -NMR spectra of reconstituted flavodoxin were acquired on a Bruker CXP-300 NMR spectrometer, under conditions as previously described [2,22]. By irradiating at the proton frequency in addition to applying a systematic increase of this frequency in steps of 10 Hz and detecting the changes in fine structure of the ^{13}C resonances, the resonance positions of the protons attached to the ^{13}C enriched atoms of the ribityl side chain of FMN could be detected.

Reduction and reoxidation experiments were conducted by the addition of the desired amount of a dithionite solution to the anaerobic solution of flavodoxin in the oxidized state as previously described [7]. All samples contained 9 to 15 mM flavodoxin in solutions consisting of potassium phosphate or potassium pyrophosphate or a mixture of both phosphates ranging from 50 mM to 330 mM. The pH of the solutions before dissolving the flavodoxin varied between 7.0 - 8.3.

All measurements were done using a mixture of 10% $^2\text{H}_2\text{O}$ /90% H_2O , except in cases where a specific deuterium content was desired. The amide exchange experiment was done by dissolving the freeze dried protein in $^2\text{H}_2\text{O}$, pH 7.6, at room temperature. Immediately after dissolving the protein, the NMR sample tube was inserted into the magnet and 4 NOESY experiments (mixing time 150 ms), taking 14.2 hours each, were performed at 41 $^\circ\text{C}$. After 108 hours at room temperature two additional NOESY spectra were acquired.

Phase-sensitive double quantum filtered Cosy [23,24], NOESY [25] and 2D Homonuclear Hartmann Hahn transfer [26] spectra were acquired on a Bruker AM500 at 33 $^\circ\text{C}$ and a Bruker AM600 at 30 and 41 $^\circ\text{C}$. The carrier frequency coincided with the water resonance.

To acquire the NOESY spectra a mixing time of 150 ms was used, no zero quantum filter has been used. During the accumulation of the HoHaHa spectra the MLEV-17 composite pulse, including two 2.5 ms trimpulses, lasted 90 ms. In the DQF-Cosy and NOESY experiments specific irradiation of the water resonance took place at all times except during the data acquisition period. In contrast in the HoHaHa experiments irradiation took only place during the relaxation delay period which lasted in all 2D experiments 2.5 s. The number of scans, including four dummy scans, varied between 52 and 148 and the number of increments varied between 360 and 540, the total acquisition time was 14-58 hours.

After data acquisition all further data-handling was performed on a Microvax II computer and a Vaxstation 2000 using software obtained from Dr. R. Boelens, modified to our specific requirements. The data were digitally filtered using sine bell or squared sine bell window functions shifted by various increments and zero-filled prior to Fourier transformation as described in the figure legends. After the double Fourier transformation of the data of the 2D-NMR experiment baseline corrections with a fourth order polynomial were performed according to Pearson [27]. The 2D-NMR spectra are presented as contour plots with levels increasing by a factor of 1.3.

Results and discussion

Sequential resonance assignments

The assignments in the NMR spectra of flavodoxin in the oxidized state were done by applying the sequential resonance assignment procedure as developed by the group of Wüthrich [3-6]. This procedure comprises of the search for as many individual amino acid residues as possible which can subsequently be assigned to a specific amino acid residue by making use of sequential NOE effects involving

neighbouring NH, C α H and C β H protons. Comparing the sequential fragments to the primary sequence of flavodoxin [28,29] results in sequence specific assignments.

During the assignment of the oxidized state we benefitted greatly from the assignments of the two-electron reduced state of *M. elsdenii* flavodoxin as generally only resonances of protons in the immediate vicinity of the protein-bound flavin (Fig. 1) appeared to be affected by the reduction state of the protein. These protons are characterized in the 2D-NMR spectra by altered resonance positions and are thereby easily recognized (Figs. 2 and 3). The majority of the assigned cross peaks of amino acid residues not being part of the flavin binding region could immediately be transferred from the spectra of the reduced to the oxidized state of the protein.

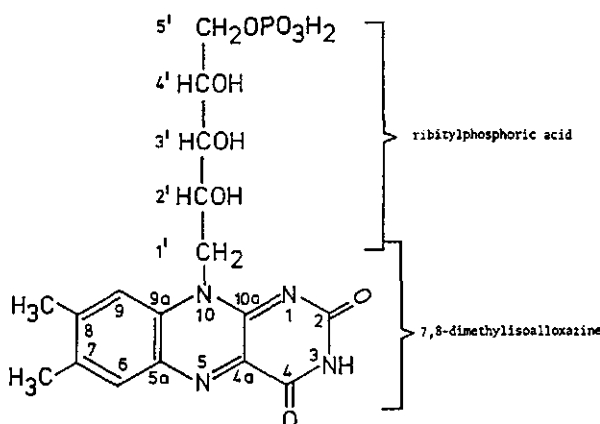


Fig. 1 Structure of riboflavin 5'-phosphate (FMN).

A significant simplification of the complex 2D-NMR spectra of the oxidized state was achieved when the sample was brought to the full semiquinone state. Due to the paramagnetic properties of the isoalloxazine ring in the semiquinone state [30], resonances of protons in the flavin binding region become broadened or disappear completely from the spectrum (Fig. 4). The remaining proton resonances in the 2D-NMR spectra have chemical shifts and cross peak patterns as in the oxidized state, so no conformational changes occur outside the flavin binding region on going from the oxidized to the one-electron reduced state (Figs. 3 and 4). Varying the semiquinone percentage in a mixture of oxidized and one-electron reduced flavodoxin molecules does not result in a varying sphere around the flavin of protons being affected by the paramagnetism of the flavin, as no fast electron transfer occurs between these molecules [7,31]. A distance dependent intensity

decrease of all cross peaks being directly affected by the flavin semiquinone is expected. This property has not been exploited. There has been a continuous feedback of information gathered from spectra corresponding to the oxidized, semiquinone and hydroquinone state of flavodoxin during the assignment procedure. Advantages of this feedback should not be underestimated in the assignment of a protein the size of flavodoxin.

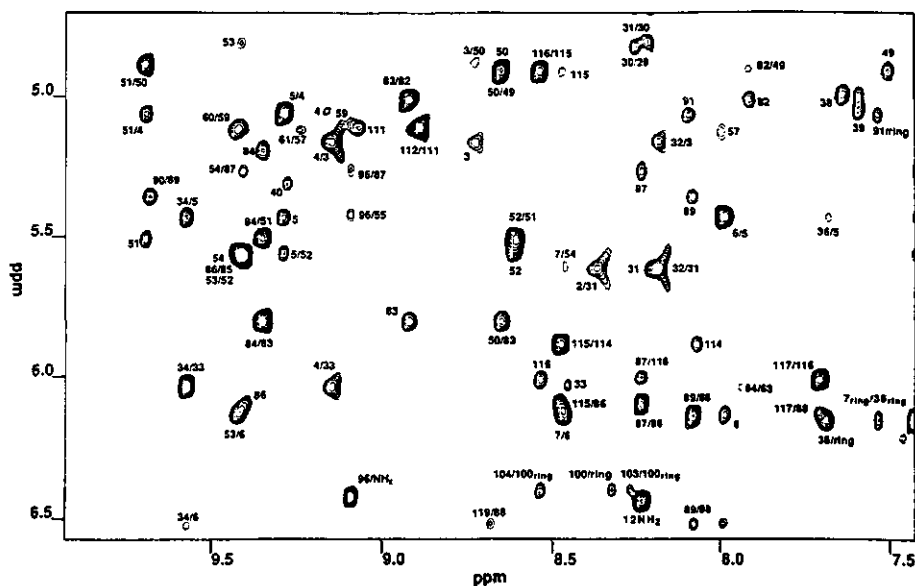


Fig. 2 Part of a 600 MHz NOESY spectrum of two-electron reduced *M. elsdenii* flavodoxin in 90% H_2O /10% D_2O , pH 8.3, 41 $^\circ\text{C}$, illustrating the wealth of information obtained from this spectrum. The mixing time was 150 ms, the spectral resolution is 4.1 Hz/point in ω_2 direction and 8.1 Hz/point in ω_1 direction. The cross peaks are labeled ω_2/ω_1 . The spectrum was processed with a sine-bell shifted by 15° in t_2 and a squared sine-bell shifted by 22.5° in t_1 dimension.

Analysis of spin systems

Individual residues were found in the reduced state of the protein by using experiments like DQF-Cosy and HoHaHa which give information about scalar coupled protons within a particular spin system. 54 unique spin systems, 24 AMX spin systems and 10 'long side chain' spin systems were found in the initial stage of the sequential assignment procedure [7]. All these spin systems could be directly transferred to the corresponding DQF-Cosy, HoHaHa and NOESY spectra of the

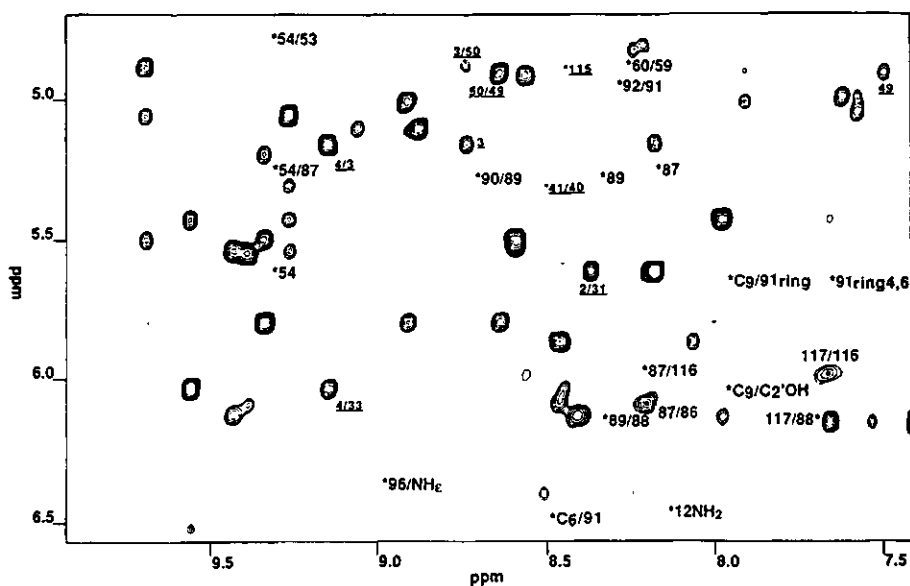


Fig. 4 The same spectral region of a 600 MHz spectrum as presented in Fig. 3 but acquired using one-electron reduced *M. elsdonii* flavodoxin in 90% H_2O /10% $\text{D}_2\text{H}_2\text{O}$, pH approximately 7.8, 41 $^{\circ}\text{C}$ (mixing time 150 ms). Positions of cross peaks broadened or missing due to the paramagnetism of the flavin moiety in the semiquinone state, as compared to the oxidized state of the protein, are labeled with an asterisk. For clarity cross peaks having only one contour level in Fig. 3 and no level in this figure are not labeled. Cross peaks having different positions ($\Delta\text{ppm} \geq 0.07$ ppm) or intensities as compared to the oxidized state, resulting from pH differences between the samples have underlined labels. Invariable cross peaks have not been labeled. Processing and resolution as in Fig. 2.

The amide proton resonance of G80 has a low intensity in spectra of the reduced state due to the high pH required for complete reduction of the protein (approximately pH=8.3) [35]. In spectra of the oxidized state the intensity of the amide proton resonance of G80 is much higher as a result of a decreased exchange rate caused by the lower pH of the solution. The same appeared to be the case for the amide proton resonances of V41, D48, N118, D122 and E126 (See e.g. 41/40 in Fig. 3). In all these cases the spectra of the oxidized state were crucial for making sequential assignments involving these residues. Small differences in cross peak position concerning exchangeable protons resulting from pH differences between the samples have also been observed (Fig. 3).

Some spin systems (including M1, V2, E3, V31, V44, V49, V66, L85, F86 and G87) exhibited chemical shift differences greater than or equal to 0.07 ppm on going to the oxidized state of the protein (see Table 1). They could however be easily detected by comparing intra- and interresidual connectivity patterns in NOESY spectra of both reduction states (taking into account connectivity patterns as observed in correlated spectra (DQF-Cosy and HoHaHa)). Figs. 2 and 3 illustrate this for some resonances of V2 and E3.

Sequential assignments

After transferring spin systems, a parallel search for sequential d_{NN} , $d_{\alpha N}$ and $d_{\beta N}$ connectivities started in NOESY spectra of the oxidized and two-electron reduced states, in order to find unique spin systems. A NOESY spectrum with a mixing time of 0.15 s was used as the main spectrum for making the sequential assignments in the oxidized state. Sequential connectivities observed are summarized in Fig. 6. Resonance positions of spin systems (Table 1) were taken from the NOESY spectrum because it has a superior resolution, especially in crowded regions, as compared to other types of spectra. Proton resonances of 88 of the 137 amino acid residues had chemical shift differences not greater than or equal to 0.07 ppm between both redox states (Table 1). Of the total number of 632 assigned resonances in the reduced state, 85 % exhibited a chemical shift difference not greater than or equal to 0.07 ppm on going from the reduced to the oxidized state (six of the proton resonances of the reduced state could not be assigned in the oxidized state, Table 1). These slight differences, in addition to the larger changes in resonance positions, could be used in solving ambiguities in different spectral regions of both the oxidized and reduced states. The amide proton of M1 could not be assigned in any of the three redox states of the protein. It is expected to exchange too rapidly with the solvent molecules to be detected. Once a sequence specific assignment had been made unambiguously for a backbone proton which had not yet been completely assigned to its side chain protons, we started searching for additional assignments for these protons.

In this section sequential assignments concerning the flavin binding region will be discussed as they were difficult to establish in some cases and concern the functional part of the molecule. This region comprises W7-T13, C54-E63, S88-W96 and N118-E119.

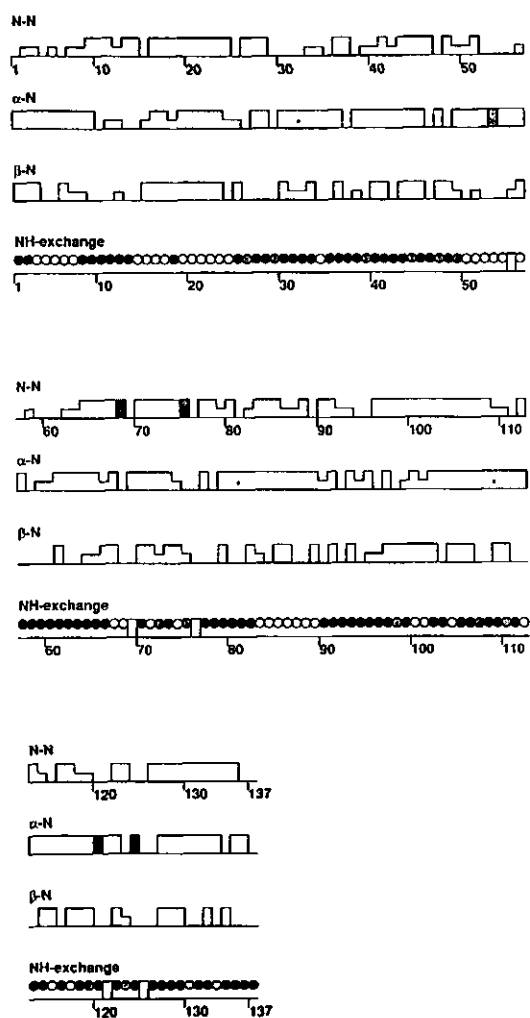


Fig. 6 Sequential NOE contacts observed in the 150 ms NOESY spectrum of oxidized *M. elsdenii* flavodoxin, pH 7.0, 41 °C. Weak NOE's have been indicated by small boxes. In case of doubts, no contact has been depicted. Contacts labeled with an asterisk indicate that a NOESY spectrum of the same sample at 30 °C has been used either to solve ambiguities or to take advantage of the shifted water resonance. The grey boxes represent respectively $d_{\alpha\delta}$, $d_{N\delta}$, $d_{N\delta}$, $d_{\alpha\delta}$ and $d_{\alpha\delta}$ connectivities involving proline residues. Black-filled, grey-filled and open circles indicate amide protons with fast, intermediate and slow exchange rates, respectively. Amide protons with slow exchange rates were present during the 28.4 h taking first two $^2\text{H}_2\text{O}$ exchange NOESY experiments (pH 7.0, 41 °C). Amide proton resonances corresponding to the black-filled circles had no detectable intensity in the second $^2\text{H}_2\text{O}$ exchange NOESY experiment.

Amino acid residues W7-T13 were easily found using the connectivity pattern as established for the reduced protein combined with the unchanged resonance positions of Y6, E14, G9 and G11 (see Fig. 6 and Table 1). The amide proton resonances of N12 and T13 and their corresponding connectivity patterns were easily recognized because they are the most down-field shifted resonances of flavodoxin as a result of hydrogen bonding to the phosphate group of the flavin [12].

Relatively small chemical shift differences (≤ 0.15 ppm) for residues in the phosphate binding region of the protein (which is close to the periphery of the molecule) are expected to result from pH differences (see [36]) between oxidized (pH 7.0) and reduced (pH=8.3) solutions of the protein. The distance from the isoalloxazine moiety to the phosphate is approximately 8 Å, thus the flavin ring cannot influence these resonance positions by ring current effects. No redox state-dependent conformation differences in the phosphate binding region are observed as judged from cross peak intensities in NOESY spectra.

Establishing sequential connectivities from C54 to E63 started with the unchanged resonances of G53, D64 [7], and the previously determined resonances of A56 and the methyl groups of L62 [33,34]. C54 could easily be determined via strong $d_{\alpha N}$ connectivities with G53, its small chemical shift variation and its NOE connectivities which are identical to those of the reduced state of the protein. P55 could then be assigned using its strong $d_{\alpha N}$ contact with A56, strong NOE connectivities of its C_{α} proton with the methyl of A56 and with one C_{α} proton of G87 as in the reduced state. In addition strong NOE's were observed from the C_{δ} protons of P55 to the amide proton of C54 as for two-electron reduced flavodoxin.

When making the assignments the complete NOE connectivity pattern as determined for the reduced state at that time was used as reference. This caused problems in assigning M57-E61 in the oxidized state as the NOE intensities changed. Resonances also shifted drastically (up to 1.79 ppm), sometimes to crowded regions of the spectrum (as for G58, E60, E61 and G92). The amide proton of M57 was detected via a $d_{\alpha N}$ contact and a NOE to the methyl group of A56 (as in the reduced state). G58 was extremely difficult to detect as no Cosy connectivity and only a low intensity HoHaHa cross peak has been detected. The amide proton resonance of G58 lies in a crowded area of the NOESY spectra concerning connectivities involving aromatic resonances. Its resonance position has been assigned using a $d_{\alpha N}$ connectivity with M57. Clear NOE contacts between C_6H of the flavin and the amide proton and $C_{\alpha}H$'s of G58 have been found. A weak NOE connectivity between the amide proton of G58 and the amide proton of a serine spin system was observed. The latter was thus assigned to S59. $d_{\alpha N}$ Connectivities with G58 coincide with other cross peaks of the amide proton resonance of S59 (one connectivity coincides with the intraresidual $NH-C_{\beta}H$ connectivity of S59).

Starting at the $C_{\alpha}H$ position of S59 a $d_{\alpha N}$ connectivity was found to a spin system yet unassigned. This was regarded as E60. The corresponding $C_{\alpha}H$ resonance of E60 has a NOE contact with the methyl of A56 as in the reduced state, further confirming the assignment. L62 could be determined using the previously assigned methyl groups in combination with results from correlated spectra. A not yet assigned strong NOE contact with its amide proton resonance was considered to result from the C_{α} proton of E61. The typical resonance position of the amide proton of E63 combined with a NOE contact pattern identical to that of the reduced state of the protein made its assignment easy. Assigning G58, E60 and E61 in spectra of the oxidized state of the protein was quite difficult as compared to other residues.

In assigning the region S88-W96 we started with S88, whose resonances could be immediately transferred from spectra of the reduced state as no significant chemical shift differences occurred (Table 1). Via a $d_{\alpha N}$ connectivity, the amide proton resonance of Y89 was detected. Its C_{α} proton was easily found despite the heavy amide proton resonance overlap in the oxidized state as the amide proton and $C_{\alpha}H$ resonances shift considerably on changing the redox state. The $C_{\alpha}H$ and ring proton resonances of Y89 were already correctly assigned by Moonen et al. [34], but the C_{β} protons were not. These incorrect assignments resulted from coinciding $C^{\delta 2}H$ and $C^{\delta}H$ resonances of F86 and Y89 and from assigning the C_{β} protons by the use of only NOESY spectra (the C_{β} protons of F86 were in fact wrongly considered as the C_{β} protons of Y89). In this study two weak HoHaHa connectivities of C_{β} protons to the C_{α} proton of Y89 were detected and were further confirmed by strong NOE connectivities to the C_{δ} protons of the ring. No indications of a different orientation of Y89 in oxidized *M. elsdenii* flavodoxin as compared to Y88 in oxidized *Clostridium MP* flavodoxin were found in contrast to previous interpretations [34]. Intense $d_{\alpha N}$ and $d_{\beta N}$ connectivities, starting at Y89, were found to an amide proton resonance which appeared to be of a glycine residue, so it was assigned to G90. Of W91 all resonances, with the exception of the amide proton and NH_{ϵ} , have already been previously assigned [33,34]. This combined with correlated spectra, a d_{NN} and a weak $d_{\alpha N}$ connectivity starting at G90, resulted in the complete assignment of W91. A d_{NN} and $d_{\alpha N}$ contact starting at W91 was found to an amide proton resonance, assigned to G92, a weak intraresidual $NH-C_{\alpha}H$ HoHaHa connectivity could be detected for this spin system. One serine spin system was yet unassigned. Therefore it had to be S93. Its amide proton resonance has a weak intensity in NOESY spectra thus requiring the postponement of its assignment to the final stage.

Assigning G94-W96 was no arduous task despite chemical shift differences as compared to the reduced state. It started with $d_{\alpha N}$ and d_{NN} connectivities from S93 to G94, followed by a $d_{\alpha N}$ connectivity to the amide proton resonance of E95. No

d_{NN} connectivity with G94 was observed (as in the reduced state). The sequential connectivity pattern on going to A99 was identical to the reduced state of the protein (despite chemical shift variations).

The amide proton resonance intensity of N118 is influenced by the pH of the solution [7]. It is almost absent in the reduced state and manifest in the oxidized state (see Fig. 5). Its altered resonance position was detected via a strong $d_{\alpha N}$ connectivity with V117. The amide proton resonance of E119 was in turn assigned via a strong $d_{\alpha N}$ contact with N118. Discussion of sequence specific assignments concerning the flavin binding region is now completed. Resonances of the complete apoprotein have been summarized in Table 1.

Flavin assignments

In assigning resonances from the flavin in the oxidized state use has been made of structural information available concerning the two-electron reduced state of the protein [8,12]. The three-dimensional structure of the flavin binding region of oxidized *Clostridium MP* flavodoxin was also used as NMR studies have shown that the flavin binding regions of both proteins are very similar [22]. Resonances of $CH_3(7\alpha)$ and $CH_3(8\alpha)$ of the flavin (Fig. 1) were assigned by Moonen and Müller [33] and the resonance positions were confirmed in this 2D-NMR study (Table 2). A HoHaHa and Cosy connectivity of $CH_3(7\alpha)$ with a resonance at 8.48 ppm was found. A strong NOE connectivity between both resonances was present in the NOESY spectra and the resonance is strongly dependent on the reduction state of the protein. Therefore it was assigned to C_6H of the flavin. The $CH_3(8\alpha)$ protons exhibit a very strong NOE connectivity with a resonance at 7.95 ppm which therefore is assigned to C_9H of the flavin. In addition a Cosy connectivity is found. C_6H and C_9H resonate at positions different from those which would have been expected on the basis of a previous study [33]. This study probably suffered from difficulties in analyzing difference spectra to determine these resonances of the holoprotein and the protein reconstituted with 7-methyl-10-ribityl-isoalloxazine-5'-monophosphate (i.e. replacement of the methyl group at C(8) by a proton).

Table 1: 1H chemical shifts (ppm) of *M. elsdenii* flavodoxin in the oxidized state (pH 7.0, 41 0C). Resonance positions of two-electron reduced *M. elsdenii* flavodoxin are given in brackets (from van Mierlo et al. [7], pH 8.3, 41 0C). In the case of a chemical shift difference $\geq \pm 0.07$ ppm, the chemical shift position of the corresponding resonance of the oxidized state has been given in bold letter type.

Residue	NH	C α H	C β H	Others
Met1		4.00(3.74)	2.17,2.07(2.21,2.04)	C γ H 2.53(2.51)
Val2	8.56(8.33)	4.49(4.40)	2.04(2.03)	C γ H 0.79,0.70(0.81,0.71)
Glu3	8.93(8.69)	5.11(5.15)	2.16,1.84(2.17,1.85)	
Ile4	9.19(9.11)	4.99(5.05)	2.07(2.08)	C γ H3 1.00(1.02) C γ H2 1.59(1.61) C δ H 0.70(0.64)
Val5	9.23(9.25)	5.39(5.42)	1.45(1.48)	C γ H 0.57,-0.32(0.60,-0.31)
Tyr6	7.91(7.95)	6.05(6.11)	2.68,2.74(2.73,2.78)	C δ H 6.56(6.60) C ϵ H 6.51(6.49)
Trp7	8.33(8.43)	4.45(4.46)	3.18,3.19(3.24,3.24) C δ H	NH 9.93(9.89) 7.49(7.50) C ζ 2H 7.46(7.47) C ζ 1H 7.16(7.19) C ζ 3H 6.95(7.06) C ζ 3H 7.27(7.38) OH 7.93(8.06)
Ser8	5.90(5.82)	4.34(4.36)	3.54,3.43(3.58,3.43)	
Gly9	10.37(10.43)	3.77,3.72(3.79,3.79)		C γ H 1.23(1.21)
Thr10	9.27(9.35)	4.71(4.66)	4.57(4.59)	
Gly11	7.55(7.55)	3.63,4.41(3.64,4.43)		NH1 6.43(6.42) NH2 8.12(8.21)
Asn12	11.39(11.49)	4.64(4.63)	2.65,3.23(2.64,3.25)	C γ H 1.39(1.49) OH 6.21(6.17)
Thr13	11.30(11.40)	3.82(3.86)	4.40(4.43)	
Glu14	7.20(7.17)	3.25(3.30)		
Ala15	7.96(7.97)	4.14(4.16)	1.65(1.65)	
Met16	7.99(8.01)	3.77(3.79)	2.57(2.58) CH3	C γ H 3.02*(3.03*) 2.13**(2.15**)
Ala17	8.21(8.27)	3.27(3.30)	0.91(0.91)	
Asn18	7.84(7.86)	4.33(4.32)	2.92,2.75(2.93,2.76)	

Glu19	8.03(8.04)	3.97(3.97)	2.10,2.07(2.13,2.09)	C ¹ H3	0.37(0.38)
Ile20	8.81(8.81)	3.31(3.33)	1.28(1.29)	C ¹ H2	1.52,0.72(1.53,0.74)
				C ^δ H	-0.44(-0.43)
Glu21	8.72(8.71)	3.43(3.47)	2.08,2.00(2.09,2.02)		
Ala22	7.70(7.67)	3.98(3.98)	1.44(1.46)		
Ala23	7.55(7.57)	4.16(4.18)	1.59(1.61)		
Val24	8.41(8.42)	3.37(3.38)	2.11(2.12)	C ¹ H	1.08,0.77(1.08,0.77)
Lys25	8.23(8.17)	4.26(4.31)	1.81(1.83)	C ^δ H	1.73*,1.63*(1.73*,1.65*)
				C ^ε H	2.94*(2.96*)
Ala26	8.15(8.17)	4.13(4.14)	1.49(1.50)		
Ala27	7.39(7.40)	4.38(4.39)	1.45(1.47)		
Gly28	7.83(7.83)	3.73,4.23(3.75,4.25)			
Ala29	7.30(7.33)	4.77(4.81)	1.34(1.36)		
Asp30	8.22(8.22)	4.77(4.75)	2.68,2.51(2.69,2.52)		
Val31	8.24(8.17)	5.63(5.60)	2.03(2.06)	C ¹ H	0.95,0.87(0.95,0.88)
Glu32	8.19(8.15)	4.68(4.66)	1.98,2.07(1.99,2.10)	C ¹ H	2.28(2.25)
Ser33	8.41(8.43)	6.00(6.01)	3.65,3.54(3.66,3.58)		
Val34	9.52(9.53)	4.54(4.53)	2.05(2.06)	C ¹ H	0.95,0.82(0.97,0.84)
Arg35	8.18(8.17)	4.41(4.45)		C ^δ H	6.12(6.12)
Phe36	7.60(7.65)	3.22(3.25)	2.51,2.41(2.52,2.43)	C ^ε H	7.38(7.40)
				C ^ζ H	7.13(7.15)
Glu37	10.21(10.24)	4.12(4.13)	2.18,2.23(2.20,2.27)	C ¹ H	2.37(2.40)
Asp38	7.59(7.62)	4.97(4.98)	3.00,2.56(3.00,2.59)		
Thr39	7.54(7.56)	5.01(5.03)	3.91(3.97)	C ¹ H	1.13(1.15)
Asn40	9.22(9.24)	5.27(5.29)	2.90,2.90(2.91,2.91)	NH1	7.32**(?)
Val41	8.49(8.49)	3.31(3.31)	1.70(1.62)	C ¹ H	0.51,0.43(0.55,0.44)
Asp42	8.01(7.98)	4.30(4.31)	2.54,2.59(2.57,2.60)		
Asp43	8.10(8.07)	4.44(4.45)	2.65,2.59(2.70,2.59)		
Val44	7.73(7.75)	3.63(3.72)	2.24(2.25)	C ¹ H	1.33,1.02(1.35,1.05)

Ala45	8.28(8.30)	3.92(3.98)	1.44(1.48)		C ^γ H	0.97,0.79(0.98,0.85)
Ser46	7.28(7.28)	4.45(4.45)	4.12,3.99(4.12,4.03)		C ^γ H3	0.81(0.85)
Lys47	7.54(7.59)	4.52(4.54)	2.00,1.82**(1.98,1.90)**		C ^γ H2	1.44(1.45)
Asp48	7.84(7.85+)	4.52(4.55)	2.73,2.83(2.74,2.83)		C ^γ H	1.44(1.47)
Val49	7.52(7.48)	4.78(4.89)	1.99(2.06)		C ^δ H	0.65,0.53(0.68,0.56)
Ile50	8.57(8.61)	4.80(4.87)	1.66(1.64)		C ^γ H	1.74(1.75)
Leu51	9.66(9.65)	5.46(5.49)	2.08,1.15(2.10,1.18)		1.11,0.98(1.11,0.99)	
Leu52	8.52(8.57)	5.49(5.54)	1.94,1.47(1.95,1.52)			
Gly53	9.37(9.37)	4.76,1.76(4.79,1.80)	C ^δ H			
Cys54	9.28(9.36)	5.55(5.60)			SH	4.52(5.05)
Pro55	-	5.29(5.40)	2.84,2.79(2.86,2.86)		C ^γ H	1.39**(1.85)
Ala56	6.32(6.46)	2.29(2.67)	2.37,1.62(2.32,2.07*)		C ^δ H	4.34,4.85(4.39,4.95)
Met57	7.46(7.96)	3.61(5.11)	-0.04(0.09)		C ^γ H	?(2.29*)
Gly58	7.39(6.95)	3.98,4.11(3.72,3.86)	0.99,1.80**(1.15,1.60**)			
Ser59	9.09(9.05)	4.83(5.10)			C ^γ H	?(2.62*)
Glu60	8.23(9.39)	3.80(3.73)	3.87,4.01(3.71,3.90)		C ^γ H	(2.25*,?)(2.34,2.34)
Glu61	8.33(9.19)	4.49**(4.54)	2.44*,2.18*(2.41*,2.10*)		C ^γ H	1.02(1.06)
Leu62	7.73(7.56)	4.02(4.19)	2.05*,1.71(2.07,1.79)		C ^δ H	-0.25,-0.74(-0.22,-0.64)
Glu63	5.84(6.00)	3.26(3.24)	1.40,0.73(1.39,0.73)		C ^γ H	-0.31,1.21*(0.30,1.22*)
Asp64	7.97(7.91)	4.07(4.10)	1.41,?(1.47,0.74*)			
Ser65	8.20(8.22)	4.30(4.31)	2.57,?(2.58,2.68)			
Val66	10.79(10.88)	4.00(4.02)	3.91,3.82(3.93,3.82)		C ^γ H	0.96,0.79(0.97,0.80)
Val67	7.78(7.82)	2.54(2.57)	1.60(1.65)		C ^γ H	0.57,0.33(0.59,0.37)
Glu68	8.52(8.55)	4.15(4.15)	1.99(2.05)			
Pro69	-	4.27(4.27)	2.25(2.25)		C ^γ H	1.82(1.82)
			C ^δ H			3.41,3.08(3.43,3.11)

Phe70	7.07(7.10)	4.12(4.13)	3.14,3.14(3.15,3.15)	C ^δ H C ^ε H C ^ζ H C ^δ H C ^ε H C ^ζ H C ^η H	7.30(7.30) 7.33(7.34) 7.16(7.11) 7.26(7.27) 6.72(?) 7.00(?) 1.21(1.23)
Phe71	9.76(9.81)	4.15(4.19)	3.03,3.03(3.06,3.06)		1.61(1.66) 1.24,1.04(1.28,1.05)
Thr72	8.56(8.55)	3.69(3.71)	4.27(4.28)		
Asp73	7.25(7.26)	4.49(4.48)	2.60,2.46(2.62,2.46)		
Leu74	8.40(8.42)	3.91(3.93)	1.90(1.92)		
Ala75	8.12(8.13)	3.71(3.73)	1.13(1.13)		
Pro76	-	4.45(4.46)	2.41,1.79(2.41,1.80)	C ^η H C ^δ H	1.97(1.98) 3.58(3.59)
Lys77	8.19(8.21)	4.38(4.39)	1.87(1.89)		
Leu78	7.59(7.60)	4.22(4.19)	2.09(2.10)		
Lys79	7.02(7.05)	3.57(3.60)	1.97,1.85*(1.99,1.82*)	C ^δ H C ^δ H C ^ε H	0.86**,0.66**(0.89**,0.68***) 1.58(1.59) 3.06(3.07)
Gly80	7.79(7.77)	4.19,3.88(4.21,3.89)			
Lys81	8.16(8.15)	4.71(4.68)	1.95,?(1.97,1.85*)	C ^η H C ^δ H	1.39*(1.43*) 1.66*(1.66*)
Lys82	7.96(7.88)	4.94(5.00)	2.17,2.17(2.18,2.18)	C ^η H C ^δ H C ^ε H C ^η H	1.55*,1.42*(1.57*,1.42*) 1.68*(1.67*) 3.05(3.03) 0.86,0.86(0.88,0.88)
Val83	8.86(8.88)	5.75(5.79)	1.57(1.59)		
Gly84	9.34(9.31)	5.14,3.30(5.18,3.32)			
Leu85	7.33(7.35)	5.49(5.54)	1.48,0.39(1.52,0.46)	C ^η H C ^δ H C ^δ H C ^ε H C ^ζ H C ^ε H	0.91(0.94) 0.01,-0.40(0.05,-0.39) 6.68(6.69) 6.83(6.84) 6.83(6.82) 7.32(7.32)
Phe86	9.37(9.29)	6.05(6.08)	3.12,2.89(3.14,2.91)		

Gly87	8.16(8.20)	5.18, 4.01(5.25, 4.06)		$C\delta^2H$	7.09(7.09)
Ser88	6.56(6.53)	6.09(6.11)	3.70, 3.70(3.72, 3.72)	OH	6.64(6.49)
Tyr89	8.32(8.05)	5.25(5.34)	2.84, 2.74(3.13, 2.64)	$C\delta^1H$	7.10(7.08)
				$C\delta^2H$	6.65(6.60)
Gly90	8.67(9.64)	4.69, 3.72(4.41, 3.54)			
Trp91	6.83(8.06)	4.92(5.05)	3.38, 3.38(3.49, 3.27)	NH	10.13(10.07)
				$C\delta^1H$	7.12(7.11)
				$C\delta^2H$	6.45(7.78)
				$C\eta^2H$	5.61(6.95)
				$C\delta^3H$	6.80(7.10)
				$C\epsilon^3H$	7.60(7.52)
Gly92	8.26(10.05)	4.47(?)			
Ser93	9.61(9.65)	4.80(4.63)	3.99, 3.90(4.01, 3.88)		
Gly94	9.22(9.48)	4.04, 3.58(4.04, 3.67)		$C\eta^1H$	2.49*, 2.40*(2.70*, 2.38)
Glu95	9.36(8.86)	4.05(4.03)	2.24, 2.09(2.17, 2.03)	NH	
Trp96	9.43(9.75)	4.43(4.39)	3.21, 2.96(3.26, 3.00)	$C\delta^1H$	8.96(9.05)
				$C\delta^2H$	6.33(6.40)
				$C\eta^2H$	7.38(7.38)
				$C\delta^3H$	7.10(7.10)
				$C\epsilon^3H$	6.60(6.61)
				$C\eta^1H$	7.42(7.45)
Met97	6.88(6.74)	3.98(3.99)	1.42, -0.16(1.39, -0.17)	$C\eta^1H$	2.09**, 2.03(2.10**, 2.01)
				CH3	?(1.56**)
Asp98	7.26(7.35)	4.25(4.24)	2.69, 2.69(2.71, 2.68)		
Ala99	7.67(7.88)	4.22(4.22)	1.55(1.57)		
Trp100	8.31(8.29)	4.43(4.44)	3.28, 3.00(3.33, 3.03)	NH	6.17(6.12)
				$C\delta^1H$	6.38(6.36)

Lys101						C ² H	6.72(6.73)
						C ¹² H	7.34**(7.33**)
						7.00**(7.08**)	
						C ¹ H	1.31,1.12(1.31,1.13)
Gln102						C ⁸ H	1.58(1.59)
						C ⁶ H	2.84(2.85)
						OH	3.68(3.68)
Arg103						C ⁷ H	0.96(0.96)
Thr104						C ⁷ H	2.52(2.53)
Glu105						OH	5.38(5.39)
						C ⁷ H	1.51(1.52)
						C ⁷ H	1.13(1.13)
Asp106						C ⁷ H	0.77,0.77(0.79,0.79)
Thr107						C ⁷ H3	0.68**(0.68**)
						C ⁷ H2	0.86,1.06(0.87,1.09)
						C ⁸ H	0.55(0.57)
Gly108						C ⁷ H	0.91(0.95)
Ala109						C ⁷ H3	0.78(0.79)
Thr110						C ⁷ H2	1.15,1.67(1.15,1.67)
Val111						C ⁸ H	0.60(0.61)
Ile112						C ⁷ H	0.90,0.72(0.89,0.72)
Gly113						NH1	7.14(6.91)
						NH2	6.00(6.23)
						C ⁷ H	2.03*(2.02*)
Thr114							
Ala115							
Ile116							
Val117							
Asn118							
Glu119							

Met120	7.42(7.41)	4.52(4.44)	2.04(2.06)	C ¹ H	2.68*, 2.57*(2.71*, 2.57*)
Pro121		4.46*(4.46*)		C ² H	3.49, 4.39*(3.48, 4.36*)
Asp122	8.05(8.05)	4.55(4.55)	2.68, 2.41(2.68, 2.41)		
Asn123	10.49(10.49)	4.04(4.06)	2.90, 2.79(2.91, 2.81)		
Ala124	9.21(9.22)	4.54(4.55)	1.68(1.68)		
Pro125		4.29(4.29)	2.42, 2.02(2.42, 2.01)	C ¹ H	2.18(2.18)
				C ² H	4.21**, 4.15**(4.19**, 4.14**)
Glu126	10.32(10.32)	4.07(4.08)	1.84, 1.99(1.85, 1.99)	C ¹ H	2.97, 2.43(2.96, 2.47)
Cys127	7.07(7.07)	3.60(3.62)	3.31, 2.60(3.33, 2.61)	SH	1.90(1.90)
Lys128	6.91(6.92)	3.73(3.74)	1.86, 1.77(1.89, 1.79)	C ¹ H	1.36, 1.29(1.38, 1.30)
				C ² H	1.60(1.61)
				C ³ H	2.94(2.92)
Glu129	8.37(8.36)	3.97(3.98)	2.01, 2.01(2.02, 2.02)	C ¹ H	2.37, 2.23(2.38, 2.24)
Leu130	7.33(7.32)	4.18(4.20)		C ¹ H	1.33(1.34)
				C ² H	0.71, 0.67(0.71, 0.67)
Gly131	8.00(7.99)	3.54, 3.45(3.55, 3.47)			
Glu132	8.32(8.30)	3.70(3.70)	2.05, 1.91(2.07, 1.93)	C ¹ H	2.42(2.43)
Ala133	7.84(7.83)	4.01(4.02)	1.43(1.45)		
Ala134	8.28(8.26)	3.77(3.79)	1.34(1.35)		
Ala135	7.82(7.80)	3.79(3.81)	1.48(1.49)		
Lys136	7.13(7.14)	4.40(4.41)	1.73, 1.65(1.74, 1.66)	C ¹ H	1.50(1.50)
				C ² H	1.95(1.97)
				C ³ H	2.96(2.97)
Ala137	7.04(7.06)	3.99(3.99)	1.41(1.43)		

- One asterisk indicates resonances belonging to a specific amino acid residue (manifested via Cosy or HoHaHa cross peaks) with a tentatively determined position in the amino acid side chain.
- Two asterisks indicate tentative resonance positions, determined exclusively via Noesy spectra.
- A question mark is used when the corresponding resonance is unknown.
- The amide resonance position of D48 in the two-electron reduced state has been determined using the 2D-NMR spectra of the partially-reduced and the oxidized states of the protein.

Table 2: ^1H and some ^{13}C resonances (in ppm) of oxidized FMN bound to the apoflavodoxin from *M. elsdenii*.

^1H resonances	ox	red(taken from [7])	
N_3H	?	9.39	
C_6H	8.48	6.48	
$\text{CH}_3(7\alpha)$	2.66	2.04	
$\text{CH}_3(8\alpha)$	2.75	2.10	
C_9H	7.95	6.09	
$\text{C}_1'\text{H}$	4.48 4.54	2.82	3.36
$\text{C}_2'\text{H}$	4.09	3.74	
$\text{C}_2'\text{OH}$	6.00	6.86	
$\text{C}_3'\text{H}$	3.35	3.01	
$\text{C}_3'\text{OH}$	n.o.	n.o.	
$\text{C}_4'\text{H}$	3.92*	3.99*	
$\text{C}_4'\text{OH}$?	5.96*	
$\text{C}_5'\text{H}$	3.75 3.83	3.38	3.38
^{13}C resonances	ox	red(taken from [7])	
C_1'	45.30	46.50	
C_2'	69.30	66.09	
C_5'	64.85	65.15	

- The $\text{C}_1'\text{H}$, $\text{C}_2'\text{H}$ and $\text{C}_5'\text{H}$ resonances were assigned using selectively enriched FMN molecules. The resonances labeled with an asterisk were assigned on the basis of NOESY spectra using the tertiary structure information which we had already gathered that time.

- Flavin ^{13}C resonances were determined using selectively ^{13}C enriched flavins.

Resonance positions of ribityl side chain protons $\text{C}_1'\text{H}$, $\text{C}_2'\text{H}$ and $\text{C}_5'\text{H}$, could be determined by using modified flavins selectively ^{13}C enriched in the ribityl part of the FMN molecule. The $\text{C}_2'\text{OH}$ resonance was identified by its Cosy connectivity to the $\text{C}_2'\text{H}$ resonance and its disappearance on dissolving the protein in deuterium oxide. The $\text{C}_3'\text{H}$ resonance has been assigned based on its HoHaHa connectivity with $\text{C}_2'\text{H}$ and its strong NOE's with the $\text{C}_1'\text{H}$ resonances, in analogy with the assignments in reduced flavodoxin [12]. No $\text{C}_3'\text{OH}$ resonance has been found. Its position on the surface of the molecule will result in fast exchange of this proton with the saturated solvent [7]. $\text{C}_4'\text{H}$ has been tentatively assigned based on NOE's with $\text{C}_\alpha\text{H}(89)$, $\text{C}_2'\text{OH}$, C_9H and $\text{NH}(90)$. Resonances of N_3H and $\text{C}_4'\text{OH}$ have not been detected. Flavin assignments are summarized in Table 2.

Secondary and tertiary structure: comparing the redox states

Secondary structure

After visually comparing the type and intensity of sequential connectivities observed in NOESY spectra outside the flavin binding region in the three redox states, we have to conclude that the secondary structure remains identical. Figs. 2, 3 and 4 are illustrations of the equivalence of the structures. So, *M. elsdenii* flavodoxin in the oxidized state contains five helices: N12-A26 (1); V41-A45 (2); D64-L74 (3); E95-D106 (4) and E126-A135 (5) and five strands of β -sheet: V2-Y6 (1); V31-R35 (2); V49-G53 (3); K82-Y89 (4) and T110-N118 (5) as deduced for the two-electron reduced state of the protein [12]. The amide proton exchange against deuterons (Fig. 6) is virtually identical between the oxidized and two-electron reduced state of the protein. In the case of the amide protons of E14, E19, A22, T39, V49, V67, E68, A75, N98, W100, T104 and T110 a slight decrease in exchange rate is observed, believed to result from the lower pH of the solution as compared to the fully reduced state [7].

Tertiary structure

Using long-range NOE's it is possible to position the secondary structure elements in space and determine the fold of a protein. Non-sequential interresidual NOE cross peaks connect amino acid residues which although far apart in the primary sequence are in close spatial proximity of each other. Visual analysis of the NOESY spectra led us to the conclusion that the tertiary structures of oxidized, one-electron and two-electron reduced flavodoxin are, with the exception of the flavin binding region, identical. Figs. 2, 3 and 4 illustrate the correspondence in NOE connectivity pattern of the protein in its three redox states. Based on similarity to the two-electron reduced state we can conclude that the tertiary structure of the oxidized state comprises a central parallel β -sheet with the connectivity pattern 2-1-3-4-5, surrounded on both sides by two α -helices, respectively helices nos. 1 and 5 on one side and helices nos. 3 and 4 on the opposite side of the sheet (see Fig. 7). The majority of amide protons present in the β -sheet have diminished exchange rates with deuterons. Even after 170 h these amide protons are still present (Fig. 6). Amide protons being part of the α -helices of flavodoxin have higher exchange rates resulting from the better accessibility and expected greater flexibility of these structures as compared to β -sheet structures [37,38].

Not only based on the similarity in NOE contacts, but also on the correspondence of the ^1H NMR chemical shifts between the two redox states (Table 1) we can conclude that the tertiary structure remains identical, except in the immediate flavin binding region. Chemical shifts are sensitive not only to local electronic structure,

protonation equilibria, and hydrogen bonding but also to shielding effects that result from the formation of secondary and tertiary structure on protein folding [6,39-41].

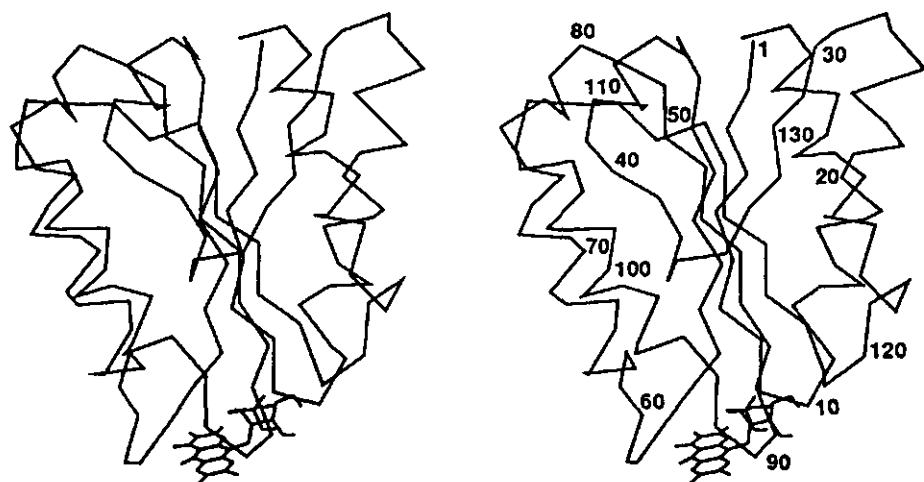


Fig. 7 Stereo drawing showing the C_{α} and FMN atoms of two-electron reduced *M. elsdenii* flavodoxin as determined from NMR and restrained molecular dynamics [12]. The structure has been generated by averaging the restrained molecular dynamics trajectory going from 60 to 120 ps. For more details see [12].

Despite the theoretical difficulties in interpreting 1H chemical shifts, correspondence of chemical shifts between two redox states of a protein is a valuable indication of structural similarity. Only 22 of the 109 amino acid residues outside the flavin binding region have proton chemical shift differences greater than or equal to 0.07 ppm on going from the quinone to the hydroquinone state. Chemical shift differences of 17 of these residues do not exceed the relatively small value of 0.10 ppm (I4, V31, V41, V44, K47, V49, I50, V66, K82, L85, F86, G87, D98, W100, K101, A109 and M120) (Table 1). The small inequivalences are likely to be the result of pH differences between samples of the reduced (pH=8.3) and the oxidized (pH=7.0) protein. In addition, small differences in ionic strength will also partly account for the observed differences. No NOE contact differences involving these residues have been observed. Five of the 22 residues exhibit chemical shift differences between 0.10 and 0.50 ppm, M1, V2, E3, M97 and A99 (Table 1). NOE cross peaks involving M1, V2 and E3 exhibit a characteristic lineshape in reduced flavodoxin. The extraordinary lineshape immediately disappears on a slight decrease of the pH (± 0.5 unit) on oxidation of the solution. The lineshape differences are expected to result from an instability of a saltbridge at pH 8.3 in this

region of the protein (involving residues E3, E32, D43 and K47) [12]. This instability disappears on lowering the pH resulting in normal lineshapes (Fig. 4). Further lowering of the pH of the solution to 7.0 (oxidized flavodoxin) results in a downfield shift of resonances, without changing the NOE connectivity pattern, probably resulting from protonation of elements of the saltbridge. Protonation of α -carboxylates can result in considerable downfield shifts of neighbouring amide protons, as demonstrated for the amide proton of the C-terminal residue of a linear tetrapeptide by Bundi and Wüthrich [42]. Slight conformational variations between the redox states as a result of pH and ionic strength might explain the chemical shift differences observed for the amide protons of M97 and A99 (Table 1). No NOE contact differences were however observed in this region of the protein.

Using 2D-NMR techniques it was relatively easy to determine the correspondence in structure outside the flavin-binding region of oxidized and reduced flavodoxin. Using crystallography it would have taken many years to compare these regions of the protein, as demonstrated for the closely related *Clostridium MP* flavodoxin [13-15]. Automated cross peak analysis of the NOESY spectra of both redox states of *M. elsdenii* flavodoxin might result in the observation of differences between both redox states outside the flavin binding region which have not been visually detected in the over-crowded spectra. Differences, if they exist, will however be quite subtle.

The FMN binding site

a. Conformation differences

The flavin-binding region is depicted for the reduced state of the protein in Fig. 8. The flavin phosphate primarily interacts with residues W7-T13. No conformation differences were detected in this region of the protein upon changing the redox state as based on NOE cross peak intensities. Several residues, including C54-E63 and S88-W96, exhibit large chemical shift differences on going from the oxidized to the two-electron reduced protein (Table 1). These residues are in the immediate vicinity of the isoalloxazine moiety and as this comprises the functional part of the molecule it received particular attention. No redox state dependent NOE differences were observed on going from C54 to A56 and from L62-E63. Chemical shift variations resulted from changes in local magnetic field caused by the flavin.

The NOE connectivities of M57 in the two redox states remained the same as far as we could observe. However, a NOE between the amide protons of respectively M57 and E61, which is prominent in the reduced state, is absent in the oxidized state. Side chain-side chain NOE connectivity variations in the high field part of the 2D-NMR spectrum involving M57 are difficult to analyze because of heavy cross

peak overlap. The same also holds true for the aliphatic side chains of other residues in the isoalloxazine binding region. Despite these problems we do not expect large redox state dependent side chain variations (>0.5 Å) in this region of the protein. Differing NOE connectivities concerning the amide proton resonances would then have been observed as a consequence of the compactness of flavodoxin.

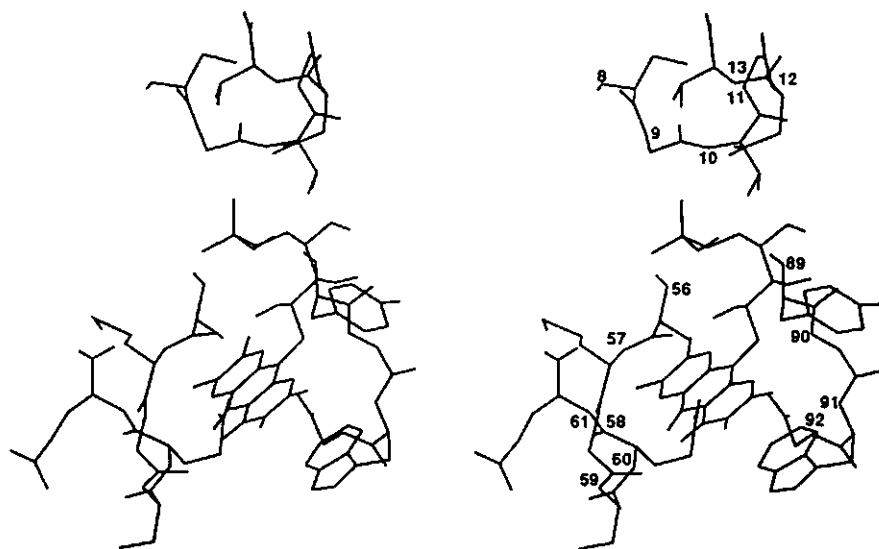


Fig. 8 Stereo drawing showing the environment of the isoalloxazine and the phosphate group of two-electron reduced *M. elsdenii* flavodoxin (the structure has been averaged over a restrained molecular dynamics trajectory going from 60 to 120 ps, see [12]). The region includes S8-T13, A56-E61 and Y89-G92. Amide protons have been labeled.

NOE's connecting $C_{\alpha}H$'s of G58 with $C_{\beta}H$ weaken on going to the fully reduced state of the protein while contacts involving the amide proton remain identical. The amide proton of S59 shows strongly increased NOE connectivities with one $C_{\alpha}H$ of G58 (3.86 ppm) and one $C_{\beta}H$ resonance (3.90 ppm). The other strong NOE connectivity with the amide proton of S59 can be the result of $C_{\alpha}H$ of G58 (3.72 ppm) and/or of one of its own $C_{\beta}H$ resonances (3.71 ppm). We cannot exclude both possibilities due to peak overlap. In the oxidized state we do not observe NOE connectivities between the amide proton of S59 and $C_{\alpha}H$'s of G58. The NOE connectivity between S59 $C_{\alpha}H$ and both $C_{\beta}H$'s remains identical. In addition, the NOE connectivity between $C_{\alpha}H$ of S59 and the amide proton of E60 increases on going to the reduced state of the protein.

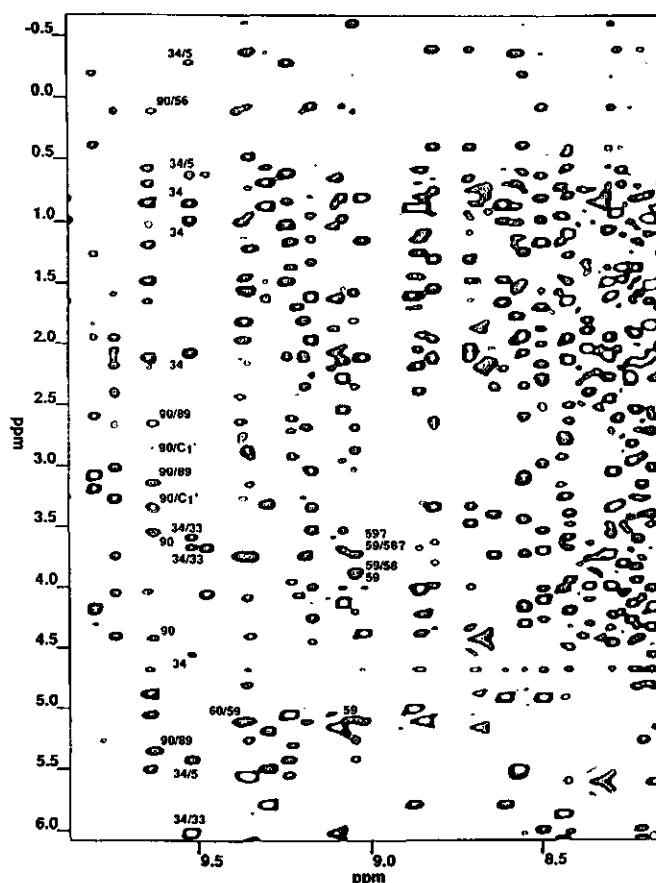


Fig. 9 Part of a 600 MHz NOESY spectrum of two-electron reduced *M. elsdenii* flavodoxin in 90% H_2O /10% $^2\text{H}_2\text{O}$, pH 8.3, 41 $^\circ\text{C}$, illustrating several NOE connectivities involving amide protons of V34, S59, E60 and G90. The NH90/C1' connectivities disappear on reconstitution of the protein with FMN selectively enriched with ^{13}C at the 1' sidechain position. Processing and resolution as in Fig. 2.

Figs. 9 and 10 illustrate several of the observed differences. NOE's between C α H of E60 and NH of E61 and between NH of E61 and C α H of A56 increase on going to the fully reduced state. All other NOE connectivities in this region of the protein, including contacts with the isoalloxazine moiety, remain identical as judged by eye.

Crystallographers observed co-ordinate differences at the peptide link between G57 and D58 after the superposition of the semiquinone and oxidized states of the closely related *Clostridium MP* flavodoxin [14]. The orientation of this peptide is drastically altered as a consequence of the reduction of the adjoining FMN as the carbonyl of G57 is expected to form a hydrogen bond with the N(5)H of the flavin.

of the amide proton of E60. The position of the amide proton of E61 is also changed on reduction of the protein (deduced from missing or lowering of NOE contacts with NH57, C α H56 and C α H60). This proton is in close proximity to the forementioned peptide link. In the case of *Clostridium MP* flavodoxin no changes in amide position of E61 have been reported [14].

In the region S88-W96 we observe a slight decrease in NOE intensity between C α H(89) and C2'OH on going to the fully reduced state. This probably results from a faster exchange of the latter proton with the solvent, caused by increasing the pH of the solution. The connectivity pattern of C2'OH remains identical as is the case for the C α H of Y89. In the case of G90, an intensity increase of NOE connectivities between the amide proton and the C1' protons of the ribityl side chain are observed (see Figs. 9 and 10). In addition, the d_{NN} connectivity with W91 increases. No further intensity changes were observed in this region of the protein. We expect that the amide proton of G90 is slightly displaced to the N₁ position of the isoalloxazine ring in the hydroquinone form in order to strengthen the hydrogen bond. N₁ becomes negatively charged on two-electron reduction of the flavin [22]. No convincing indications, based on NOE intensities, were found for differing positions of W91 on reduction. Differences observed for W90 in the case of the related *Clostridium MP* flavodoxin probably result from the influence of intermolecular contacts in the crystals, as suggested by Smith et al. [14].

For N118 and E119 no conformation differences have been observed. No indications were found for a change in conformation of the flavin on reduction.

b. Chemical shift differences

Analysis of chemical shift variations of protons surrounding the isoalloxazine ring on going from the oxidized to the reduced state should yield information concerning the function of the protein. Since the majority of proton resonances have been assigned in both redox states it is now possible to do this. For a correct and detailed prediction of the variations many theoretical difficulties have first to be overcome (including e.g.: ring current variations, electron distribution of the flavin and conformational differences of the protein). However, a perforce rough view can lead to interesting observations.

Changes in mobility in the flavin binding region are not expected on two-electron reduction of the oxidized molecule. In both redox states strong NOE connectivities between the constituting amino acid residues and between several residues and the flavin are detected. In addition the NOE for the N₃H group was determined to be very small in both redox states, indicating that the isoalloxazine is tightly bound to the protein [22]. Previously suggested differences in 'flipping rate' around the C β -C γ

axis of the ring of Y89 between the two redox states [34] have been shown not to exist [7].

The C_{1'} protons of the ribityl side chain are positioned in the plane of the isoalloxazine moiety closest to the pyrazine part of the molecule (Fig. 1). No conformational differences, as judged from NOESY spectra concerning these protons, were detected on reduction of the protein. A considerable upfield shift is observed (Table 2) which must be the consequence of a decreased ring current effect of the pyrazine part of the flavin. The C_α proton of M57 exhibits one of the largest downfield shifts of the apoprotein on reduction of the flavin (1.50 ppm downfield, Table 2). This proton is situated directly above the pyrazine part of the flavin (Fig. 8, clear NOE's between C_αH(57) and C₆H are observed in both redox states) and shows no detectable conformation differences. Its chemical shift difference is in accordance with a strongly decreased ring current in the pyrazine part of the flavin on two-electron reduction. The aromatic part of W91 is situated opposite to M57 and close to the isoalloxazine. C(7)H of W91 is the nearest atom to the N(5) atom of the flavin as evidenced by a clear NOE with N(5)H in the reduced state of the protein. No convincing conformation differences concerning this residue were observed between the two redox states based on NOESY spectra. C(6)H and C(7)H of W91 exhibit large downfield shifts on reduction (respectively: 1.34 and 1.33 ppm, Table 2), again consistent with a decrease in pyrazine ring current effects. Detailed analysis of these chemical shift variations might result in the conclusion that the indole part of W91 is shifting with respect to the isoalloxazine moiety on reduction as proposed for the closely related *Clostridium MP* flavodoxin [14]. However based on NOESY spectra we do not observe such an effect. The conclusion of Moonen et al. [34] concerning a shift of the indole part of W91 on reduction must therefore be regarded as tentative.

Amide proton resonances showing large downfield shifts on reduction include NH(60), NH(61), NH(90), NH(91) and NH(92). These shifts are caused by conformation changes (E60, E61 and G90) and possibly by altering hydrogen bonding interactions with the pyrimidine part of the isoalloxazine (E60, G90, W91 and G92). On reduction the electron density of the pyrimidine part alters and N₁ becomes negatively charged [22]. Hydrogen bonds to the pyrimidine part are expected to be influenced by the increased charge density in the reduced state. Owing to the lack of a detailed ring current model it is not possible to predict whether the ring current effect caused by the pyrimidine part will alter.

The amide proton of S59 has almost no chemical shift difference although it is in close proximity to the isoalloxazine. This is expected to result from the conformation change of the peptide unit linking G58 and S59, as already observed from altering NOE intensities.

G58 is the residue which is in closest proximity to the benzene part of the isoalloxazine ring (Fig. 8). As a reduction state dependent conformation change occurs in this part of the protein it is not possible to predict from the chemical shifts if a difference in ring current in the benzene part of the flavin occurs on reduction of the protein.

Concluding remarks

On reduction of *M. elsdenii* flavodoxin to the semiquinone state subtle conformation changes in the flavin binding region take place. These conformation changes correspond to an activation barrier in the transition between the oxidized and semiquinone state of the protein. The tertiary structure outside the immediate isoalloxazine binding region remains essentially unchanged. On further reduction of the protein to the two-electron reduced state no further conformation changes are expected, the fast electron exchange between the semiquinone and hydroquinone state prevents structural rearrangements. *M. elsdenii* flavodoxin is predestinated for one-electron transfer reactions by shuttling between the semiquinone and hydroquinone states. No difference in water accessibility of the flavin is observed on going from the oxidized to the reduced state as judged from the exchange characteristics of the corresponding amide protons with deuterium oxide (Fig. 6 and see [7]). Flexibility changes in the flavin binding region on reduction of the protein are not expected as judged from many strong NOE connectivities in this part of the molecule in both redox states.

Conformation changes in *M. elsdenii* flavodoxin are expected to result in a close contact of the backbone carbonyl group of the peptide unit linking G58-S59 with N(5)H of the flavin in the semiquinone and two-electron reduced states of the protein. The semiquinone state is stabilized as compared to the oxidized state [1]. Hydrogen bonding between the carbonyl of G58 and N(5)H of the neutral flavin is very likely to account for this. The situation is analogous to *Clostridium MP* flavodoxin [14]. As a result of changes in the forementioned peptide unit, the amide position of E61 is also changed, probably to stabilize this altered peptide unit orientation. On reduction of the neutral semiquinone state of *M. elsdenii* flavodoxin, N₁ becomes negatively charged [22] and the flavin becomes anti-aromatic [43] in contrast to the oxidized state. The latter is evidenced by a decrease in ring current effect of the pyrazine part of the isoalloxazine moiety on the protein. The amide proton of G90 is slightly displaced towards the N₁ position of the flavin. The crucial negative charge on the N₁ position in the hydroquinone state is expected to be destabilized by its local microenvironment [12] in which no charged group is present within a distance of 6 Å of N₁ as deduced from the tertiary structure (Fig. 8),

as compared to the uncharged situation, resulting in the main contribution to the low redox potential of the semiquinone/hydroquinone couple of *M. elsdenii* flavodoxin.

Two-dimensional NMR experiments have allowed a detailed analysis of the tertiary structure of *M. elsdenii* flavodoxin in its redox states. Conformation differences in the flavin binding region on going from the oxidized to the hydroquinone state of the protein could be detected using NOESY spectra. Differences in ring current effects on reduction of the isoalloxazine moiety were observed by analyzing chemical shift variations of protons in the immediate vicinity of the isoalloxazine part. A more detailed analysis of the relationship between chemical shift position and reduction state of the protein using the tertiary structures of both the oxidized (yet to be generated) and the fully reduced states [12] should reveal further important information concerning the relationship between tertiary structure and function of this interesting macromolecule.

Acknowledgement

All 2D-NMR experiments have been done at the HF-SON NMR-Facility Nijmegen (The Netherlands). Help of Dr. J. de Vlieg and Mr. P. Lijnzaad in generating Figs. 7 and 8 is greatly appreciated. Dr. A. Bacher supplied us with ^{13}C labeled FMN which we greatly acknowledge. We are indebted to Dr. R. D. Hall for carefully reading the manuscript. This study was carried out under the auspices of the Netherlands Foundation for Chemical Research (SON) with financial aid from the Netherlands Organization for the Advancement of Pure Research (NWO).

References

1. Mayhew, S.G. & Ludwig, M.L. (1975) *Enzymes 3rd Ed.* 12, 57-118.
2. Moonen, C.T.W. & Müller, F. (1982) *Biochemistry* 21, 408-414.
3. Wüthrich, K., Wider, G., Wagner, G. & Braun, W. (1982) *J. Mol. Biol.* 155, 311-319.
4. Wagner, G. & Wüthrich, K. (1982) *J. Mol. Biol.* 155, 347-366.
5. Billeter, M., Braun, W. & Wüthrich, K. (1982) *J. Mol. Biol.* 155, 321-346.
6. Wüthrich, K. (1986) *NMR of proteins and nucleic acids*, Wiley, New York.
7. Mierlo van, C.P.M., Vervoort, J., Müller, F. & Bacher, A. (1990) *Eur. J. Biochem.* 187, 521-541.
8. Mierlo van, C.P.M., Müller, F. & Vervoort, J. (1990) *Eur. J. Biochem.*, (in press).

9. van Gunsteren, W.F., Kaptein, R. & Zuiderweg, E.R.P. (1983) in *Nucleic Acid Conformation and Dynamics* (Olson, W.K. Ed.) Report of NATO/CECAM Workshop, pp. 79-92, Orsay, France.
10. Kaptein, R., Zuiderweg, E.R.P., Scheek, R.M., Boelens, R. & van Gunsteren, W.F. (1985) *J. Mol. Biol.* 182, 179-182.
11. Clore, G.M., Brünger, A.T., Karplus, M. & Gronenborn, A.M. (1986) *J. Mol. Biol.* 191, 523-551.
12. Mierlo van, C.P.M., Lijnzaad, P., Vervoort, J., Müller, F., Berendsen, H.J.C. and de Vlieg, J. (1990) *Eur. J. Biochem.*, (submitted).
13. Burnett, R.M., Darling, G.D., Kendall, D.S., LeQuesne, M.E., Mayhew, S.G., Smith, W.W. & Ludwig, M.L. (1974) *J. Biol. Chem.* 249, 4383-4392.
14. Smith, W.W., Burnett, R.M., Darling, G.D. & Ludwig, M.L. (1977) *J. Mol. Biol.* 117, 195-225.
15. Ludwig, M.L., Burnett, R.M., Darling, G.D., Jordan, S.R., Kendall, D.S. & Smith, W.W. (1976) in *Flavins and Flavoproteins* (Singer, T.P., ed.) pp. 393-404, Elsevier, Amsterdam.
16. Mayhew, S.G. & Massey V. (1969) *J. Biol. Chem.* 244, 794-802.
17. Wassink, J.H. & Mayhew, S.G. (1975) *Anal. Biochem.* 68, 609-616.
18. Vervoort, J., O'Kane, D., Müller, F., Bacher, A., Strobl, G. & Lee, J. (1990) *Biochemistry*, (in press).
19. Sedlmaier, H., Müller, F., Keller, P.J. & Bacher, A. (1987) *Z. Naturforsch.* 42c, 425-429.
20. Hausinger, R.P., Honek, J.F. & Walsh, C. (1986) *Methods Enzymol.* 122, 199-209.
21. Nielsen, P., Rauschenbach, P. & Bacher, A. (1986) *Methods Enzymol.* 122, 209-220.
22. Vervoort, J., Müller, F., Mayhew, S.G., van den Berg, W.A.M., Moonen, C.T.W. & Bacher, A. (1986) *Biochemistry* 25, 6789-6799.
23. Marion, D. & Wüthrich, K. (1983) *Biochem. Biophys. Res. Commun.* 113, 967-974.
24. Rance, M., Sörenson, O.W., Bodenhausen, G., Wagner, G., Ernst, R.R. & Wüthrich, K. (1983) *Biochem. Biophys. Res. Commun.* 117, 479-485.
25. Bodenhausen, G., Kogler, H. & Ernst, R.R. (1984) *J. Magn. Res.* 58, 370-388.
26. Bax, A. & Davis, D.G. (1985) *J. Magn. Reson.* 65, 355-360.
27. Pearson, G.A. (1977) *J. Magn. Reson.* 27, 265-272.
28. Tanaka, M., Haniu, M., Yasunobu, K., Mayhew, S. & Massey, V. (1973) *J. Biol. Chem.* 248, 4354-4366.
29. Tanaka, M., Haniu, M., Yasunobu, K., Mayhew, S. & Massey, V. (1974) *J. Biol. Chem.* 249, 4397.

30. Müller, F. (1983) *Curr. Top. Chem.* 108, 71-107.
31. Moonen, C.T.W. & Müller, F. (1984) *Eur. J. Biochem.* 140, 303-309.
32. Moonen, C.T.W., Hore, P.J., Müller, F., Kaptein, R. & Mayhew, S.G. (1982) *FEBS Lett.* 149, 141-146.
33. Moonen, C.T.W. & Müller, F. (1984) *Eur. J. Biochem.* 140, 311-318.
34. Moonen, C.T.W., Scheek, R.M., Boelens, R. & Müller, F. (1984) *Eur. J. Biochem.* 141, 323-330.
35. Mayhew, S.G. (1978) *Eur. J. Biochem.* 85, 535-547.
36. Wüthrich, K. & Wagner, G. (1979) *J. Mol. Biol.* 130, 1-18.
37. Bhaskaran, R. & Ponnuswamy, P.K. (1984) *Int. J. Protein Res.* 24, 180-191.
38. Bhaskaran, R. & Ponnuswamy, P.K. (1988) *Int. J. Protein Res.* 32, 241-255.
39. Szilágyi, L. & Jardetzky, O. (1989) *J. Magn. Reson.* 83, 441-449.
40. Wagner, G., Pardi, A. & Wüthrich, K. (1983) *J. Am. Chem. Soc.* 105, 5948-5949.
41. Pardi, A., Wagner, G. & Wüthrich, K. (1983) *Eur. J. Biochem.* 137, 445-454.
42. Bundi, A. & Wüthrich, K. (1979) *Biopolymers* 18, 299-311.
43. Müller, F., Vervoort, J., van Mierlo, C.P.M., Mayhew, S.G., van Berkel, W.J.H. & Bacher, A. (1987) in *Flavins and Flavoproteins* (Edmondson, D.E. & McCormick, D.B., eds.) pp. 261-270, Walter de Gruyter & Co., Berlin.

Chapter 6

Three-dimensional Clean TOCSY-NOESY NMR study of *Megasphaera elsdenii* flavodoxin in the oxidized state

Sybren S. Wijmenga¹, and Carlo P. M. van Mierlo²

1. National HF-NMR Facility, Laboratory of Biophysical Chemistry, Faculty of Science, University of Nijmegen, Toernooiveld 6525 ED Nijmegen, The Netherlands.

2. Department of Biochemistry, Agricultural University, Wageningen, The Netherlands.

Summary

The value of a 3D non-selective TOCSY-NOESY spectrum for making sequential resonance assignments in proteins is demonstrated using the relatively large *Megasphaera elsdenii* flavodoxin (molecular mass 15 kDa) in the oxidized state. An easy and concise way for the analysis of cross peaks in a 3D spectrum is given. In addition, non-selective TOCSY-NOESY is compared with selective TOCSY-NOESY and nonselective NOESY-TOCSY. Sequential assignments in various secondary structure elements of flavodoxin are made using the f1f3 and f1f2 planes.

Introduction

Flavodoxins are a group of small proteins (molecular mass ranging from 14 kDa to 23 kDa) functioning as low-potential electron transfer proteins [1]. They contain non-covalently bound riboflavin-5'-phosphate (FMN) as prosthetic group and have been found in several sources of bacteria and algae. The protein-bound flavin can occur in the oxidized, one-electron reduced (semiquinone) and the two-electron reduced (hydroquinone) state.

Recently, 2D-NMR techniques have been used to study in detail the solution structures of *M. elsdenii* flavodoxin (137 amino acid residues) in the reduced as well as in the oxidized state. The sequential assignments of the ^1H NMR spectra of the two-electron reduced *M. elsdenii* flavodoxin have been described [2]. Based on these assignments, using interresidual NOE connectivities the secondary structure elements of two-electron reduced *M. elsdenii* flavodoxin were determined [3]. The tertiary structure has been generated using restrained molecular dynamics [4-6] with 509 interresidual distance restraints, which had been extracted from NOESY spectra [7]. A detailed analysis of the solution structure, which strongly resembles the crystal structures of the related *Clostridium MP* flavodoxin [8-9], has been made [7]. The sequential assignments of the ^1H NMR spectrum of *M. elsdenii* flavodoxin in the oxidized state have recently been described as well [10]. From this study the conformational differences between the oxidized and the semiquinone, and the hydroquinone states became clear [10].

In the past few years two-dimensional NMR has been applied successfully for the sequential assignments in spectra of relatively small-sized proteins (e.g. BPTI, 58 amino acid residues [11,12]). Several sequential resonance assignments have been made on proteins not exceeding 90 amino acid residues [12-28]. Assignments of proteins of larger sizes have only recently been made, including those for spinach plastocyanin (99 residues [29]), and hen egg white lysozyme (129

residues [30]). *M. elsdenii* flavodoxin with its 137 amino acid residues, is therefore the largest protein of which a complete resonance assignment has been done. The sequential assignments of larger proteins is hampered by the larger intrinsic line widths and the substantial increase in numbers of cross peaks, both resulting in considerable overlap of resonances in the 2D-NMR spectra.

Obviously, spreading the resonances in a crowded 2D-NMR spectrum into three dimensions will considerably decrease overlap. This can be done by means of three-dimensional NMR techniques. In 3D-NMR an additional evolution time is incorporated into a 2D-NMR pulse sequence. A 3D-NMR experiment can thus be envisioned as a combination of two 2D-NMR experiments. The 3D-NMR experiments published until now [31-42], can be divided into two groups, Homonuclear 3D-NMR experiments and Heteronuclear 3D-NMR experiments. In Homonuclear 3D-NMR two ^1H 2D-NMR correlation experiments are combined. The most useful for the purpose of resonance assignment seem to be those 3D-NMR experiments in which the distance information, as obtained from a NOESY experiment [43], is combined with J-coupling information, obtained from a TOCSY experiment [44-47]. Two Homonuclear 3D-NMR experiments (NOESY-TOCSY) have been published in which the full proton spectral width was utilized [31,32]. To limit measuring time and size of data matrices the proton frequency domain can be restricted by using selective excitation pulses. This method has been used in a NOESY-TOCSY as well as in a TOCSY-NOESY experiment [33-35]. In Heteronuclear 3D-NMR a proton-heteronucleus correlation experiment is combined with a proton-proton correlation experiment. Of the Heteronuclear experiments the most useful seem those, in which a HMQC experiment [48-50] is combined either with a NOESY experiment, giving a HMQC-NOESY [36,37] or NOESY-HMQC [38,39] or if the HMQC is combined with a TOCSY, leading to a HMQC-TOCSY [40] or TOCSY-HMQC [41]. In each of these Hetero 3D-NMR experiments either only proton-proton distance information is present (e.g. NOESY-HMQC) or only proton J-coupling information (e.g. HMQC-TOCSY). To have both proton-proton distance and J-coupling information present in one 3D Hetero NMR experiment one could combine the HMQC with TOCSY and NOESY, leading to e.g. a HMQC(TOCSY)-NOESY [42]. For proteins the advantage of Hetero 3D-NMR over Homonuclear 3D-NMR lies in the larger spectral dispersion of e.g. ^{15}N compared to ^1H . On the other hand, only ^{15}N enriched proteins are amenable to Hetero 3D-NMR experiments.

The increased line width of the resonances, due to the longer tumbling time of larger proteins in solution, leads not only to less resolved spectra but also to a diminished number of relay peaks in the TOCSY spectra. The latter is partly due to the influence of ROE peaks in a TOCSY spectrum, which are of opposite sign to the regular TOCSY cross peaks, stemming from J-coupled protons. The ROE cross

peaks are due to the NOE effect and are thus present between protons, which are in close proximity. In the Clean-TOCSY experiment [51], ROE cross peaks are compensated by regular NOE cross peaks of opposite sign, by inserting delays in the MLEV17 spinlocking pulse sequence. The use of Clean-TOCSY will thus lead to more intense cross peaks between J-coupled protons than in a regular TOCSY experiment. For the 3D-NMR experiment we have therefore chosen to use Clean-TOCSY instead of TOCSY. We have further decided for reasons discussed below to use TOCSY-NOESY instead of NOESY-TOCSY. The full experimental details of the Clean-TOCSY-NOESY experiment, in which the full proton spectral width was utilized, and which was performed on *M. elsdenii* flavodoxin in the oxidized state, are published elsewhere [52]. This paper is concerned with the interpretation of the 3D spectrum. It is divided into two parts. In the theoretical section a method is described for the interpretation of Homonuclear 3D-NMR spectra, as well as a method for the assignment of 3D-NMR TOCSY-NOESY spectra of proteins. In this context, a theoretical comparison will be made between the Clean TOCSY-NOESY experiment and other comparable Homonuclear 3D-NMR techniques, i.e. selective TOCSY-NOESY and non-selective NOESY-TOCSY. In the second part the interpretation and assignment method is applied to the Clean TOCSY-NOESY spectrum of *M. elsdenii* flavodoxin in the oxidized state, providing a check on the assignments found by 2D methods and showing the value of 3D experiments.

Materials and Methods

Flavodoxin from *M. elsdenii* was isolated and purified as described previously [53]. For the NMR experiments a 23 mM sample of *M. elsdenii* flavodoxin in the oxidized state was used in a solution consisting of a 250 mM mixture of 20% potassium pyrophosphate and 80% potassium phosphate, at pH 7.0, 41°C, in 10%²H₂O/90%H₂O. The sample was kept under oxygen during the 3D-NMR experiment. The 3D Clean TOCSY-NOESY experiment, the pulse sequence of which is given in Fig. 1, was done on a Bruker AM600 operating at 600 MHz. To suppress the strong water signal the water resonance was irradiated during the relaxation delay of 1.0 s. The delays in the Clean-MLEV17 pulse sequence between the 90° and 180° pulses, were taken to be 2.6 times the 90° pulse length. The 90° pulse length in the MLEV17 pulse sequence was set to a value of 14.2 μs equal to the other 90° pulses in the 3D-NMR pulse sequence. The Clean-MLEV17 composite pulse length, including two 2.5 ms trim pulses, lasted 92.1 ms. The NOESY mixing time was set to 100 ms. For each of the 120 *t*₁ values, FID's were measured for 256 different *t*₂ values. Each FID of 1024 data points (*t*₃) was the accumulation of 4 scans, preceded by 2 dummy scans. The spectral width in *f*₁ and

f2 was set to 8333.3 Hz to cover fully the proton spectral width, while in f3 a spectral width of 16666.6 Hz was used, twice the proton spectral width. The latter method leads to smaller base line distortions in the proton spectral area. Time Proportional Phase Incrementation was used to achieve quadrature detection in the t_1 as well as in the t_2 direction. The complete 3D experiment took 4 days of which approximately 30% is due to disk IO.

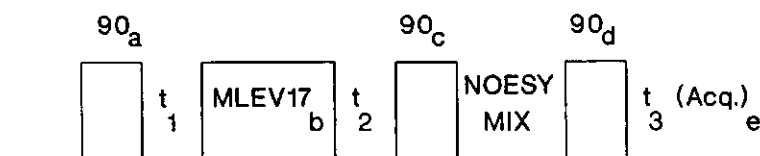


Fig. 1 Pulse sequence for the 3D Clean TOCSY-NOESY experiment. The phase cycling used is follows: $a = x, -x$ (+TPPI(t_1), (+TPPI(t_2)); $b = y$ (+TPPI(t_2)); $c = y, y$; $d = y, y$; acquisition $e = y, -y$. Time Proportional Phase Increments are used in the t_1 and t_2 time domains, TPPI(t_1) stands for TPPI in the t_1 direction. Water irradiation takes place during the relaxation delay period. The carrier is placed at the water resonance.

All data processing was done on an ASPECT3000 computer. In the t_1 direction the data were zero-filled from 120 to 1024 data-points and in t_2 direction from 256 to 512 points. No zero filling was done in the t_3 direction. In all directions the same window function was applied, i.e. a $\pi/4$ shifted quadratic sine filter. After Fourier transformation of the t_3 direction, only the part of the spectrum downfield from the water resonance in f_3 was Fourier transformed with respect to t_1 and t_2 . After phasing to pure absorption, the real points were retained, giving a 3D data set of $512 \times 256 \times 256$ data points. Finally, in all sections perpendicular to f_2 a baseline correction along f_3 was applied.

A. Theoretical Aspects

A 3D-NMR spectrum can be represented as a 3D cube [31,32], such as the one shown in Fig. 2. The coordinates of a cross peak in the 3D-NMR spectrum, f_1 , f_2 , and f_3 respectively, depend on the transfer route the magnetization has followed during the 3D pulse sequence. If no transfer of magnetization occurs during any of the two mixing periods, the coordinates f_1 , f_2 , and f_3 will be all equal. The cross

peaks, for which $f_1=f_2=f_3$, will consequently lie on the body diagonal of the 3D cube.

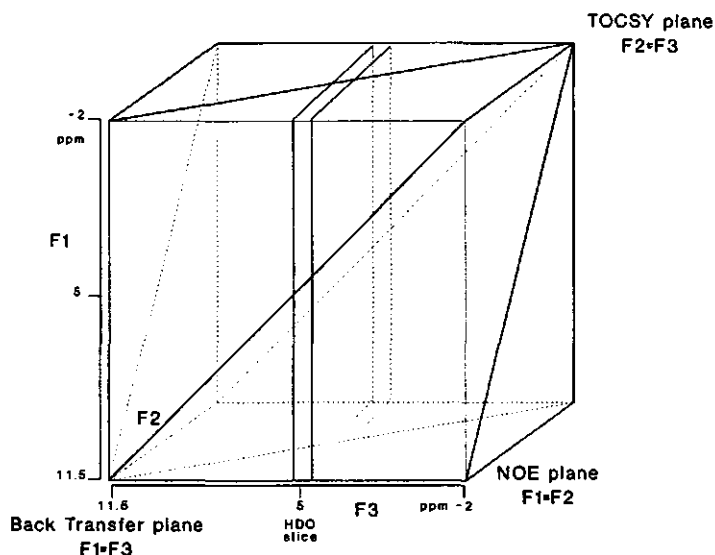


Fig. 2 Cube presentation of a 3D NOESY-TOCSY spectrum. The three basic planes (Back Transfer, NOESY and TOCSY), as well as the body diagonal have been indicated. Slices spoiled by the residual water are indicated in f_3 dimension.

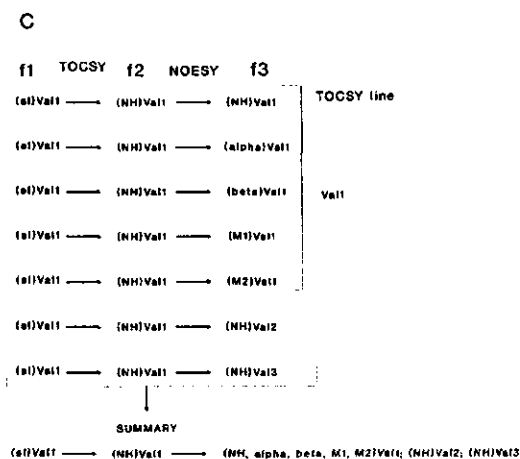
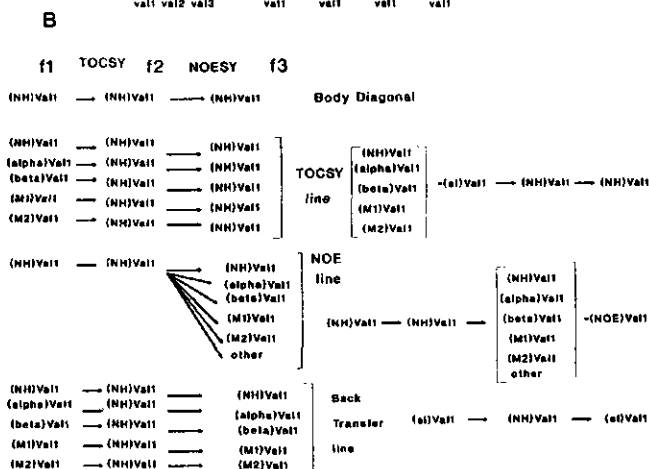
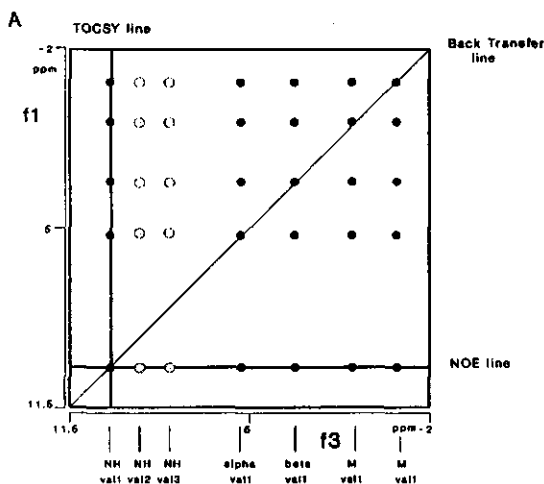
In addition, three diagonal planes are present in the 3D cube. If transfer of magnetization takes place only during the first mixing period (here the spinlock period) the resulting cross peaks will all end up on the diagonal plane for which, $f_2=f_3$. A 2D TOCSY spectrum will be visible in this plane in the case of a 3D TOCSY-NOESY experiment, while in the case of a 3D NOESY-TOCSY experiment this plane contains a 2D NOESY spectrum. These diagonal planes can thus be called, respectively, a TOCSY plane and a NOESY plane. If only during the second mixing period transfer takes place, the corresponding diagonal plane for a TOCSY-NOESY experiment can be called the NOESY plane, while for a NOESY-TOCSY experiment, it may be called the TOCSY plane. Finally, the magnetization can be transferred during the first mixing period and then back during the second mixing period, so that $f_1=f_3$. The diagonal plane with $f_1=f_3$ is thus called the Back Transfer plane, for both the TOCSY-NOESY as for the NOESY-TOCSY experiment.

Analysis of planes perpendicular to one of the axes

For the analysis of 3D spectra one can best make use of planes perpendicular to one of the axes of the 3D cube. In Fig. 3a a plane perpendicular to the f_2 axis is shown, called a f_1f_3 plane. In this plane we have schematically represented the cross peaks, as they may appear for a valine amino acid residue, in the case of a 3D TOCSY-NOESY spectrum. We shall use valine to exemplify the method of analysis of a 3D TOCSY-NOESY spectrum. The f_1f_3 plane is assumed to dissect the f_2 axis at the NH resonance frequency of this valine amino acid residue ($f_2=(\text{NH})\text{Val}$). A number of characteristic properties of the f_1f_3 plane follow directly from the dissection of the 3D cube by this plane. Firstly, the cross peak at $f_1=f_2=(\text{NH})\text{Val}=f_3$, i.e. at the position where the f_1f_3 plane dissects the body diagonal, stems from magnetization that has not been transferred during any of the mixing periods. Secondly, three lines are indicated in Fig. 3a. They result from the dissection of the f_1f_3 plane with the three diagonal planes. The TOCSY line results from the dissection of the f_1f_3 plane by the TOCSY plane. The dissection of the f_1f_3 plane by the NOESY plane gives the NOE line. Finally, the dissection by the Back Transfer plane gives the diagonal, and is called the Back Transfer line. As Fig. 3a shows, in addition to the cross peaks on the TOCSY-, NOE- and BT line, also other cross peaks are present, that do not lie on any of these lines.

To analyze the complete set of cross peaks present in the planes perpendicular to any one of the axes of the 3D-NMR spectrum, we feel that a magnetization transfer route scheme as given in Figs. 3b and 3c, provides for an easy and concise way. In Fig. 3b, we define the notation, while in Fig. 3c, we have drawn schematically the magnetization routes, that lead to the cross peaks in the f_1f_3 plane as presented in Fig. 3a. To prevent overcrowding in Fig. 3a and subsequent figures, only interresidual NOE contacts to other amide protons but not to aliphatic protons are shown.

- Fig. 3** **A.** f_1f_3 plane of a TOCSY-NOESY spectrum through the f_2 amide resonance position of a valine spin system showing the TOCSY, NOE and Back Transfer line. Only interresidual NOE connectivities to other amide protons and not to aliphatic protons are shown.
- B.** Notation of the magnetization transfer routes resulting in the body diagonal, the TOCSY-, NOE- and Back Transfer line.
- C.** Schematic presentation of the magnetization transfer routes (as defined in Fig. 3B) that lead to cross peaks in a f_1f_3 section of a TOCSY-NOESY spectrum (Fig. 3A).



As indicated in the magnetization transfer route scheme in Fig. 3b, the array of cross peaks on the TOCSY line can be written in a short hand notation as (sl)Val1-(NH)Val1-(NH)Val1, where (sl)Val1 stands for an array of cross peaks forming the spinlock pattern of this valine. It is the type of pattern that would be present on the vertical line through the NH resonance in a 2D TOCSY spectrum. The short hand notation given above allows for a concise way of identifying an amino acid residue in a 3D spectrum. The NOE line can also easily be represented, i.e. (NH)Val1-(NH)Val1-(NOE)Val1, as shown in Fig. 3b. This route stands for the cross peaks, that stem from magnetization that has been transferred only during the NOE mixing period from (NH)Val1 to other protons. In fact, it represents the set of cross peaks that is present on the horizontal line through the amide resonance position of the corresponding Val in a 2D NOESY spectrum. For other protons then (NH)Val1 similar routes can be written. For example, (α)Val1-(α)Val1-(NOE)Val1, represents, the NOE line in the f1f3 plane through the (α)Val1 resonance position. It is important to realize that contrary to (sl)Val1, (NOE)Val1 in itself is an ill defined quantity. The reason for this is that the set of cross peaks that appear on the NOE line, depend on their history. For example, (α)Val1 may have other interresidual contacts then (NH)Val1, and therefore the set of cross peaks on the NOE line through (α)Val1 may be different from the NOE line through (NH)Val1. The set of cross peaks on the NOE line is defined however when the history is taken into account, e.g. the routes (NH)Val1-(NOE)Val1, or (α)Val1-(NOE)Val1 do define the set of cross peaks. On the other hand, (sl)Val1 does define the set of cross peaks, because during the spinlock mixing period only intraresidual transfer occurs. Finally, the diagonal of the f1f3 plane can be written as (sl)Val1-(NH)Val1-(sl)Val1. On the Back Transfer line, only cross peaks appear that belong to one and the same spin system. With the shorthand notations thus defined one can readily derive, all the cross peaks shown in Fig. 3a. This is shown in the magnetization transfer route scheme of Fig. 3c. Since the f1f3 plane is at f2=(NH)Val1, only cross peaks appear that stem from magnetization that has the NH frequency of Val1 during f2. We expect to find the following cross peaks: firstly, the TOCSY line (sl)Val1-(NH)Val1-(NH)Val1. Secondly, (NH)Val1 may transfer its magnetization to other protons belonging to Val1 during the NOE mixing period, so that one gets as well (sl)Val1- (NH)Val1-($\alpha,\beta,M1,M2$)Val1, i.e. the vertical spinlock pattern of Val1 ((sl)Val1) is repeated at the resonance positions of the α , β , M1 and M2 protons of Val1. Each of these (sl)Val1 patterns will always have a diagonal cross peak because back transfer is always intraresidual, i.e. to Val1. As also indicated in Fig. 3c, the NH proton of Val1 may have additional NOE contacts, e.g. to a NH proton of another amino acid residue. In the example of Fig. 3, NOE contacts are assumed to exist to (NH)Val2 and (NH)Val3. This can be written in shorthand notation as

(sl)Val1-(NH)Val1-(NH)Val2, (NH)Val3, i.e. the (sl)Val1 pattern appears also at the f3 frequency of (NH)Val2 and (NH)Val3. If a Back Transfer cross peak is present, i.e. a cross peak on the diagonal, this immediately identifies this resonance as belonging to the same amino acid residue that has its NH resonance at f1=f2=f3. Overlap of two or more NH resonances, a situation that occurs quite often for a protein of the size of flavodoxin, is immediately recognized from the cross peak pattern in the f1f3 plane.

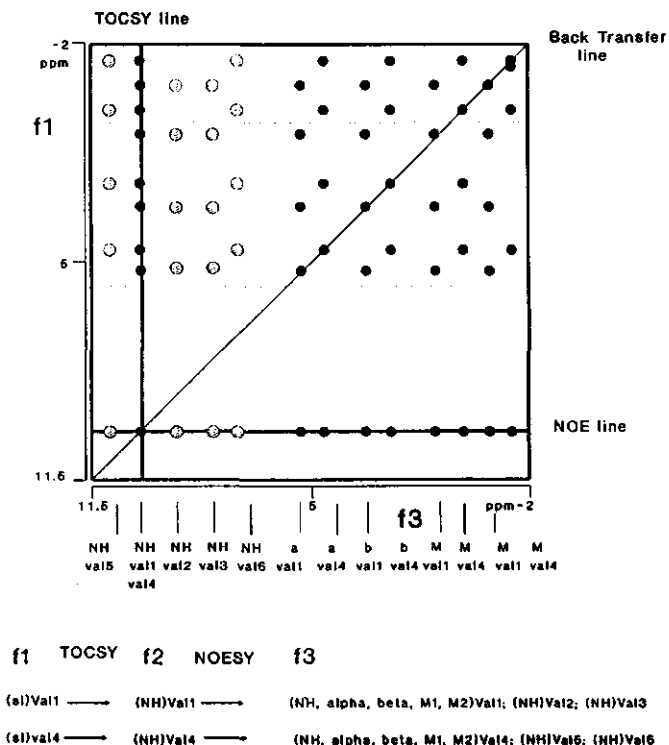


Fig. 4 f1f3 plane expected for the situation of two overlapping valine amide resonances. Only interresidual NOE contacts to other amide protons and not to the aliphatic region are shown. The magnetization transfer routes leading to the various cross peaks are also given. The region surrounded by dashed lines is observed when selecting the aliphatic region in f1 (see text).

This is exemplified in Fig. 4. Here we assume that the amide proton of Val4 has the same f2 NH resonance position as the amide proton of Val1. The following cross peaks are then expected, as one can easily derive using the magnetization transfer route scheme of Fig. 4. For Val1, one may have (sl)Val1-(NH)Val1-

$((\text{NH}, \alpha, \beta, \text{M1}, \text{M2})\text{Val1}; (\text{NH}, \alpha, \beta, \text{M1}, \text{M2})\text{Val2}; (\text{NH}, \alpha, \beta, \text{M1}, \text{M2})\text{Val3})$ if there are also NOE contacts to Val2 and Val3 and for Val4: $(\text{sl})\text{Val4}-(\text{NH})\text{Val4}-((\text{NH}, \alpha, \beta, \dots)\text{Val4}; (\text{NH}, \alpha, \beta, \dots)\text{Val5}; (\text{NH}, \alpha, \beta, \dots)\text{Val6})$ if there are also NOE contacts of $(\text{NH})\text{Val4}$ to Val5 and Val6. Two sets of spinlock patterns will thus be visible, i.e. of Val1 and Val4. Only on the TOCSY line the spinlock patterns of Val1 and Val4 overlap.

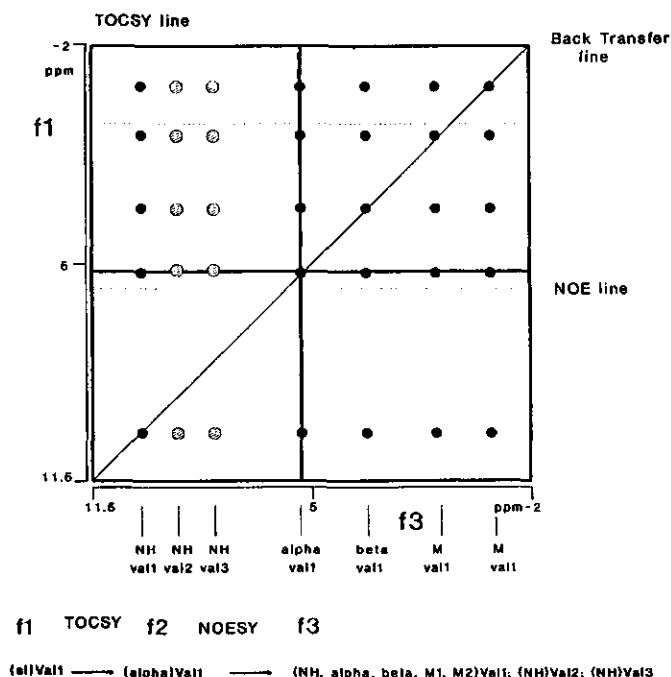


Fig. 5 f_1f_3 plane through the $(\alpha)\text{Val}$ resonance position in f_2 . Only interresidual NOE contacts to other amide protons and not to aliphatic protons are shown. The magnetization transfer routes leading to the cross peaks in this plane are also given. The region surrounded by dashed lines is observed when selecting the aliphatic region in f_1 (see text).

The same spinlock pattern that is present in the f_1f_3 plane at f_2 of $(\text{NH})\text{Val1}$, is also present in the f_1f_3 planes through, e.g. f_2 of $(\alpha)\text{Val1}$ and $(\beta)\text{Val1}$. This is schematically shown in Fig. 5, the magnetization transfer route is also given. In case, the f_1f_3 plane is through, for example f_2 of $(\alpha)\text{Val1}$, additional NOE contacts may appear which differ from contacts observed when the f_1f_3 plane is through $(\text{NH})\text{Val1}$ at f_2 , and $(\alpha)\text{Val1}$ may overlap with other α protons, but this does not

hamper the possibility to identify the Val1 amino acid residue as follows from the discussion above. A $f1f3$ section through the (α) Val1 resonance does provide an additional check on the assignment. In this respect the question of transfer of magnetization through the spin system during the spinlock mixing period is of importance. If for example during the spinlock mixing period transfer of magnetization to the amide proton occurs only from the α proton and no relaying takes place, the spinlock pattern as seen in the $f1f3$ plane through (NH)Val1 will be cutoff at the α resonance. The $f1f3$ plane through (α) Val1 may then be helpful in that it may provide more spinlock relay cross peaks, i.e. to the β , ... protons.

Summarizing: the $f1f3$ plane provides through the sl pattern a means of identifying an amino acid residue. If overlap of resonances is present at e.g. $f2$ of NH, the repeating sl pattern in the $f1f3$ plane for each NOE contact of these NH's makes it possible to identify the overlapping NH resonances, responsible for the NOE contact. Secondly, the same sl pattern is also present in the $f1f3$ planes through other resonances of that spin system, providing additional confirmation of the assignment of a spin system and in case relaying is not sufficient during the spinlock mixing period it may help to further identify an amino acid residue. Finally, a Back Transfer cross peak on the diagonal indicates that this cross peak is due to magnetization transfer to or from a proton within one spin system with its NH proton resonating at $f1=f2=f3$.

To analyze the $f1f2$ plane a similar method can be used as for the $f1f3$ plane. In the $f1f2$ planes the TOCSY line is still the vertical line, while the NOE line and the BT line are interchanged. The NOE line is now the diagonal and the BT line is the horizontal one along the $f2$ axis. As example we use again the valine amino acid residue. The cross peak pattern in the $f1f2$ plane through the NH resonance of Val1 at $f3$ is schematically shown in Fig. 6. As follows from the magnetization transfer route scheme all the magnetization that ends up on the NH of Val1 during t_3 , is visible in the $f1f2$ plane. From Fig. 6, it also follows directly, that in the $f1f2$ plane at the resonance positions of respectively, (α) Val1, (β) Val1, $(M1)$ Val1, and $(M2)$ Val1 along $f2$, the spinlock pattern of Val1 ((sl)Val1) can be observed as well. However, if (NH)Val1 has a NOE contact to another spin system the spinlock pattern of that spin system (amino acid residue) is observed at, e.g. $f2=(\text{NH})\text{Val2}$, and $f2=(\text{NH})\text{Val3}$. In such a case the magnetization transfer route is, (sl)Val2-(NH, α , β , ...)Val2-(NH)Val1. In this notation the spinlock cross peak patterns that appear on the vertical lines with $f2$ equal to, respectively, the NH, α , β ,... resonance positions of Val2, may be compared with the cross peak patterns appearing vertically on these same resonance positions in a 2D TOCSY spectrum. A similar route can be written down for the other amino acid residue to which an NOE contact exists, i.e. to Val3. The spinlock pattern of the amino acid residues (here Val2 and Val3) with which Val1

has a NOE contact, will thus be observed. The case of overlap at the NH resonance position in the f1f2 plane is considered in Fig. 7. Contrary, to the situation in a f1f2 plane, one can not establish solely from a f1f2 section whether it is Val1 or Val4 that has NOE contacts to Val2, Val3, Val5 or Val6. Using the f1f3 plane and the f1f2 plane simultaneously provides the identification. With the aid of the f1f3 plane one can establish the resonance position of the NH proton with which Val1 has a NOE contact. The f1f3 plane does not provide information concerning the type of amino acid residue that resonates at that NH proton position. This information is provided by the f1f2 plane.

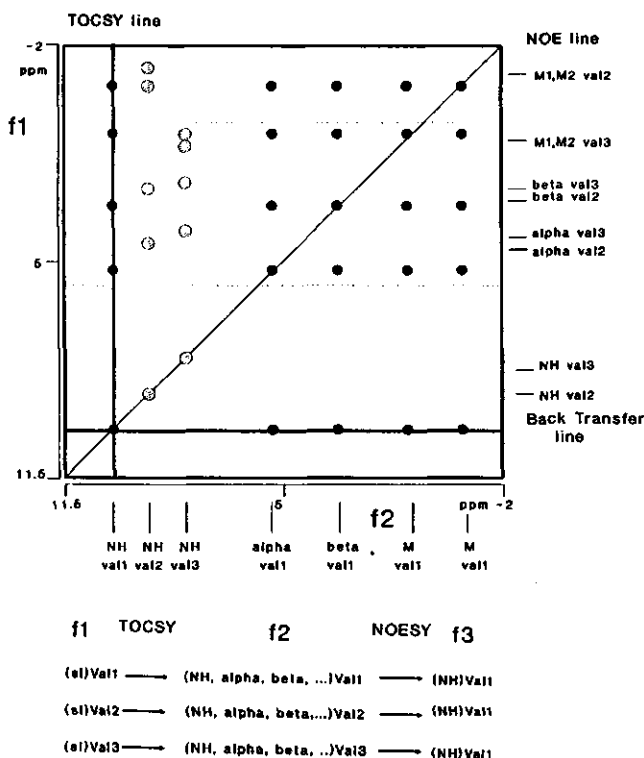


Fig. 6 f1f2 plane through the f3 amide resonance of a valine spin system. Only interresidual NOE contacts to other amide protons and not to aliphatic protons are shown. The corresponding spin systems are recognized by their TOCSY pattern. The magnetization transfer routes leading to cross peaks in this plane are also given. The region surrounded by dashed lines is observed when selecting the aliphatic region in f1 (see text).

Summarizing: the f1f3 planes are very useful to identify the type of spin system (amino acid residue) at a certain resonance position (NH), especially in case of overlap. The f1f3 planes also provide the resonance positions of the protons with which the amide proton has a NOE contact. The f1f2 plane through those proton resonances provides then the type of amino acid residue to which the contact is.

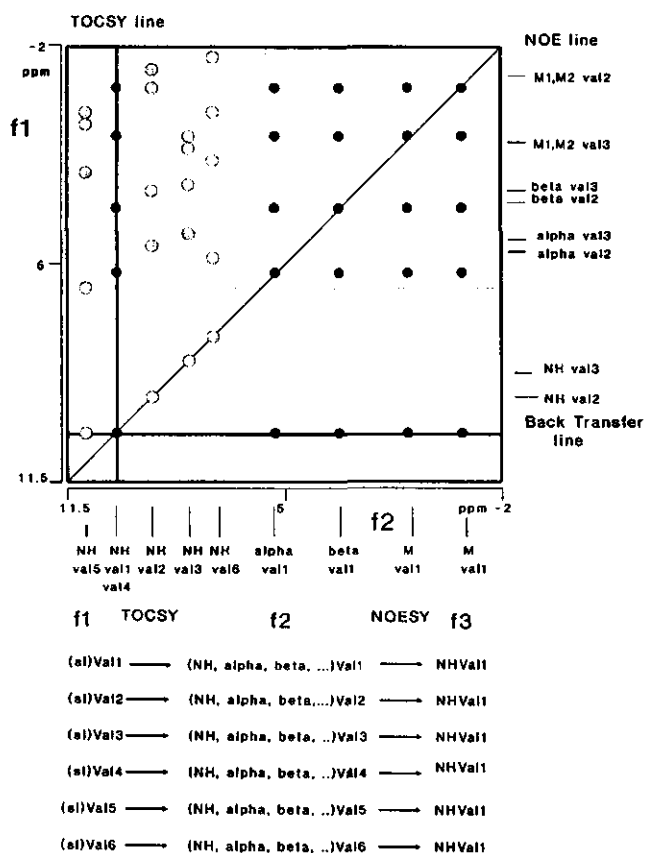


Fig. 7 f1f2 plane through the overlapping f3 amide resonance positions of two valine spin systems (Val1, Val4). The figure illustrates the difficulties in determining the specific interresidual NOE connectivities of the two amide protons of these valines. The magnetization transfer routes have also been indicated. The region surrounded by dashed lines is observed when selecting the aliphatic region in f1 (see text).

Finally, we consider the f2f3 plane. The TOCSY line will now lie on the diagonal, while the Back Transfer line is the vertical one along the f2 axis. The NOE line lies

horizontally along the f_3 axis. Note again that in principle the sl pattern is present on the vertical line (on the BT line), i.e. only cross peaks belonging to one spin system will appear there. One sees (NH)Val1-(sl)Val1-(NH)Val1. To a different spin system X one gets, (NH)Val1-(sl)Val1-(NH, α , β ...)X. The Val1 sl pattern repeats itself for each NOE contact of Val1. In the f_2f_3 planes a similar set of cross peak patterns may thus be expected as one gets for the f_1f_3 planes. However, when compared to f_1f_3 planes the magnetization transfer routes leading to the cross peaks that define a sl pattern at a NOE contact are different. Consequently, in the f_2f_3 plane a sl pattern may lack cross peaks, due to the absence of a NOE contact.

Consideration of the aspect of H₂O suppression

Because of the presence of residual water signal, slices from the 3D cube perpendicular to the f_3 axis close to the water line cannot be used, these slices are indicated in the 3D cube representing the 3D-NMR spectrum (Fig. 2). In these planes severe baseline distortions will occur. A band of the order of 0.3 to 0.4 ppm around the water resonance cannot be used because it is not amenable to baseline correction. If the water is suppressed via saturation, in addition, α -protons that lie directly under the water line may be bleached. The magnetization from the route (α)X-(sl)X-(NOE)X, i.e. a plane perpendicular to f_1 will be bleached. Although in a f_1f_3 plane with f_2 through the resonance position of an α proton that lies under the water line, the α proton will be absent but other protons belonging to the same spin system may still be visible. The reason being that this α proton may acquire magnetization during the spinlock mixing period. An example will be shown in the 3D TOCSY-NOESY spectrum of flavodoxin.

Comparison of selective TOCSY-NOESY and non-selective TOCSY-NOESY

Oschkinat et al. [35] have presented the results of selective TOCSY-NOESY experiments and discussed in detail the practical problems involved. The most useful selection turns out to be the one in which the aliphatic region in the f_1 direction is selected. In the f_1f_3 and f_1f_2 planes certain regions will thus be missing. These regions are indicated in figures 4 to 7 used in the foregoing discussion. As can be seen from these figures, the use of selective excitation strongly restricts the areas in the 3D spectrum that can be analyzed. For f_1f_3 planes through a NH resonance position, the NH to NH NOE contacts will not be visible. This may hamper the identification of the spin system, as one has to rely on relay cross peaks. In a f_1f_3 section through an α proton resonance the spinlock cross peak to

its NH will not be visible. Therefore it cannot be identified as intraresidual. Using a f_1f_3 plane through its NH resonance position the α proton resonance can be identified as intraresidual when the α proton resonates upfield from the water line. In addition, the aromatic amino acid residues cannot be recognized from cross peaks in the aromatic region. Only in the f_2f_3 planes the full spectrum will be visible, although a set of planes will be missing, i.e. the ones lowfield of the water resonance. However, as discussed before for the f_2f_3 plane in a non-selective TOCSY-NOESY, the repeating sl pattern may lack cross peaks, due to the absence of a NOE contact.

Also an experiment was done in which the NH region was selected in f_1 and in f_2 the aliphatic region [35]. Such a selection prohibits the use of the sl pattern to identify a spin system, as is evident from the forementioned figures. No f_1f_3 slices are available through NH resonance positions. For the assignment of resonances in α -helices slices through the NH resonance are quite useful, because of the NOE contacts between NH resonances. In addition, as pointed out by the authors selective pulses lead to base line distortions, in particular if a strong diagonal cross peak is present. These base line distortions made the aliphatic region uninterpretable.

Comparison of non-selective TOCSY-NOESY with non-selective NOESY-TOCSY

In the non-selective NOESY-TOCSY experiment slightly different spectra are obtained as compared to the non-selective TOCSY-NOESY experiment. We consider the sections f_1f_3 , f_1f_2 and f_2f_3 and compare these for the two types of 3D-NMR experiments in terms of the assignment method. Some subtle differences between the two methods exist. We will consider first the f_1f_3 plane. The sl pattern lies now horizontally along f_3 and repeats itself for each NOE contact. Because of the residual water signal perpendicular to the f_3 axis and the t_1 noise on the highfield side the identification of the sl pattern of a particular amino acid residue is not as easy as in a TOCSY-NOESY experiment. These disturbances hamper the possibility to resolve overlap using these repeating TOCSY lines in the f_1f_3 plane of a NOESY-TOCSY when compared to a TOCSY-NOESY experiment. Secondly, in the f_2f_3 plane of a NOESY-TOCSY, the NOE line is the diagonal, while the TOCSY line is along the f_3 axis and the BT line along the f_2 axis. The magnetization route is then as follows (NH)Val1-(NOE)Val1-(sl)Val1,(sl)Val2,... For each NOE contact of (NH)Val1 a sl pattern may appear in the f_2f_3 sections along the f_3 axis, e.g. the sl pattern of Val1 repeats for each intraresidual NOE contact. In addition, for each interresidual NOE contact of (NH)Val1 to a specific spin system the corresponding

sl pattern of that spin system is seen. The main drawback, since the TOCSY line lies along the f_3 axis, is the residual water signal and t_1 noise, which will disturb the sl pattern. The undisturbed region lowfield of the water resonance is for both types of experiments of low value.

Finally, in the f_1f_2 plane, the plane the least disturbed by experimental artefacts in both types of experiments, the TOCSY line lies along the diagonal, while the NOE line lies vertically along the f_1 axis and the Back Transfer line is horizontally along the f_2 axis. A diagonal cross peak identifies itself as intraresidual, because they stem from magnetization transfer during only the spinlock period. All the off diagonal cross peaks in the f_1f_2 planes indicate NOE contacts as pointed out in references [31] and [32]. With the aid of the magnetization transfer route scheme the cross peaks expected in f_1f_2 can be derived. For a f_1f_2 plane through the $f_3=(\text{NH})\text{Val1}$, one finds $(\text{NOE})\text{Val1}-(\text{NH},\alpha,\beta,\text{M1},\text{M2})\text{Val1}-(\text{NH})\text{Val1}$. The $(\text{NOE})\text{Val1}$ pattern repeats itself as vertical lines at the Val1 resonance positions. This repeating pattern may lack cross peaks due to the absence of a NOE, not facilitating the interpretation of the spectra. If the NOE pattern has a diagonal cross peak in the horizontal direction it is easily seen that this cross peak is due to an intraresidual contact. NOE contacts to another spin system lead to NOE patterns that do not have diagonal cross peaks in horizontal direction. However, this also means that in case two NH protons have the same resonance position (and e.g. strong d_{NN} contacts) it will be difficult to distinguish the overlapping NH resonances, favouring the f_1f_3 planes of a TOCSY-NOESY where such ambiguities are easy to resolve.

B. Application to flavodoxin.

In this section we shall analyze the 3D TOCSY-NOESY spectrum of *M. elsdenii* flavodoxin in the oxidized state for the purpose of resonance assignments. The analysis will be done in examples of the main secondary structure elements of flavodoxin. As shown in the stereo drawing (Fig. 8a), flavodoxin contains various structural elements, such as 5 parallel β -sheet strands and 5 α -helices, as well as turns [7].

Assignment in a TOCSY-NOESY spectrum of a β -sheet

The parallel β -sheet of *M. elsdenii* flavodoxin is characterized by a number of short NH to α H distances. $d_{\alpha\text{N}}(i,i+1)$ is very short, while some long range $d_{\alpha\text{N}}(i,j)$ distances are relatively short and of the same order as the intraresidual $d_{\alpha\text{N}}(i,i)$ distance. A f_1f_3 slice through an α proton resonance position provides on the NOE line a number of contacts to the NH region, see Fig. 9a where a f_1f_3 slice is taken

through f2 = (α)Ser33. First the intraresidual contact with its own NH is observed and secondly, a very strong sequential contact to (NH)Val34. Some long range contacts may also be present. In Fig. 9a a contact is seen from (α)Ser33 to (NH)Ile4. The sequential contact can be identified most easily, because of its high NOE intensity. At the frequencies of (NH)_i, (NH)_{i+1} and (NH)_j the sl pattern of amino acid residue i repeats itself. In Fig. 9a all three NOE contacts of (α)Ser33 show the sl pattern of Ser33. Note that a slice through an α proton resonance position, instead of through the corresponding NH resonance position is expected to enhance the intensity of the cross peaks to the aliphatic protons on the sl lines.

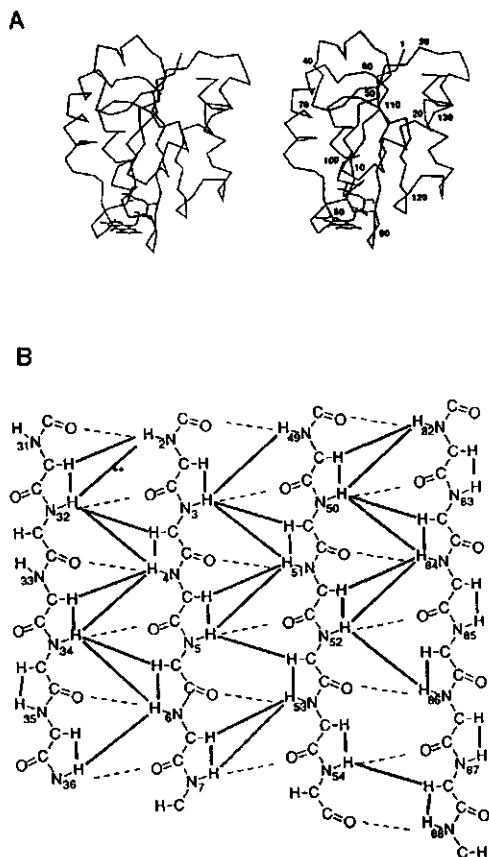


Fig. 8 A. Stereo drawing showing the C α and FMN atoms of two-electron reduced *M. elsdenii* flavodoxin as determined from NMR and restrained molecular dynamics [7].

B. Schematic presentation of part of the parallel β -sheet of flavodoxin. Dashed lines indicate hydrogen bonds as expected regarding the relative position of the strands and amide hydrogen characteristics [3]. Solid bold lines indicate NOE connectivities between protons observed in a 150 ms NOESY spectrum. Bold lines with asterisks represent NOE connectivities observed after building the β -sheet [3].

Finally, overlap is resolved because of the fact that the sl pattern repeats itself at each NOE contact. In conjunction with the f1f3 sections one can use the f1f2 sections to establish the type of amino acid residue to which the NOE contact is, in order to obtain additional checks on the sequential contact. This may be of help in finding a starting point for the sequential assignment.

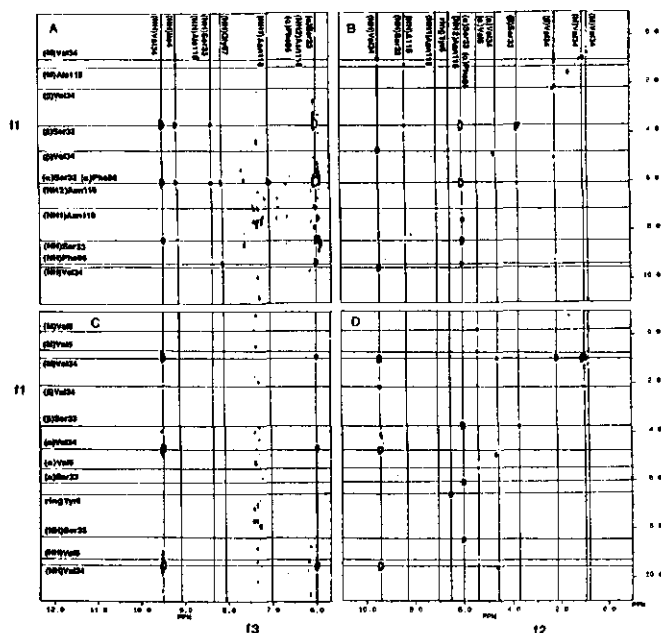


Fig. 9

- A. f1f3 plane through f2= (α)Ser33. Cross peaks are labeled ω1/ω3.
- B. f1f2 plane through f3= (α)Ser33. Cross peaks are labeled ω1/ω2.
- C. f1f3 plane through f2=(NH)Val34. Cross peaks are labeled ω1/ω3.
- D. f1f2 plane through f3=(NH)Val34. Cross peaks are labeled ω1/ω2.

In fact, various ways of checking the assignment exist. One can take a f1f2 slice through αH. This slice provides the sl pattern of the amino acid residue to which the NOE contact is, as shown for example for Val34 in Fig. 9b. A f1f3 slice through the NH resonance position of that NOE contacted residue (e.g. Val34) provides the same information (Fig. 9c). Finally, a f1f2 slice through the NH resonance position of the NOE contacted residue confirms the assignments. For example the f1f2 slice through (NH)Val34 (Fig. 9d) shows on the sl line at (NH)Val34 the sl pattern of Val34 and at f2=(α)Ser33 the sl pattern of Ser33. The presence of an aromatic

amino acid residue is directly obvious from additional cross peaks in the lowfield region of the spectrum.

We have used this procedure to identify and check the assignments of the flavodoxin protein in the oxidized state [10]. Part of the β -sheet of flavodoxin is shown in Fig. 8b [7], together with the amino acid residue numbering scheme. Fig. 10 shows an example of the sequential walk in the β -sheet of the flavodoxin. The f1f3 plane through the α proton resonance position is placed side by side with the f1f2 plane through the NH resonance position of the sequential contact. We start at the f1f3 plane for which $f_2 = 4.70 - 4.80$ ppm. In this range lies amongst others the α resonance of Val49 as taken from the assignments given in ref. [10]. The f1f3 plane immediately exemplifies several issues. The expected pattern of cross peaks in such a plane is as shown in Fig. 5. The transfer of magnetization is according to (sl)Val49-(α)Val49-(NH,...)Val49;(NH,...)Ile50;(NH...)Asp48. For another coinciding α proton at f_2 another set of sl lines will be visible in the plane. Using the vertical repeating sl lines it is immediately seen, which NOE contacts belong to the same α proton. Several α resonances overlap in Fig. 10a. Focussing on (α)Val49, one very strong NOE contact and two weaker contacts are seen on the NOE line. The cross peak on a sl line which coincides with the NOE line has not always the highest intensity. This can be understood directly from the magnetization transfer route resulting in these cross peaks. The intensity of a cross peak on the sl line not coinciding with the NOE line (which is presumed now to be on an α H position) stems from magnetization that is transferred first from a J-coupled proton to the α -proton via the spinlock mixing time and then from α via the NOE mixing time to an NH. The intensity of a cross peak on the NOE line stems from transfer of magnetization from α H during the NOE mixing time only. The α proton magnetization left after the sl mixing period may thus be less than the magnetization transferred to it during the sl mixing period. The three sl lines related to (α)Val49, reveal beside the α resonance also the resonance positions of the NH-, β - and methyl protons of Val49. To establish which of the three sl lines belongs to an intraresidual NH contact, f_3 of that sl line must equal f_1 on the BT line. Since the strongest NOE contact is expected to be the sequential α N NOE contact, the amino acid residue with NH at $f_3=8.6$ ppm, is the sequential contact and this must be Ile50, as follows from the amino acid sequence.

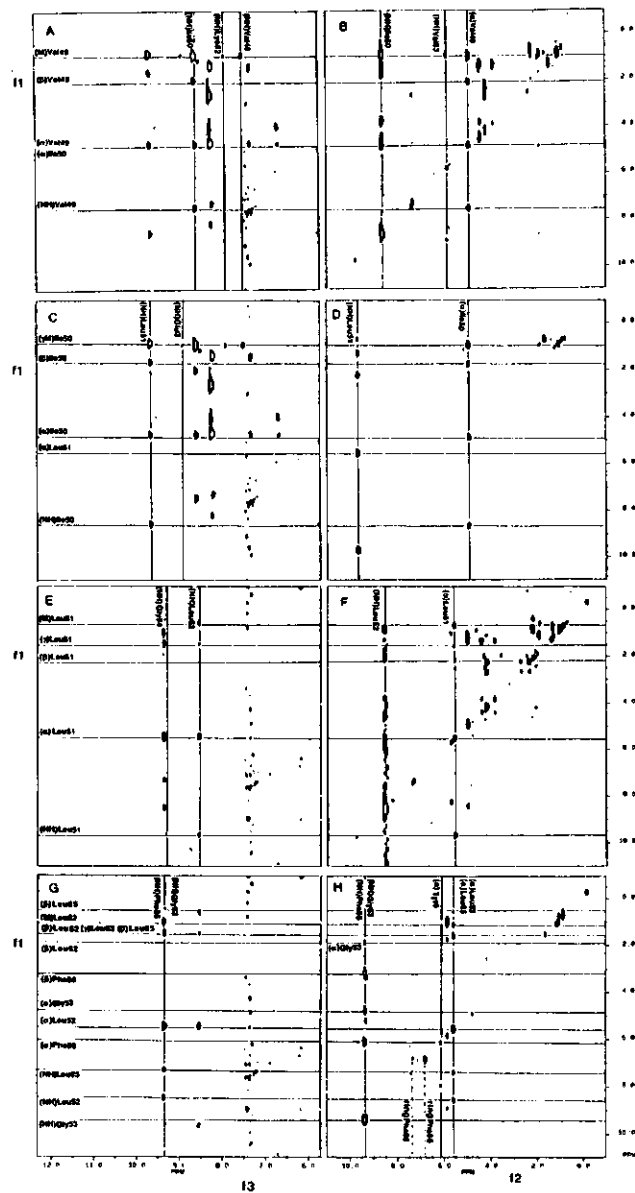


Fig. 10 Example of a sequential walk, using a TOCSY-NOESY spectrum, in part of the central β -sheet of oxidized *M. elsdenii* flavodoxin. f1f3 planes are placed side by side with f1f2 planes. Cross peaks are labeled as described in the former figures. (See text).

The related f_1f_2 plane through the NH50 resonance position (Fig. 10b) shows, because of the strong (NH)Ile50 to (α)Val49 NOE contact, the sl pattern of Val49 again at $f_2 = (\alpha)\text{Val49}$, confirming the slice has been taken at the right NH resonance position. From the sl pattern in the f_1f_2 slice at $f_2 = (\text{NH})\text{Ile50}$ the (α)Ile50 resonance position can be found. The f_1f_3 slice through (α)Ile50 (Fig. 10c) confirms the sl pattern of Ile50, and provides the next sequential NOE contact. In this particular case (α)Val49 and (α)Ile50 overlap. This made the sequential walk difficult in the 2D spectra. Here no ambiguity exists. The next sequential contact from (α)Ile50 to (NH)Leu51 can directly be found using the f_1f_3 slice through (α)Ile50 (Fig. 10c). The f_1f_2 slice through (NH)Leu51 (Fig. 10d) provides the resonance position of (α)Leu51, and from the f_1f_3 slice through (α)Leu51 (Fig. 10e) the next sequential contact is obtained. Analogously, the sequential walk is further shown in Figs. 10f to 10h unto amino acid residue Gly53.

In addition to sequential NOE's also long range NOE's may be present. For example, in the f_1f_2 plane through (NH)Ile50 (Fig. 10b) such a NOE contact is seen. That this contact is from the NH of Ile50 is confirmed by a f_1f_3 plane through (NH)Ile50 (not shown). In the f_1f_2 plane through (NH)Ile50, the sl pattern at this NOE contact provides the NH, αH and side chain resonance positions of this residue. It turns out to be Val83. This contact thus provides the step into the adjacent strand of the β -sheet (see Fig. 8b). Starting at this residue one can go either forward along the chain, via the strong NOE contact with (NH)Gly84, or backwards through the NH of Val83, in the same manner as shown in Figs. 10. Other long range contacts that show up are between (α)Ile50 and (NH)Glu3 (Fig. 10a), between (α)Val49 and (NH)Lys82 (Fig. 10a) and between (NH)Gly53 and (α)Tyr6 (Fig. 10h).

Assignment in a TOCSY-NOESY spectrum of an α -helix

In an α -helical structural part of a protein the most relevant sequential distance used is the d_{NN} distance. A f_1f_3 section through NH of for example valine provides two sequential distances. The sl pattern provides then as discussed in the theoretical section the amino acid residue from which the NOE contact originates, because the corresponding sl pattern appears for each NOE contact of this residue (see Fig. 3a). Note again that overlap in the f_1f_3 planes is resolved in that way. Using in the f_1f_2 slice through a specific NH the sl pattern on the NH position of the sequential NOE contacts, one can identify the type of amino acid residues to which the contacts are (Fig. 6). A f_1f_3 slice through the (α)_i resonance position may provide further help in identifying the amino acid residue or confirm the identification.

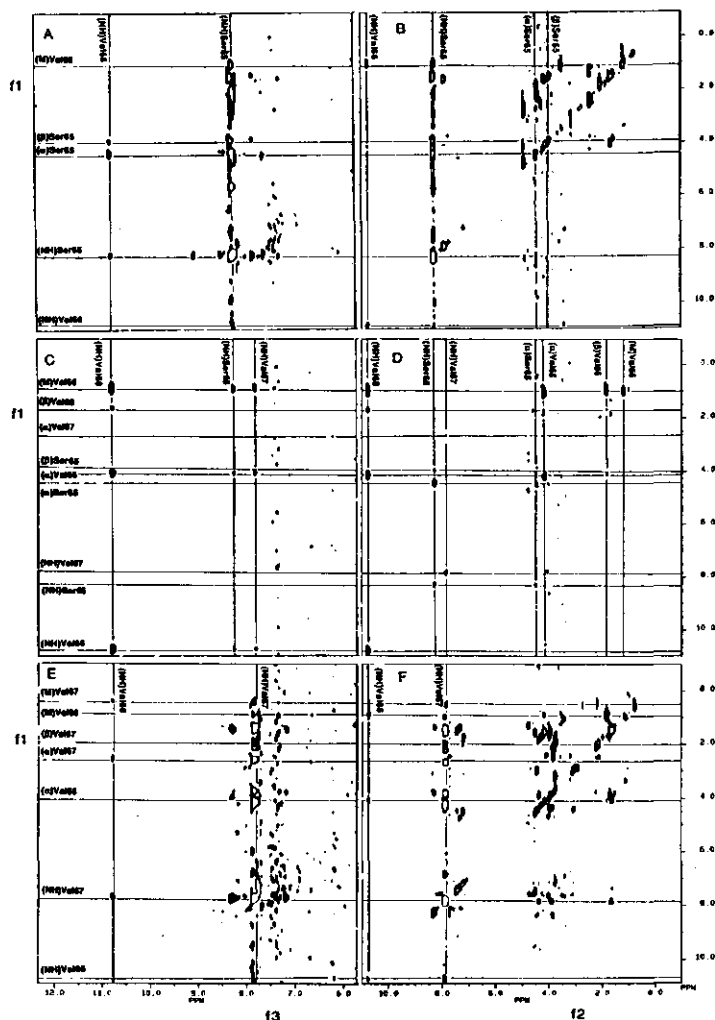


Fig. 11 Example of a sequential walk, using a TOCSY-NOESY spectrum, in part of an α -helix of oxidized *M. elsdenii* flavodoxin. f1f3 planes are placed side by side with f1f2 planes. Cross peaks are labeled as described in the former figures. (See text).

Using this procedure we have checked the assignments as found by 2D methods [10]. In Figs. 11 a small part of the sequential walk in an α -helical part of flavodoxin is shown, going from Ser65 to Val67. The f1f2 planes through NH provide additional confirmation. Notice for example that in Fig. 11d, on the NOE line (diagonal) the α , β and methyl protons appear of Val66, together with cross peaks between them. The f1f3 slice through (NH)Ser65 (Fig. 11a) provides the NOE contact to (NH)Val66. The sl pattern of Val66 can be read off from the f1f2 slice through (NH)Ser65 (Fig. 13b). The f1f3 slice through (NH)Val66 (Fig. 11c) provides two contacts, one back to Ser65 and another to Val67. The sl pattern of Val66 is

repeated at these NOE contacts. The f1f2 slice through (NH)Val66 (Fig. 11d) shows the sl pattern of both Ser65 and Val67. Finally, the f1f3 slice through (NH)Val67 (Fig. 11e) provides the NOE contact back to (NH)Val66, while in the f1f2 plane through (NH)Val67 (Fig. 11f) the sl pattern of Val66 is seen back. These additional checks are useful if the sl pattern does not repeat completely. Figs. 11a, 11c, and 11e show at the (NH)Val66 resonance position the sl patterns of respectively, Ser65, Val66 and Val67.

Assignment in a TOCSY-NOESY spectrum of turns

In Figs. 12, a sequential walk is shown from Ala26, which is the last residue that is part of an α -helix, through Ala27, Gly28, Ala29, which are part of a turn, to Asp30 and Glu32 which are again part of a β -sheet strand. The sequential walk can be done by the joined use of both f1f3- and f1f2 planes.

Starting at the f1f3 slice through (NH)Ala27 (Fig. 12a), two NOE contacts show up quite clearly. These contacts must be to (NH)Ala26 and (NH)Gly28. Because the sl pattern is repeating at each NOE contact, it is possible to resolve overlap, which is clearly present here. The f1f3 slice through (NH)Gly28 provides a sequential contact to (NH)Ala29 (Fig. 12b). This contact lies in a noisy region of the spectrum, which makes the identification difficult. Also the contact from (NH)Gly28 to (NH)Ala27 is obscured now. However, a f1f3 slice through (NH)Ala29 (Fig. 12c) shows the contact to (NH)Gly28. The corresponding sl pattern at (NH)Gly28 confirms the correct assignment as being Ala29 (Fig. 12c). Also a weak NOE contact is seen that could be to (NH)Asp30 (not visible in Fig. 12c). A f1f2 slice taken through the (α)Ala29 resonance position shows the (α)Ala29 to (NH)Ala29 contact and in addition, quite clearly the (α)Ala29 to (NH)Asp30 is seen (Fig. 12d). Herewith, the contact is confirmed to stem from (NH)Ala29. A f1f2 slice through (NH)Asp30 (Fig. 12e) confirms the contact to (α)Ala29. It also shows that the (α)Asp30 resonance position is coinciding with the (α)Ala29 resonance.

At this stage an interesting case of severe overlap of resonances evolves that can be resolved. The f1f3 slice through (NH)Val31 (Fig. 12h) shows the contact to the α proton resonance region. The contact is intraresidual, since the sl pattern of Val31 appears when taking a f1f3 slice through the corresponding α resonance position (Fig. 12f). In addition, another sl pattern appears in Fig. 12h, at (α)Val31, implying that another NH proton, which overlaps with (NH)Val31, contacts with (α)Val31 as well. The f1f2 plane through (α)Val31 (Fig. 12g) confirms the internal contact, as well as establishes the other contact, which has its α proton resonance position at 4.68 ppm (observed at lower contour levels then presented in Fig. 12g) and its β proton resonance position at 2.68 ppm.

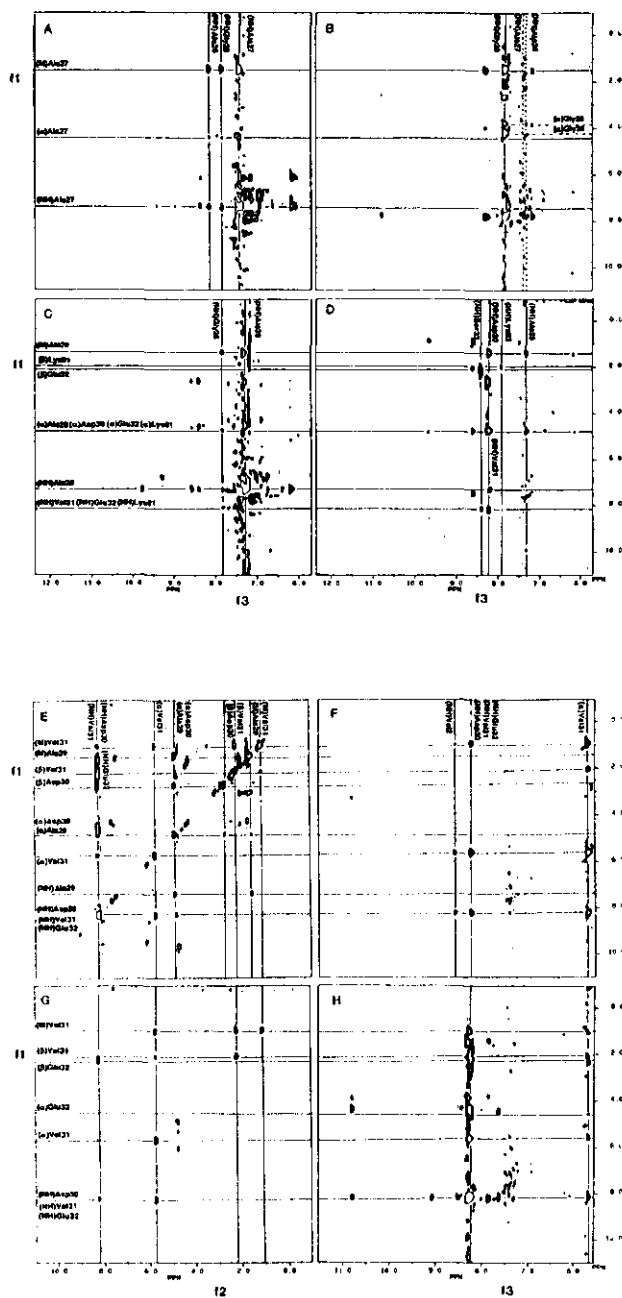


Fig. 12 Example of a sequential walk, using a TOCSY-NOESY spectrum, in a turn of oxidized *M. elsdenii* flavodoxin. Figs. 12a-d and Figs. 12f,g represent f1f3 planes, and Figs. 12e,g represent f1f2 planes. Cross peaks are labeled as described in the former figures. (See text).

This is consistent with the assignment of amino acid residue Glu32. In Fig. 12f (f1f3 slice through α Val31) also a long-range NOE contact to (NH)Val2 is seen, stemming from (α)Val31. In Fig. 12d and 12e, (f1f3 slice through (α)Val31 (and others) and f1f2 slice through (NH)Asp30 (and others)) it is seen that (α)Ala29 and (α)Asp30 overlap. Furthermore, an intraresidual contact is visible between (α)Asp30 and (NH)Asp30 (Fig. 12e).

Bleached α -protons can recover during the 3D experiment through relay contacts in the TOCSY period. This makes it possible, as compared to 2D methods, to observe α N contacts (characteristic for β -sheet strands) when taking a f1f3 slice through the bleached f2 resonance position. An example is shown in Fig. 12d, where proton resonances of Lys82 are observed through its $d_{\alpha N}$ contact with (NH)Lys82. Such a $d_{\alpha N}$ contact is not observed in a 2D-NMR spectrum acquired under the same circumstances.

In conclusion, we have demonstrated the value of acquiring a 3D-NMR non-selective Clean TOCSY-NOESY spectrum for assigning a protein the size of *M. elsdenii* flavodoxin. A straightforward method for interpreting such a spectrum, using magnetization transfer route schemes as described in the figures, has been given. The method, using f1f3 and f1f2 planes of the 3D spectrum, has been successfully applied for making sequential assignments in various secondary structure elements of flavodoxin. A comparison of this 3D experiment with a selective TOCSY-NOESY and a non-selective NOESY-TOCSY experiment has been made. We expect that non-selective 3D TOCSY-NOESY spectra will become an important additional tool, beside the well-known 2D-NMR spectra, for assigning relatively large proteins.

Acknowledgements

We thank Mr. P. Lijnzaad and Dr. J. de Vlieg for help in generating figure 8a. The measurements were performed at the HF-SON NMR-facility Nijmegen (The Netherlands). This study was carried out under the auspices of the Netherlands Foundation for Chemical Research (SON) with financial aid from the Netherlands Organization for the Advancement of Pure Research (NWO).

References

1. Mayhew, S.G. & Ludwig, M.L. (1975) *Enzymes 3rd Ed.* 12, 57-118.
2. van Mierlo, C.P.M., Vervoort, J., Müller, F. & Bacher, A. (1990) *Eur. J. Biochem.* 187, 521-541.

3. van Mierlo, C.P.M., Müller, F. & Vervoort, J. (1990) *Eur. J. Biochem.*, (in press).
4. van Gunsteren, W.F., Kaptein, R. & Zuiderweg, E.R.P. (1983) in *Nucleic Acid Conformation and Dynamics* (Olson, W.K., ed.) Report of NATO/CECAM Workshop, pp. 79-92, Orsay, France.
5. Kaptein, R., Zuiderweg, E.R.P., Scheek, R., Boelens, R. & van Gunsteren, W.F. (1985) *J. Mol. Biol.* 182, 179-182.
6. Clore, G.M., Brünger, A.T., Karplus, M. & Gronenborn, A. (1986) *J. Mol. Biol.* 191, 523-551.
7. van Mierlo, C.P.M., Lijnzaad, P., Vervoort, J., Müller, F., Berendsen, H.J.C. & de Vlieg, J. (1990) *Eur. J. Biochem.*, (submitted).
8. Burnett, R.M., Darling, G.D., Kendall, D.S., Lequesne, M.E., Mayhew, S.G., Smith, W.W. & Ludwig, M.L. (1974) *J. Biol. Chem.* 249, 4383-4392.
9. Smith, W.W., Burnett, R.M., Darling, G.D. & Ludwig, M.L. (1974) *J. Mol. Biol.* 117, 195-225.
10. van Mierlo, C.P.M., van der Sanden, B.P.J., van Woensel, P., Müller, F., Bacher, A. & Vervoort, J. (1990) *Eur. J. Biochem.*, (submitted).
11. Wüthrich, K., Wider, G., Wagner, G. & Braun, W. (1982) *J. Mol. Biol.* 155, 311-319.
12. Wagner, G. & Wüthrich, K. (1982) *J. Mol. Biol.* 155, 347-366.
13. Wider, G., Lee, K.H. & Wüthrich, K. (1982) *J. Mol. Biol.* 155, 367-388.
14. Neuhaus, D., Wagner, G., Vasák, M., Kägi, J.H.R. & Wüthrich, K. (1985) *Eur. J. Biochem.* 151, 257-273.
15. Wagner, G., Neuhaus, D., Worgötter, E., Vasák, M., Kägi, J.H.R. & Wüthrich, K. (1986) *Eur. J. Biochem.* 157, 275-289.
16. Kline, A.D. & Wüthrich, K. (1986) *J. Mol. Biol.* 192, 869-890.
17. Klevit, R.E., Drobny, G.P. & Waygood, E.B. (1986) *Biochemistry* 25, 7760-7769.
18. van de Ven, F.J.M. & Hilbers, C.W. (1986) *J. Mol. Biol.* 192, 389-417.
19. van de Ven, F.J.M. & Hilbers, C.W. (1986) *J. Mol. Biol.* 192, 419-441.
20. Otting, G., Steinmetz, W.E., Bougis, P.E., Rochat, H. & Wüthrich, K. (1987) *Eur. J. Biochem.* 168, 609-620.
21. Bach, A.C., Selsted, M.E. & Pardi, A. (1987) *Biochemistry* 26, 4389-4397.
22. Sukumaran, D.K., Clore, G.M., Preuss, A., Zarbock, J. & Gronenborn, A.M. (1987) *Biochemistry* 26, 333-338.
23. Zuiderweg, E.R.P., Mollison, K.W. & Carter, G.W. (1988) *Biochemistry* 27, 3568-3580.
24. Zuiderweg, E.R.P., Kaptein, R. & Wüthrich, K. (1988) *Eur. J. Biochem.* 137, 279-292.

25. Basus, V.J., Billeter, M., Love, R.A., Stroud, R.M. & Kuntz, I.D. (1988) *Biochemistry* 27, 2763-2771.
26. Montelione, G.T., Wüthrich, K. & Scheraga, H.A. (1988) *Biochemistry* 28, 195-203.
27. Robertson, A.D., Westler, W.M. & Markley, J.L. (1988) *Biochemistry* 27, 2519-2529.
28. Chazin, W.J., Hugli, T.E. & Wright, P.E. (1988) *Biochemistry* 27, 9139-9148.
29. Driscoll, P.C., Hill, H.A.O. & Redfield, C. (1987) *Eur. J. Biochem.* 170, 279-292.
30. Redfield, C. & Dobson, C. (1988) *Biochemistry* 27, 122-136.
31. Vuister, G.W., Boelens, R. & Kaptein, R. (1989) *J. Magn. Res.* 80, 176-185.
32. Vuister, G.W., de Waard, P., Boelens, R., Vliegthart, J.F.G. & Kaptein, R. (1989) *J. Am. Chem. Soc.* 111, 772-774.
33. Oschkinat, H., Griesinger, C., Kraulis, P.J., Sörensen, O.W., Ernst, R.R., Gronenborn, A.M. & Clore, G.M. (1988) *Nature* 332, 374-376.
34. Oschkinat, H., Cieslar, C., Clore, G.M. & Gronenborn, A.M. (1989) *J. Magn. Res.* 81, 212-216.
35. Oschkinat, H., Cieslar, C., Holak, T.A., Clore, G.M. & Gronenborn, A.M. (1989) *J. Magn. Res.* 83, 450-472.
36. Fesik, S.W. & Zuiderweg, E.R.P. (1988) *J. Magn. Res.* 78, 588-593.
37. Zuiderweg, E.R.P. & Fesik, S.W. (1989) *Biochemistry* 28, 2387-2391.
38. Marion, D., Kay, L.E., Sparks, S.W., Torchia, D. & Bax, A. (1989) *J. Am. Chem. Soc.* 111, 1515-1517.
39. Kay, L.E., Marion, D. & Bax, A. (1989) *J. Magn. Res.* 84, 72-84.
40. Wijmenga, S.S., Hallenga, K. & Hilbers, C.W. (1989) *J. Magn. Res.* 84, 634-642.
41. Marion, D., Driscoll, P.C., Kay, L.E., Wingfield, P.T., Bax, A., Gronenborn, A.M. & Clore, G.M. (1989) *Biochemistry* 28, 6150-6156.
42. Wijmenga, S.S. & Hilbers, C.W. (1990) *J. Magn. Res.*, (submitted); Wijmenga, S.S., Hallenga, K. & Hilbers, C.W. (1989) *Bull. Magn. Res.*, (submitted).
43. Macura, S. & Ernst, R.R. (1980) *Mol. Phys.* 41, 95-117.
44. Braunschweiler, L. & Ernst, R.R. (1983) *J. Magn. Res.* 53, 521-528.
45. Davis, D.G. & Bax, A. (1985) *J. Am. Chem. Soc.* 107, 2820-2822.
46. Davis, D.G. & Bax, A. (1985) *J. Am. Chem. Soc.* 107, 7197-7198.
47. Bax, A. & Davis, D.G. (1985) *J. Magn. Res.* 65, 355-360.
48. Müller, L. (1979) *J. Am. Chem. Soc.*, 101, 4481-4484.
49. Bax, A., Griffey, R.H. & Hawkins, B.L. (1983) *J. Magn. Res.* 55, 301-315.
50. Summers, M.F., Marzilli, L.G. & Bax, A. (1986) *J. Am. Chem. Soc.* 108, 4285-4294.

51. Griesinger, C., Otting, G., Wüthrich, K. & Ernst, R.R. (1988) *J. Am. Chem. Soc.* 110, 7870-7872.
52. Wijmenga, S.S. & van Mierlo, C.P.M. (1990) *J. Mag. Res.*, (to be published).
53. Mayhew, S.G. & Massey, V. (1969) *J. Biol. Chem.* 244, 794-802.

Chapter 7

A two-dimensional ^1H NMR study on the apoflavodoxin of *Megasphaera elsdenii*

Carlo P.M. van Mierlo, Annette van der Toorn and Jacques Vervoort

Department of Biochemistry, Agricultural University, Dreyenlaan 3, 6703BC Wageningen, The Netherlands.

Summary

Apoflavodoxin from *Megasphaera elsdenii* has been studied using two-dimensional ^1H NMR techniques. The large majority of the proton resonances of amino acid residues outside the flavin binding region has been assigned. The protein appears to be highly structured which is in contrast to results reported from far-uv-circular dichroism studies. The structure of the protein is nearly identical to that of the corresponding holoprotein in its three redox states. Differences are observed in the flavin binding region, as expected.

Introduction

Flavodoxins are a group of small flavoproteins (molecular mass ranging from 14 to 23 kDa) functioning as low-potential electron transfer proteins [1]. They contain non-covalently bound riboflavin-5'-phosphate (FMN) as prosthetic group. The uncrystallizable flavodoxin of *Megasphaera elsdenii* (137 amino acid residues, 15 kDa) has been studied in detail by using two-dimensional ^1H NMR techniques. Virtually all proton resonances of the oxidized and two-electron reduced protein have been assigned [2,3]. Based on these sequential assignments, using interresidual NOE connectivities, the secondary structure elements were determined [3,4]. The tertiary structure of two-electron reduced *M. elsdenii* flavodoxin has been determined using restrained molecular dynamics [5,6] with 509 interresidual distance constraints which have been extracted from NOESY spectra [7].

Conformation changes in the flavin binding region do occur on one-electron reduction of the oxidized protein [3], resulting in an activation barrier in the transition from the oxidized to the one-electron reduced protein [8]. The absence of such a barrier in the transition between the one- and two-electron reduced protein predestinates *M. elsdenii* flavodoxin for one-electron transfer reactions by shuttling between these two states [8]. The local microenvironment of the flavin is expected to electrostatically destabilize the flavin relative to water resulting in the low redox potential for the transition between the one- and two-electron reduced protein [7,9].

Questions arise like: how does the apoprotein, of which no crystal is available, look like, is it partly folded? Which structural changes do occur on binding of FMN to the apoflavodoxin of *M. elsdenii* to create such a specific microenvironment in the holoprotein? Using modern two-dimensional NMR techniques we try to tackle questions like this. In this paper we report on the preliminary results obtained for *M. elsdenii* apoflavodoxin, resonance assignments are given and a comparison of the structures of the apo- and holoprotein is made.

Materials and Methods

Flavodoxin of *M. elsdenii* was isolated and purified as previously described [11]. The apoflavodoxin was prepared according to the method of Wassink and Mayhew [12]. To get rid of trichloro acetic acid and to get the NMR samples in the appropriate salt conditions, use was made of molecular sieve chromatography (Biogel P-6Dg). The final samples contain approximately 10 and 15 mM apoflavodoxin in solutions consisting of potassium phosphate and potassium pyrophosphate in concentrations ranging from 200 mM to 300 mM. All samples were freshly prepared before the 2D-NMR measurements. The pH of the samples varied between 6.1 and 7.3. All measurements were done using a mixture of 10% $^2\text{H}_2\text{O}$ /90% H_2O , except in cases a specific deuterium content was desired.

Phase-sensitive double quantum filtered Cosy [13,14], NOESY [15] and 2D Homonuclear Hartmann Hahn transfer [16] spectra were acquired at 30 $^\circ\text{C}$ using time-proportional phase incrementation (TPPI) in t_1 to achieve f_1 quadrature detection at a Bruker AM600. The carrier frequency coincided with the water resonance. To acquire the NOESY spectra a mixing time of 150 ms was used, no zero quantum filter has been used. The MLEV-17 composite pulse, including two 2.5 ms trim pulses, lasted between 80 and 90 ms. In the DQF-Cosy and NOESY experiments specific irradiation of the water resonance took place at all times except during the data acquisition period. In contrast in the HoHaHa experiments irradiation took only place during the relaxation delay period which lasted in all 2D experiments 2.5 s. The number of scans, including dummy scans, varied between 34 and 108, whereas the number of increments varied between 393 and 611, the total acquisition time was 16-40 hours. The data-handling was performed as previously described [2]. The 2D-NMR spectra are presented as contour plots with levels increasing by a factor of 1.3.

Results and discussion

The 1D-NMR spectrum of apoflavodoxin from *M. elsdenii* shows a remarkable spread of resonances (Fig. 1), comparable to the spectra of the holoprotein in its three redox states [17,18]. This suggests a highly ordered structure and lead us to acquiring several 2D-NMR spectra to gain more specific insights.

Fig. 2A depicts part of the NOESY spectrum of *M. elsdenii* flavodoxin in the oxidized state, sequence specific assignments are added (taken from [3]). In fig. 2B the same part of the NOESY spectrum of the apoprotein is shown with corresponding sequence specific assignments. As can be seen there is considerable overlap with respect to chemical shift positions and NOE effects

between the spectra (such overlap is observed for the complete NOESY spectrum), so large parts of the tertiary structures of the holo- and apoprotein will be very alike. However, differences between the spectra are also observed. In Fig. 2 a sequential pathway, characteristic for an β -sheet strand, as obtained by using the sequential resonance assignment procedure [19] is shown for both holo- and apoprotein. Cross peaks in the spectra of the apoprotein are broader than the corresponding ones in the holoprotein (at comparable concentrations) making the former spectra more difficult to interpret (see Fig. 2).

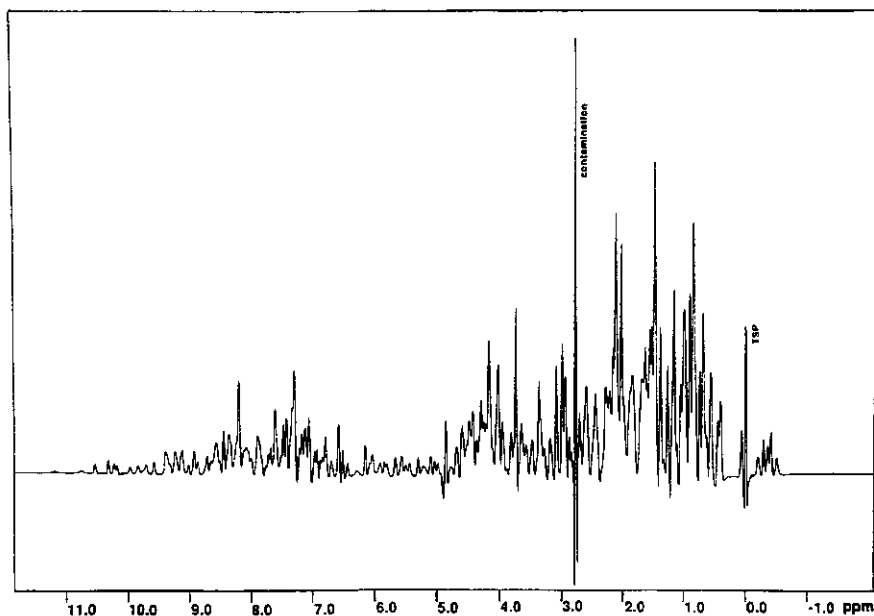


Fig. 1 ^1H NMR spectrum (4096 data points) at 600 MHz of approximately 10 mM apoflavodoxin from *M. elsdenii* (pH 6.1, 30 $^{\circ}\text{C}$, solvent is H_2O). The resolution of the spectrum was enhanced by a sine multiplication, the sine bell was shifted by 15 degrees.

Because of considerable overlap between the ^1H 2D-NMR spectra of the apo- and holoprotein, and the known assignments of the holoprotein in two redox states [2,3], we decided not to start making sequential assignments by searching for individual spin systems in the correlated spectra, as normally done [19]. Instead by comparing NOESY spectra of the oxidized and reduced state with NOESY spectra of the apoprotein, we could easily transfer assigned spin systems to the latter spectra greatly facilitating the sequential assignments of the apoprotein. Assignments of individual spin systems of the apoprotein were then checked by

Residue	NH	C α H	C β H	others
Met1		4.07(3.74)	2.24,---(2.21,2.04)	C γ H 2.58(2.51)
Val2	8.59(8.33)	4.53(4.40)	2.02(2.03)	C γ H 0.84,0.74(0.81,0.71)
Glu3	9.02(8.69)	5.11(5.15)	2.20,1.88(2.17,1.85)	
Ile4	9.21(9.11)	5.05(5.05)	2.08(2.08)	C γ H3 1.04(1.02)
				C γ H2 1.63(1.61)
				C δ H 0.65(0.64)
Val5	9.32(9.25)	5.45(5.42)	1.49(1.48)	C γ H 0.63,-0.28(0.60,-0.31)
Tyr6	7.91(7.95)	6.04(6.11)	2.77,2.77(2.78,2.73)	C δ H 6.60(6.60)
Trp7	8.37(8.43)	4.88(4.46)	3.30(3.24)	C δ H 6.51(6.49)
				NH ϵ 9.97(9.89)
				C δ^1 H 7.53(7.50)
				C δ^2 H 7.49(7.47)
				C γ^2 H 7.25(7.19)
				C δ^3 H ---(7.06)
				C δ^3 H ---(7.38)
				OH ---(8.06)
Ser8	---(5.82)	4.04*(4.36)	3.57*,3.67*(3.58,3.43)	
Gly9	---(10.43)	3.82*,3.70*(3.79,3.79)		C γ H 1.20*(1.21)
Thr10	---(9.35)	---(4.66)	4.59*(4.59)	
Gly11	---(7.55)	4.43*,3.70*(4.43,3.64)		
Asn12	---(11.49)	---(4.63)	3.14*,2.76*(3.25,2.64)	NH1 ---(6.42)
				NH2 ---(8.21)
Thr13	---(11.40)	3.88*(3.86)	---(4.43)	C γ H 1.47*(1.49)
				OH ---(6.17)
Glu14	7.23(7.17)	---(3.30)		
Ala15	7.93(7.97)	4.17(4.16)	1.67(1.65)	
Met16	8.09(8.01)	3.81(3.79)	2.61(2.58)	C γ H 3.05*(3.03*)
Ala17	8.19(8.27)	3.32(3.30)	0.95(0.91)	C δ H 2.17*(2.15*)

Asn18	7.85(7.86)	4.36(4.32)	2.96,2.79(2.93,2.76)	NH1,2	3.39(---)
Glu19	8.08(8.04)	4.02(3.97)	2.15,2.09(2.13,2.09)	C ¹ H3	0.41(0.38)
Ile20	8.87(8.81)	3.34(3.33)	1.32(1.29)	C ¹ H2	1.56,0.76(1.53,0.74)
				C ² H	-0.40(-0.43)
Glu21	8.72(8.71)	3.48(3.47)	2.13,2.04(2.09,2.02)		
Ala22	7.72(7.67)	4.01(3.98)	1.48(1.46)		
Ala23	7.61(7.57)	4.20(4.18)	1.63(1.61)	C ¹ H	1.12,0.79(1.08,0.77)
Val24	8.46(8.42)	3.39(3.38)	2.14(2.12)	C ² H	1.64*, --- (1.73*, 1.65*)
Lys25	8.26(8.17)	4.28(4.31)	1.85(1.83)	C ³ H	--- (2.96*)
Ala26	8.20(8.17)	4.16(4.14)	1.51(1.50)		
Ala27	7.42(7.40)	4.42(4.39)	1.49(1.47)		
Gly28	7.87(7.83)	4.26,3.78(4.25,3.75)			
Ala29	7.33(7.33)	4.77(4.81)	1.38(1.36)		
Asp30	8.36(8.22)	4.75(4.75)	2.73,2.58(2.69,2.53)	C ¹ H	1.00,0.91(0.95,0.88)
Val31	8.35(8.17)	5.67(5.60)	2.08(2.06)	C ¹ H	2.33(2.25)
Glu32	8.21(8.15)	4.69(4.66)	2.00,2.12(1.99,2.10)		
Ser33	8.56(8.43)	6.05(6.01)	3.69,3.56(3.66,3.58)	C ¹ H	0.99,0.86(0.97,0.84)
Val34	9.58(9.53)	4.60(4.53)	2.08(2.06)		
Arg35	8.25(8.17)	4.40(4.45)	3.05*(---)		
Phe36	7.63(7.65)	3.27(3.25)	2.60,2.46(2.52,2.43)	C ² H	6.16(6.12)
				C ³ H	7.43(7.40)
				C ⁴ H	7.18(7.15)
				C ¹ H	2.43(2.40)
Glu37	10.23(10.24)	4.17(4.13)	2.24,2.24*(2.27,2.20)	C ¹ H	1.17(1.15)
Asp38	7.62(7.62)	5.02(4.98)	3.05,2.61(3.00,2.59)		
Thr39	7.60(7.56)	5.04(5.03)	3.96(3.97)	NH1	7.11(---)
Asn40	9.26(9.25)	5.31(5.29)	2.93(2.91)	NH2	7.74(---)
Val41	8.58(8.49)	3.33(3.31)	1.74(1.62)	C ¹ H	0.56,0.45(0.55,0.44)
Asp42	8.12(7.98)	4.33(4.31)	2.62,2.62(2.60,2.57)		

Asp43	8.13(8.07)	4.46(4.45)	2.63,2.63(2.70,2.59)	C ¹ H	1.38,1.06(1.35,1.05)
Val44	7.77(7.75)	3.65(3.72)	2.29(2.25)		
Ala45	8.37(8.30)	3.95(3.98)	1.49(1.48)		
Ser46	7.31(7.28)	4.48(4.45)	4.15,4.02(4.12,4.03)		
Lys47	7.59(7.59)	4.58(4.54)	2.19*,---(1.98*,1.90*)		
Asp48	7.91(7.85)	4.58(4.55)	2.88,2.77(2.83,2.74)	C ¹ H	1.01,0.85(0.98,0.85)
Val49	7.55(7.48)	4.79(4.89)	2.02(2.06)	C ¹ H3	0.86(0.85)
Ile50	8.64(8.61)	4.78(4.87)	1.70(1.64)	C ¹ H2	1.48(1.45)
Leu51	9.71(9.65)	5.50(5.49)	2.13,1.19(2.10,1.18)	C ¹ H	1.49(1.47)
Leu52	8.61(8.57)	5.57(5.54)	2.01,1.56(1.95,1.52)	C ² H	0.71,0.57(0.68,0.56)
				C ¹ H	1.79(1.75)
				C ² H	1.16,1.01(1.11,0.99)
Gly53	9.38*(9.37)	4.70*,1.82*(4.79,1.80)		SH	---(5.05)
Cys54	9.38(9.36)	5.67(5.60)	2.94,2.81(2.86,2.86)	C ¹ H	1.56*(1.85)
Pro55		5.23(5.40)	2.72,2.08*(2.32,2.07*)	C ² H	4.50*,4.90*(4.39,4.95)
Ala56	6.81(6.46)	2.70(2.67)	0.40(0.09)	C ¹ H	---(2.29*)
Met57	---(7.96)	---(5.11)	---,---(1.15,1.60*)		
Gly58	---(6.95)	---(3.86,3.72)			
Ser59	---(9.05)	---(5.10)	---,---(3.90,3.71)	C ¹ H	---(2.62*)
Glu60	---(9.39)	---(3.73)	---,---(2.41*,2.10*)	C ¹ H	---,---(2.34,2.34)
Glu61	---(9.19)	---(4.54)	---,---(2.07,1.79)	C ¹ H	1.13(1.06)
Leu62	8.19(7.56)	4.20(4.19)	1.47,0.89(1.39,0.73)	C ² H	-0.19,-0.49(-0.22,-0.64)
				C ¹ H	---,---(1.22*,0.30)
Glu63	5.99(6.00)	3.61(3.24)	---,---(1.64,0.74*)		
Asp64	8.04(7.91)	4.16(4.10)	---,2.59(2.68,2.58)		
Ser65	8.34(8.22)	4.33(4.31)	3.96,3.86(3.93,3.82)	C ¹ H	1.02,0.85(0.97,0.80)
Val66	10.76(10.88)	4.05(4.02)	1.67(1.65)	C ¹ H	0.65,0.43(0.59,0.37)
Val67	8.00(7.82)	2.59(2.57)	2.07(2.05)		

Glu68	8.76(8.55)	4.20(4.15)	2.34(---)	C7H	1.91*(1.82)
Pro69		4.30(4.27)	2.35*, 2.29*(---, 2.25)	CδH	3.45, 3.17(3.43, 3.11)
Phe70	7.12(7.10)	4.17(4.13)	3.18, 3.18(3.15, 3.15)	CδH	7.33(7.30)
				CεH	7.32(7.34)
				CδH	7.13(7.11)
Phe71	9.84(9.81)	4.18(4.19)	3.10, 3.10(3.06, 3.06)	CδH	7.29(7.27)
				CεH	7.38(---)
Thr72	8.67(8.55)	3.77(3.71)	4.30(4.28)	C7H	1.26(1.23)
Asp73	7.29(7.26)	4.52(4.48)	2.65, 2.52(2.62, 2.46)		
Leu74	8.45(8.42)	3.99(3.93)	---(1.92)	C7H	---(1.66)
				CδH	---, ---(1.28, 1.05)
Ala75	8.21(8.13)	3.76(3.73)	1.19(1.13)		
Pro76		4.49(4.46)	2.45*, 1.82*(2.41, 1.80)	C7H	2.00*(1.98)
				CδH	3.62*(3.59)
Lys77	8.24(8.21)	4.44(4.39)	1.91(1.89)		
Leu78	7.60(7.60)	4.16(4.19)	---(2.10)	CδH	---, ---(0.89*, 0.68*)
Lys79	7.15(7.05)	3.63(3.60)	2.02, 1.84*(1.99, 1.82*)	CδH	1.55*(1.59)
				CεH	3.09(3.07)
Gly80	7.83(7.77)	4.24, 3.92(4.21, 3.89)			
Lys81	8.19(8.15)	4.65(4.68)	2.00, 1.85*(1.97, 1.85*)	C7H	---(1.43*)
				CδH	---(1.66*)
Lys82	8.00(7.88)	4.90*(5.00)	2.22, 2.22(2.18, 2.18)	C7H	---, 1.45*(1.57*, 1.42*)
				CδH	1.69*(1.67*)
				CεH	---(3.03)
Val83	8.93(8.88)	5.81(5.79)	1.62(1.59)	C7H	0.90, 0.90(0.88, 0.88)
Gly84	9.37(9.31)	5.20, 3.35(5.18, 3.32)			
Leu85	7.34(7.35)	5.58(5.54)	1.56, 0.51(1.52, 0.46)	C7H	0.98(0.94)
				CδH	0.08, -0.34(0.05, -0.39)

Phe86	9.40(9.29)	6.09(6.08)	3.18,2.95(3.14,2.91)	C^{δ1}H C^{ε1}H C^{ε2}H C^{ε3}H C^{ε4}H	6.71(6.69) 6.86(6.84) 6.86(6.82) 7.37(7.32) 7.13(7.09)
Gly87	8.20(8.20)	5.24,4.12(5.25,4.06)			
Ser88	6.80(6.53)	5.92(6.11)	3.70,3.70(3.72,3.72)	OH	---(6.49)
Tyr89	8.56(8.05)	5.00(5.34)	2.97,2.76(3.13,2.64)	C^δH C^εH	7.05(7.08) 6.59(6.60)
Gly90	---(9.64)	---,---(4.41,3.54)			
Trp91	7.82*(8.06)	4.90*(5.05)	3.48*,3.37*(3.49,3.27)	NH C^{δ1}H C^{ε2}H C^ηH C^{ε3}H C^{ε3}H	10.18*(10.20) 7.29*(7.11) 7.45*(7.78) 7.22*(6.95) ---(7.10) 7.49*(7.52)
Gly92	---(10.05)	---,---(---,---)			
Ser93	---(9.65)	---(4.63)	---,---(4.01,3.88)		
Gly94	9.07*(9.48)	3.96*,3.69*(4.04,3.67)		C^ηH	2.63*,2.42*(2.70*,2.38)
Glu95	9.76*(8.86)	4.13*(4.03)	2.27*,2.12*(2.17,2.03)	NH	9.23*(9.05)
Trp96	---(9.75)	---(4.39)	3.38*,2.69*(3.26,3.00)	C^{δ1}H C^{ε2}H C^{η2}H C^{ε3}H C^{ε3}H	6.69*(6.40) 7.47*(7.38) 7.13*(7.10) 6.60*(6.61) 7.45*(7.45)
Met97	6.96(6.74)	4.13*(3.99)	---, +0.08*(1.39,-0.17)	C^ηH C^δH	---,---(2.10*,2.01) ---(1.56*)
Asn98	7.42(7.35)	4.28(4.24)	2.71,---(2.71,2.68)		
Ala99	7.66(7.88)	4.26(4.22)	1.59(1.57)		

Trp100	8.36(8.29)	4.54(4.44)	3.37,3.11(3.33,3.03)	NH C ^δ H C ^ε H C ^η H C ^θ H	6.29(6.12) 6.45(6.36) 6.80(6.73) 7.30*(7.33*) 7.06*(7.08*)
Lys101	9.16(9.18)	3.55(3.52)	1.99,1.62(1.96,1.59)	C ^γ H C ^δ H C ^ε H NH	1.32,1.15(1.31,1.13) --(1.59) 2.88(2.85) 6.93(---)
Gln102	7.69(7.65)	4.14(4.12)	2.48,2.25(---,2.25)	NH	6.93(---)
Arg103	8.20(8.23)	(4.25)		OH	--(3.68)
Thr104	8.56(8.50)	4.27(3.99)	--(4.08)	C ^γ H	--(0.96)
Glu105	9.12(9.09)	4.15(4.12)	2.29,2.12*(2.27,2.12*)	C ^γ H	2.57(2.53)
Asp106	8.29(8.23)	4.61(4.56)	2.97,2.84(2.95,2.80)	C ^γ H	1.55(1.52)
Thr107	7.51(7.48)	4.35(4.31)	4.47(4.42)	OH	--(5.39)
Gly108	8.02(7.94)	4.47,3.95(4.44,3.91)			
Ala109	7.56(7.55)	4.68(4.65)	1.28(1.30)	C ^γ H	1.16(1.13)
Thr110	8.93(8.86)	4.39(4.37)	3.99(3.99)	C ^γ H	0.82,0.82(0.79,0.79)
Val111	9.13(9.03)	5.11(5.09)	2.12(2.09)	C ^γ H3	0.70*(0.68*)
Ile112	8.94(8.85)	4.26(4.21)	1.97(1.91)	C ^γ H2	1.09*,0.86*(1.09,0.87)
				C ^δ H	0.58(0.57)
Gly113	6.97(6.93)	4.15,4.01(4.15,3.97)			
Thr114	8.16(8.03)	5.85(5.86)	4.03(3.99)	C ^γ H	0.97(0.95)
Ala115	8.52(8.44)	4.90*(4.90)	1.17(1.14)		
Ile116	8.63(8.50)	5.91(5.99)	2.22(2.26)	C ^γ H3	0.86(0.79)
				C ^γ H2	1.70,1.17(1.67,1.15)
				C ^δ H	0.69(0.61)
Val117	7.59(7.67)	4.47(4.38)	2.19(2.16)	C ^γ H	0.91,0.75(0.89,0.72)

Asn118	8.51(8.33)	4.04(3.70)	2.48,2.36(2.47,2.30)	NH1 NH2 C γ H C γ H C δ H	7.06(6.91) 6.59(6.23) ---(2.02*) ---,---(2.71*,2.57*) 3.51*,---(3.48,4.36*)
Glu119	8.08(8.65)	3.46(3.39)	---,---(2.34,2.15)		
Met120	---(7.41)	4.61*(4.44)	---(2.06)		
Pro121		4.42*(4.46*)			
Asp122	8.12(8.05)	4.57(4.55)	2.71,2.43(2.68,2.41)		
Asn123	10.54(10.49)	4.09(4.06)	2.94,2.83(2.91,2.81)	NH1 NH2	7.50(---) 6.89(---)
Ala124	9.24(9.22)	4.57(4.55)	1.70(1.68)		
Pro125		4.31(4.29)	2.44,2.03(2.42,2.01)	C γ H C δ H	2.17(2.18) 4.20*,---(4.19*,4.14*)
Glu126	10.32(10.32)	4.11(4.08)	---,---(1.99,1.85)	C γ H	3.00,2.50(2.96,2.47)
Cys127	7.08(7.07)	3.65(3.62)	3.34,2.63(3.33,2.61)	SH	---(1.90)
Lys128	6.98(6.92)	3.76(3.74)	1.89,1.81(1.89,1.79)	C γ H C δ H	1.39,1.32(1.38,1.30) 1.63(1.61)
				C ϵ H	---(2.92)
Glu129	8.44(8.36)	3.99(3.98)	2.04,2.04(2.02,2.02)	C γ H	2.41,2.27(2.36,2.24)
Leu130	7.36(7.32)	4.23(4.20)	---(---)	C γ H C δ H	---(1.34) ---,---(0.71,0.67)
Gly131	8.06(7.99)	3.57,3.48(3.55,3.47)			
Glu132	8.39(8.30)	3.74(3.70)	2.11,1.94(2.07,1.93)	C γ H	2.46(2.43)
Ala133	7.88(7.83)	4.05(4.02)	1.48(1.45)		
Ala134	8.33(8.26)	3.82(3.79)	1.39(1.35)		
Ala135	7.90(7.80)	3.82(3.81)	1.52(1.49)		
Lys136	7.19(7.14)	4.42(4.41)	1.78,---(1.74,1.66)	C γ H C δ H C ϵ H	1.55(1.50) 1.98(1.97) ---(2.97)
Ala137	7.07(7.06)	4.03(3.99)	1.45(1.43)		

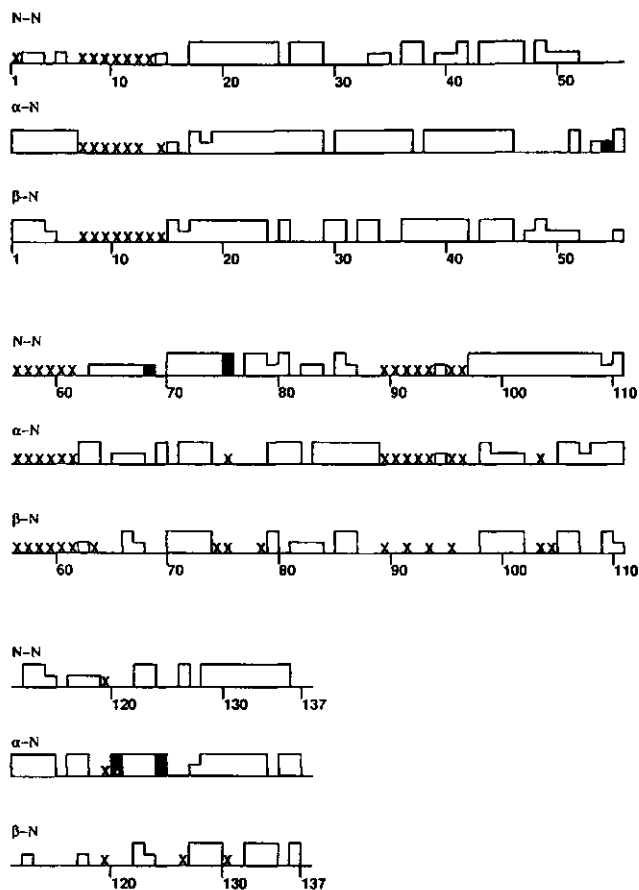


Fig. 3 Sequential NOE contacts observed in the 150 ms NOESY spectrum of approximately 10 mM apoflavodoxin of *M. elsdenii*, pH 6.1, 30 °C. Weak NOE's have been indicated by small boxes. In case of doubts, no contact has been depicted. The grey boxes indicate respectively, $d_{\alpha\delta}$, $d_{N\delta}$, $d_{N\delta}$, $d_{\alpha\delta}$ and $d_{\alpha\delta}$ connectivities involving proline residues. Crosses indicate that connectivities could not be established because of missing assignments.

By analyzing sequential (Fig. 3) and long-range NOE connectivities, which are virtually identical to the connectivities observed for the holoprotein, and based on the identity in chemical shifts (Table 1), we can conclude that the apoflavodoxin of *M. elsdenii* consists, just as in case of the holoprotein, of a central parallel β -sheet consisting of 5 strands. Strand 1: Val2-Tyr6, strand 2: Val31-Arg35, strand 3: Val49-Gly53 (many $C_{\alpha}H$'s resonate close to the water frequency, so Fig. 3 does not reflect the extended chain characteristics), strand 4: Lys82-Tyr89 (possible disturbance at

Y89), strand 5: Thr110-Asn118, the connectivity pattern is 2-1-3-4-5. This sheet is surrounded on both sides by two α -helices: helix 1: Asn12-Ala26 (possible disturbance at Asn12-T13), helix 2: Asp64-Leu74 (possibly disturbed at Asp64-Glu68), helix 3: Met97-Asp106 (possibly extended to Glu95), helix 4: Glu126-Ala135. The secondary and tertiary structure characteristics outside the flavin binding region of the apoprotein are virtually identical when compared to the holoprotein in its three redox states. A "...significant loss of secondary structure (increase in random coil) accompanying flavin removal from the apoprotein" as observed by far-uv-circular dichroism techniques [10] we do not observe.

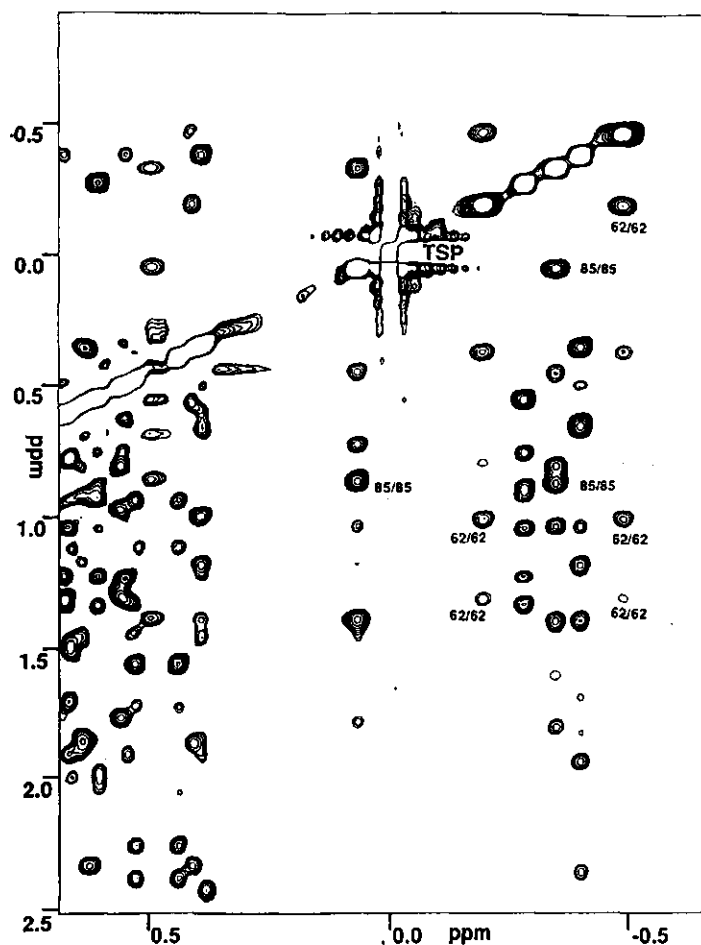


Fig. 4 A. Part of the highfield region of a 600 MHz NOESY spectrum (mixing time 150 ms) of apollavodoxin from *M. elsdenii* in 10%²H₂O/90%¹H₂O, pH 6.1, 30 °C. The concentration of the apollavodoxin is approximately 10 mM. TSP was added as reference to this sample. Processing and resolution as in Fig. 2A.

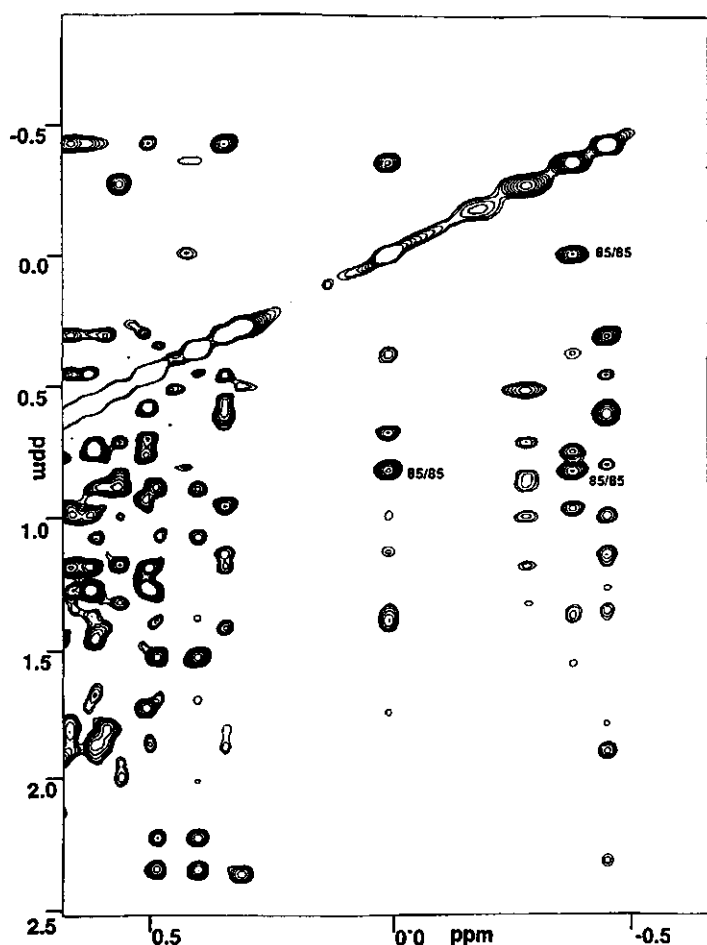


Fig. 4 B. Same part of the highfield region of a 600 MHz NOESY spectrum (mixing time 150 ms) as depicted in Fig. 4A of apoflavodoxin from *M. elsdenii* in 10%²H₂O/90%¹H₂O, pH 7.3, 30 °C. The concentration of the apoflavodoxin is approximately 15 mM. No TSP was added. Processing and resolution as in Fig. 2A. Notice the strong broadening of several cross peaks as compared to Fig. 4A.

Of the amino acid residues outside the flavin binding region, resonances of Met1, Val2, Glu3, Asp30, Ser33, Val41, Asp42, Lys47, Asp64, Ser65, Val66, Val67, Glu68, Thr72, Lys82, Phe86, Met97, Ala99, Trp100, Thr104, Thr114, Ile116 and M120 show proton chemical shift differences, when compared to the corresponding resonances of the holoprotein, which exceed 0.10 ppm but do not exceed 0.35 ppm (see Table 1). Many of these resonances have already been reported to be pH sensitive in the holoprotein without showing NOE contact differences involving these protons [3,7]. In case of the apoflavodoxin both pH and temperature are lower

when compared to the experiments involving the holoprotein explaining the chemical shift differences observed for the forementioned residues. The largest shifts are observed for resonances of Met1, Val2 and Glu3, probably resulting from protonation of elements of the saltbridge they take part in, as has been reported for the holoprotein [3,7].

Of the residues in the flavin binding region the aliphatic proton resonances in the phosphate binding region (Trp7-Thr13) were assigned based only on overlap with the corresponding cross peaks in Cosy, HoHaHa and NOESY spectra of the holoprotein. Amide resonances in this region of the protein were not detected expected to result from fast exchange with the solvent, since the strong hydrogen bonding of these amides with the phosphate [7] is not present anymore.

In the isoalloxazine binding region many proton resonances have not (yet) been assigned, preventing structural analysis (no proton resonances have been assigned at all of Met57, Gly58, Ser59, Glu60, Glu61, Gly90, Gly92 and Ser93). This can be the result from several things. The amide protons in this region might exchange to fast with the saturated solvent (at pH 6.1, 30 °C) to be detected as the specific hydrogen bonding of these amides, known to exist with the flavin in the holoprotein, will have disappeared. Secondly, interconversion with an intermediate rate on the NMR time scale between several possible conformations of the amino acid residues in the unstable flavin binding region can result in broadening of these cross peaks beyond detection (explaining why beside amide resonances many aliphatic proton resonances have not been detected in this region of the protein). Such an interconversion between conformations has been observed for trapped intermediates in the folding of Basic Pancreatic Trypsin Inhibitor [20]. These multiple conformations in the isoalloxazine binding region might be caused by specific interactions (during collisions) between the apoflavodoxin molecules. Raising the concentration of the apoflavodoxin from approximately 10 to 15 mM results in a decrease of T₂ of all proton resonances and an additional broadening, in some cases beyond detection, of several resonances of protons in the flavin binding region. Fig. 4 illustrates this for the methyl resonances of L62. A considerable part of the sample containing 15 mM apoflavodoxin precipitated during the measurements (which lasted 3 days), whereas the 10 mM samples contained only a minor fraction of precipitate at the end of the experiments. Apoflavodoxin is clearly not as stable as the holoprotein of which stable concentrations could be reached up to 23 mM, pH 7.0, 41 °C, over a period of several weeks. The severe concentration dependent broadening of resonances is not solely restricted to the isoalloxazine binding region, resonances of a few residues in the immediate neighbourhood of this region are also broadened (e.g.

all protons of Gly53 , Gly87 and Val67 are broadened beyond detection in the 15 mM sample).

In conclusion it has been shown that the apoflavodoxin of *M. elsdenii* has a highly ordered structure. The tertiary structures of the apo- and holoprotein of *M. elsdenii* are virtually identical outside the flavin binding region. Proton resonances of several amino acid residues in the flavin binding region have not yet been assigned, possibly the result of multiple conformations (extra flexibility) in this region of the protein. The latter might be of importance for flavin binding. The apoprotein is relatively stable but less stable than the holoprotein, a well known feature of partly folded proteins [21].

By lowering the temperature and the concentration of the apoprotein samples, in combination with 2D-NMR experiments in which no selective irradiation of the water resonance takes place (e.g. using a jump-return pulse sequence), we intend to assign the remaining resonances of protons in the flavin binding region. This will reveal interesting detailed information on the conformation and dynamics of the flavin binding region of this partly folded protein and the structural changes accompanied by flavin binding. The relatively high stability of apoflavodoxin further gives the opportunity to study the unfolding of this protein by NMR on varying the experimental conditions.

Acknowledgements

Measurements were performed at the HF-SON NMR Facility Nijmegen (The Netherlands). This study was carried out under the auspices of the Netherlands Foundation for Chemical Research (SON) with financial aid from the Netherlands Organization for the Advancement of Pure Research (NWO).

References

1. Mayhew, S.G. & Ludwig, M.L. (1975) *Enzymes 3rd Ed.* 12, 57-118.
2. van Mierlo, C.P.M., Vervoort, J., Müller, F. & Bacher, A. (1990) *Eur. J. Biochem.* 187, 521-541.
3. van Mierlo, C.P.M., van der Sanden, B.P.J., van Woensel, P., Müller, F. & Vervoort, J. (1990) *Eur. J. Biochem.*, (submitted).
4. van Mierlo, C.P.M., Müller, F. & Vervoort, J. (1990) *Eur. J. Biochem.*, (in press).
5. Kaptein, R., Zuiderweg, E.R.P., Scheek, R.M., Boelens, R. & van Gunsteren, W.F. (1985) *J. Mol. Biol.* 182, 179-182.

6. Clore, G.M., Brünger, A.T., Karplus, M. & Gronenborn, A.M. (1986) *J. Mol. Biol.* **191**, 523-551.
7. van Mierlo, C.P.M., Lijnzaad, P., Vervoort, J., Müller, F., Berendsen, H.J.C. & de Vlieg, J. (1990) *Eur. J. Biochem.*, {submitted}.
8. Moonen, C.T.W. & Müller, F. (1984) *Eur. J. Biochem.* **140**, 303-309.
9. Moonen, C.T.W., Vervoort, J. & Müller, F. (1984) in *Flavins and Flavoproteins* (Bray, R.C., Engel, P.C. & Mayhew, S.G., eds.) pp. 493-496, Walter de Gruyter & Co., Berlin-New York
10. D'Anna, J.A. & Tollin, G. (1972) *Biochemistry* **11**, 1073-1080.
11. Mayhew, S.G. & Massey, V. (1969) *J. Biol. Chem.* **244**, 794-802.
12. Wassink, J.H. & Mayhew, S.G. (1975) *Anal. Biochem.* **68**, 609-616.
13. Marion, D. & Wüthrich, K. (1983) *Biochem. Biophys. Res. Commun.* **113**, 967-974.
14. Rance, M., Sörenson, O.W., Bodenhausen, G., Wagner, G., Ernst, R.R. & Wüthrich, K. (1983) *Biochem. Biophys. Res. Commun.* **117**, 479-485.
15. Bodenhausen, G., Kogler, H. & Ernst, R.R. (1984) *J. Magn. Res.* **58**, 370-388.
16. Bax, A. & Davis, D.G. (1985) *J. Magn. Reson.* **65**, 355-360.
17. van Schagen, C.G. & Müller, F. (1981) *FEBS Lett.* **136**, 75-79.
18. Moonen, C.T.W. & Müller, F. (1984) *Eur. J. Biochem.* **140**, 311-318.
19. Wüthrich, K. (1986) *NMR of proteins and nucleic acids*, Wiley, New York.
20. States, D.J., Creighton, T.E., Dobson, M. & Karplus, M. (1987) *J. Mol. Biol.* **195**, 731-739.
21. Creighton, T.E. (1985) *J. Phys. Chem.* **89**, 2452-2459.

Summary

^1H NMR techniques have been applied for a thorough study of the uncrystallizable *Megasphaera elsdenii* flavodoxin in its three redox states. The aim of the research project described in this thesis was to obtain answers regarding questions concerning the redox potential regulation of FMN by the protein and the observed activation barrier occurring between the oxidized and one-electron reduced redox states of the protein. Detailed information about the structure of the, from a NMR point of view, challenging large protein in solution was gathered.

Applying the sequential resonance assignment procedure using phase-sensitive 2D-correlated spectroscopy (DQF-Cosy, HoHaHa, DQ experiments) and phase-sensitive nuclear Overhauser enhancement spectroscopy (NOESY) to two-electron reduced *M. elsdenii* flavodoxin, essentially complete proton assignments for its 137 amino acid residues have been made. In addition all proton resonances of the two-electron reduced flavin were assigned, using ^{13}C -enriched FMN molecules. An exception has to be made for $\text{C}_3'\text{OH}$ which exchanges too fast with solvent molecules to be detected. The presence of a fast electron shuttle between the paramagnetic semiquinone and the diamagnetic hydroquinone state of the protein was extensively exploited during the assignment procedure to create a varying proton sphere around the flavin which depended on the semiquinone percentage in the samples. Protons in this sphere are characterized in the 2D-NMR spectra by either complete disappearance or broadening of the corresponding cross peaks thereby simplifying the complex 2D-NMR spectra of the protein and labelling these protons with regard to their distance to the flavin.

The assignments of the two-electron reduced state of *M. elsdenii* flavodoxin provided the starting point of further studies on the protein as described in this thesis. The secondary structure of the protein has been determined by visual, qualitative inspection of sequential connectivities involving C_αH , C_βH and NH protons observed in NOESY spectra. The global fold of the protein was then established by using nonsequential interresidual NOE connectivities as primary source of information. *M. elsdenii* flavodoxin consists of a central parallel β -sheet including five strands surrounded on both sides by a pair of α -helices. The flavin is non-covalently bound at the periphery of the molecule. The protein is very stable and compact as reflected by the unexpected observation of several hydroxyl and sulfhydryl groups at 41 $^\circ\text{C}$ and pH 8.3 with water as solvent, and the extremely slow exchange of 32 amide protons against deuterium oxide under the same experimental conditions.

Comparing the secondary structure elements and the global fold of two-electron reduced *M. elsdenii* flavodoxin with the crystal structures of oxidized as well as

one-electron reduced *Clostridium MP* flavodoxin it became clear that there is a high structural similarity between both flavodoxins. Therefore the crystal structure of the semiquinone state of *Clostridium MP* flavodoxin was used to build by amino acid residue replacement a plausible starting structure for the restrained molecular dynamics calculations on two-electron reduced *M. elsdenii* flavodoxin. These calculations, using 509 experimental interresidual NOE distance restraints (including one *non*-NOE in the flavin binding region) which are all very well spread over the molecule, resulted in a tertiary structure of two-electron reduced *M. elsdenii* flavodoxin which satisfies the experimental restraints very well (maximum NOE violation 0.66 Å, the potential energy of the structure is -2278 ± 122 kJ mol⁻¹). For the first time the three-dimensional structure of a flavoprotein has been elucidated by NMR.

The tertiary structure of *M. elsdenii* flavodoxin is highly defined with the exception of the flavin. The latter is expected to result from performing the RMD simulation without water molecules and without proper charges on the flavin (phosphate dianionic and N₁ negatively charged). Water plays an important role in regions of the molecule accessible to solvent molecules. The negatively charged phosphate is strongly hydrogen bonded by peptide dipoles in the region Trp7-Thr13 of the protein. Amide protons involved in phosphate binding are characterized by their very lowfield resonance positions. This study shows that these amides are solvent accessible as they exhibit fast exchange with deuterated solvent on the timescale of a NOESY exchange experiment (at pH 8.3, 41 °C). Under the same experimental conditions also part of the isoalloxazine binding region is accessible to solvent molecules. The possibility of measuring exchange characteristics of individual protons by NMR signifies important additional information on protein tertiary structure.

Taking into account this solvent accessibility of both the phosphate and part of the isoalloxazine binding region and the stabilizing effects of it on charges, it is proposed that the role of electrostatic interactions between the negatively charged phosphate and N₁ on the redox potential of flavodoxin will be less dominant than proposed. The destabilization of the negatively charged N₁ in two-electron reduced flavodoxin by its local microenvironment as compared to the uncharged N₁ in the semiquinone state (both relative to their energies in water) is expected to be an important contribution to the redox potential. The amide exchange against deuterons and several typical line shapes in the 2D-NMR spectra are consistent with the structure generated.

Greatly benefiting from the assignments made of the two-electron reduced state, essentially complete sequential assignments have been made of oxidized *M. elsdenii* flavodoxin, including flavin assignments. Based on identity in NOE

contacts and in chemical shift positions of the protons, it is concluded that the tertiary structure outside the immediate flavin binding region remains identical on going from the oxidized to the reduced state of the protein. However, functionally important conformation changes in the flavin binding region do occur on reduction as observed by NMR. The orientation of the peptide link between Gly58 and Ser59 is altered (bringing the carbonyl group in close contact to N5H) as well as the position of the amide of Glu61. The semiquinone state is stabilized as compared to the oxidized state. These subtle conformation changes account for the activation barrier occurring in the transition from the oxidized to the one-electron reduced state of the protein. On additional reduction of the protein to the two-electron reduced state no further conformation changes are expected as a fast electron exchange between the semiquinone and the hydroquinone state prevents structural rearrangements. *M. elsdenii* flavodoxin is thereby predestined for one-electron transfer reactions by shuttling between the semiquinone and hydroquinone states, as has already been shown by previous studies. No difference in water accessibility and flexibility in the flavin binding region are observed on reduction. On two-electron reduction the flavin becomes anti-aromatic as evidenced by a decrease in ring current effect of the pyrazine part of the isoalloxazine moiety on the apo region of the protein.

A three-dimensional non-selective Clean TOCSY-NOESY ^1H NMR study of *M. elsdenii* flavodoxin in the oxidized state has been performed to demonstrate the value of the experiment for making sequential resonance assignments in relatively large proteins. An easy and concise way for the analysis of cross peaks has been given and sequential assignments in various secondary structure elements of flavodoxin are made confirming the assignments made by 2D-NMR results. Additional information has also been obtained. Non-selective TOCSY-NOESY has been compared with selective TOCSY-NOESY and non-selective TOCSY-NOESY.

Finally, apoflavodoxin of *M. elsdenii* has been studied using 2D-NMR techniques. The large majority of proton resonances outside the flavin binding region has been assigned. By analyzing sequential and long-range NOE connectivities, which are virtually identical to the connectivities observed for the holoprotein, and based on identity in chemical shifts, it is concluded that the structure of the protein outside the flavin binding region is nearly identical to that of the holoprotein in its three redox states. This is in contrast to results reported from far-uv-circular dichroism studies. Many proton resonances in the isoalloxazine binding region have not (yet) been assigned, possibly resulting from multiple conformations in this region of the protein, preventing structural analysis.

Samenvatting

^1H NMR technieken zijn toegepast op het niet kristalliseerbare *Megasphaera elsdenii* flavodoxine. Het eiwitmolecuul is diepgaand bestudeerd in haar drie redox-toestanden. Het doel van het onderzoek dat beschreven staat in dit proefschrift, was om antwoorden te verkrijgen op vragen betreffende de regulering van de redox-potentiaal van het FMN door het eiwit, en de geobserveerde activerings-barriere in de overgang van de geoxideerde naar de een-electron gereduceerde toestand van het eiwit. Gedetailleerde informatie werd verkregen over de structuur in oplossing van het, voor NMR-begrippen, uitdagend grote eiwit.

Toepassen van de sequentiele resonantie-toekenning-procedure op spectra van het twee-electronen gereduceerde *M. elsdenii* flavodoxine resulteerde in een vrijwel volledige toekenning van de protonresonanties van de 137 aminozuur residuen. Hierbij werd gebruik gemaakt van fasegevoelige 2D-gecorrleerde spectroscopie (DQF-Cosy, HoHaHa, DQ experimenten), en fasegevoelige nucleair Overhauser enhancement spectroscopie (NOESY). Tevens zijn alle protonresonanties van het twee-electronen gereduceerde flavine toegekend door gebruik te maken van ^{13}C verrijkte FMN moleculen. Een uitzondering dient hierbij gemaakt te worden voor het $\text{C}_3'\text{OH}$ proton dat te snel met oplosmiddel-moleculen uitwisselt zodat het niet gedetecteerd wordt. De aanwezigheid van een snelle electronen-uitwisseling tussen de paramagnetische semiquinon en de diamagnetische hydroquinon toestand van het eiwit is intensief gebruikt tijdens de toekenning-procedure. Hiermee werd een variabele protonruimte (die afhankelijk is van het semiquinon percentage in de monsters) rond het flavine gecreeerd. Protonen in dit gebied worden gekarakteriseerd door de volledige verdwijning of verbreding van hun kruispieken. De gecompliceerde 2D-NMR spectra vereenvoudigen daardoor, en de betreffende protonen zijn ge-oormerkt met betrekking tot hun afstand ten opzichte van het flavine.

De toekenning van de twee-electronen gereduceerde toestand van het *M. elsdenii* flavodoxine vormde het beginpunt van verdere studies aan het eiwit zoals gepresenteerd in dit proefschrift. De secundaire structuur van het eiwit is bepaald via visuele, kwalitatieve inspectie van de sequentiele contacten tussen C_αH , C_βH en NH protonen, zoals geobserveerd in de NOESY spectra. Inzicht in de globale vouwing van het eiwit werd daarna verkregen door gebruik te maken van niet-sequentiele interresiduele NOE contacten als primaire bron van informatie. *M. elsdenii* flavodoxine wordt gevormd door een centrale, parallele β -sheet bestaande uit vijf strengen die aan beide zijden omgeven is door twee α -helices. Het flavine is niet-covalent gebonden aan de periferie van het molecuul. Flavodoxine is zeer stabiel en compact; dit komt tot uitdrukking in de onverwachte observatie van

verschillende hydroxyl en sulfhydryl groepen bij 41 °C en een pH van 8.3 met water als oplosmiddel, en in de zeer langzame uitwisseling van 32 amide protonen tegen deuterium oxide onder dezelfde experimentele omstandigheden.

Vergelijking van de secundaire structuur-elementen en de globale vouwing van het twee-electronen gereduceerde *M. elsdenii* flavodoxine met de kristal-structuren van zowel het geoxideerde als het een-electron gereduceerde *Clostridium MP* flavodoxine liet zien dat er een zeer hoge structurele overeenkomst tussen beide eiwitten bestaat. Besloten werd de kristal-structuur van het *Clostridium MP* flavodoxine in de semiquinon toestand om te bouwen middels substitutie van aminozuren. Dit resulteerde in een acceptabele startstructuur voor de moleculaire dynamica berekeningen met afstandsrestricties aan het twee-electronen gereduceerde *M.elsdenii* flavodoxine. De 509 experimenteel verkregen interresiduele NOE afstandsrestricties (inclusief een zogenaamde *non*-NOE) liggen zeer goed verspreid over het molecuul. De berekeningen resulteerden in een tertiare structuur die goed voldeed aan de experimentele restricties (maximale NOE schending 0.66 Å, de potentieele energie van de structuur is -2278 ± 122 kJ mol⁻¹). Voor het eerst werd hiermee de drie-dimensionale structuur van een flavine-eiwit verkregen met behulp van NMR.

De tertiare structuur van het *M. elsdenii* flavodoxine is goed gedefinieerd met uitzondering van het flavine. Het laatste wordt waarschijnlijk veroorzaakt doordat de RMD simulatie werd gedaan zonder water-moleculen en correcte ladingen op het flavine (fosfaat dianionisch en N₁ negatief geladen). Water speelt een belangrijke rol in gebieden van het molecuul die toegankelijk zijn voor water-moleculen. De negatief geladen fosfaat groep wordt sterk waterstofbrug-gebonden door de peptide-dipolen in het gebied Trp7-Thr13 van het eiwit. Amide protonen die betrokken zijn in de fosfaat-binding zijn gekarakteriseerd door hun sterk laagveld verschoven resonantie-posities. Deze studie toont tevens aan dat deze amides toegankelijk zijn voor oplosmiddel-moleculen, ze vertonen een snelle uitwisseling met gedeutereerd oplosmiddel op de tijdschaal van een NOESY-uitwisselings-experiment (bij pH 8.3 en 41 °C). Onder dezelfde experimentele omstandigheden is ook een gedeelte van de isoalloxazine groep toegankelijk voor water-moleculen. De mogelijkheid om met behulp van NMR individuele uitwisselingssnelheden van protonen te meten vormt een bron van belangrijke extra informatie betreffende de tertiare structuur van een eiwit.

De rol van electrostatistische interacties tussen de negatief geladen fosfaat en de N₁ in de regulering van de redoxpotentiaal van het flavodoxine is vermoedelijk minder belangrijk dan verondersteld werd. Dit wordt geconcludeerd naar aanleiding van de oplosmiddel-toegankelijkheid van zowel de fosfaat als gedeeltes van het isoalloxazine en de stabiliserende werking daarvan op ladingen.

De destabilisatie van de negatief geladen N_1 in het twee-electronen gereduceerde flavodoxine door zijn lokale micro-omgeving, vergeleken met die van de ongeladen N_1 in de semiquinon toestand (beiden relatief ten opzichte van hun energieën in water), levert vermoedelijk een belangrijke bijdrage aan de redoxpotentiaal. De amide-uitwisseling met deuterium oxide en de typische lijnvorm van een aantal kruispijken in de 2D-NMR spectra zijn consistent met de gegenereerde structuur van het flavodoxine.

Vrijwel complete sequentiele resonantie-toekenningen, inclusief flavine-toekenningen, zijn gedaan aan het geoxideerde *M. elsdenii* flavodoxine. Groot voordeel werd hierbij ondervonden van de toekenningen van de twee-electronen gereduceerde toestand van het eiwit. Er werd, op grond van overeenkomstige NOE contacten en chemische verschuivingen van protonen, geconcludeerd dat de tertiäre structuur van het eiwit buiten het directe flavine-bindingsgebied vrijwel identiek is in de geoxideerde en de gereduceerde toestand. Echter, functioneel belangrijke conformatie-veranderingen treden wel op in het flavine-bindingsgebied bij reductie, zoals geobserveerd is met behulp van NMR. De orientatie van de peptide-binding tussen Gly58 en Ser59 verandert (waarbij de carbonylgroep in de directe omgeving van N_5H komt), evenals de positie van het amideproton van Glu61. De semiquinon toestand wordt gestabiliseerd in vergelijking met de geoxideerde toestand. De subtiele conformatieveranderingen verklaren de activeringsbarrière die optreedt in de overgang van de geoxideerde naar de een-electron gereduceerde toestand van het eiwit. Bij verder reduceren van het eiwit naar de twee-electronen gereduceerde toestand vinden geen conformatieveranderingen plaats, daar de snelle electronen-uitwisseling tussen de semiquinon en hydroquinon toestand structurele veranderingen uitsluit. *M. elsdenii* flavodoxine is daarom voorbestemd voor een-electron overdragende reacties door te pendelen tussen de semiquinon en hydroquinon toestand, zoals reeds door studies in het verleden is aangetoond. Er wordt geen verschil in watertoegankelijkheid of flexibiliteit in het flavine-bindingsgebied geobserveerd bij reductie. Het flavine wordt anti-aromatisch bij twee-electronen reductie zoals blijkt uit de afname van kringstroom effecten van het pyrazine gedeelte van de isoalloxazine groep op het apo-gedeelte van het eiwit.

Een drie-dimensionale niet-selectieve Clean TOCSY-NOESY 1H NMR studie van *M. elsdenii* flavodoxine in de geoxideerde toestand toonde de waarde van dit experiment voor het maken van sequentiele resonantietoekenningen in relatief grote eiwitten aan. Een eenvoudige en beknopte methode voor de analyse van kruispijken is gegeven. Sequentiele resonantie-toekenningen in verschillende secundaire structuurelementen van het eiwit zijn gemaakt, de toekenningen zoals verkregen met 2D-NMR resultaten werden bevestigd. Daarnaast werd ook extra

informatie verkregen. Niet-selectieve TOCSY-NOESY is vergeleken met selectieve TOCSY-NOESY en met niet-selectieve TOCSY-NOESY.

Tenslotte is het apoflavodoxine met behulp van 2D-NMR technieken bestudeerd. Vrijwel alle resonanties van protonen die niet tot het flavine bindingsgebied behoren zijn toegekend. Uit de sterke overeenkomst van sequentiele en long-range NOE contacten met die van het holo-eiwit, en op grond van overeenkomst in chemische verschuivingen, wordt geconcludeerd dat de structuur van het apo-eiwit buiten het flavine-bindingsgebied vrijwel identiek is aan dat van het holo-eiwit in haar drie redoxtoestanden. Dit is in tegenstelling met resultaten verkregen uit ver-uv-circulair-dichroïsme studies. De meerderheid van de proton-resonanties in het isoalloxazine-bindingsgebied zijn (nog) niet toegekend. Dit is mogelijk het gevolg van meerdere conformaties in dit gebied van het eiwit, waardoor structurele analyse bemoeilijkt wordt.

Curriculum vitae

Carlo van Mierlo is geboren op 18 november 1959 in Wehl. Na het volgen van de kleuter- en lagere school in zijn woonplaats werd het diploma ongedeeld VWO in 1978 aan het Sint Ludgercollege te Doetinchem behaald. In hetzelfde jaar werd de studie Moleculaire Wetenschappen aan de Landbouwhogeschool Wageningen begonnen. Het doctoraal-examen omvatte de hoofdvakken Moleculaire Fysica (Prof. Dr. T. Schaafsma, Dr. H. van As), de Natuurkunde (Prof. Dr. P. Bruijn, Ir. C. Vriesinga) en als bijvak de Wiskunde (Prof. Dr. B. van Rootselaar). Het hoofdvak Moleculaire Fysica bestond uit het bestuderen van het effect van vatdiameter en pulsrepetitietijd op stromingsmetingen met behulp van NMR (de π -pulsmethode). Het hoofdvak Natuurkunde bestond uit de Quantum Mechanica en de Theoretische Natuurkunde. De onderzoeksstage werd uitgevoerd bij Philips Medical Systems te Best (Ir. P. van Dijk), en richtte zich op de kwantificatie van stroming en de studie van stromingsartefacten in NMR-afbeeldingen gebruik makend van NMR-beeldvormings-technieken. De studie werd in mei 1985 afgesloten. Vanaf half juni 1985 werd aan deze dissertatie gewerkt in dienst van de Nederlandse Organisatie voor Wetenschappelijk Onderzoek (NWO). Sedert augustus 1989 was de auteur in tijdelijke dienst van de Landbouwniversiteit Wageningen. Per 1 januari 1990 is de auteur in dienst getreden van het MRC Laboratory of Molecular Biology, Cambridge, Groot-Britannië.